Government of Saskatchewan
Ministry of the Economy

Report 264

Rare Earths in Saskatchewan: Mineralization Types, Settings, and Distributions

by
Charles Normand

2014

Government of Saskatchewan
Ministry of the Economy

Report 264

Rare Earths in Saskatchewan: Mineralization Types, Settings, and Distributions

by
Charles Normand

2014

Printed under the authority of the
Government of Saskatchewan

Cover: Photographs showing different styles of rare earth element mineralization observed at four locations in the Precambrian Shield of northern Saskatchewan:

Top left: Folded diopside-biotite-apatite vein in granitic gneiss, Hoidas South apatite-allanite occurrence, Hoidas Lake, Zemlak Domain, Saskatchewan.

Top right: Reddish apatite breccia containing dark vein/dyke fragments composed of diopside and allanite, JAK zone apatite-allanite developed REE prospect with resources, Hoidas Lake, Zemlak Domain, Saskatchewan. The matrix of the breccia consists mainly of large, light-coloured, centimetre-sized apatite crystals set in medium- to fine-grained apatite.

Bottom left: Deformed biotite-monazite–rich layer containing white granitic pegmatite feldspar knots in psammitic gneiss, Oldman River monazite occurrence, Beaverlodge Domain, Saskatchewan. Up to 20 vol. % monazite is observed locally in the biotite-rich layers at this locality.

Bottom right: Monazite-bearing, biotite-rich stringer-like veins cutting psammopelitic gneiss and white granitic pegmatite, Nevins Lake, Beaverlodge Domain, Saskatchewan. Total rare earth concentrations exceeding 1 wt. % have been reported from biotite-rich stringers cutting white, feldspar-rich granitic pegmatites at this locality.

This product is available for viewing at:

Publications Office
Saskatchewan Ministry of the Economy
2101 Scarth Street, 3rd floor
Regina, SK S4P 2H9
TEL (306) 787-2528
FAX (306) 787-2488
Website: http://economy.gov.sk.ca/

and the La Ronge office.

Normand, C. (2014): Rare Earths in Saskatchewan: Mineralization Types, Settings, and Distributions; Saskatchewan Ministry of the Economy, Sask. Geological Survey, Rep. 264, 105p.

Technical editing and desktop publishing:
R.F. Davie, RnD Technical

Released August 2014
Saskatchewan Geological Survey

Foreword

The occurrence of rare earth element (REE) mineralization was first documented in Saskatchewan in the 1950s following the discovery of widespread allanite-rich veins in the Hoidas Lake–Nisikkatch Lake area. Interest was raised again in the late 1960s when monazite mineralization was noted in the Archie Lake area, but the evaluation of these occurrences remained stagnant until the 2000s when the importance of REE as an essential component in specialized technologies began to be recognized. The demand for REE was exacerbated by diminishing export quotas imposed by China, the country that currently supplies more than 90% of the world's REE. The majority of Saskatchewan remains underexplored for REE mineralization, and currently the only primary REE deposit with defined resources is the JAK zone at Hoidas Lake.

Data in this report are a combination of industry securities filings, press releases, assessment files, and Saskatchewan Geological Survey field data collection. References to historical reserves, resources, grades, or tonnages, except for the JAK zone, may not be compliant with NI 43-101 or Canadian Institute of Mining, Metallurgy and Petroleum standards of reporting.

This report contains previously unpublished information and is a comprehensive review of the current state of knowledge of Saskatchewan's REE occurrences and deposits, and should provide a valuable tool for anyone exploring for or studying REE in the province.

Gary Delaney, *Ph.D., P.Geo.*
Chief Geologist
Saskatchewan Geological Survey
Minerals, Lands, and Resource Policy Division
Saskatchewan Ministry of the Economy

February 2014

Executive Summary

Three hundred and fourteen georeferenced spot rare earth element (REE) mineral locations, bedrock geochemical anomalies, occurrences, and prospects were compiled from literature. The REE at these locations may be the principal or a secondary commodity.

Mineralization containing significant REE concentrations in Saskatchewan can be subdivided into three broad categories based on the percentage ratio of the total heavy REE (THREE) and Y to that of the total REE (TREE). These categories are: 1) mineralization in which REE are the principal commodity and in which the percentage of the (THREE+Y)/TREE ratio is less than, or equal to, 20, including monazite-dominant and allanite+apatite–dominant types; 2) U-rich mineralization in which REE are a secondary, but important commodity and the percentage of the (THREE+Y)/TREE ratio is greater than 20, including intrusion-associated, vein-type, and unconformity-related types; and 3) mineralization in which REE are the principal commodity and the percentage of the (THREE+Y)/TREE ratio is greater than 90, mainly sandstone-hosted, diagenetic-hydrothermal xenotime types. Mineralization in category 1 is hosted entirely by high-grade metamorphic rocks older than *ca.* 1.75 Ga. Monazite-dominant types are generally hosted by paragneiss and allanite+apatite–dominant types by orthogneiss. Intrusion-associated and vein-type, low-grade U mineralization (category 2) occur in a wide variety of >1.75 Ga metamorphosed rock types. Unconformity-related U (category 2) and sandstone-hosted diagenetic-hydrothermal xenotime (category 3) mineralization are mostly restricted in their occurrence to the Athabasca Basin.

No REE have been produced in the past or are currently being produced in the Province of Saskatchewan. Resource estimates, however, are available for three deposits. The first deposit for which a resource estimate was made available is the MAW REE zone, a sandstone-hosted diagenetic-hydrothermal xenotime occurrence in the Wheeler River area of the Athabasca Basin. This subeconomic resource, evaluated in the mid-1980s prior to the standards of disclosure for mineral projects in Canada provided by National Instrument 43-101 (NI 43-101; Canadian Securities Administrators, 2011), is estimated to contain 462 664 t grading 0.21 wt. % Y_2O_3. The most important resource estimate published for a deposit in Saskatchewan is for the allanite+apatite–dominant Hoidas Lake deposit of alkaline affinity. An NI 43-101–compliant, combined Measured and Indicated Resource estimate of 2 560 835 t grading 2.027 wt. % TREE was established for the deposit in 2009. Rare earth elements as a secondary commodity were identified in intrusion-associated U mineralization known as the Fraser Lakes zone B, located in the Wollaston Domain approximately 50 km east of Key Lake. An NI 43-101–compliant Inferred Resource estimate of 10 354 926 t grading 0.03 wt. % U_3O_8 and 0.003, 0.006, 0.001, and 0.007 wt. % La_2O_3, Ce_2O_3, Yb_2O_3, and Y_2O_3, respectively, was announced for the deposit in 2012.

During the past six years, interest in REE by exploration companies has focussed on the potential value-added secondary REE commodity associated with U mineralization outside the Athabasca Basin, and on HREE-rich sandstone-hosted xenotime mineralization in the Athabasca Basin. Although HREE, Y, and Sc are known to be present in anomalous concentrations in unconformity-related U deposits, no published NI 43-101–compliant Resource estimate exists for these. It is estimated, approximately, that more than 4 000 to 10 000 t THREE+Y and 190 to 470 t Sc are (were) contained in the ensemble of the unconformity-related U deposits of the Athabasca Basin. Other types of deposits that may contain valuable and recoverable REE, and to date are untested, include kaolin deposits such as those in the Whitemud Formation of southern Saskatchewan. Apatite mineralization in the Athabasca Basin offers attractive exploration targets for xenotime. Such apatite mineralization may have acted as reactive horizons favourable for deposition of xenotime from HREE+Y–rich fluids, particularly where strongly fractured zones occur.

Acknowledgements

The information presented in this report benefited from material obtained from, or informative and inspiring discussions with, Jeanette, Alan Anderson, Kevin Ansdell, Ken Ashton, Don Baker, Scott Bell, Robert Berman, Raymond Bernatchez, Sean Bosman, Jarrod Brown, Colin Card, Jim Clark, Tom Drivas, Andy DuFrane, Kimberley Halpin, Charles Harper, Alex Knox, Robert Martin, Christine McKechnie, Michelle McKeough, Artas Migdisov, Ryan Morelli, Deirdre O'Donohoe, Yuanming Pan, David Quirt, Murray Rogers, Karl Schimann, Vlad Sopuck, and Anthony (Willy) Williams-Jones.

Part of the information included in this report was obtained from fieldwork undertaken in the course of four summer seasons, during which the author was ably assisted by Devin Anderson, Kyle Blazek, Dillon Johnstone, Travis Legault, Andrew Masurat, Mark Matthews, Brian McEwan, and Andrew Smith, and gained from the support of Ken Ashton, Gary Delaney, Bernadette Knox, and John Pearson.

Thomas Love, Bill Slimmon, and Dustin Zmetana provided invaluable support in GIS and all matters computer related. Tom Bonli aided in obtaining electron microprobe data at the University of Saskatchewan. Advice and encouragement by Jason Berenyi and Gary Delaney helped in bringing this study to completion.

Reviews of the original manuscript by Murray Rogers and Anthony E. Williams-Jones, and editorial handling helped to greatly improve the quality of this report.

Contents

Figures

Tables

Introduction

Exploration for rare earth elements (REE) in Saskatchewan intensified significantly following a sharp increase in demand and price for these metals in the early 2000s and cutbacks in export quotas from China, which is by far the world's leading producer of these metals. Consequently, the development of a comprehensive database of the locations, ore deposit models, and exploration tools for REE mineralization in Saskatchewan is required.

This report is part of an ongoing research project aimed at evaluating the REE resources and potential for new discoveries in the Province of Saskatchewan. It updates the most extensive past compilation reports published on the subject by Harper (1987) and MacDougall (2002), the map of Gent *et al.* (1995), the Saskatchewan Geological Survey metallogenic map series, and the Saskatchewan Mineral Deposit Index (SMDI). The present report contains a compilation of 314 georeferenced spot locations where anomalous concentrations of REE, as evidenced by bulk rock geochemical analyses and presence of REE-bearing minerals, have been reported. Detailed descriptions are provided for the most interesting mineralization for which sufficient information is available.

According to the International Union of Pure and Applied Chemistry (IUPAC), the REE comprise the fifteen Group 3 lanthanide elements, yttrium (Y), and scandium (Sc). The lanthanide elements are, in increasing order of atomic mass, lanthanum (La), cerium (Ce), praseodymium (Pr), neodymium (Nd), promethium (Pm)[1], samarium (Sm), europium (Eu), gadolinium (Gd), terbium (Tb), dysprosium (Dy), holmium (Ho), erbium (Er), thulium (Tm), ytterbium (Yb), and lutetium (Lu). The lanthanides are often subdivided into light REE (LREE), comprising La, Ce, Pr, Nd, and Sm, and heavy REE (HREE), comprising Eu, Gd, Tb, Dy, Ho, Er, Tm, Yb, and Lu. This subdivision of REE into LREE and HREE has been adopted in this report. Values for the average abundances of combined LREE and combined HREE in the upper continental crust, given by Rudnick and Gao (2003), are 133 ppm and 15 ppm, respectively. Ce is 63 times more abundant than Eu, 90 times more abundant than Tb, and 210 times more abundant than Tm.

The LREE are widely used in a variety of applications ranging from polishing powders to the fabrication of automotive catalytic converters to the production of strong permanent magnets. Similarly, the much rarer and more valuable HREE (*e.g.*, 99.99% Eu oxide selling for US$2150 per kg vs. 99.5% Ce oxide selling for US$12 per kg; HEFA Rare Earth Canada Co. Ltd., URL <http://www.baotou-rareearth.com/>, 31 Dec 2012) have wide applications, such as in the fabrication of specialized glasses and in the stabilization of performance of permanent magnets at elevated temperatures (Gupta and Krishnamurthy, 2005; Walters and Lusty, 2010). It is estimated that demand for LREE will be satisfied for the long term due to the existence of very large resources in many parts of the world. Economic resources of the more valuable HREE are, however, much less abundant and concerns about the ability of the industry to satisfy forecasted demand in the future have been widely expressed in the press.

There are presently no mines producing REE in Saskatchewan and none have produced this commodity in the past. There are, however, several active projects in the province where at least two companies are involved primarily in exploration for REE: the Hoidas Lake allanite-apatite deposit (Great Western Minerals Group Ltd., 2009) and the Archie Lake monazite *occurrence*[2] (Quantum Rare Earth Developments Corp., 2010, 2011). Recent analyses of individual grab samples from the Archie Lake and two other undeveloped monazite occurrences (Alces Lake and Kulyk Lake) returned grades comparable to those encountered in the world-class Steenkampskraal deposit, South Africa (Andreoli *et al.*, 2006; Hancox and Jones, 2012; Great Western Minerals Group Ltd., 2012). However, the REE grades in, and vertical and lateral extents of, these monazite occurrences remain to be determined.

Several U exploration companies, notably CanAlaska Uranium Ltd., Eagle Plains Resources Ltd., and JNR Resources Inc. (acquired by Denison Mines Corp. in 2013), have taken advantage of the increased interest in REE during the last five years or so, and have shown that most of the U occurrences on their properties contain anomalous REE concentrations. This suggests that virtually all untested U (and Th) deposits, prospects or occurrences in Saskatchewan may be considered as having REE potential, especially HREE. Recent work has shown that REE-enriched, U-rich or U-poor mineralization in the Wollaston Domain are hosted by a wide variety of rock types, reflecting a number of complex fluid, melt, and rock interaction processes for their origin, including liquid immiscibility (Watkinson and Mainwaring, 1976; McKeough and Lentz, 2011; McKeough *et al.*, 2011a, 2011b), hybridization (McKeough and Lentz, 2011; McKeough *et al.*, 2013), intrusion-associated calcic and alkalic metasomatism (Kremer *et al.*, 2010, 2011; Mercadier *et al.*, 2012), and, in part, inheritance of detrital or

[1] All Pm isotopes are radioactive and have short half-lives. This metal is practically nonexistent in the Earth's crust, so it is not considered in this report.
[2] Use of italics indicates that it conforms to the classification scheme of Rogers and Hart (1995).

authigenic material (McKechnie *et al.*, 2012b; McFarlane and McKeough, 2013a). Also of importance, the richest unconformity-associated U deposits in the Athabasca Basin contain appreciable HREE concentrations and, in some cases, Sc (*e.g.*, up to ~1000 ppm Dy and greater than 600 ppm Sc at the McArthur River mine; Saskatchewan Ministry of the Economy (SME) Assessment File[3] 74H-0048), and may represent an important source of HREE and Sc in the future.

As mentioned above, no current or past mines have produced REE in the province of Saskatchewan. Likewise, REE reserves for these metals have not been established for any deposit. Data on REE resources are, however, available for three deposits. The earliest resource determination, which predates the introduction of NI 43-101–compliant regulations, was provided by Union Oil Company of Canada Inc. for the "Wheeler River Yttrium Prospect" (Knox, 1985, 1986), also known as the "MAW REE zone" xenotime deposit (MacDougall, 1990; Quirt et al, 1991; Hanly, 2001; SMDI[4] #2160), located in the Athabasca Basin. Total drill-indicated and possible resources of 462 664 t (510,000 short tons) grading 0.21% Y_2O_3 (0.1% cutoff) were estimated (Knox, 1985, 1986) for this deposit.

The project that has seen the most development to date is being conducted by Great Western Minerals Group Ltd. at Hoidas Lake, near the extreme northeastern corner of the province. Total Measured and Indicated Resources for the JAK zone are 2 560 835 t grading 2.027% TREE (1.5% cutoff) and the deposit is noted for its high concentration of Nd (Barr Engineering Company, 2009; Great Western Minerals Group Ltd., 2009). More recently, resources have been published for a U-REE project developed in the Fraser Lakes area, located in the Wollaston Domain approximately 50 km east of Key Lake, by JNR Resources Inc. The Fraser Lakes zone B is estimated to contain an Inferred Resource of 10 354 926 t grading 0.03% U_3O_8, 0.003% La_2O_3, 0.006% Ce_2O_3, 0.007% Y_2O_3, and 0.001% Yb_2O_3 (0.01% U_3O_8 cutoff; Armitage and Sexton, 2012). Resource estimates for these three deposits are compiled in Table 1.

Table 1 – REE resource estimates for the Fraser Lakes zone B, Hoidas Lake JAK zone, and MAW REE zone deposits.

Deposit	Fraser Lakes	Hoidas Lake				MAW
Zone	B	JAK				REE
Company holding ground as of February 2014	Denison Mines Corp.	Great Western Minerals Group Ltd.				Denison Mines Corp.
Cut-off grade	0.01% U_3O_8	1.5% TREE				0.1% Y_2O_3
Resource category	Inferred	Measured[1]	Indicated[1]	Total Measured + Indicated[1]	Inferred[1]	Indicated
Tonnes	10 354 926	963 808	1 597 027	2 560 835	286 596	462 664
TREE (%)	n. r.	2.142	1.958	2.027	1.784	n. r.
La_2O_3 (%)	0.003	0.520	0.483	n. r.	0.441	n. r.
Ce_2O_3 (%)	0.006	1.138	1.046	n. r.	0.953	n. r.
Pr_2O_3 (%)	n. r.	0.149	0.136	n. r.	0.119	n. r.
Nd_2O_3 (%)	n. r.	0.537	0.478	n. r.	0.427	n. r.
Sm_2O_3 (%)	n. r.	0.070	0.064	n. r.	0.061	n. r.
Eu_2O_3 (%)	n. r.	0.014	0.013	n. r.	0.012	n. r.
Gd_2O_3 (%)	n. r.	0.032	0.029	n. r.	0.029	n. r.
Tb_2O_3 (%)	n. r.	0.003	0.002	n. r.	0.002	n. r.
Dy_2O_3 (%)	n. r.	0.009	0.008	n. r.	0.008	n. r.
Y_2O_3 (%)	0.007	0.029	0.028	n. r.	0.029	0.210
Er_2O_3 (%)	n. r.	0.006	0.006	n. r.	0.006	n. r.
Yb_2O_3 (%)	0.001	0.001	0.001	n. r.	0.001	n. r.
U_3O_8 (%)	0.030	n. r.	n. r.	n. r.	n. r.	n. r.
NI 43-101 compliant?	Yes	Yes				No
Source of data	Armitage and Sexton (2012)	Barr Engineering Company (2009)				Knox (1985, 1986)
Company involved in resource assessment	JNR Resources Inc.	Great Western Minerals Group Ltd.				Union Oil Company of Canada Ltd.

[1] Ordinary kriging interpolated Resource estimate.

Abbreviations: n. r., not reported.

Values for individual REE oxide grades in the JAK zone were obtained by converting values for REE metal grades reported in Barr Engineering Company (2009, Table 18).

[3] Saskatchewan Ministry of the Economy (SME) assessment files can be consulted at http://www.smad.gov.sk.ca.
[4] Saskatchewan Mineral Deposit Index (SMDI) can be consulted at http://www.economy.gov.sk.ca/SMDI.

The wide variety of mineralization in which REE occur in Saskatchewan is discussed in detail in the "Classification of Saskatchewan REE Mineralization" section of this report. For the present work, the discussion relies heavily on published bulk-rock geochemical analyses, which were obtained at different times and from different laboratories using different sample digestion and analysis methods. Only data obtained from total sample digestion were considered.

General Considerations

The subdivision of the REE into LREE and HREE discussed in the "Introduction" did not include Sc and Y. Although Y is lighter than La (88.9 grams/mole vs. 138.9 grams/mole), it is often grouped with the HREE because its effective ionic radius (and therefore its size) is comparable to that of the heavier trivalent lanthanides in similarly co-ordinated crystallographic sites (VIII-fold) of HREE-rich minerals such as xenotime and uraninite (Smyth *et al.*, 2000; Boatner, 2002).

Sc is the lightest of the REE (44.96 grams/mole) and also has the smallest effective ionic radius (in VI-fold co-ordination, Sc^{3+} 74.5 picometres (pm), Y^{3+} 104 pm, La^{3+} 117 pm, Lu^{3+} 100 pm; Shannon, 1976). In the upper Earth's crust, Sc most commonly substitutes for Al^{3+} and Fe^{3+} in minerals, which explains its tendency to be dispersed as a trace constituent in rocks (Raade *et al.*, 2002). The concentration of Sc in minerals rarely exceeds 1000 ppm. There are ~16 minerals that contain essential Sc, but most are extremely rare. Nevertheless, exceptional Sc enrichment has been documented in residual deposits resulting from weathering of mafic-ultramafic rocks (Van Huet *et al.*, 2010), and the element can occur in significant concentrations in U deposits (Tarkhanov *et al.*, 1992; Naumov, 2008). Some Al phosphate-sulphate (APS) minerals of the alunite supergroup (Bayliss *et al.*, 2010) are also reported to contain significant Sc (Frondel *et al.*, 1968; Shubat, 1988). Although Sc may be enriched in certain minerals that also contain an abundance of the other REE, significant differences in its geochemical behaviour in magmatic and hydrothermal systems (*e.g.*, solid-liquid partition coefficients) justify separate treatment of this REE.

The REE are generally present in minerals in the trivalent state. Under appropriate redox conditions, however, Eu and Ce may occur predominantly in the divalent or tetravalent state, respectively. Divalent Eu is well known to partition into plagioclase that crystallized from magma (Weill and Drake, 1973) and Ce^{4+} into Mn hydroxide nodules formed on the seafloor (Corliss *et al.*, 1978) and into hydrothermal zircon (Hoskin and Schaltegger, 2003).

The REE tend to be dispersed in rocks, occurring in trace amounts in a wide variety of minerals, and are difficult to separate. For this reason, it was thought that they were rare. However, as is now well known, the REE, and particularly the LREE, are not rare (Muecke and Moeller, 1988). According to data presented in Rudnick and Gao (2003), Ce and Zn have similar abundances in the upper continental crust (63 and 67 ppm, respectively). On the other hand, HREE are much rarer and more valuable, Lu and Tm being present in concentrations of ~0.3 ppm and occupying an intermediate position between Sb (0.4 ppm) and Bi (0.16 ppm) in abundance. The concentration of Sc in the upper continental crust averages 14 ppm (Rudnick and Gao, 2003), intermediate between those of Pb (17 ppm) and Nb (12 ppm).

Mineralogy is of major importance in evaluating REE mineralization. Some minerals are enriched in LREE, others in HREE, and still others may contain the full range of REE in various relative proportions. Some, such as monazite and bastnäsite, are easily amenable to metallurgical processing and REE separation, whereas other, more chemically complex or refractory minerals require complicated and costly processing (Gupta and Krishnamurthy, 2005). REE minerals also provide clues on the origin of the mineralization that host them and may contain elements that can be detected by geophysical methods (*e.g.*, U and Th). At present, well over 300 mineral species that contain essential REE have been approved by the International Mineralogical Association (IMA), and a large number of others may contain minor to major REE proportions (*e.g.*, apatite and titanite).

REE minerals recognized from Saskatchewan mineralization include monazite (LREE), allanite (LREE), cheralite (LREE), xenotime (HREE), and rare chevkinite (LREE) and bastnäsite (LREE). Euxenite-polycrase (LREE and HREE) and fergusonite (HREE) are also reported to occur at a few localities. Other important REE-bearing minerals that, where present in appreciable amounts, can contribute significantly to the total REE content of mineralization, include apatite (LREE and HREE), titanite (LREE and HREE), uraninite-thorianite and pitchblende (LREE and HREE), thorite (LREE and HREE), brannerite (LREE and HREE), coffinite and secondary U minerals (LREE and HREE), and solid solutions among various APS minerals of the alunite supergroup (LREE).

Among the REE-bearing minerals listed above, monazite, allanite, apatite, uraninite-thorianite, thorite and pitchblende, and xenotime are the main REE minerals in Saskatchewan mineralization. Commonly, only one or two of these minerals control the bulk of the REE contained at any given location. The most prevalent associations are monazite (locally +thorite+allanite+xenotime), allanite+apatite, uraninite-thorianite+thorite+allanite, uraninite and/or pitchblende, and xenotime. These associations characterize different types of mineralization that originated from a variety of ore-forming processes and form the basis for the classification of REE mineralization presented in this report.

Classification of Saskatchewan REE Mineralization

REE mineralization in Saskatchewan can be classified according to its bulk REE distribution and REE-bearing minerals present, and level of enrichment in U with respect to Th. In view of this, the mineralization was subdivided into three broad categories:

1) mineralization in which the LREE (Sc is treated separately and Y is treated with the HREE), and allanite+apatite or monazite, predominate (THREE+Y ≤20% of TREE), and which are characterized by U/Th ratios <1 (min 0.001, max 10, mean 0.439, median 0.089, n = 390; Figures 1 and 2);
2) U-enriched, intrusion-associated (median U/Th 1.15, n = 27), vein-type (median U/Th 818, n = 29) or unconformity-related U (median U/Th 229, n = 320), mixed REE mineralization in which THREE+Y (±Sc) account for more than 20% of the total of the contained REE (median 60.8%, n = 441; Figures 1 and 2), and in which REE mineralogy is complex; and
3) mineralization in which HREE+Y represents more than 90% of the total of the contained REE and in which REE mineralogy is essentially represented by xenotime; limited data show U/Th ratios ranging between 1.1 and 73.7 (median 4, n = 25; Figures 1 and 2); the presence of variable proportions of APS minerals may result in a decrease in the percentage of (HREE+Y)/TREE to below 90.

The mineralization types were further assigned to five categories, mainly according to REE grade; the REE grade, in many cases, may be represented by only a limited number of surface grab samples. In most cases, other metals were

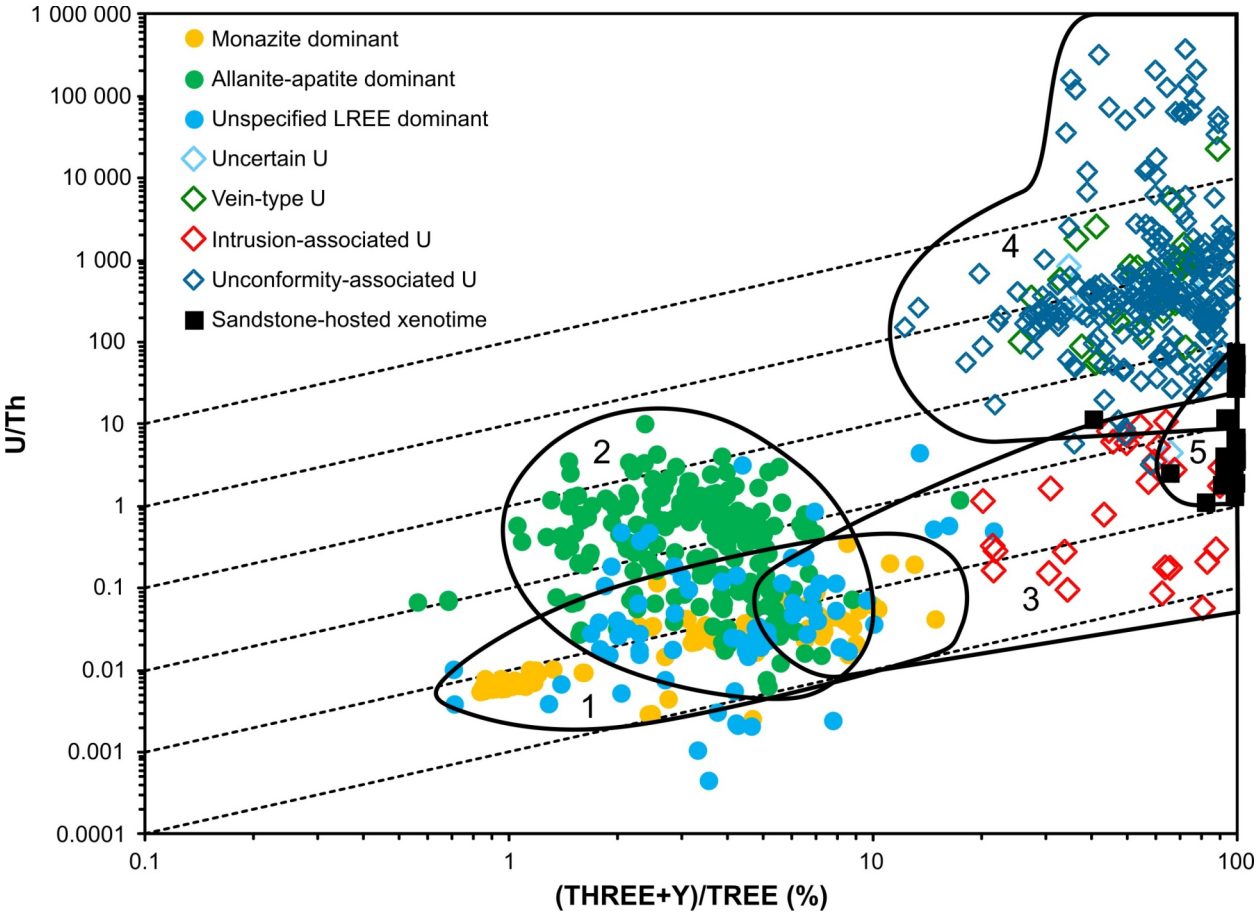

Figure 1 – Log-log plot of the relationship between U/Th and the proportion of THREE+Y relative to TREE for REE-bearing mineralization in Saskatchewan. Filled circles represent LREE-dominant mineralization in which the percentage of (THREE+Y)/TREE is ≤20. Open diamond symbols represent various types of U-rich mineralization. Black squares represent sandstone-hosted xenotime mineralization. Roughly hand-contoured fields labelled 1, 2, 3, 4, and 5 correspond to monazite-dominant, allanite+apatite–dominant, intrusion-associated U, unconformity-associated and vein-type U, and sandstone-hosted xenotime mineralization, respectively.

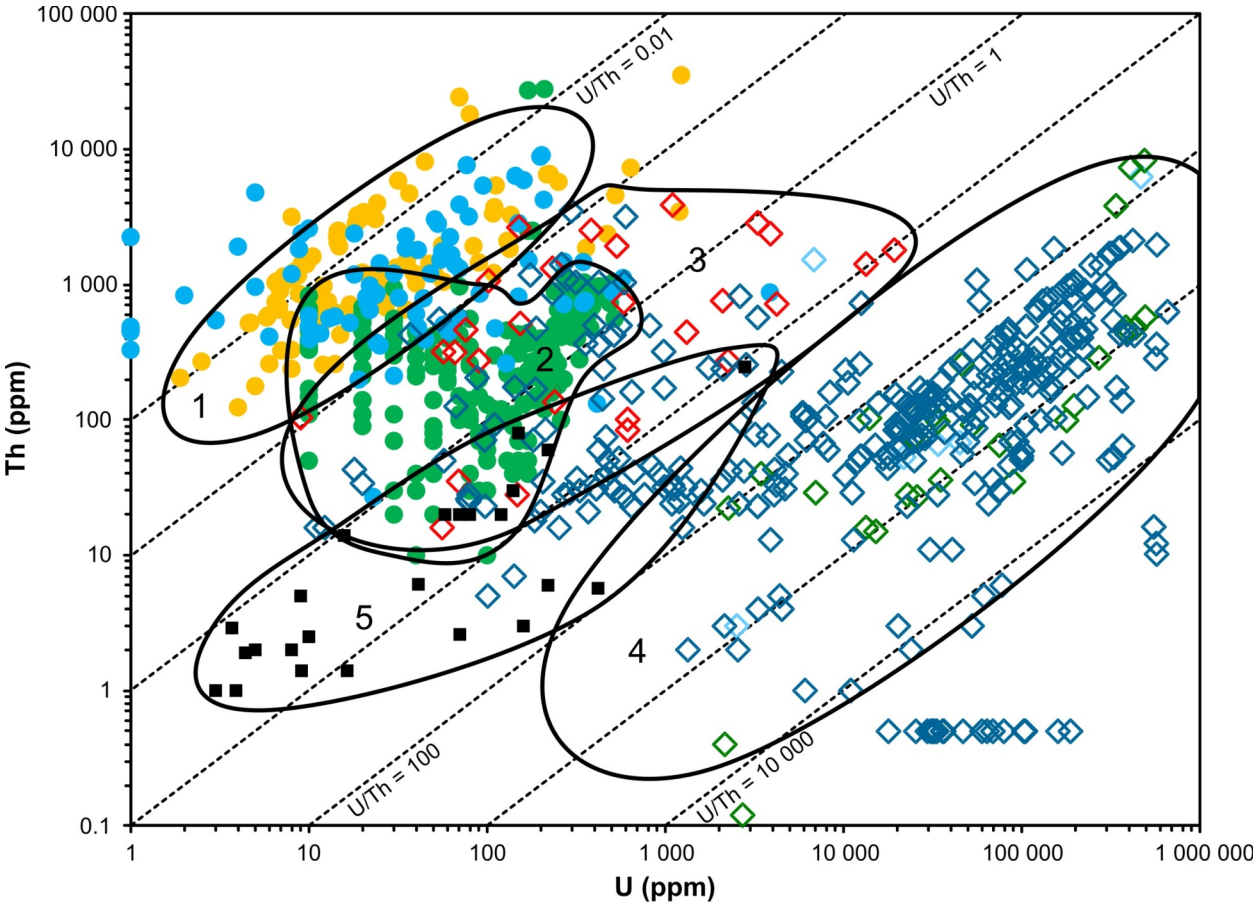

Figure 2 – Log-log plot of the relationship between U and Th concentrations in REE-bearing mineralization in Saskatchewan. Data symbols and fields are the same as in Figure 1. The proportion of THREE+Y relative to TREE in the mineralization generally increases from left to right (with the exception of sandstone-hosted xenotime mineralization, which contains the highest proportion of THREE+Y. Sc enrichment is also associated with the mineralization showing the highest U/Th signature. The mineralization types considered and the sources of data used in Figures 1 and 2 can be found in Tables 3 to 10, and 13.

not taken into account. The categories represent a partial, condensed, and highly simplified version of the qualitative mineral potential evaluation procedures presented in Rogers and Hart (1995). Following the recommendations of Rogers and Hart (1995), minimum total rare earth oxide (TREO) grade requirements of 0.50%[5], or 1% monazite equivalent, for occurrences and prospects, and half that value[6] for a bedrock geochemical anomaly, were selected.

For THREE+Y, severe limits were imposed on concentrations obtained from bulk-rock geochemical data to establish minimum grade requirements for each category. In most advanced REE projects throughout the world, where deposits are enriched in THREE+Y, the combined concentration of these metals in resource assessments varies between ~1000 ppm (*e.g.*, Zeus, Canada; Saucier *et al.*, 2012) and ~4300 ppm (*e.g.*, Lofdal, Namibia; Siegfried and Hall, 2012). An estimated market value for xenotime of approximately five times that of monazite per kilogram of mineral was calculated based on current FOB prices (China) for individual REO (>99% purity). For this reason, the minimum grade requirement for THREE+Y for occurrences and prospects was set at 1000 ppm, and that for a bedrock geochemical anomaly at 500 ppm. The simplified categories and their minimum grade requirements adopted in this report are as follows:

1) ***bedrock REE geochemical anomaly***, where at least one sample returned TREE concentrations of ≥0.25 and <0.50%, or THREE+Y concentrations of ≥0.05 and <0.10%.

[5] 1% monazite equivalent is roughly equivalent to 0.45% TREE, which was rounded off for the purpose of this report to 0.50% TREE.
[6] 0.25% TREE.

2) ***REE occurrence***, where at least one sample returned TREE concentrations of ≥0.50%, or THREE+Y concentrations of ≥0.10%.
3) ***REE prospect***, where at least three drill-hole intersections meet grade requirements for an REE occurrence over a minimum width of 1 m. For steeply dipping bodies, vertical extension of outcropping mineralization is proven to a depth of at least greater than 20 m.
4) ***developed REE prospect without resources or reserves***, where "mineralization is present in three dimensions as defined by a delineation drill/exploration program. Mineralization is present for a significant distance along strike and down-dip, with numerous intersections that meet or exceed the minimum grade-width standard" (Rogers, pers. comm., 2012) of ≥0.50% TREE per metre or ≥0.10% THREE+Y per metre. "Reserve-resource figures have not been published or the published reserves-resources do not meet the minimum grade-tonnage standard" (100 000 t at 1.0% REO; Rogers, pers. comm., 2012).
5) ***developed REE prospect with resources and/or reserves***, where "mineralization is present in three dimensions as defined by a delineation drill/exploration program. Mineralization is present for a significant distance along strike and down-dip, with numerous intersections that meet or exceed the minimum grade-width standard" (Rogers, pers. comm., 2012) of ≥0.50% TREE per metre or ≥0.10% THREE+Y per metre. "Published reserves-resources meet or exceed the minimum grade-tonnage standard" (100 000 t at 1.0% REO; Rogers, pers. comm., 2012).

The classification scheme necessarily echoes the REE mineralogy, which may be simple (*i.e.*, the REE are essentially contained in one mineral) or complex (*i.e.*, two or more minerals contain the bulk of the REE). Data on REE prospects, occurrences, bedrock geochemical anomalies, and mineral locations in Saskatchewan are presented in tables and figures in appropriate sections of this report. Although no economic potential has been demonstrated for mineral locations, the literature still provides valuable descriptions and chemical data that can be used, for example, for radiometric characterization and reference localities for future dating purposes. Data for the various classes of mineralization were compiled from the SMDI, exploration and mining company reports (SME assessment files, NI 43-101 reports through SEDAR[7] or company websites) and corporate news releases, Saskatchewan Geological Survey reports, and peer-reviewed papers in scientific journals.

Many of the common REE-rich minerals (*e.g.*, monazite, allanite, and xenotime) contain appreciable concentrations of Th and/or U. Similarly, most U- and Th-rich minerals (*e.g.*, uraninite-thorianite, uraninite, pitchblende, thorite) contain REE. Consequently, most of the REE mineralization in Saskatchewan was discovered by the examination of airborne and ground radiometric anomalies during U exploration. Until recently, however, Th-rich anomalies were not considered beneficial targets for the discovery of economic U mineralization. Anomalies characterized by elevated U/Th ratios, generally >1, have systematically been favoured and the potential of Th to predict the occurrence of REE mineralization was overlooked. Detailed exploration work and REE geochemical analyses made available in the past decade by exploration companies, however, have revealed that Th-rich occurrences are generally also rich in REE (most commonly in the LREE) at the margin of Archean inliers in the Wollaston Domain, particularly in the Foster lakes (Upper Foster Lake, Middle Foster Lake, and Lower Foster Lake) and Karin Lake areas (McKeough *et al.*, 2010; McKeough and Lentz, 2011; McKeough *et al.*, 2011a, 2011b; McKeough *et al.*, 2013; McFarlane and McKeough, 2013b) and the southeastern Fraser Lakes area (McKechnie *et al.*, 2012a, 2012b).

Exploration efforts for REE deposits throughout the world are currently focussed on the search for mineralization associated with alkaline rocks. Carbonatite-associated mineralization hosts the majority of the LREE resources in bastnäsite and other LREE carbonates (*e.g.*, Mountain Pass, California; Bear Lodge, Wyoming; Montviel, Quebec; Sarfartoq, Greenland; Mount Weld, Australia; Wigu Hill, Tanzania; Zandkopsdrift, South Africa). Peralkaline (alkalinity index (AI) >1), silica-saturated (*e.g.*, Strange Lake, Quebec-Labrador; Bokan Mountain, Alaska) and silica-undersaturated (*e.g.*, Ilimaussaq, Greenland; Thor Lake, Northwest Territories; Red Wine, Quebec; Norra Karr, Sweden) rocks having a variable feldspathoid silica-saturation index (FSSI; Frost and Frost, 2008) contain the most sought after HREE-rich resources, which are hosted by a wide variety of rare minerals, such as those of the eudialyte group (Johnsen *et al.*, 2003).

Peralkaline rocks are uncommon in Saskatchewan, only having been reported, albeit as minor occurrences, from Hoidas Lake (Halpin, 2010). Nepheline-sodalite syenite occurs at Lyle Lake, but the chemistry of the rocks shows a miaskitic (AI <1) signature (Quirt, 1992). Miaskitic alkaline rocks rarely contain economic REE deposits, although peralkaline or agpaitic varieties, as well as carbonatites and zones of fenitized wallrock that may contain economic

[7] System for Electronic Document Analysis and Retrieval maintained by Canadian Securities Administrators at http://www.sedar.com/search/search_form_pc_en.htm (accessed 20 Jan 2014).

REE concentrations, locally occur associated with them. Large-tonnage, low-grade, low-Th, HREE-enriched, ion-adsorption clay deposits or other deposits believed to have originated partly from such processes, which can be mined at low cost, also attract considerable attention (*e.g.*, Grande Vallée property of Orbite Aluminae Inc., Gaspésie, Quebec (Doran *et al.*, 2012); Stromberg prospect of TUC Resources Ltd, Northern Territory, Australia). The REE concentration of large residual clay deposits in Saskatchewan, such as those in the Whitemud Formation, remains essentially unknown.

Although there has been no commercial REE production to date in Saskatchewan, available data indicate that the unconformity-related U and sandstone-hosted xenotime deposits show the greatest potential for developing economic, high-value, HREE-enriched resources. Uraninite in the unconformity-related U deposits of the Athabasca Basin can contain up to ~4 wt. % TREE, of which up to 99% is HREE+Y.

LREE-Dominant Mineralization (THREE+Y ≤20% of TREE)

The most significant LREE-dominant mineralization in Saskatchewan is generally characterized by U/Th ratios <1 (chemical and radiometric) and can be further divided into those where monazite is the predominant, or an important, REE mineral (Tables 2 and 3; Figure 3) and those where allanite and apatite are the predominant REE minerals (Table 4; Figure 4). Other paragenetic types of LREE-dominant mineralization probably occur, but critical mineralogical information is lacking for a large proportion of these (Table 5; Figure 5).

Mineralization of simple REE mineralogy, in which monazite is the dominant REE mineral, occurs in close spatial association with clastic sedimentary rocks that have been metamorphosed to the upper amphibolite or granulite facies and subjected to some level of partial melting. Mineralization of more complex REE mineralogy, in which allanite is one of the predominant minerals, is generally hosted by granitoid rocks. Monazite is a common rock-forming mineral, occurring as a minor to trace constituent in virtually every rock type present in northern Saskatchewan. Localities where monazite is reported to occur, at least locally, in proportions exceeding 10% by volume are not numerous and include Alces Lake (SMDI #1283 and #1453; locations 3 to 6, Table 3), Archie Lake (SMDI #1552; location 21, Table 3), and Oldman River (SMDI #1332; location 7, Table 3) in the Beaverlodge Domain, and Kulyk Lake in the Wollaston Domain (SMDI #0985; location 74, Table 3). Locations of monazite-dominant mineralization for which at least one sample analysis returned TREE concentrations >0.25 wt. % are shown in Figure 3. All monazite locations in Saskatchewan are enriched in Th (Th/TREE averaging ~0.18) and, as expected, present elevated La_N/Yb_N[8] signatures (averaging ~275). They usually show low Eu/Eu*[9] values (<0.2), with the exception of the Kulyk Lake occurrence (location 74, Table 3), where values of ~0.6 are calculated from monazite-rich bulk-rock geochemical data (consistent with SPI Supplies Kulyk Lake electron microprobe monazite standard AS1240-AB, for which Eu/Eu* is 0.5).

LREE minerals of the monazite group have among the highest contents of REE. They typically contain >50 wt. % combined REE oxides, have been used as a primary source of REE for nearly 100 years, and their metallurgy is well known (Gupta and Krishnamurthy, 2005). Monazite-group minerals comprise five IMA-approved monoclinic orthophosphate species with the general formula $X(P,Si,S)O_4$, where major cations in IX-fold co-ordinated *X* sites (Boatner, 2002) are predominantly the LREE Ce, La, Nd, Pr and Sm (some varieties relatively rich in Eu and Gd also exist), and Ca and Th. The species include cheralite ($CaTh(PO_4)_2$), monazite-(Ce)[10], monazite-(La), monazite-(Nd), and monazite-(Sm). Monazite-(Ce) is by far the most common species (Spear and Pyle, 2002), followed by, and not necessarily in order, monazite-(La) and monazite-(Nd). Monazite-(Sm) is very rare (Masau *et al.*, 2002). Concentrations of Y and HREE in monazite depend on temperature, the bulk composition of the system considered, the presence and composition (substitution exchange vectors; also dependent on T, P, and bulk system composition) of other phases into which Y and HREE can partition (*e.g.*, garnet, titanite, apatite), and are limited by saturation with xenotime (Gratz and Heinrich, 1997; Pyle *et al.*, 2001; Mogilevsky, 2007; Spear and Pyle, 2010). An example of a deposit in which monazite is rich in Y and HREE is the Steenkampskraal deposit in South Africa, where the mineral contains up to 10 wt. % $Gd_2O_3+Dy_2O_3+Y_2O_3$ (Andreoli *et al.*, 1994).

Monazite that was formed at elevated temperatures usually contains significant Th. Solid solution can be extensive at elevated temperatures between the isostructural monazite-group minerals monazite ($LREEPO_4$) and cheralite ($CaTh(PO_4)_2$), and huttonite ($ThSiO_4$), according to the heterovalent exchange reactions $LREE^{3+} + P^{5+} \leftrightarrow Th^{4+} + Si^{4+}$ and $2LREE^{3+} \leftrightarrow Ca^{2+} + Th^{4+}$ (Linthout, 2007). Considering the monazite-dominant compositions (50 to

[8] Normalization values used throughout this report are for C1 chondrite from Anders and Grevesse (1989).
[9] Arithmetically calculated throughout this report as $Eu_N/(0.5 \times (Gd_N + Sm_N))$.
[10] See Bayliss and Levinson (1988) for notation of REE minerals.

Table 2 – Abbreviations and chemical formulas of minerals listed in Tables 3 to 6.

Mineral Name	Abbreviation	Chemical Formula[b]
Allanite	Aln[a]	$Ca(Ln^{d},Y,Ca)(Fe^{2+},Fe^{3+})Al_2(Si_2O_7)(SiO_4)O(OH)$[c]
Apatite	Ap[a]	$Ca_5(PO_4)_3(F,Cl,OH)$[e]
Barite	Brt[a]	$BaSO_4$
Bastnäsite	Bst	$(Ln,Y)CO_3F$
Bornite	Bn[a]	Cu_5FeS_4
Chalcopyrite	Ccp[a]	$CuFeS_2$
Cheralite	Che	$CaTh(PO_4)_2$[f]
Chevkinite	Cvk	$(Ln,Ca,Na,Th)_4(Fe^{2+},Mg)_2(Ti,Fe^{3+})_3Si_4O_{22}$
Coffinite	Cof	$U(SiO_4)_{1-x}(OH)_{4x}$
Euxenite-polychrase series	Eux-Pol	$(Y,Ca,Ln,Hln^{g},U,Th)(Nb,Ta,Ti)_2O_6$ - $(Y,Ca,Ln,Hln,U,Th)(Ti,Nb,Ta)_2O_6$
Fluorite	Fl[a]	CaF_2
Galena	Gn[a]	PbS
Goethite	Gth[a]	α-$Fe^{3+}O(OH)$
Gummite	Gum	Mixture of uranium oxides
Hyalophane	Hap	$(K,Ba)Al(Si,Al)_3O_8$
Hematite	Hem[a]	α-Fe_2O_3
Ilmenite	Ilm[a]	$Fe^{2+}TiO_3$
Ilmeno-hematite	Ilm-Hem	Ilmenite-hematite solid solution
Magnetite	Mag[a]	$Fe^{2+}Fe_2{}^{3+}O_4$
Molybdenite	Mol[a]	MoS_2
Monazite	Mnz[a]	$Ln\,PO_4$[h]
Pitchblende	Ptb	Massive, often botryoidal, pitchy form of uraninite
Pyrite	Py[a]	FeS_2
Pyrochlore-microlite series	Pcl[a]-Mrl	$(Ca,Na)_2Nb_2O_6(OH,F)$ - $(Ca,Na)_2Ta_2O_6(O,OH,F)$
Pyrrhotite	Po[a]	$Fe_{1-x}S$
Sphalerite	Sp[a]	ZnS
Thorianite	Thn	ThO_{2i}[i]
Thorite	Thr[a]	$(Th,U)SiO_4$
Titanite	Ttn[a]	$CaTiSiO_5$
Uraninite	Urn[a]	UO_2
Uranothorite	Utr	U-rich thorite
Xenotime	Xtm[a]	$(Y,Hln^{i})PO_4$
Zircon	Zrn[a]	$ZrSiO_4$

[a] From Whitney and Evans (2010).

[b] From Mandarino (1999). Exact species for REE minerals are generally unspecified and a modified, more general formula is provided. In those where light lanthanides predominate, the term *Ln* is employed. In those where heavy lanthanides predominate, the term *Hln* is employed.

[c] Modified from Ercit (2002).

[d] *Ln*: mostly Ce and La.

[e] Most commonly fluorapatite.

[f] From Linthout (2007). Forms a series with huttonite ($ThSiO_4$) and monazite, and can contain significant *Ln* and Si concentrations.

[g] *Hln*: mostly Dy, Er, and Gd or Yb.

[h] Forms a series with huttonite and cheralite, and can contain significant Th, Ca, and Si concentrations.

[i] Forms a series with uraninite. Thorianite, uraninite, and other Th- and/or U-rich minerals can contain appreciable REE concentrations.

Table 3 – LREE-dominant mineralization in which monazite is the principal REE mineral.

Location #	Name	Category	SMDI #	Location[1]				Mineralization type	Minerals[2]		References
				NTS Area	Easting	Northing	Domain		Main REE	Others	
1	Nadir Bay	Occurrence	none	74N/16	313080	6637556	Zemlak	Metamorphic-metasomatic	Mnz; minor to trace retrograde Aln, Ap	Minor Ilm, Py; trace Sp, Ccp, Mol	Normand (2010a, 2010b)
2	RA2010-13	Bedrock geochemical anomaly			309899	6635747			Mnz		Normand (2010a, 2010b)
3	Alces Lake	Occurrences	1283, 1336	74N/09	329243	6618116	Beaverlodge		Mnz; minor to trace retrograde Aln, Ap, REE carbonate	Py, Zrn; trace U-Th silicates, Urn, Gn	Normand (2010a, 2010b)
4					329249	6618249					
5					329233	6618141					
6		Bedrock geochemical anomaly			329275	6618415					
7	Oldman River	Occurrence	1332		327287	6611784			Mnz	Urn, iron oxides, Py	Robinson (1955); Normand (2011a, 2011b)
8	Nevins Lake	Occurrences	none	74O/12	340729	6600004			Mnz	Py	SME Assessment File 74O12-0049; Normand (2012, 2013).
9					340479	6600984					
10					340521	6600806					
11					340865	6600723					
12					340575	6600840					
13					340507	6600999					
14		Bedrock geochemical anomalies			340537	6600931					
15					340533	6600909					
16					340608	6600778					
17					340449	6601387					
18					340467	6601278					
19					340689	6599706					
20					340751	6599939					
21	Archie Lake	Occurrence	1552	74O/05	345193	6596848		Fossil placer	Mnz	Ilm, Zrn	Harper (1986); Smith and Cathro (2010); Normand (2011a, 2011b)
22	Schaffer Lake	Occurrence	none		344800	6596282		Intrusion-associated (some Mnz inherited)	Mnz (locally >1%; euhedral to 7 mm)		Normand (2011a, 2011b)
23	Nordbye Lake	Prospect	0653	64M/03	590226	6549908	Mudjatik (N)		Mnz; Aln and Xtm reported but not confirmed		MacDougall (2002); SME Assessment File 64M03-0011
24	Alexander Lake area	Occurrences	none	74H/02	518523	6337005	Wollaston				
25					516038	6335412					
26		Bedrock geochemical anomaly			514508	6335075					
27	Walker River area	Occurrences			500100	6322552					
28					509290	6332434					
29					503245	6326536					
30					503428	6325790					
31					500100	6322550					
32					504902	6332540					
33					506162	6329722					
34					509325	6332445					
35					502928	6326635					
36					503016	6326410					
37					502274	6323268					
38					503093	6326484					
39					502239	6323206					
40					509730	6332710					
41					502121	6329051					
42		Bedrock geochemical anomalies			509596	6332504					
43					502251	6326422					
44					502334	6323309					
45					505028	6327747					
46					507956	6330975					
47					500100	6322552					
48					509311	6333949					
49					502532	6329052					
50					509253	6332441					
51					506654	6331838					
52					502276	6323272					
53					503047	6326428					
54					502120	6328941					
55					503296	6327462					
56					502333	6323308					
57					504966	6326993					
58	Fraser Lakes area (zone B)	Occurrences	1122, 1127		504270	6322625					
59					503294	6321957					
60					504271	6322629					
61					504897	6322530					
62		Bedrock geochemical anomalies			505049	6322535					
63					504261	6322615					
64					505016	6322412					
65	Fraser Lakes area (zone A)	Occurrences	none		500657	6320179					
66					500476	6320198					
67		Bedrock geochemical anomaly			500562	6320117					
68	Grab sample G-1000	Occurrence	2023	74H/04	461928	6322667		Polymetallic, structurally controlled vein-shear	Che, Aln		SME Assessment File 74H04-0028
69	Yellow Lake	Occurrences	0999	74A/14	492259	6305334		Intrusion-associated (some Mnz inherited)	Mnz	Ilm, Ap	SME Assessment File 74A14-0047; McKeough *et al.* (2010, 2013)
70					492263	6305336					
71	Rona	Occurrences	0983	74A/11	481880	6289764			Mnz		SME Assessment File 74A14-0047; McKeough *et al.* (2010, 2013)
72					481886	6289789					
73					481911	6289509					
74	Kulyk Lake	Occurrence	0985		470779	6275810			Mnz; trace Xtm	Mag, Hem, Ilm-Hem, Zrn, Ap	SME Assessment File 74A11-0053; Watkinson and Mainwaring (1976); McKeough and Lentz (2011); McKeough *et al.* (2010, 2013)

Table 3 (continued) – LREE-dominant mineralization in which monazite is the principal REE mineral.

Location #	Name	Sample #	Source of Data	TREE (wt. %)	(THREE+Y)/TREE (%)	Eu/Eu*	La_N/Yb_N	U (wt. %)	Th (wt. %)	Th/TREE	U/Th
1	Nadir Bay	GC-2	Normand (2010a)	1.27	4.8	ins. dat.	42	0.002	0.12	0.10	0.0163
2	RA2010-13	10CN310		0.33	2.1	ins. dat.	42	<0.002	0.07	0.20	<0.0350
3	Alces Lake	10CN469		28.90	2.3	0.04	1498	0.123	3.54	0.12	0.0347
4		10CN416-1		17.63	2.5	0.04	914	0.007	2.42	0.14	0.0029
5		10CN421-1		13.05	2.8	0.04	994	0.008	1.82	0.14	0.0044
6		10CN414-1		0.36	ins. dat.	ins. dat.	ins. dat.	<0.002	0.06	0.15	<0.0333
7	Oldman River	n. r.	Robinson (1955)	n. r.; up to 20% Mnz	ins. dat.	ins. dat.	ins. dat.	0.263	5.40	ins. dat.	0.0487
8	Nevins Lake	329007	SME Assessment File 74O12-0049	>0.74	<5.3	0.06	>79	0.006	0.20	<0.27	0.0286
9		329027		>0.67	<2.3	0.07	>602	0.004	0.15	<0.22	0.0236
10		329206		>0.71	<2.9	0.06	>330	0.005	0.14	<0.20	0.0332
11		329222		>0.74	<3.9	0.05	>338	0.004	0.12	<0.16	0.0317
12		329010		>0.54	<1.1	0.09	966	0.001	0.10	<0.19	0.0124
13		329215		>0.50	<2.4	0.06	267	0.001	0.08	<0.16	0.0170
14		329216		>0.44	<2.2	0.09	500	0.001	0.09	<0.20	0.0103
15		329217		>0.43	<1.9	0.07	491	0.001	0.08	<0.19	0.0119
16		329218		>0.43	<1.7	0.06	677	0.001	0.07	<0.16	0.0150
17		329220		>0.40	<2.1	0.11	267	0.001	0.07	<0.18	0.0173
18		329214		>0.40	<1.9	0.10	620	0.001	0.07	<0.18	0.0104
19		329005		0.31	2.7	0.34	98	0.001	0.05	0.18	0.0144
20		329031		0.31	3.1	0.08	333	0.002	0.05	0.15	0.0418
21	Archie Lake	38391	Smith and Cathro (2010)	29.2	0.6	0.07	2346	0.011	>1.00	>0.03	<0.0110
22	Schaffer Lake	—	Normand (2011a)	n. r.; locally abundant Mnz to 7 mm in diameter	ins. dat.	ins. dat.	ins. dat.	0.0068 (eU)	0.212 (eTh)	ins. dat.	0.031 (eU/eTh)
23	Nordbye Lake	01-33-0005	MacDougall (2002)	>0.9	low (ins. dat.)	ins. dat.	ins. dat.	<0.0003	0.241	<0.27	<0.001
24	Alexander Lake area	WA0706037	SME Assessment File 74H02-0043	1.28	8.5	0.17	31	0.120	0.35	0.27	0.3468
25		WA0703027	SME Assessment File 74H02-0043	0.83	6.6	0.16	103	0.009	0.15	0.18	0.0616
26		WA08-O-0039	SME Assessment File 74H02-0045	0.38	4.9	0.11	261	0.002	0.06	0.17	0.0264
27	Walker River area	WA0703044	SME Assessment File 74H02-0043	3.56	6.0	0.06	99	0.064	0.73	0.21	0.0874
28		WA08-O-1014	SME Assessment File 74H02-0045	2.65	4.7	0.08	211	0.001	0.32	0.12	0.0025
29		WA0702052	SME Assessment File 74H02-0043	1.45	8.1	0.13	169	0.005	0.12	0.08	0.0429
30		WA07B1081	SME Assessment File 74H02-0043	1.17	3.9	0.26	160	0.004	0.18	0.15	0.0206
31		WA0703046	SME Assessment File 74H02-0043	1.13	5.5	0.09	102	0.013	0.18	0.16	0.0728
32		WA08-O-2020	SME Assessment File 74H02-0045	1.10	7.4	0.05	142	0.011	0.37	0.34	0.0294
33		WA0701049	SME Assessment File 74H02-0043	0.98	4.4	0.00	105	0.002	0.07	0.07	0.0238
34		WA08-O-0049	SME Assessment File 74H02-0045	0.92	4.6	0.09	113	0.005	0.13	0.14	0.0386
35		WA0701073	SME Assessment File 74H02-0043	0.88	7.3	0.00	188	0.003	0.10	0.12	0.0255
36		WA0701076	SME Assessment File 74H02-0043	0.76	8.6	0.04	161	0.001	0.07	0.09	0.0152
37		WA0703038	SME Assessment File 74H02-0043	0.68	3.6	0.13	250	0.003	0.13	0.20	0.0231
38		WA0701074	SME Assessment File 74H02-0043	0.59	7.3	0.00	181	0.002	0.06	0.10	0.0320
39		WA0701092	SME Assessment File 74H02-0043	0.56	3.9	0.13	314	0.002	0.12	0.22	0.0194
40		WA08-O-0051	SME Assessment File 74H02-0045	0.56	5.8	0.10	115	0.006	0.11	0.19	0.0543
41		WA0701085	SME Assessment File 74H02-0043	0.52	3.6	0.06	202	0.001	0.03	0.06	0.0242
42		WA08-O-1017	SME Assessment File 74H02-0045	0.48	5.9	0.10	169	0.003	0.07	0.14	0.0396
43		WA0702059	SME Assessment File 74H02-0043	0.46	10.4	0.09	51	0.003	0.05	0.12	0.0549
44		WA0701089	SME Assessment File 74H02-0043	0.44	3.2	0.06	208	0.001	0.03	0.07	0.0215
45		WA0702032	SME Assessment File 74H02-0043	0.43	6.5	0.00	108	0.001	0.04	0.10	0.0230
46		WA0703060	SME Assessment File 74H02-0043	0.42	3.3	0.08	128	0.001	0.05	0.13	0.0221
47		WA0703045	SME Assessment File 74H02-0043	0.41	7.0	0.09	54	0.011	0.12	0.30	0.0893
48		WA0705055	SME Assessment File 74H02-0043	0.34	7.1	0.08	51	0.001	0.03	0.07	0.0469
49		WA0703031	SME Assessment File 74H02-0043	0.33	4.9	0.16	153	0.002	0.05	0.17	0.0331
50		WA08-O-2053	SME Assessment File 74H02-0045	0.30	3.5	0.16	458	0.002	0.04	0.14	0.0351
51		WA0705066	SME Assessment File 74H02-0043	0.28	3.5	0.03	126	0.000	0.01	0.04	0.0323
52		WA0703036	SME Assessment File 74H02-0043	0.28	3.7	0.14	247	0.001	0.06	0.22	0.0224
53		WA0701075	SME Assessment File 74H02-0043	0.27	8.8	0.10	172	0.001	0.02	0.09	0.0335
54		WA0703032	SME Assessment File 74H02-0043	0.26	3.8	0.11	125	0.001	0.03	0.10	0.0231
55		WA07B1067	SME Assessment File 74H02-0043	0.26	6.8	0.00	46	0.001	0.03	0.10	0.0541
56		WA0701091	SME Assessment File 74H02-0043	0.25	5.0	0.10	157	0.001	0.05	0.21	0.0227
57		WA0702031	SME Assessment File 74H02-0043	0.25	3.2	0.05	168	0.001	0.02	0.07	0.0281
58	Fraser Lakes area (zone B)[3]	WA08-O-2024	SME Assessment File 74H02-0045	2.17	9.0	0.06	92	0.011	0.54	0.25	0.0207
59		WA08-O-1012		1.95	11.2	0.09	81	0.047	0.24	0.12	0.1992
60		WA08-O-0027		1.15	7.8	0.06	83	0.025	0.58	0.50	0.0438
61		WA08-O-2019		0.81	6.7	0.05	149	0.011	0.34	0.42	0.0321
62		WA08-O-0016		0.48	7.1	0.08	132	0.006	0.16	0.33	0.0367
63		WA08-O-0026		0.45	14.9	0.07	23	0.014	0.33	0.73	0.0415
64		WA08-O-2012		0.25	8.4	0.09	73	0.004	0.10	0.40	0.0392
65	Fraser Lakes area (zone A)	WA08-O-0012		2.83	13.0	0.08	55	0.036	0.19	0.07	0.1925
66		WA08-O-2002		0.61	10.0	0.07	48	0.013	0.21	0.35	0.0616
67		WA08-O-0013		0.37	9.2	0.10	80	0.004	0.07	0.18	0.0534
68	Grab sample G-1000	G-1000	SME Assessment File 74H04-0028	< 21 wt. % Che[4]	ins. dat.	ins. dat.	ins. dat.	avg. 0.00305, max. 0.084 (Cheralite 0.4%)	n. r. (Cheralite 10 to 20%)	ins. dat.	ins. dat. (Cheralite 0.02 to 0.04)
69	Yellow Lake	TMKLR005	SME Assessment File 74A14-0047	1.88	8.6	0.02	116	0.005	0.30	0.16	0.0168
70		JBKLR-009		1.77	8.1	0.06	112	0.004	0.19	0.10	0.0189
71	Rona	BMFLR-005	SME Assessment File 74A14-0047	0.92	7.9	0.08	153	0.015	0.29	0.31	0.0526
72		BMFLR-004		0.58	7.9	0.09	121	0.017	0.15	0.26	0.1132
73		BMFLR-001		0.56	6.9	0.08	162	0.007	0.13	0.24	0.0530
74	Kulyk Lake	AGKJR 001	SME Assessment File 74A11-0053	22.36	2.6	0.61	895	0.053	0.46	0.02	0.1146
		AGKJR 003		6.96	3.0	0.58	379	0.0084	0.193	0.03	0.0435

[1] All location co-ordinates given in UTM Zone 13N, NAD 83.
[2] See Table 2 for list of mineral abbreviations.
[3] Additional diamond-drill hole core analyses available in SME Assessment File 74H02-0044.
[4] Estimation from maximum bulk rock and cheralite U concentrations.
Abbreviations: avg., average; ins. dat., insufficient data; max., maximum; n. r., not reported.

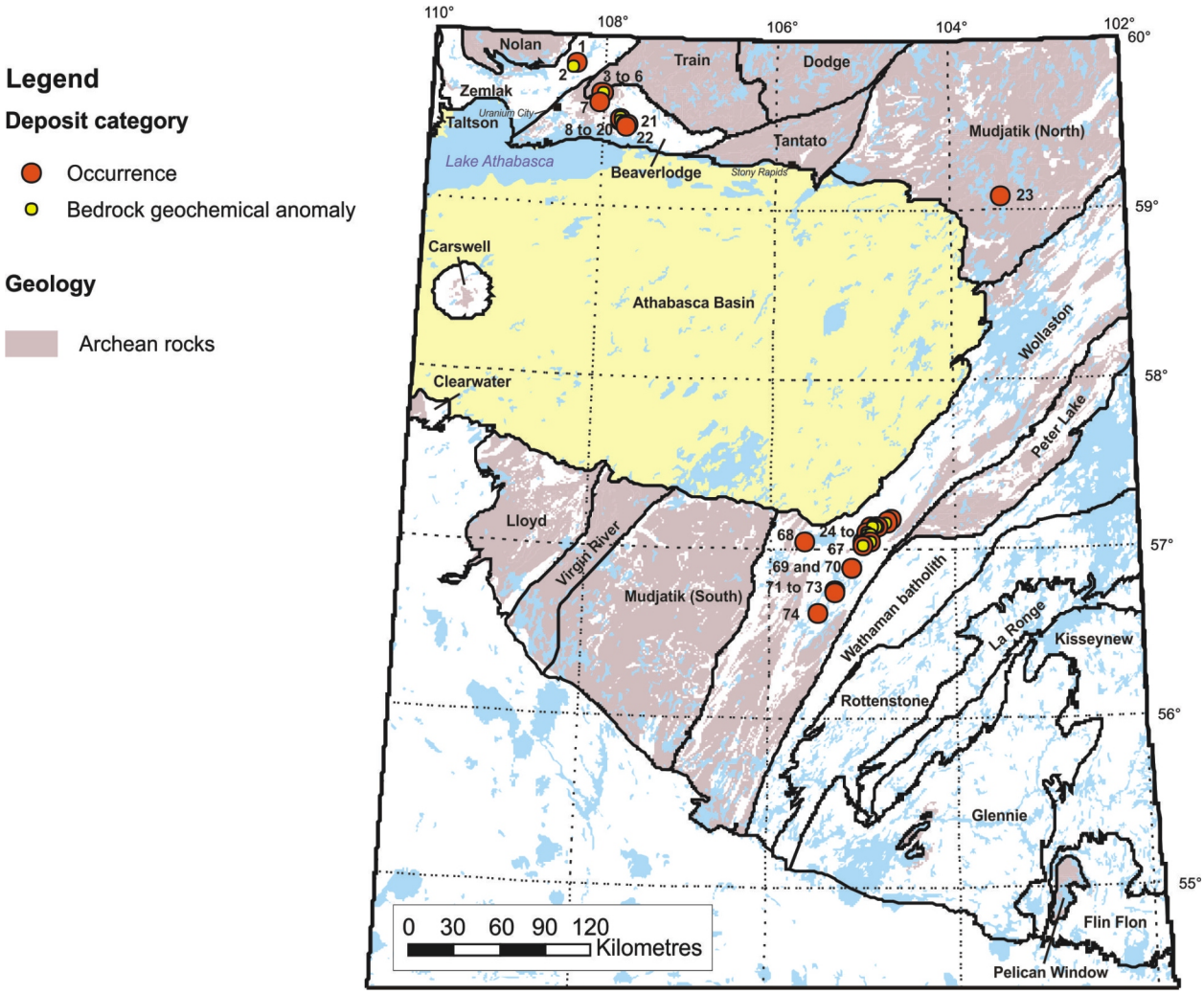

Figure 3 – Location of LREE-dominant mineralization ((THREE+Y)/TREE ≤20%) in the Precambrian Shield of Saskatchewan where monazite is the predominant REE mineral. Proterozoic sedimentary rocks of the Athabasca Basin are shown in light yellow. Areas in purple show the distribution of Archean rocks[11] and domains are labelled. Numbers beside location symbols refer to 'Location #' column in Table 3. Bedrock geology layer merged from 1:250 000 scale Compilation Bedrock Geology Map Series of the Precambrian Shield area of Saskatchewan.

100 mol. % $REEPO_4$) in the monazite-huttonite-cheralite series, Th concentrations can theoretically reach up to ~42 wt. % along the monazite-huttonite join. Similar substitutional schemes can be written using U^{4+} instead of Th^{4+}. U is generally present in monazite in much lower concentrations (rarely above 1 wt. %) than Th. Examples of occurrences where U-rich monazite (>2 wt. % U) is reported include: 1) as a replacement product of U-rich apatite in a pegmatoid (Ziemann *et al.*, 2005); 2) in some pegmatites (Gramaccioli and Segalstad, 1978); and 3) in association with U-rich granites (Förster, 1998). Most monazite-rich mineralization in Saskatchewan, however, has bulk U/Th values between 0.1 and 0.01, mirroring comparatively U-poor monazite compositions. What is particularly interesting about these examples of monazite-rich mineralization is that virtually each occurs in, or in proximity to, predominantly clastic metasedimentary rock packages of Paleoproterozoic age lying on top of a predominantly felsic igneous basement, commonly of Archean age. Examples of this include the Archie Lake, Alces Lake, and Oldman River occurrences that are closely associated with the contact between Murmac Bay group supracrustal rocks and underlying orthogneiss (Normand, 2010a, 2010b, 2011a, 2011b) of uncertain age, and occurrences in the Foster lakes (McKeough *et al.*, 2010) and Fraser Lakes (McKechnie *et al.*, 2012a, 2012b) areas, and around the Karin Lake dome, which is cored by Archean basement (Annesley and Madore, 1989).

Monazite solubility in metaluminous to peraluminous granitic melts is quite low (<500 ppm below 850°C; D <1 and <8% H_2O; equation 1 in Montel, 1993), even lower in melts in which P concentration is buffered by apatite (Tin,

Table 4 – LREE-dominant mineralization in which allanite and apatite are the principal REE minerals.

Location #	Name	Category	SMDI #	Location[1]				Mineralization Type	Minerals[2]		References
				NTS Area	Easting	Northing	Domain		Main REE	Others	
75	JAK REE zone	Developed prospect with Resources	1612	74O/13	343559	6647708	Zemlak	Vein/dyke (deformed)	Aln, Ap; minor to trace Ttn, Bst, Cvk, Mnz	Zrn, Hap	Hogarth (1957); Harvey et al. (2002); Gunning and Card (2005); Barr Engineering Company (2009); Normand and McEwan (2009); Normand *et al.* (2009); Halpin (2010); Normand (2010a, 2010b); Pandur *et al.* (2013a, 2013b); SME Assessment File 74O13-NW-0021
76	Hoidas Lake South	Occurrence	1611		341544	6645321			Aln, Ap	Hap	Hogarth (1957); Normand and McEwan (2009); Normand *et al.* (2009); Halpin (2010)
77	Nisikkatch Lake	Occurrence	1610		337576	6640703			Aln	Hap	Hogarth (1957); Gunning and Card (2005); Normand and McEwan (2009); Normand *et al.* (2009); Halpin (2010)
78	Bear Lake	Occurrence	none		307952	6633417			Aln, Ap, Ttn	Minor Mag; trace Urn, Zrn, Fl (late), Py, Gn, Brt	de Zoysa (1974); Normand (2010a, 2010b)

Table 4 (continued) – LREE-dominant mineralization in which allanite and apatite are the principal REE minerals.

Location #	Name	Sample #	Source of Data	TREE (wt. %)	(THREE+Y)/TREE (%)	Eu/Eu*	La_N/Yb_N	P_2O_5 (wt. %)	Y (wt. %)	Sr (ppm)	Ba (ppm)	U (wt. %)	Th (wt. %)	Th/TREE	U/Th
75	JAK REE zone	799468	SME Assessment File 74O13-NW-0023	9.9	1.2	0.70	1904	0.17	0.022	13400	10200	< 0.001	0.291	0.03	< 0.003
		Averages (±1 standard deviation) of 65 samples with ≥30 wt. % P_2O_5		3.6 (0.7)	5.7 (1.1)	0.83 (0.04)	180 (51)	30 to 40	0.06 (0.02)	8373 (2459)	3808 (4745)	< 0.05	0.11 (0.04)	0.03	< 0.79
		Allanite-rich (average of 2 ICP-MS analyses)	Halpin (2010)	15.2	0.8	0.74	5107	0.04	0.020	5851	4356	0.007	0.626	0.04	0.01
		Apatite-rich (average of 10 ICP-MS analyses)		3.2	6.6	0.86	146	27.59	0.067	7310	4589	0.008	0.088	0.03	0.12
76	Hoidas Lake South	HS-AL (40% allanite, 25% apatite)		8.8	1.2	0.72	2435	1.74	0.020	3807	2443	0.008	0.356	0.04	0.02
77	Nisikkatch Lake	n. r.	Normand (unpublished data)	n. r.	ins. dat.	ins. dat.	ins. dat.	n. r.	n. r.	n. r.	n. r.	0 to 0.0096 (eU)	0.054 to 0.24 (eTh)	ins. dat.	ins. dat.
78	Bear Lake	10CN326-1 (titanite-apatite-allanite-rich)	Normand (2010a)	1.95	17.4	0.79	12	5.46	0.149	1790	453	0.033	0.028	0.01	1.18
		10CN326-4 (allanite)		16.1	0.7	0.64	>3220	0.05	0.018	2690	115	0.017	0.250	0.02	0.07

[1] All location co-ordinates given in UTM Zone 13N, NAD 83.

[2] See Table 2 for list of mineral abbreviations.

Abbreviations: ins. dat., insufficient data; n. r., not reported; N, north; S, south.

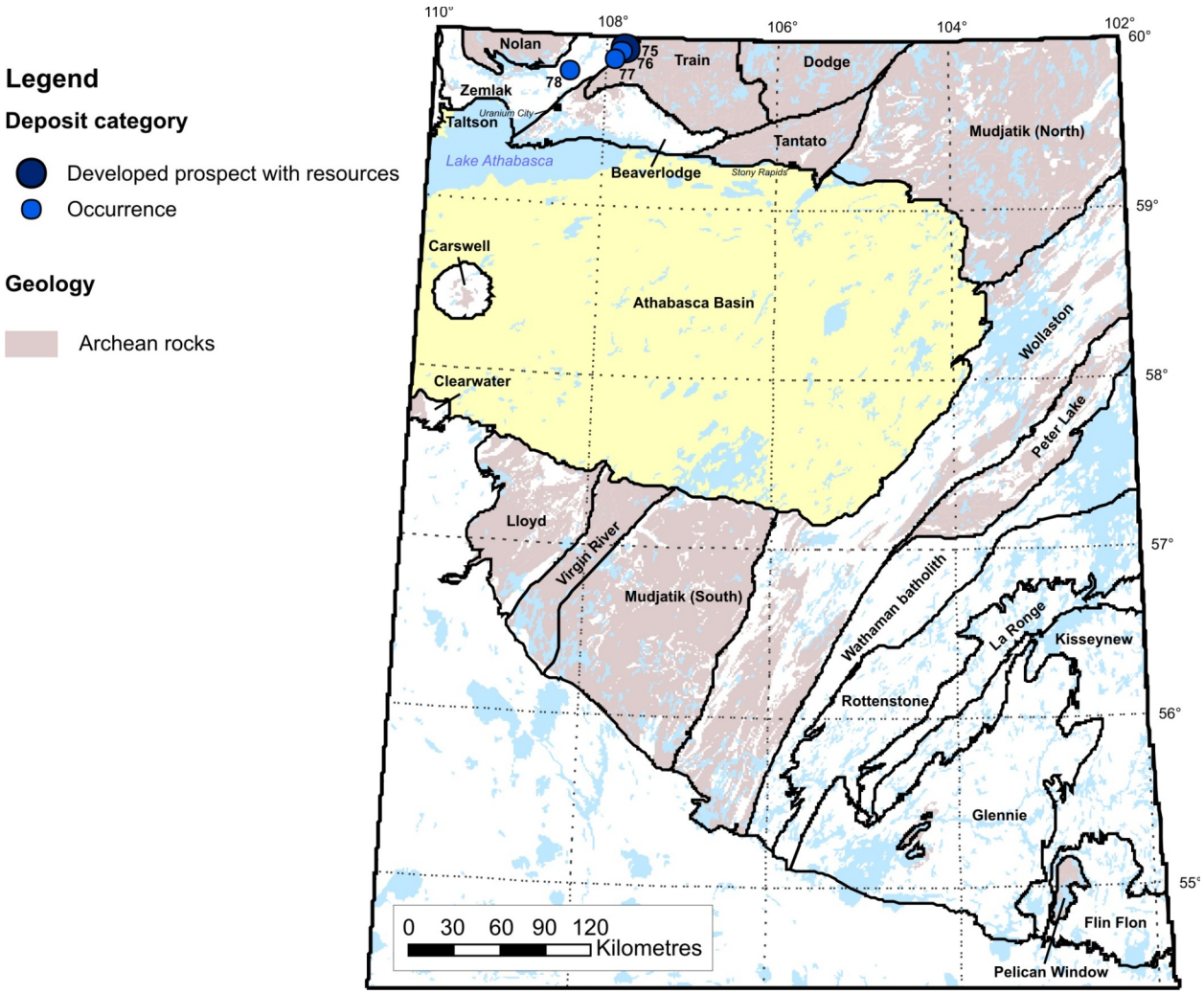

Figure 4 – Location of LREE-dominant mineralization ((THREE+Y)/TREE ≤20%) in the Precambrian Shield of Saskatchewan where allanite and apatite are the predominant REE minerals. Proterozoic sedimentary rocks of the Athabasca Basin are shown in light yellow. Areas in grey show the distribution of Archean rocks and domains are labelled. Numbers beside location symbols refer to 'Location #' column in Table 4.

2007; Skora and Blundy, 2012). Monazite solubility increases dramatically with increased peralkalinity of the melts and can reach thousands of parts per million, although elevated F contents may tend to counteract this somewhat (Tin, 2007), perhaps due to saturation with REE fluorides.

Monazite solubility in hydrothermal fluids at low temperatures (<400°C), even in electrolyte-rich solutions, is also very low (Williams-Jones *et al.*, 2012). Experimental work by Pourtier *et al.* (2010) suggested that dissolution of $NdPO_4$ in excess of 1000 ppm can be achieved in dilute NaCl aqueous solutions at very high temperatures. Much lower solubility, however, was obtained for $CePO_4$ by Tropper *et al.* (2011) at similar temperatures and fluid salinities. Percentage-level dissolution of $CePO_4$ was obtained in NaF-rich fluids from hydrothermal experiments conducted at 800°C and 1 GPa by Tropper *et al.* (2013). The NaF concentrations used in their experiments were very elevated (>2%) and atypical of most natural hydrothermal systems. Naturally occurring NaF, villiaumite, is encountered only in undersaturated, alkaline agpaitic rocks, commonly in the company of rare, exotic, REE-bearing carbonates, phosphates, and silicates (*e.g.*, steenstrupine-(Ce)). Villiaumite may occur as disseminations, such as in lujavrite in the Ilimaussaq Complex (Sørensen, 1997), in large metre-sized lenses in pegmatites and as a late-forming mineral in ussingitized hyperagpaitic rocks (Sørensen and Larsen, 2001; Yakovenchuk *et al.*, 2003; Pekov *et al.*, 2005; see also Shchekina *et al.*, 2013).

Table 5 – LREE-dominant mineralization in which REE mineralogy is not specified.

Location #	Name	Category	SMDI #	Geographic location[1]				Mineralization Type	References
				NTS Area	Easting	Northing	Domain		
79	Lamont Lake	Bedrock geochemical annomaly	2124, 2125, 1532 (area of)	74N13	225337	6654280	Zemlak		SME Assessment File 74N13-NW-0014
80					343061	6586540			
81					338710	6592206			
82					341360	6591022			
83					341515	6591239			
84					340713	6588303			
85					341339	6591038			
86		Occurrences			340886	6587793			
87	Adair Bay		1568, 1569a, 1570, 1781, 1782 (area of)		341314	6588506			
88					342383	6588293			
89					341224	6588316			
90				74O/05	342165	6586636			SME Assessment File 74N08-0162
91					341572	6589508			
92					341282	6591451			
93					341268	6588736			
94		Bedrock geochemical anomalies			341754	6586503			
95					341433	6591104	Beaverlodge		
96					353132	6588544			
97	Natukam Peninsula	Occurrences	1690 (area of)		353198	6588578			
98					350363	6587299			
99					354624	6589741			
100					388761	6587529			
101					388062	6587416			
102					388019	6587334			
103					388059	6587345			
104	North Stolar Lake area	Occurrences	none		387977	6587382			SME Assessment File 74O09-0023
105					388054	6587409			
106				74O/07	388194	6587372			
107					387877	6587304			
108		Bedrock geochemical anomalies			389310	6588397			
109					388286	6587501			
110					406732	6586202			
111	Smith River	Occurrences	1577 (area of)		406828	6585957	Tantato		SME Assessment File 74O09-0024
112					406823	6585946			
113	West Tait Lake	Occurrence		74O/09	430615	6603767	Train		SME Assessment File 74O09-0023
114					663307	6533986			
115		Occurrences			663298	6533975			
116					663299	6533978			
117	Charcoal 6			64L/16	663168	6533318			
118					663334	6533965	Wollaston	Intrusion-associated	
119		Bedrock geochemical anomalies			662065	6532507			SME Assessment Files 64L16-0025 and -0026; Kremer et al. (2010, 2011)
120			none		663320	6533964			
121	Hara 12	Occurrences			662235	6559075			
122				64M/01	663033	6559263			
123	Hara 5	Occurrences			670056	6570025	Mudjatik (N)		
124					669403	6566612			
125	Hook Lake Zone	Bedrock geochemical anomaly			672014	6550559			
126	Reid Bay	Occurrence		64L/09	671750	6514250			
127	DDH KEY005	Occurrence		74H/04	454979	6334154			SME Assessment File 74H04-0120
128	Pegmatite Lake	Bedrock geochemical anomaly	1003, 1004 (area of)		491161	6308595			
129	South Pipe Lake	Bedrock geochemical anomaly	1006 (area of)	74A/14	488120	6307580			SME Assessment File 74A14-0047
130	Craig Bay	Bedrock geochemical anomaly	1001 (area of)		491222	6301739			
131	Gateway Uranium Mines uranium showing no. 3	Occurrence	0977		480807	6287113			
132	Nate	Occurrence	none	74A/11	486497	6277722			Brown (2011)
133	Eldorado Dyke U-REE showing	Occurrence	0980		470082	6274795			Mawdsley (1957); McKeough *et al.* (2010); McKeough and Lentz (2011)
134	Lower Foster Lake	Bedrock geochemical anomaly	none		482480	6274346			SME Assessment File 74A11-0052
135	Roper Island–Daly Lake	Occurrence		74A/12	460953	6264654			SME Assessment File 74A12-0014
136	MacPherson Lake	Bedrock geochemical anomaly	0986 (area of)	74A/11	484357	6263147			SME Assessment File 74A11-0052
137					428984	6263147			
138	Nigeria	Occurrences	none	74B/09	428981	6263140			SME Assessment File 74A12-0014
139					428979	6263140	Wollaston		
140									
	Narrows Lake	Occurrence	0941		450388	6250355			SME Assessment File 74A05-0049
141		Bedrock geochemical anomaly			450385	6250355			
142	Welsh Rapids	Bedrock geochemical anomaly	none		458306	6253757			SME Assessment File 74A12-0014
143					449090	6238879			
144					449087	6238857			
145				74A/05	449090	6238851			
					449090	6238851			
146	Pipewrench Lake	Bedrock geochemical anomalies	0940a, 0940b, 0942 (area of)		449093	6238837			SME Assessment File 74A05-0048
					449093	6238837			
					449093	6238837			
147					449090	6238846			
148					449091	6238853			
149					449096	6238830			
150	Cup Lake	Occurrences	n. r.	74B/02	n. r.	n. r.	Mudjatik (S)		Rare Earth Minerals PLC (2011)

Table 5 (continued) – LREE-dominant mineralization in which REE mineralogy is not specified.

Location #	Name	Sample #	Source of Data	TREE (wt. %)	(THREE+Y)/TREE (%)	Eu/Eu*	La_N/Yb_N	U (wt. %)	Th (wt. %)	Th/TREE	U/Th
79	Lamont Lake	38112	SME assessment file 74N13-NW-0014	0.35	3.9	0.12	195	0.0069	0.058	0.16	0.0022
80	Adair Bay	FT065	SME assessment file 74N08-0162	2.69	1.8	0.09	1006	0.0070	0.391	0.15	0.0179
81		CH225		1.66	2.7	0.08	228	0.0018	0.239	0.14	0.0075
82		MG124		1.43	2.3	0.09	771	0.0062	0.225	0.16	0.0276
83		CH227		1.27	2.3	0.08	999	0.0035	0.228	0.18	0.0154
84		FT064		1.12	2.1	0.14	521	0.0056	0.176	0.16	0.0318
85		MG125		1.09	2.3	0.09	598	0.0025	0.144	0.13	0.0174
86		FT063		1.02	2.0	0.10	559	0.0346	0.073	0.07	0.4746
87		FT055		0.88	1.9	0.09	1783	0.0018	0.119	0.14	0.0151
88		FT062		0.83	6.5	0.09	91	0.0347	0.147	0.18	0.2361
89		FT054		0.82	2.0	0.12	954	0.0005	0.096	0.12	0.0052
90		JR475		0.80	2.9	0.08	247	0.0150	0.082	0.10	0.1836
91		FT053		0.57	4.1	0.09	286	0.0030	0.121	0.21	0.0248
92		MG123		0.56	2.4	0.26	208	0.0356	0.076	0.14	0.4684
93		JR480		0.54	1.8	0.11	1197	0.0091	0.086	0.16	0.1059
94		FT050		0.44	2.0	0.13	311	0.0032	0.080	0.18	0.0400
95		CH226		0.38	6.0	0.13	79	0.0111	0.048	0.12	0.2332
96	Natukam Peninsula	MG106		0.80	1.4	0.08	590	0.0008	0.120	0.15	0.0067
97		MG105		0.56	1.7	0.10	409	0.0024	0.086	0.15	0.0278
98		FT044		1.01	1.9	0.09	1006	0.0270	0.148	0.15	0.1824
99		MG126		1.05	1.8	0.14	1202	0.0063	0.166	0.16	0.0380
100	North Stolar Lake area	TR028	SME assessment file 74O09-0023	2.36	1.3	0.14	2760	0.0010	0.260	0.11	0.0038
101		JR378		0.93	3.0	0.18	209	0.0061	0.045	0.05	0.1359
102		CC294		1.23	2.3	0.07	3143	0.0269	0.072	0.06	0.3752
103		CC295		0.88	5.6	0.15	80	0.0045	0.039	0.04	0.1142
104		TR017		0.76	2.3	0.16	341	0.0024	0.037	0.05	0.0645
105		TR019		0.74	4.2	0.17	113	0.0030	0.021	0.03	0.1415
106		TR022		0.67	4.4	0.17	68	0.0414	0.013	0.02	3.1364
107		TR016		0.65	3.1	0.17	179	0.0019	0.020	0.03	0.0955
108		CC297		0.38	2.0	0.21	343	0.0021	0.081	0.21	0.0260
109		WM332		0.28	6.9	0.10	33	0.0023	0.003	0.01	0.8519
110	Smith River	OM458	SME assessment file 74O09-0024	2.90	0.7	0.04	1588	0.0077	0.764	0.26	0.0101
111		CH171		1.09	0.7	0.08	1140	0.0009	0.239	0.22	0.0038
112		CH170		0.80	0.7	0.07	1470	0.0009	0.183	0.23	0.0048
113	West Tait Lake	TP019	SME assessment file 74O09-0023	0.58	1.3	0.02	802	<0.0002	0.088	0.15	<0.0023
114	Charcoal 6	RD058	SME assessment files 64L16-0025 and -0026	3.30	2.8	0.19	350	0.0095	0.54	0.16	0.0176
115		KTK039		3.10	2.9	0.20	328	0.0208	0.424	0.14	0.0491
116		KTK041		2.46	3.3	0.17	905	0.0005	0.48	0.20	0.0010
117		KTK043		1.25	4.3	0.14	690	0.0004	0.191	0.15	0.0021
118		KTK040		0.42	4.2	0.19	303	0.0003	0.055	0.13	0.0055
119		KTK044		0.37	4.2	0.19	234	0.0001	0.045	0.12	0.0022
120		RD059		0.25	3.8	0.25	304	0.0001	0.033	0.13	0.0030
121	Hara 12	DC297		1.66	5.0	0.01	214	0.0079	0.319	0.19	0.0248
122		DC300		1.37	4.9	0.01	395	0.0053	0.282	0.21	0.0188
123	Hara 5	GM301		1.23	3.5	0.08	298	0.0001	0.225	0.18	0.0004
124		WM212		0.83	6.0	0.09	299	0.0066	0.141	0.17	0.0468
125	Hook Lake zone	GM048		0.31	4.2	0.22	250	0.0001	0.046	0.15	0.0022
126	Reid Bay	JR045		0.51	4.7	0.20	269	0.0001	0.0489	0.10	0.0020
127	DDH KEY005	011-0185	SME assessment file 74H04-0120	>7.55	5.5	0.02	200	0.0203	0.906	<0.12	0.0224
		011-0186		>7.20	5.1	0.02	236	0.0199	0.883	<0.12	0.0225
		011-0189		5.19	4.7	0.02	179	0.0144	0.637	0.12	0.0227
		011-0194		5.12	6.6	0.02	130	0.0161	0.592	0.12	0.0271
		011-0183		1.55	5.2	0.03	199	0.0041	0.180	0.12	0.0227
		011-0184		0.81	5.0	0.04	224	0.0022	0.099	0.12	0.0223
		011-0187		0.70	4.8	0.04	165	0.0024	0.084	0.12	0.0283
		011-0192		0.63	5.0	0.04	146	0.0021	0.078	0.12	0.0272
		011-0196		0.58	5.1	0.05	135	0.0021	0.073	0.13	0.0291
		011-0188		0.33	4.9	0.08	164	0.0012	0.044	0.13	0.0266
		011-0191		0.29	5.0	0.05	152	0.0010	0.039	0.14	0.0256
128	Pegmatite Lake	JBKLR050	SME assessment file 74A14-0047	0.39	6.0	0.07	166	0.0040	0.061	0.15	0.0659
129	South Pipe Lake	JBKLR054		0.26	7.1	0.06	74	0.0048	0.121	0.46	0.0397
130	Craig Bay	TMKLR001		0.28	6.8	0.09	182	0.0041	0.048	0.17	0.0849
131	Gateway Uranium Mines uranium showing no. 3	JBFLR-001		0.52	6.3	0.16	290	0.0044	0.079	0.14	0.0556
132	Nate	NTKJR004	Brown (2011)	1.20	7.3	ins. dat.	ins. dat.	0.0690	0.465	0.39	0.1484
133	Eldorado Dyke U-REE showing	27	McKeough and Lentz (2011)	0.79	10.1	0.02	50	0.0055	0.153	0.19	0.0359
134	Lower Foster Lake	JMKJR001	SME assessment file 74A11-0052	0.34	7.2	0.11	127	0.0057	0.051	0.15	0.1129
135	Roper Island–Daly Lake	5162	SME assessment file 74A12-0014	0.67	9.9	0.18	120	<0.0002	0.119	0.18	<0.0011
136	MacPherson Lake	TMKJR019	SME assessment file 74A11-0052	0.46	13.5	0.28	19	0.3870	0.088	0.19	4.4128
137	Nigeria	5034	SME assessment file 74A12-0014	0.73	7.8	0.07	264	0.0002	0.084	0.11	0.0024
138		5033		0.57	7.8	0.07	294	<0.0002	0.066	0.12	<0.0030
139		5031		0.54	8.1	0.08	272	<0.0002	0.061	0.11	<0.0033
		5032		0.25	8.4	0.10	214	<0.0002	0.027	0.11	<0.0075
140	Narrows Lake	10819	SME assessment file 74A05-0049	0.76	14.7	0.11	34.8	0.0580	0.112	0.15	0.5179
		10820		0.67	16.2	0.11	27.5	0.0506	0.088	0.13	0.5724
141		10714		0.25	21.5	0.13	22.1	0.0128	0.026	0.10	0.4885
142	Welsh Rapids	5154	SME assessment file 74A12-0014	0.35	9.7	0.19	48	0.0025	0.036	0.10	0.0704
143	Pipewrench Lake	9782	SME assessment file 74A05-0048	0.48	3.4	ins. dat.	233	n. r.	0.048	0.10	ins. dat.
144		9766		0.36	3.6	ins. dat.	257	n. r.	0.039	0.11	ins. dat.
145		9734		0.33	4.8	0.06	258	0.0022	0.065	0.20	0.0338
		9732		0.30	4.5	0.03	194	0.0006	0.041	0.14	0.0145
146		9654		0.32	4.3	0.05	245	0.0014	0.058	0.18	0.0240
		9653		0.28	4.8	0.04	231	0.0017	0.052	0.18	0.0326
		9659		0.27	4.7	0.03	248	0.0010	0.049	0.18	0.0202
147		9705		0.31	4.5	ins. dat.	269	0.0010	0.059	0.19	0.0169
148		9748		0.28	4.7	0.02	244	0.0013	0.056	0.20	0.0230
149		9676		0.26	4.6	0.04	215	0.0010	0.049	0.18	0.0205
150	Cup Lake	n. r.	Rare Earth Minerals PLC (2011)	7.5 (excluding Y, Ho, Tm, Yb, Lu)	2 (excluding Y, Ho, Tm, Yb, Lu)	0.11	ins. dat.	n. r.	n. r.	ins. dat.	ins. dat.

[1] All location co-ordinates given in UTM Zone 13N, NAD 83.
Abbreviations: DDH, diamond-drill hole; ins. dat., insufficient data; n. r., not reported; N, north; S, south.

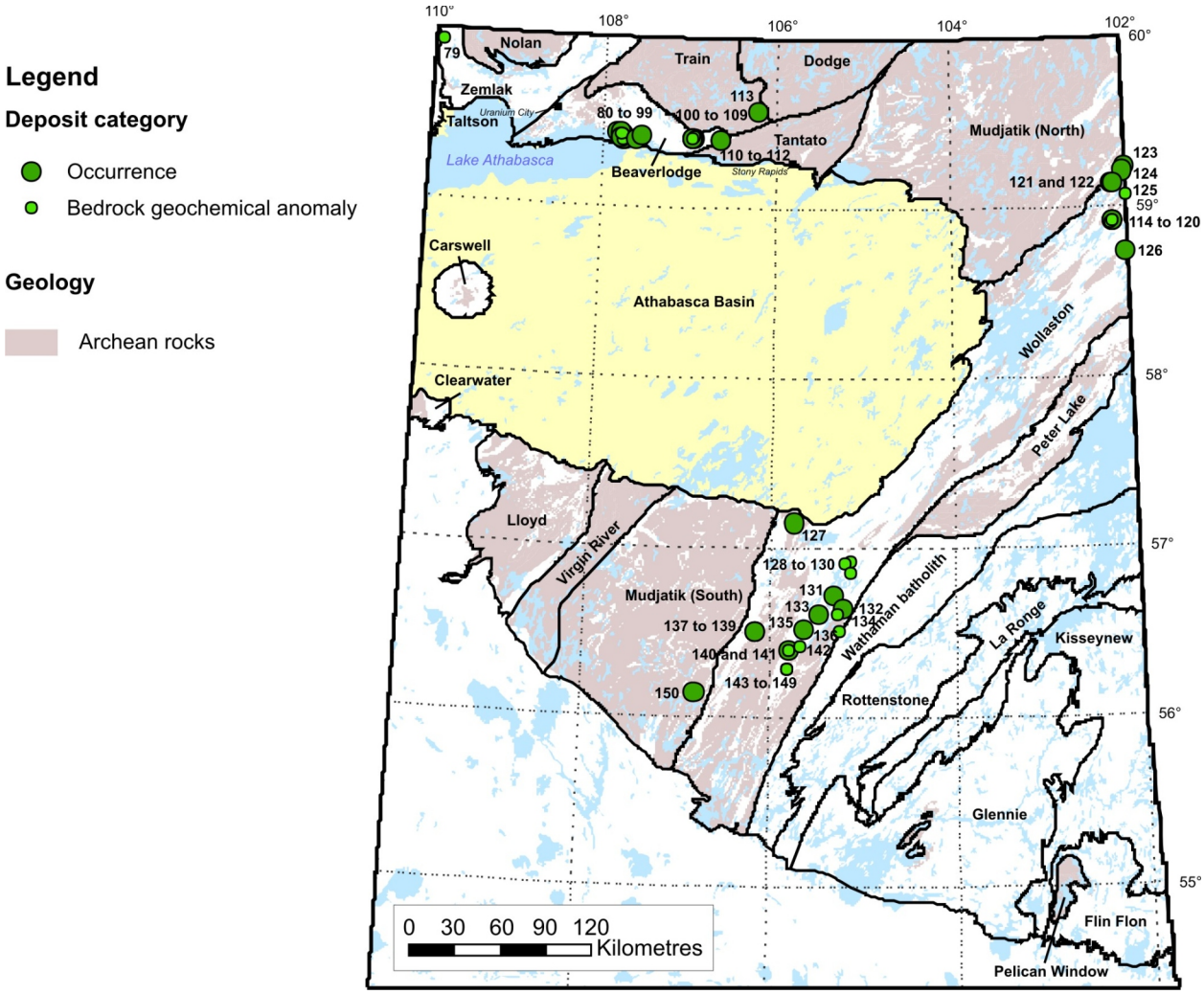

Figure 5 – Location of LREE-dominant mineralization ((THREE+Y)/TREE ≤20%) in the Precambrian Shield of Saskatchewan where REE mineralogy remains largely unknown. Proterozoic sedimentary rocks of the Athabasca Basin are shown in light yellow. Areas in grey show the distribution of Archean rocks and domains are labelled. Numbers beside location symbols refer to 'Location #' column in Table 5.

In general, measured or estimated F concentrations in hydrothermal fluids associated with granitic magmas are well below 5000 ppm (Banks *et al.*, 1994; McCaig *et al.*, 2000; Penniston-Dorland and Ferry, 2005; Yardley, 2013). However, exceptionally elevated F concentrations of 0.7 to 4.8%, in addition to 1.5 to 9.7% SO_4 and 13.2 to 15.4% Cl, have been reported to occur in fluid inclusions contained in omphacite and garnet present in Caledonian eclogite from Norway (Svensen *et al.*, 2001). Potentially, thousands of parts per million monazite could be dissolved in such F- and SO_4-rich fluids, although the effect of saturation levels of REE fluorides or other solid REE phases at elevated temperatures (>400° to 500°C) would need to be addressed. Destabilization of REE fluoride complexes would be expected during formation of such F-rich minerals as amphiboles, micas, apatite, and fluorite (*e.g.*, granulite- to amphibolite-facies retrograde fluids), leading to precipitation of REE minerals. Sulphate reduction (at T >300° to 400°C), which could be accompanied by precipitation of sulphides, might be a possible mechanism for destabilization of REE-sulphate complexes.

The presence of abundant monazite in biotite-rich metasomatites associated with a syenite intrusion in the Ukraine was tentatively ascribed by Marchenko and Goncharova (1965) to precipitation following an impoverishment in F of the altering fluids during biotitization[11]. Although there are no experimental data for the solubility of monazite in sulphate- or carbonate-rich brines at elevated pressures and temperatures, theoretical estimations of, and experimentally determined, association constants for REE-sulphate and REE-carbonate complexes (Wood, 1990;

[11] The biotite was reported to contain 2.3 to 2.4 wt. % F.

Sverjensky *et al.*, 1997; Migdisov *et al.*, 2006, Migdisov and Williams-Jones, 2008) suggest that such complexes could also be important in mass transport of REE in the deep crust. An evaluation of the effect of saturation levels for solid REE fluorides, carbonates, and fluoro-carbonates is needed to determine maximum REE concentrations in the presence of fluoride and carbonate under a wide range of physicochemical conditions.

In systems that are poor in P (and poor in ligands, such as fluoride and, presumably, carbonate that could form insoluble REE compounds), it is conceivable that REE can achieve considerable solubility (>1000 ppm) at elevated temperatures, especially when free chloride ions are available in abundance. In such a case, solubility would be limited by hydrolysis (below saturation levels for REE fluoride, carbonate, and fluoro-carbonate minerals), and introduction of P in the fluid, or reaction with phosphatic rocks, could lead to massive precipitation of monazite (this would be valid for melts as well, where magma mixing or assimilation might be involved).

Similar to monazite, allanite is a common accessory, rock-forming constituent that has been observed in a wide variety of rock types, including granitic pegmatites, granites, diorites, paragneisses, and granitic and granodioritic gneisses, of various ages in northern Saskatchewan, especially in the Zemlak Domain (Koster, 1965a, 1965b; de Zoysa, 1974; Ashton *et al.*, 2005). It occurs in elevated concentrations in one prospect with resources (the JAK zone, on the northwestern shore of Hoidas Lake) and in at least three REE occurrences in the same general area: Hoidas Lake South (SMDI #1611), Nisikkatch Lake South (SMDI #1610), and Bear Lake (de Zoysa, 1974; Normand, 2010a, 2010b). Allanite is reported from a further 18 locations in the SMDI database (Table 6; Figure 6). However, in the majority of these cases, allanite is reported to be present as a minor to trace constituent in mineralization in which U is the main commodity or for which information on the proportions of allanite present and paragenesis is lacking entirely.

Based on presently available data, it appears that all significant allanite-dominant mineralization occurs in the Zemlak Domain. By contrast with monazite, locations where allanite occur show no systematic spatial relationship with metamorphosed sedimentary rocks. In fact, at all major occurrences, allanite-rich mineralization is hosted by granitoid rocks and apatite is an important ore-forming mineral in the parageneses. This could be explained, in part and in very generalized terms, by the comparably higher Ca and lower Al chemical potentials (or partial equilibrium to higher $(a\mathrm{Ca}^{2+})^3/(a\mathrm{Al}^{3+})^2$ values) expected to characterize the chemistry of fluids flowing through granitoid rocks compared to those flowing through clastic sedimentary rocks, and comparatively low temperatures at equivalent $(a\mathrm{Ca}^{2+})^3/(a\mathrm{Al}^{3+})^2$ values with respect to monazite stability in metamorphosed silicate rocks that are higher than greenschist facies (Wing *et al.*, 2003; Janots *et al.*, 2007, 2008; Budzyñ *et al.*, 2011). A comparable general reasoning, using chemical potential of component oxides, can be applied to melts instead of hydrothermal fluids. Allanite solubility in water-saturated haplogranitic felsic melts is, similar to monazite, fairly low (Klimm *et al.*, 2008). Under appropriate $f\mathrm{O}_2$ conditions (Gieré and Sorensen, 2004), the mineral may saturate with the cooling of silicic liquids, which can be derived from melting of mafic or sedimentary rocks sufficiently enriched in CaO (Klimm *et al.*, 2008).

Allanite-subgroup minerals (Armbruster *et al.*, 2006) are members of the epidote group and are isostructural with epidote and clinozoisite. The structural formula of allanite-subgroup minerals can be written as $(\mathrm{A1A2})(\mathrm{M1M2M3})(\mathrm{Si_2O_7})(\mathrm{SiO_4})\mathrm{O}(\mathrm{OH})$, where REE occupy the largest (A2) sites in XI-fold co-ordination (Dollase, 1971). The allanite subgroup comprises 18 IMA-approved species, of which allanite-(Ce) is probably the most common. For simplicity, and in the absence of detailed chemical and crystallographic data, the term allanite is used in this report to refer to all allanite-subgroup species. Allanite most commonly contains ~15 to 25 wt. % total REE (rarely approaching 40 wt. %) and may contain minor to major concentrations of Th and U. It generally contains less than 3 wt. % $\mathrm{ThO_2}$, with a maximum of 4.9 wt. % reported by Gieré and Sorensen (2004). Concentrations of $\mathrm{UO_2}$ in allanite are usually much less than 1 wt. % (Ercit, 2002; Gieré and Sorensen, 2004). In contrast to monazite, allanite is commonly metamict due to its crystal lattice being less flexible to recovery from radiation damage and much higher annealing temperature (Poitrasson, 2004). By comparison with monazite-dominant mineralization, radiometrically and chemically measured U/Th values from allanite-dominant mineralization in Saskatchewan vary between ~1 and <0.001, due to a more complex assemblage of REE-U-Th–bearing minerals and variability in the proportion of these minerals across mineralized zones.

Experimental data on the dissolution of epidote (Rose, 1991) and monazite (Oelkers and Poitrasson, 2002) suggest that epidote dissolves at a rate at least one order of magnitude faster under ambient laboratory conditions. Price *et al.* (2005) further reported that allanite dissolves much faster than epidote in soils, probably due to its frequent metamict nature. This has implications in exploration using lake-bottom sediment geochemistry as, based on the above, lakes that reside on a substrate composed of metasedimentary rocks containing anomalous concentrations of monazite should be much less responsive to chemically derived REE accumulation than those that overlie magmatic

Table 6 – REE mineral locations.

Location #	Name	SMDI #	Location[1]				Minerals[2]		Mineralization Type	References
			NTS Area	Easting	Northing	Domain	Main REE	Others		
151	Hoidas Lake North allanite occurrence	1613	74O/13	343328	6649576	Zemlak	Aln		Intrusion-associated	Koster (1965b)
152	Fisher-Hayes uranium deposit	1644	74P/06	343328	6649576	Mudjatik (N)	Aln (tentative id.)	Urn, Gum		SMDI #1644
153	Hazleton Lake	1531	74N/13	225197	6639096	Zemlak	Eux-Pol, Pcl-Mrl			SMDI #1531
154	RA2010-05	none	74N/16	313556	6637678		Aln			Normand (2010a, 2010b)
155	Ledford		64M/16	658625	6637008	Mudjatik (N)	Aln	Mol, Mag		MacDougall (2002)
156	Laird Island uranium occurrences 2, 6, 7, and 8	1544	74N/15	275953	6635964	Zemlak	Mnz	Urn/Ptb, Gum	Shear zone-hosted vein	Lang *et al.* (1962)
157	Old South uranium showing, uranium showings B, C, D, and E, or Great West uranium showing B	1537	74N/14	273057	6635860		Aln	Ptb, Zrn (cyrtolite)	Shear zone-hosted	
158	RA2010-17	none	74N/16	307801	6633515		Aln		Intrusion-associated	Normand (2010a, 2010b)
159	American Canadian Uranium Mines Ltd showing FF-10H	1340 (?)	74N/09	313833	6626982		Mnz, Xtm	Po, Mol, Urn, Ap		Robinson (1955); SME Assessment File 74N09-0029
160	Goldfields uranium occurrence 49-TT-1 or the Nesbitt Lake uranium showing B and C zones	1474	74N/10	301463	6625245		Mnz (to 3 mm)	Hem, Py, Mol, Urn, Thr, Po, Ccp, Sp, Gn	Shear zone-hosted	Christie (1953); Robinson (1955); Lang *et al.* (1962); Beck (1969)
161	Keseechewun	none	64M/10	629514	6621453	Mudjatik (N)	Aln		Intrusion-associated	MacDougall (2002)
162	Keseechewun			630104	6620787		Aln			
163	RA2010-27		74N/09	329374	6619885	Beaverlodge	Mnz			Normand (2010a, 2010b)
164	50-TT-62		74N/10	296027	6619824	Zemlak	Mnz (euhedral to 3 mm)	Ap, Zrn (trace)		Robinson (1955)
165	RA2010-26		74N/09	327693	6618738	Beaverlodge	Mnz			Normand (2010a, 2010b)
166	Haight Lake		74O/12	354510	6611256		Mnz (locally abundant)	Zrn, Urn		Harper (1986)
167	Viking Lake (west of)	1345	74N/09	316847	6610204		Aln, Mnz	Mag, Utr, Pcl-Mrl, Zrn (cyrtolite)		Robinson (1955)
168	Pinkham Lake U-allanite pegmatites zones A and B	1672	74P/08	551302	6592468	Mudjatik (N)	Aln	Urn, yellow secondary U minerals		SMDI #1672
169	Fisher-Hayes uranium showing extension (G showing)	1758	74P/06	494112	6571398		Aln (tentative id.)	Urn		SMDI #1758
170	Pluto Bay (south shore of west arm)	1759		494871	6570964		Aln (tentative id.)	Urn		SMDI #1759
171	Nistoo	none	64M/01	664911	6569079		Aln	Mol		MacDougall (2002)
172	Ox Lake allanite showing (drill holes 4-OX-1, -3, and -4)	1145	74H/09	540302	6383394	Wollaston	Aln		Shear zone-hosted	SMDI #1145
173	Pyett Lake allanite pegmatite	0543	64E/05	580723	6366056	Peter Lake	Aln (rare; to 10 cm)		Intrusion-associated	MacDougall (1990)
174	Fire Creek uranium showing (trench)	2481	74G/05	334045	6365939	Virgin River	Aln (minor)	Urn (minor), Zrn	Shear zone-hosted	SMDI #2481
175	Lyle Lake nepheline-bearing pegmatite/plug	2639	64E/06	612074	6364383	Peter Lake	Aln (trace)	Fl, Ttn, Zrn, Mag	Intrusion-associated	Quirt (1992)
176	Sand Lake area C uranium occurrence	1008	74A/14	488851	6312767	Wollaston	Mnz (not confirmed)	Ptb; minor Py, Hem		SMDI #1008
177	Horn U showing, Jackpine U showing, or Bleasdell 4 and 6 showings, Rita's As-Cu-Be-U showing	0500	64D/09	661792	6274672	Kisseynew	Mnz (minor)	Torbernite, kasolite, uranophane		SMDI #0500
178	Cup Lake (northwest) showing no. 1 to showing no. 6	1031	74B/02	382880	6226110	Mudjatik (S)	Aln (rare)	Urn; minor Mol, uranophane, Fl, Po, Py		SMDI #1031
179	Keller Lake U-Th-Mo occurrence	1025		401236	6210090		Mnz, Aln	Minor Mol		SMDI #1025
180	Iskwatam Lake allanite showing	0375	63M/11	620410	6160066	Kisseynew	Aln			Lang *et al.* (1962)
181	PIX U-Cu±Mo showing	0798	73P/07	512227	6139107	Glennie	Aln	Ccp, Py, Mol	Vein	SMDI #0798
182	Intrepid Lake radioactive occurrences	0356	63M/07	629714	6127914	Kisseynew	Mnz		Intrusion-associated	SMDI #0356
183	Split Lake U zone, Tongue U zone, Plug U zone, Mountain U zone, Ridge U zone, East U zone, West U zone	0806	73P/08	536517	6127030	Glennie	Mnz, Aln	Urn, secondary yellow U minerals		Lang *et al.* (1962)
184	Jahala Lake uranium deposit (zones A, B, and C), North Jahala uranium showing; Jahala Lake adit	0720	73P/01	546977	6117204		Mnz (to 1 cm), Aln, Xtm	Urn, titaniferous Mag, Gth, Cof, curite, kasolite and uranophane		Mawdsley (1954); Ford (1955)
185	Lacey Lake allanite showing	0686	73I/16	550594	6091307		Aln			SMDI #0686
—	Chris-June	none	74N/14, /N15	n. r.	n. r.	Zemlak	Aln, Mnz			Lang *et al.* (1962)
—	Trojan		74O/06(?)	n. r.	n. r.	Beaverlodge	Mnz		n. r.	

Table 6 (continued) – REE mineral locations.

Location #	Name	High TREE (wt. %)	(THREE+Y)/TREE (%)	High Th (wt. %)	High U (wt. %)	Th/TREE	U/Th
151	Hoidas Lake North allanite occurrence	n. r.	ins. dat.	n. r.	n. r.	ins. dat.	ins. dat.
152	Fisher-Hayes uranium deposit	n. r.	ins. dat.	n. r.	0.45	ins. dat.	ins. dat.
153	Hazleton Lake	n. r.	ins. dat.	n. r.	n. r.	ins. dat.	ins. dat.
154	RA2010-05	0.089	3.4	0.008	<0.002	0.09	<0.25
155	Ledford	0.014	ins. dat.	0.0009	0.0002	0.06	0.22
156	Laird Island uranium occurrences 2, 6, 7, and 8	n. r.	ins. dat.	n. r.	3.85	ins. dat.	ins. dat.
157	Old South uranium showing, uranium showings B, C, D, and E, or Great West uranium showing B	n. r.	ins. dat.	n. r.	n. r.	ins. dat.	ins. dat.
158	RA2010-17	0.117	2.6	0.024	0.003	0.21	0.13
159	American Canadian Uranium Mines Ltd showing FF-10H	n. r.	ins. dat.	ins. dat.	ins. dat.	ins. dat.	ins. dat.
160	Goldfields uranium occurrence 49-TT-1 or the Nesbitt Lake uranium showing B and C zones	n. r.	ins. dat.	n. r.	0.11	ins. dat.	ins. dat.
161	Keseechewun	0.067	ins. dat.	0.0059	<0.0001	0.09	<0.017
162	Keseechewun	0.057	ins. dat.	0.0043	<0.0001	0.07	<0.023
163	RA2010-27	n. r.	ins. dat.	0.0289 (eTh)	0.00057 (eU)	ins. dat.	0.02
164	50-TT-62	n. r.	ins. dat.	11.47 in Mnz	0.161 in Mnz	ins. dat.	0.01 (Mnz)
165	RA2010-26	n. r.	ins. dat.	0.0299 (eTh)	0.00087 (eU)	ins. dat.	0.03
166	Haight Lake	n. r.	ins. dat.	n. r.	n. r.	ins. dat.	ins. dat.
167	Viking Lake (west of)	n. r.	ins. dat.	n. r.	n. r.	ins. dat.	ins. dat.
168	Pinkham Lake U-allanite pegmatites zones A and B	n. r.	ins. dat.	n. r.	n. r.	ins. dat.	ins. dat.
169	Fisher-Hayes uranium showing extension (G showing)	n. r.	ins. dat.	n. r.	0.45	ins. dat.	ins. dat.
170	Pluto Bay (south shore of west arm)	n. r.	ins. dat.	n. r.	0.45	ins. dat.	ins. dat.
171	Nistoo	0.006	ins. dat.	0.0004	0.0009	0.08	2.14
172	Ox Lake allanite showing (drill holes 4-OX-1, -3, and -4)	n. r.	ins. dat.	0.19	0.26	ins. dat.	1.37
173	Pyett Lake allanite pegmatite	n. r.	ins. dat.	n. r.	n. r.	ins. dat.	ins. dat.
174	Fire Creek uranium showing (trench)	n. r.	ins. dat.	0.137	0.15	ins. dat.	1.09
175	Lyle Lake nepheline-bearing pegmatite/plug	0.0369	ins. dat.	0.0033	0.0025	0.09	0.76
176	Sand Lake area C uranium occurrence	n. r.	ins. dat.	0.57	3.73	ins. dat.	6.54
177	Horn U showing, Jackpine U showing,or Bleasdell 4 and 6 showings, Rita's As-Cu-Be-U showing	n. r.	ins. dat.	n. r.	0.46	ins. dat.	ins. dat.
178	Cup Lake (northwest) showing no. 1 to showing no. 6	Two samples, 0.01% and 0.02% Y_2O_3	ins. dat.	0.404	0.187	ins. dat.	0.46
179	Keller Lake U-Th-Mo occurrence	n. r.	ins. dat.	0.105	0.004	ins. dat.	0.04
180	Iskwatam Lake allanite showing	n. r.	ins. dat.	n. r.	n. r.	ins. dat.	ins. dat.
181	PIX U-Cu±Mo showing	n. r.	ins. dat.	n. r.	0.23	ins. dat.	ins. dat.
182	Intrepid Lake radioactive occurrences	n. r.	ins. dat.	0.57	0.12	ins. dat.	0.21
183	Split Lake U zone, Tongue U zone, Plug U zone, Mountain U zone, Ridge U zone, East U zone, West U zone	n. r.	ins. dat.	n. r.	0.34 (0.64 in biotite clusters in scarp dyke; 1.15 in biotite in fold dyke)	ins. dat.	ins. dat.
184	Jahala Lake uranium deposit (zones A, B, and C), North Jahala uranium showing; Jahala Lake adit	n. r.	ins. dat.	n. r.	2.04	ins. dat.	ins. dat.
185	Lacey Lake allanite showing	n. r.	ins. dat.	n. r.	n. r.	ins. dat.	ins. dat.
—	Chris-June	n. r.	ins. dat.	n. r.	n. r.	ins. dat.	ins. dat.
—	Trojan	n. r.	ins. dat.	n. r.	n. r.	ins. dat.	ins. dat.

[1] All location co-ordinates given in UTM Zone 13N, NAD 83.

[2] See Table 2 for list of mineral abbreviations.

Abbreviations: id., identification; ins. dat., insufficient data; n. r., not reported; N, north; S, south.

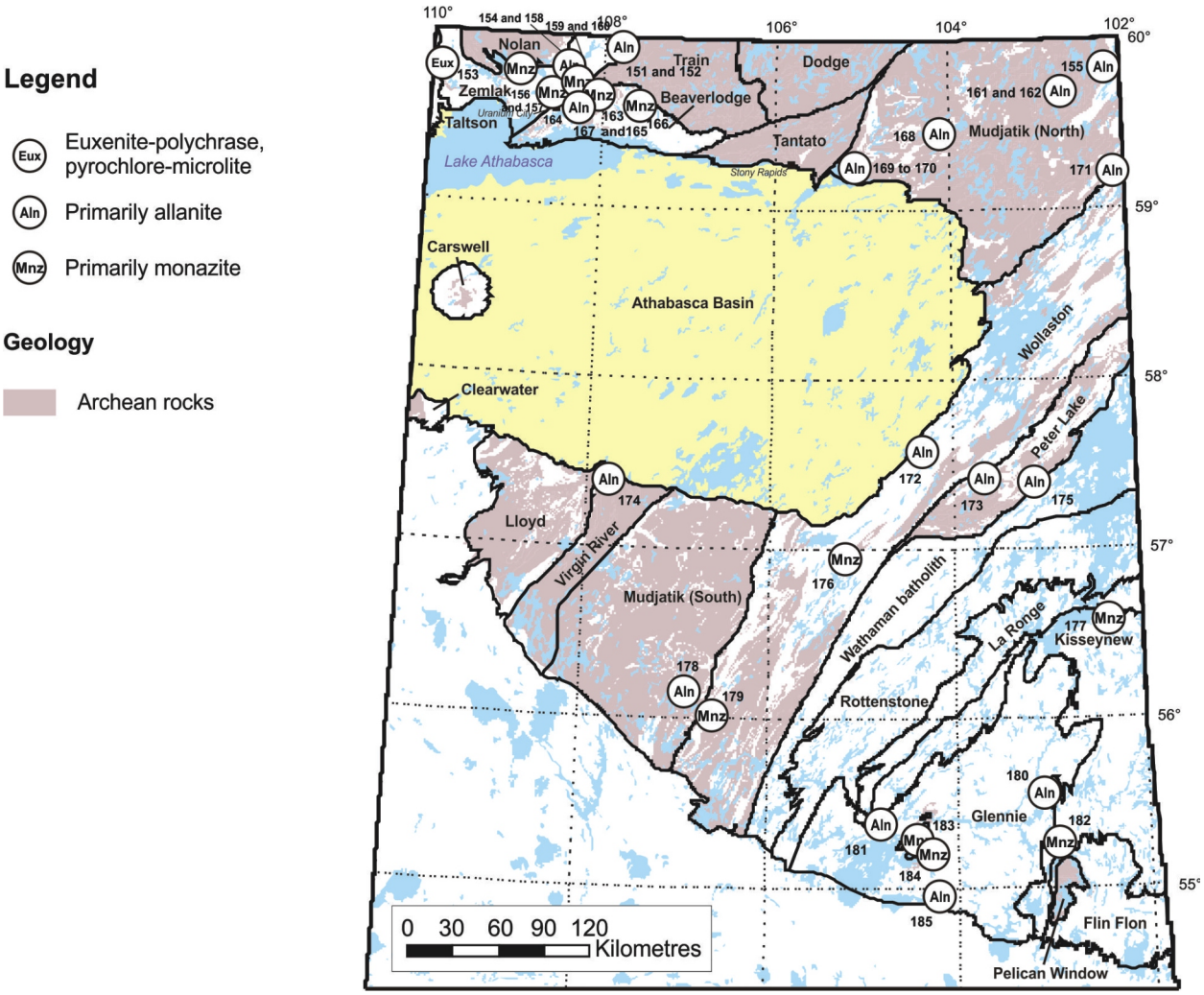

Figure 6 – Rare earth element mineral locations in the Precambrian Shield of Saskatchewan. Proterozoic sedimentary rocks of the Athabasca Basin are shown in light yellow. Areas in grey show the distribution of Archean rocks and domains are labelled. Numbers beside location symbols refer to the 'Location #' column in Table 6.

rocks containing more readily soluble REE-bearing minerals such as allanite, U-rich minerals, or apatite. The near absence of REE anomalies in lakes surrounded by supracrustal metasedimentary rocks in northern Saskatchewan[12], despite the widespread presence of monazite in those rocks, and concentration of anomalies where orthogneiss predominates may constitute evidence for this. A detailed description of the most significant LREE-dominant mineralization in Saskatchewan is given below.

Monazite-Dominant Mineralization

Monazite-dominant mineralization almost invariably occurs in or close to upper amphibolite– to granulite-facies clastic metasedimentary rocks, suggesting that these rocks may have provided the source for the REE. Monazite is locally the only REE-rich mineral in this mineralization. Minor to trace amounts of retrograde allanite+apatite, primary allanite, REE carbonates, and xenotime are reported from some locations. Zircon, thorianite, and thorite are commonly present as major to trace constituents. Apatite is an important mineral associated with monazite and Fe and Ti oxides in at least one occurrence. The mineralization can be subdivided into three types based on mineral assemblages and geological setting: 1) mineralization in which monazite is associated with a biotite-rich paragenesis; 2) mineralization in which monazite is associated with major proportions of ilmenite and minor to trace

[12] Based on the National Geochemical Reconnaissance (NGR) lake-sediment data for Saskatchewan (Hornbrook and Friske, 1988a, 1988b, 1988c; Friske *et al.*, 1994a, 1994b).

biotite; and 3) pegmatite-associated mineralization in which monazite is associated with major proportions of Fe and Ti oxides, and apatite.

For the most part — and this is undoubtedly related, in part, to concentration of exploration activity in specific sectors of the province — the monazite-rich mineralization appears to be clustered in the Beaverlodge and Wollaston domains. In the Beaverlodge Domain, known LREE-dominant mineralization is closely associated spatially with the contact between Archean rocks and Paleoproterozoic supracrustal packages consisting of quartzite, amphibolite, psammite, psammopelite, and pelite that probably belong to the Murmac Bay group. Similarly, the mineralization occurs in pelitic to psammitic Paleoproterozoic supracrustal rock packages near the contact with Archean windows in the Wollaston Domain. They are aligned along the axial trace of regional folds, notably along a 135 km stretch between Way Lake and 'Pipewrench Lake' (unofficial name)[13], or disseminated near the boundary between the Wollaston and Mudjatik domains (Figure 7). The best examples of each monazite-dominant mineralization type (local presence of >10% monazite) are the Alces Lake and Oldman River occurrences (type 1), the Archie Lake occurrence (type 2), and the Kulyk Lake occurrence (type 3). A brief description of these deposits is provided in this section.

Type 1: Mineralization in which Monazite is Associated with Biotite-Rich Parageneses

Radioactive monazite (±xenotime) mineralization associated with biotite-rich segregations in migmatitic gneiss and granitic to syenitic pegmatites has been recognized in many parts of the world (Schaller, 1933; Davidson, 1956; Young and Sims, 1961; Evans, 1964; Marchenko and Goncharova, 1965; Nechayev and Kononov, 1965; Haapala *et al.*, 1969). In northernmost Saskatchewan, elevated monazite concentrations, up to 20% by volume, in biotite-rich segregations were reported from a number of locations by Robinson (1955). "Common" monazite was reported by Ford (1955) from biotite-rich selvages bordering the Jahala Lake pegmatite located in the Glennie Domain. Mawdsley (1954) previously reported monazite crystals measuring up to 1.3 cm from the same locality but from an intermediate zone of the pegmatite, not the selvages.

Harper (1987) reported that biotite-rich segregations containing monazite in Saskatchewan occur in pegmatites or restites in gneisses of high metamorphic grade. More specifically, Harper (1986) noted that relatively quartz-poor white pegmatites containing biotite-rich segregations with monazite occur in the Nevins Lake–Forsyth Lake area. McKechnie *et al.* (2012b) described biotite-rich zones (up to 90% biotite) at the margin of pegmatites (their group B pegmatites) in the Fraser Lakes area of the Wollaston Domain that contain 1 to 2% monazite crystals measuring up to 1.1 mm in diameter. These monazite crystals have chemical ages that predate the emplacement age of the host pegmatites by >250 m.y., based on chemical ages obtained from electron microprobe analysis of uraninite from a different set of pegmatites (group B pegmatites in McKechnie *et al.*, 2012b). The monazite chemical ages are older than the youngest detrital zircons contained in Wollaston Group rocks, and inheritance from the host sedimentary succession was proposed to explain their origin.

There are considerable variations in textural and structural relationships between monazite associated with biotite-rich segregations and the hostrock. These relationships are summarized in what follows from the author's field observations (Normand, 2010a, 2010b, 2011a, 2011b, 2012, 2013) and literature descriptions. Some biotite-rich zones (>40% biotite by volume) containing significant concentrations of monazite (>1% by volume, corresponding to greater than ~0.5% by weight) were observed or described in, or at the contact of, granitic pegmatites. Other biotite-rich zones occur as layers without apparent association with intrusive rocks but invariably in high-grade metamorphosed sedimentary rocks. Biotite-monazite–rich zones associated with intrusive rocks range from thin, discontinuous selvages close to, or at the margin of, variably deformed granitic pegmatites; to extensively developed zones where only a few pegmatitic feldspar remnants are observed; to late interstitial masses of small- to medium-size crystals between large feldspar crystals in pegmatites; to coarse- to fine-grained assemblages filling fractures in cataclastic breccias affecting pegmatites; to infillings in fracture/shear zones that cut the pegmatites. Pegmatites and biotite-monazite–rich zones may be parallel to the regionally developed gneissosity or crosscut it, suggesting formation at different times (and by different processes?) during tectonic evolution of the areas where REE mineralization occurs. In all cases where monazite (and very rarely xenotime) is present, the modal abundances of the mineral are correlated with that of biotite, although small proportions also occur in feldspar and other phases. In this type of mineralization, monazite appears mostly in biotite as anhedral to euhedral, poikiloblastic or embayed, and inclusion-rich to inclusion-free crystals.

[13] Unofficial settlement and lake names will appear in single quotation marks when first mentioned. The quotation marks will be subsequently dropped.

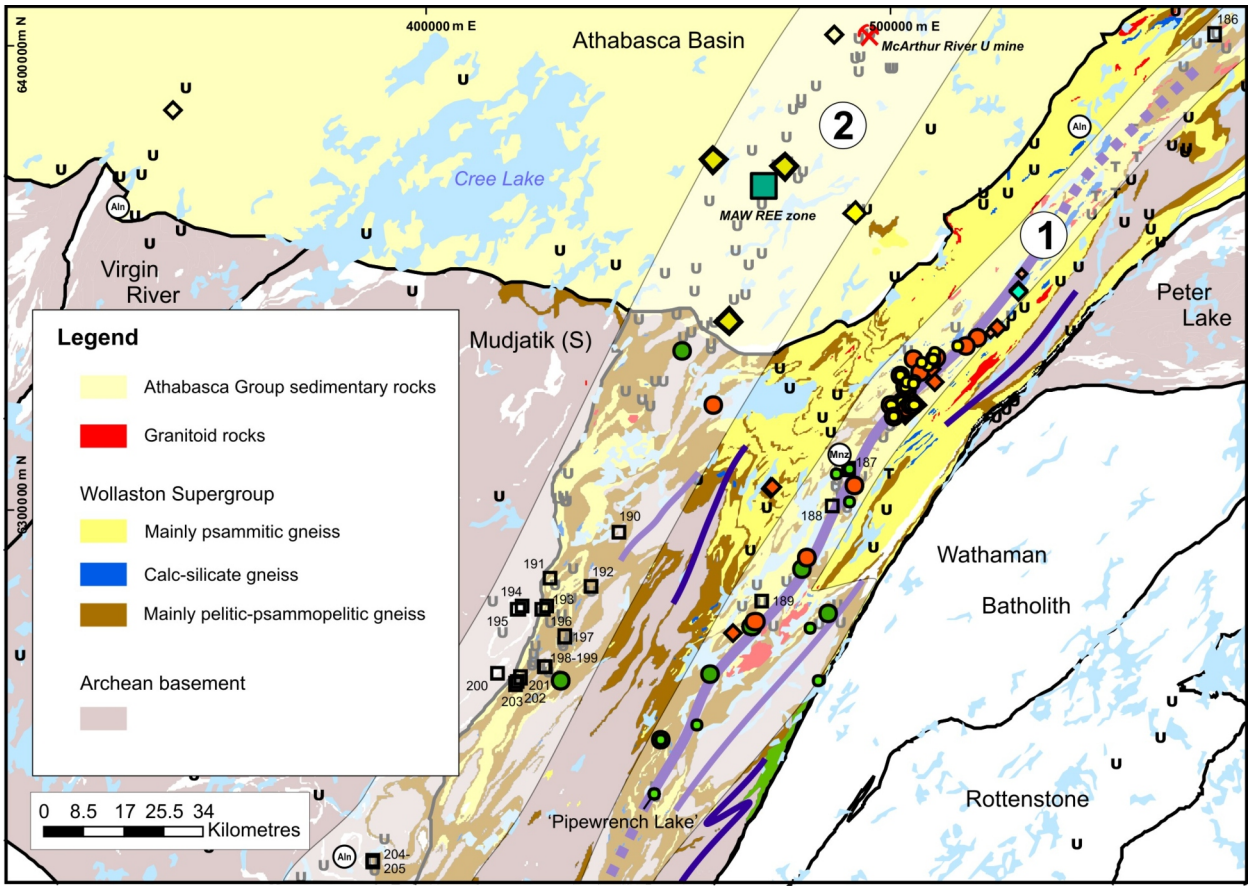

Figure 7 – Distribution of REE prospects, occurrences, bedrock geochemical anomalies, and mineral locations in the southern part of the Wollaston Domain and adjacent Mudjatik Domain and Athabasca Basin. Filled circles correspond to LREE-dominant mineralization illustrated in Figures 3, 4, and 5. Filled diamonds correspond to the location of intrusion-associated (shades of red), vein-type (light green), and unconformity-related (shades of yellow) U mineralization enriched in HREE (discussed in the "Mineralization in which THREE+Y(±Sc) Constitute >20% of the TREE" section; see Figures 12, 13 and 14). The filled square (green) corresponds to the MAW REE zone (discussed in the "Mineralization in which THREE+Y(±Sc) Constitute >90% of the TREE" section; see Figure 28). Filled symbol sizes and colours are explained in the captions of the figures. Open, numbered square symbols correspond to locations where samples containing elevated REE have been reported, but for which only partial data are available (Table 7). The mineralization is concentrated along two zones that parallel the regional, northeast-striking structural grain. The semitransparent overlay area labelled '1' corresponds to a zone of concentrated REE mineralization that lies approximately along the axial trace of a regional fold system (thick purple lines) in the Wollaston Domain. A large proportion of the mineralization is distributed along the perimeter of Archean inliers. The semitransparent overlay area labelled '2' corresponds to a zone of concentrated mineralization that lies along the boundary between the Wollaston and Mudjatik domains. U and T symbols correspond to U and Th mineralization in the SMDI database.

Elsewhere in the world, where field relationships are sufficiently clear to attribute an intrusion-associated, metasomatic origin to the biotite- and monazite-rich mineralization, this mineralization is usually developed in the form of a selvage at the margins of pegmatites (Korzhinskiy, 1955) or the margin of hydrothermal veins formed from fluids derived from the crystallization of plutonic rocks (*e.g.*, Schaltegger *et al.*, 2005). In other cases, biotite- and monazite-rich mineralization occurs in migmatites, and an association with intrusive igneous rocks is not always readily apparent.

Four models are generally proposed for the origin of the monazite-rich (>1% monazite by volume) mineralization that occurs in migmatized gneissic terrains: 1) as mechanical concentrations of detrital material, such as paleoplacers, later modified during metamorphism (Evans, 1964); 2) as refractory residues left after extensive anatexis in high-grade metamorphosed clastic sedimentary rocks (Wülser, 2009); 3) as magmatic-metamorphic and/or hydrothermal-metasomatic (re)concentrations in widely variable geological settings where multiple types of REE-rich assemblages may be present and monazite-rich mineralization may occur spatially or temporally separated from biotite-rich alteration (Young and Sims, 1961; Nechayev and Kononov, 1965; Grauch, 1989, top of p160; Aleinikoff and Grauch, 1990; Chao *et al.*, 1992; Tao *et al.*, 1996; Gillerman, 2008; Lund *et al.*, 2011;

Table 7 – Other locations where partial assay results of interest for REE have been reported.

Location #	Name	Location[1]				SMDI #	Mineralization Type	Sample #	REE Data	U (wt. %)	Th (wt. %)	U/Th	References
		NTS Area	Easting	Northing	Domain								
186	Geikie River (island on)	64E/13	569588	6402349		1708		MKORR001	1.00 wt. % TREE	0.112	n. r.	ins. dat.	Eagle Plains Resources Ltd. (undated b)
187	Vee Lake (southwest end of)	74A/14	490900	6308725		1004		n. r.	0.45 wt. % TREO	3.731	n. r.	ins. dat.	Eagle Plains Resources Ltd. (undated a)
188	Marilyn Bay		487300	6300700		none		n. r.	0.61 wt. % TREO	n. r.	n. r.	ins. dat.	
189	Kotelmach Lake (Baska)	74A/11	472084.8	6280372.9	Wollaston	0978		TMKJR012	0.39 wt. % TREE	0.004	0.048	0.0756	SME Assessment File 74A11-0052
190		74A/13	441497	6295108		none	Intrusion-associated	11532 (boulder)	0.07 wt. % La	0.003	0.047	0.0572	
191			426555	6285370		none		11652 (boulder)	0.20 wt. % La	<0.0001	0.133	<0.0008	
192			435570	6283459		near 1964		11554	0.08 wt. % La	0.034	0.067	0.5111	
193			425946	6279311		none		11603	0.11 wt. % La	<0.0001	0.123	<0.0008	
194			420682	6279245	Mudjatik (S)	none		11567	0.21 wt. % La	<0.0001	0.171	<0.0006	SME Assessment File 74B-0003
195			419838	6278630	Mudjatik (S)	none		11566 (boulder)	0.16 wt. % La	0.070	0.211	0.3336	
196	Key Lake road	74B/09	425124	6278517		none		11606	0.33 wt. % La	<0.0001	0.281	<0.0004	
197			429817	6272761	Wollaston	near 2010	Metamorphic/metasomatic?	11614	0.24 wt. % La	<0.0001	0.219	<0.0005	
198			425677	6266111		1962	Metamorphic/metasomatic?	11908	0.09 wt. % La	0.040	0.061	0.6511	
199			425661	6266100		1962	Intrusion-associated	11907	0.09 wt. % La	0.012	0.066	0.1837	
200			415280	6264824	Mudjatik (S)	none		H-05-12	0.60 wt. % La	<0.0001	0.208	<0.0005	SME Assessment File 74B09-0030
201			420306	6263842		none	Metamorphic/metasomatic?	17052	0.15 wt. % La	5.300	0.673	7.8752	
202			419663	6262953	Wollaston	none	Intrusion-associated	17013	0.08 wt. % La	0.045	0.089	0.5020	SME Assessment File 74B-0003
203		74B/08	419205	6262463		none		17001	0.07 wt. % La	0.043	0.089	0.4759	
204	Cup Lake (Rod)	74B/02	388514	6224382	Mudjatik (S)	1958	Clastic sediment–hosted U-Cu-Ni-As	0446	1.27 wt. % TREO	n. r.	n. r.	ins. dat.	Rare Earth Minerals PLC (2011)
205	Cup Lake (George)		388491	6224197		1930	Clastic sediment–hosted Uranium	0457	1.23 wt. % TREO	n. r.	n. r.	ins. dat.	

[1] All location co-ordinates given in UTM Zone 13N, NAD 83.
Other locations where boulders containing elevated REE concentrations (up to 2.8 wt. %) have been reported from the north side of Wollaston Lake are described in SME Assesment File 64L05-NE-0163.
Abbreviations: ins.dat., insufficient data; n. r., not reported; S, south.

Razafymahatratra and Montel, 2011); and 4) as magmatic accumulations in intrusive rocks (Hogge *et al.*, 2010)[14]. Grauch (1989) advanced the possibility that monazite-rich (La+Ce+Pr+Nd > 100 000 × chondrite) biotite schist from the Ruby Mountains, Nevada (Snoke *et al.*, 1979) could have originated from phosphorus-rich sediment that acted as a sink for REE. From North Carolina, Schaller (1933) reported a remarkable example of intrusion-associated monazite mineralization in a 'mica'-rich zone. He described a <4.6 m wide pegmatite dyke near Asheville that had a 0.3 m wide selvage composed of dark green mica in which a layer ranging from 2.5 to >10 cm thick contained 35% monazite (>2 mm in diameter) in single crystals measuring up to 31.5 cm in diameter and weighing up to 27 kg.

A model of hydrothermal-metasomatic development of certain biotite-monazite–rich zones observed in migmatized clastic metasedimentary rocks and white pegmatites of the Beaverlodge and Zemlak domains could involve the cooling of fluid emanations exsolved from solidifying, regionally distributed, granitic melts previously residing in the H_2O-barrier zone of the crust (Touret and Huizenga, 2011) along decompression/cooling loops of P-T-t paths[15]. It is speculated that such fluids may collect and flow preferentially along relatively permeable zones (*e.g.*, contacts between rock types of contrasting rheology, shear zones) to eventually form alteration zones characterized by large time-integrated fluid fluxes (*e.g.*, Ferry and Gerdes, 1998; Sassier *et al.*, 2006; Ague, 2011), which can be alleviated by the presence of anionic ligands, such as chloride, that promote mass transport of Mg and Fe (Vidale, 1983; Yardley, 2013). Preliminary calculations with winTWQ (version 2.34; Berman, 1991, 2007), using water properties from Haar *et al.* (1984), the hkf81.aqu thermodynamic database for aqueous species[16], and the DEC06.DAT thermodynamic database for solids, in the system KFMASH predict that biotite should be the stable K-silicate phase forming along a disequilibrium ($(a\mathrm{Mg}^{2+})/(a\mathrm{H}^{+})^2$ kept high) cooling path initiated from K-feldspar+biotite equilibria above ~575° to 600°C and ~2 to 5 kbars (below these temperatures, K-feldspar would be the stable phase).

To the best of the author's knowledge, few deposits in the world that fall in this broad category have received sufficient assessment to provide resource estimates. At Olserum, Sweden, a metamorphosed and metasomatized psammitic to pelitic sedimentary succession of Precambrian age contains apatite (containing 0.5 to 1.2% TREO)–monazite–xenotime mineralization associated with biotite–amphibole–iron oxide–rich horizons in quartzite that are believed to represent a modified placer deposit. Recent development work on the deposit by Tasman Metals Ltd. provided a drill-defined, NI 43-101–compliant Indicated Resource estimate of 4 500 000 t grading 0.60% TREO (0.4% cut-off), 34% of which is represented by HREO+Y_2O_3, including 210 ppm Dy_2O_3. An NI 43-101–compliant Inferred Resource estimate of 3 300 000 t grading 0.63% TREO, 34% of which is likewise represented by HREO+Y_2O_3, including 220 ppm Dy_2O_3, was also drill defined (Reed, 2013). Biotite-monazite–rich zones in group B pegmatites of the Fraser Lakes zone B deposit (McKechnie *et al.*, 2012b) probably contribute a major proportion of the LREE in the NI 43-101–compliant Inferred REO Resources of the deposit (Armitage and Sexton, 2012).

The most important mineralization in Saskatchewan, in terms of monazite concentration, in which monazite is associated with a biotite-rich paragenesis are the Alces Lake and Oldman River occurrences, where ≥20% monazite has been reported locally in zones largely composed of biotite (Robinson, 1955; Normand, 2010a, 2011a). A detailed description of these two deposits follows.

Alces Lake Monazite Occurrence (SMDI #1283 and #1453; Locations 3 to 6, Table 3 and Figure 3)

The occurrence is located 35 km east-northeast of Uranium City and 2 km south of Alces Lake in the Beaverlodge Domain. Monazite was first tentatively identified at this location by J.H. Wilson, who described the occurrence in 1954 (SME Assessment File 74N09-0020). Monazite-rich mineralization was exposed in a number of trenches and reported by Wilson to occur in a north-trending, biotite-rich segregation band in granitic gneiss measuring 1.2 to 1.8 m wide and ~91 m long. Numac Oil and Gas Ltd examined the occurrence in 1966 (SME Assessment File 74N-09-NE-0077) and reported strong counts in a zone measuring 2.4 m wide and 61 m long, and striking 140° and dipping 80° in massive biotite-garnet schist. A sample sent for assay returned 2.91% ThO_2 (2.56% Th), 0.04% Y_2O_3 (315 ppm Y; erroneously reported as YO_2), 0.046 and 0.03% U_3O_8 (390 to 254 ppm U), and <15 ppm Sc. Assay results for REE other than Y and Sc were not reported.

The author visited the occurrence and confirmed the presence of the monazite-rich mineralization described by Wilson (Normand, 2010a). Mineralization with abundant monazite was observed in an area measuring ~300 m by 50 m in heavily overgrown terrain where bedrock is poorly exposed. In many cases, mineralization was localized

[14] Bruns (2011) suggested the possibility of an origin from fenitization. Could there be a vaugnerite/durbachite affiliation?
[15] Assuming all water is not consumed in retrograde reactions.
[16] Note that there is no demonstrated internal consistency between the solids and aqueous species databases. Further testing, using other thermodynamic databases (*e.g.*, Holland and Powell, 1998), is needed.

using a handheld spectrometer and topsoil up to 30 cm thick had to be removed to expose mineralized bedrock. Monazite-rich zones were observed in quartzite, in interlayered paragneiss and garnet diatexite, and at the contact with red, coarse-grained, plagioclase-rich, and quartz-poor leucocratic gneiss structurally above the quartzite. A layer of amphibolite ranging from <90 to 100 m thick is reported to be present (Blake, 1955) in the immediate vicinity of the mineralization, between the quartzite and other rock types described above. All these rock units have been subjected to upper amphibolite– to granulite-facies metamorphism and have been affected by four phases of folding (F_1 to F_4 of Bethune *et al.*, 2013). Mineralization is located on the eastern limb and close to the hinge of a truncated, south-plunging (moderate) open fold (Normand, 2010b; Figure 8). The monazite mineralization coincides with an airborne radiometric anomaly measuring ~450 m in length. The anomaly is the strongest of the entire survey, which was part of an airborne multisensor geophysical survey of NTS area 74N, Tazin Lake (joint Saskatchewan Geological Survey–Geological Survey of Canada effort; Carson *et al.*, 2001). The survey recorded another anomaly measuring 300 m in length along the same flight line ~1 km to the southeast of, and in structural continuity with, the Alces Lake occurrence.

Three types of monazite mineralization were identified at the occurrence. Together, these three types form an ensemble that was recognized over a strike length of 300 m. In the first type, minor monazite is common in biotite-rich replacement zones that affect deformed pegmatitic granitoids. These pegmatitic granitoids are commonly creamy-grey in colour, show strong cataclasis, and are quartz poor. The most interesting such style of monazite mineralization occurs in a quartz-poor, foliation-parallel, tightly spaced group of white pegmatites, measuring <2.5 m wide and >40 m in strike length, in a thick quartzite unit near its upper contact with garnet diatexite and

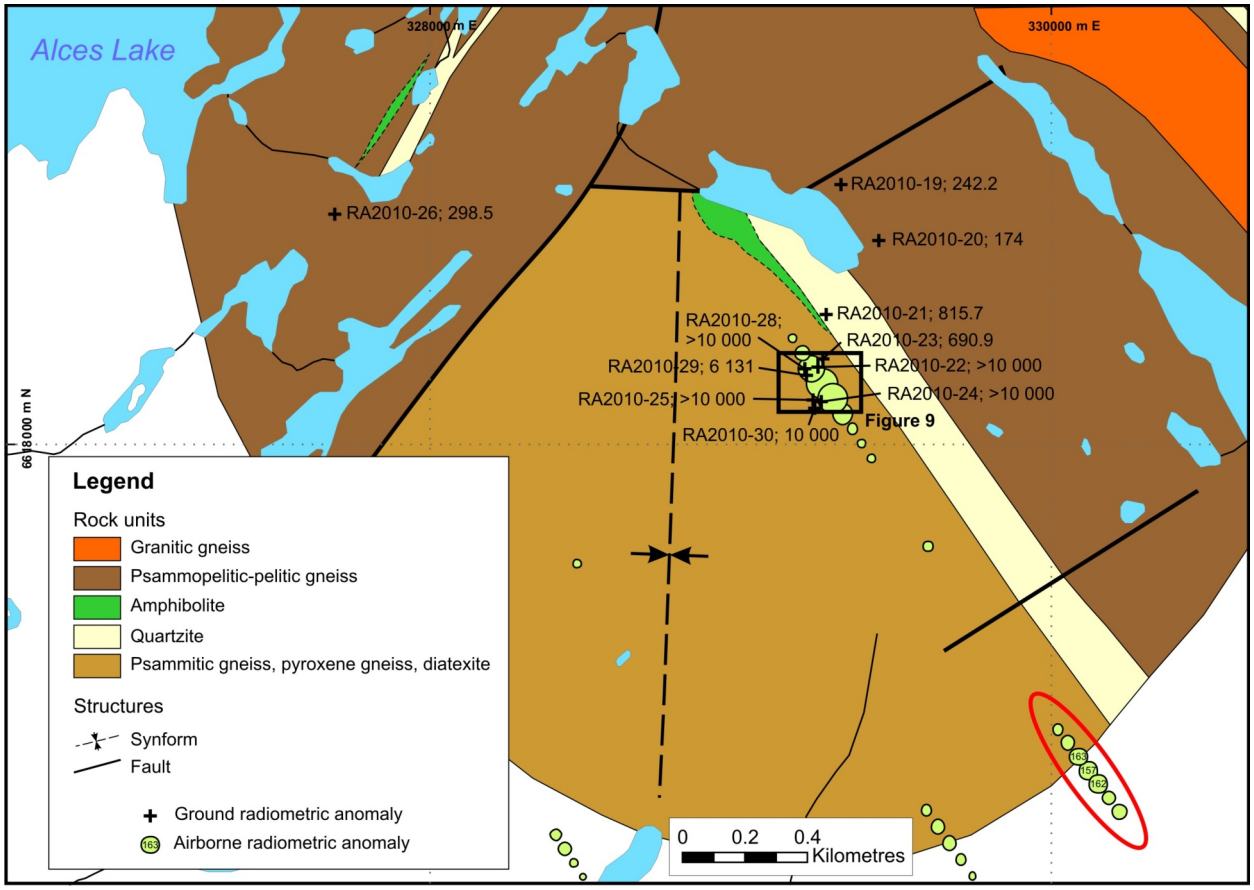

Figure 8 – Geology of the Alces Lake monazite occurrence area (modified after Blake (1955) and Normand (2010a)). Biotite-monazite–rich mineralization (RA2010-21 to -30) is located on the eastern limb of a fault-truncated synform cored by high-grade rocks of possible Archean age. The synform is enveloped by a sequence of quartzite, amphibolite, and psammopelitic to pelitic gneisses believed to correlate with rocks of the Murmac Bay group (Bethune* et al.*, 2013). If so, the outward sequence of rocks from the axial trace of the synform suggests that the units are overturned. Airborne radiometric equivalent Th (eTh) recording stations for values >50 are shown by light green–filled symbols. The data were collected as part of an airborne multisensor geophysical survey of NTS sheet 74N, Tazin Lake (joint Saskatchewan Geological Survey–Geological Survey of Canada effort; Carson* et al.*, 2001). The highest values of the entire survey coincide with the highly radioactive ground anomalies.

paragneiss (RA2010-21; Figure 8). The pegmatites are very coarse grained, are composed mainly of alkali feldspar, contain <10% quartz, and have a colour index of <5. Contacts between pegmatites and quartzite are sharp. Zones of cataclasis/breccia, comprising a biotite filling rich in monazite crystals measuring <1 mm in diameter, affect portions of the pegmatites. Bulk-rock analysis of a representative sample of mineralized breccia from that location returned 0.36 wt. % TREE and 550 ppm Th, equivalent to ~0.7% monazite by weight.

The second type of monazite mineralization consist of layers, measuring <30 cm thick, that show rough asymmetric mineral zoning at the contact between red, coarse-grained, plagioclase-rich, quartz-poor leucocratic gneiss and garnet diatexite and paragneiss (RA2010-22, -28, and -29; Figures 8 and 9). The layers tend to be biotite-allanite-pyrite rich toward the red gneiss contact and garnet rich (~60% garnet, 3 to 4 mm in diameter) toward the paragneiss contact. Layers or lenses composed of 80 to 95 vol. % monazite and measuring 1.0 to 2.5 cm in thickness occupy an intermediate position. Triple-grain junctions at 120° to one another are common between the monazite crystals that show evidence of grain reduction (mean grain size 0.36 mm, n = 102; compare with third type below; zoning in single crystals commonly truncated and abutting crystal edges). Late, retrograde chlorite replaces both biotite and garnet, and allanite rims monazite. The monazite is of the Ce-dominant variety and contains <1 wt. % of each of Si and Ca (*i.e.*, low proportions of the huttonite and cheralite components in solid solution), <0.47 wt. % Gd, and an average of 0.25 wt. % Y, 7.24 wt. % Th, 0.34 wt. % U, and 0.52 wt. % F (n = 20; Normand, unpublished wavelength-dispersive electron microprobe analysis). Bulk-rock geochemical analysis of a sample that represents the full width (~12 cm) of a contact zone layer at anomaly RA2010-22 (Figure 9) returned 17.6 wt. % TREE (Table 3) and 2.4 wt. % Th, equivalent to ~33% monazite by weight.

The third and most important type of monazite mineralization, in terms of width and concentration of monazite, is located in biotite-rich layers, up to 2 m wide, exposed in two old rock trenches (RA2010-25 and -30; Figure 9), 27 m apart on the western side of a narrow valley that corresponds to a SPOT satellite-image lineament. The area is heavily covered by bush and poorly exposed, and only hangingwall contacts of the mineralization with paragneiss are visible. These contacts parallel the regional gneissosity. The bottom parts of the trenches are filled with blocks

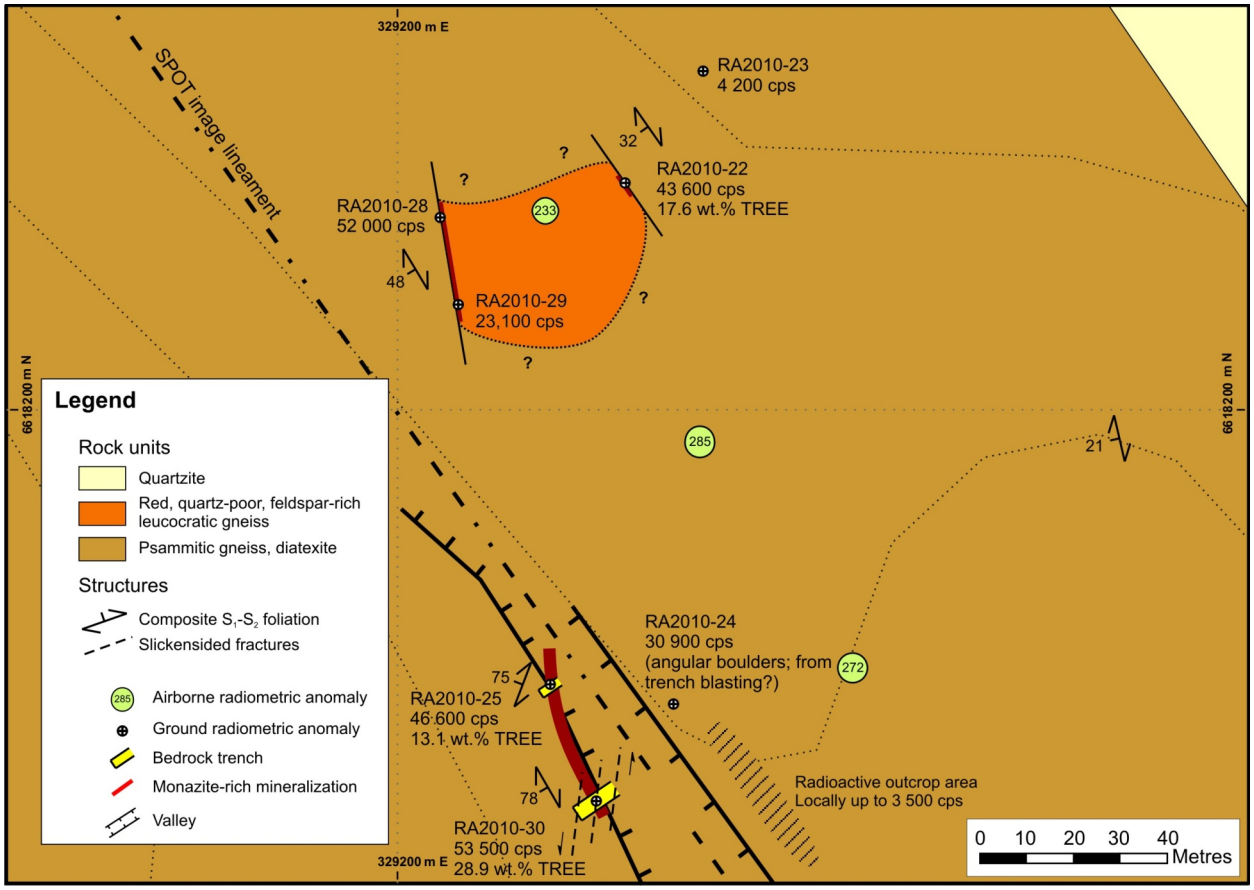

Figure 9 – Detailed geology of the outlined area on Figure 8. See text for discussion.

of blasted, mineralized, biotite-rich rock measuring up to 1 m in diameter. Radioactivity is very high in the trenches, and >20 000 total counts per second were recorded by an RS-230 spectrometer held at waist level while standing up. By visual inspection *in situ* and polished thin-section examination, the biotite-rich, chlorite-altered material was estimated to contain an average of 15 to 20 vol. % orange, subhedral to euhedral crystals measuring 0.1 to 1.8 mm in diameter (mean 0.58 mm; median 0.53 mm; n = 100). Variably chloritized biotite is typically present in proportions varying between 40 and 60 vol. % of the mineralized rock, and decreases locally where monazite is abundant. Coarse-grained, altered feldspars represent between 15 and 20 vol. % of the rock. Fe and Ti oxides, epidote-allanite, and zircon occur in minor to trace proportions. The composition of monazite in this type of mineralization is similar to that of the previous Ce-dominant variety, containing <1 wt. % of each of Si and Ca, <0.57 wt. % Gd, and averaging 0.28 wt. % Y, 7.07 wt. % Th, 0.35 wt. % U, and 0.51 wt. % F (n = 84; Normand, unpublished wavelength-dispersive electron microprobe analysis). Chemical analyses were obtained for two samples from the trenches. Concentrations of 13 and 29 wt. % TREE, and 1.8 and 3.5 wt. % Th (equivalent to 26 and 53% monazite by weight) were obtained from anomalies RA2010-25 and RA2010-30, respectively. Bulk-rock analyses of samples of types 2 and 3 monazite mineralization show strong negative Eu anomalies (Eu/Eu* of 0.04) and elevated La_N/Yb_N values (914 to 1498; Table 3). Heavy rare earth elements and Y represent <3% of the TREE in all samples analyzed, and Th/TREE ratios vary between 0.12 and 0.15 (Table 3).

Monazite shows strong evidence of alteration by fluids during late deformation events. Allanite, an unidentified REE carbonate, and unidentified Th and U silicates, galena, thorianite, and uraninite were all observed as replacement products of monazite at Alces Lake using scanning electron microscopy aided by energy-dispersive X-ray analysis. Such replacement is usually interpreted to result from a dissolution-(re)precipitation process (Cherniak *et al.*, 2004; Hetherington and Harlov, 2008; Putnis, 2009). This fluid-assisted recrystallization process was accompanied by Pb loss, similar to that shown for monazite at other localities in the world (Teufel and Heinrich, 1997; Ayers *et al.*, 1999; Crowley and Ghent, 1999), and is illustrated by calculated chemical ages that decrease sympathetically with decreased Pb contents, from 2120 Ma (8015 ppm) to 63 Ma (150 ppm). Remobilization appears to have occurred at a local scale, however, such that the bulk chemical and, by inference, radiometric U/Th signature of the occurrence was probably not modified significantly.

Although structural and textural evidence suggest a metasomatic-hydrothermal origin for type 1 monazite mineralization (and the associated biotite), the origin of types 2 and 3 monazite mineralization is less evident. Field relationships indicate that types 2 and 3 monazite mineralization are coeval and were formed, or deformed, during high-grade metamorphic events related to D_1 and/or D_2 in the Beaverlodge Domain. Normand (2010a) tentatively interpreted type 3 monazite mineralization to represent modified restitic material, largely based on textural relationships involving zircon. The concentration mechanism of monazite in type 2 mineralization is unknown. Concentration in a residue by anatexis *in situ* would require the protolith to have been exceptionally rich in monazite. Neglecting solubility and physical entrainment of monazite in the separated, rising melt, simplistic calculations show that, for extreme melting of up to 95% accompanied by 100% effective extraction of the liquid, >1 vol. % monazite would have to have been originally present in the protolith of type 2 or type 3 mineralization. Rare layers in some modern placers thought to have been enriched by tidal currents and storm-wave action are reported to have contained locally >30 and up to 90 vol. % monazite (Overstreet, 1967). Those local occurrences, however, are invariably situated within larger placer districts where ilmenite and other Fe and Ti oxides are vastly more abundant than monazite. The author is not aware of any report of ilmenite- or iron oxide–rich rocks, or extensively occurring metamorphic-equivalent silicate-facies iron formations, in the vicinity of the biotite-monazite–rich occurrences discussed here.

The position of the mineralization immediately below a perceived interface, probably an unconformity, between basal Murmac Bay group quartzite-amphibolite and underlying, potentially much older rocks, raises the possibility that pre-enrichment in monazite of these older rocks may have resulted from eluvial accumulation on saprolitic bedrock or colluvium deposits developed on comparatively Fe-Ti-oxide– and xenotime-poor bedrock. The strong negative Eu anomalies shown in bulk-rock analyses of monazite-rich samples and elevated Th concentrations shown in electron microprobe analyses of the monazite preclude a low-temperature, diagenetic/authigenic (Rosenblum and Mosier, 1983; Cabella *et al.*, 2001; Schandl and Gorton, 2004) origin for the monazite. Isotopic dating of U-bearing minerals (*e.g.*, zircon and monazite) in barren hostrock and mineralized zones should help to shed light on the origin of the monazite in the three types of mineralization.

Oldman River Monazite Occurrence (SMDI #1332; Location 7, Table 3 and Figure 3)

The occurrence is located 6.63 km south-southwest of the Alces Lake monazite occurrence, on the north and south banks of the Oldman River between Forget and MacRae lakes. Robinson (1955) reported up to 20% monazite crystals measuring between 0.2 and 1 mm in diameter from the locality, hosted by a band of massive, coarse-grained

biotite gneiss locally containing knots or phenocrysts of microcline and quartz, and suggested that this band may represent a segregation associated with granitic pegmatite. Results of a partial analysis of the monazite provided by Robinson (1955) include 5.4% Th, 0.263% U, and 0.5% Pb. Massive pyrite was also reported to occur interstitially to the monazite and biotite. No recent age data are available for the mineralization. Robinson (1955) reported a 2220 Ma $^{207}Pb/^{206}Pb$ age for a monazite concentrate from the occurrence, and much younger $^{207}Pb/^{235}U$ and $^{206}Pb/^{238}U$ ages (1780 and 1450 Ma, respectively). Using the partial analysis data reported above, the author has calculated a chemical age of 1730 Ma.

Mapping in the area in 2010 (Normand, 2010a, 2010b) revealed that the mineralization is confined to strongly migmatized psammitic gneiss mixed with various generations of granitic rocks, including pegmatites. Mineralization was found to be highly localized and scattered over a strike length estimated at between 400 and 500 m immediately above (current structural position) an ~40 m thick layer of amphibolite, and ~150 m from the contact with Murmac Bay group quartzite (Figure 10). The mineralized biotite-rich layers at this locality are generally <10 cm, and rarely ~30 cm, in thickness.

Mineralization at this occurrence shares similar structural and textural characteristics with those observed at anomaly RA2012-39, located near the southern shore of Nevins Lake (Normand, 2012, 2013). At both locations, the monazite-bearing, biotite-rich zones crosscut white pegmatites that were emplaced immediately following, or postdate by an unknown amount of time, an early, composite, S_1-S_2 gneissosity developed during D_1-D_2 events correlated with the 1940 to 1930 Ma Taltson orogeny (Bethune *et al.*, 2013). The presence of an S_4 fabric that crosscuts the monazite-bearing, biotite-rich zones indicates that their formation predates the 1910 to 1900 Ma Snowbird D_4 event (D_4 of Bethune *et al.*, 2013).

Most biotite-monazite–rich mineralization in the Beaverlodge and Zemlak domains occurs within 300 m, and as close as a few metres but rarely in, amphibolite near mixed amphibolite-quartzite layers that form the base of the

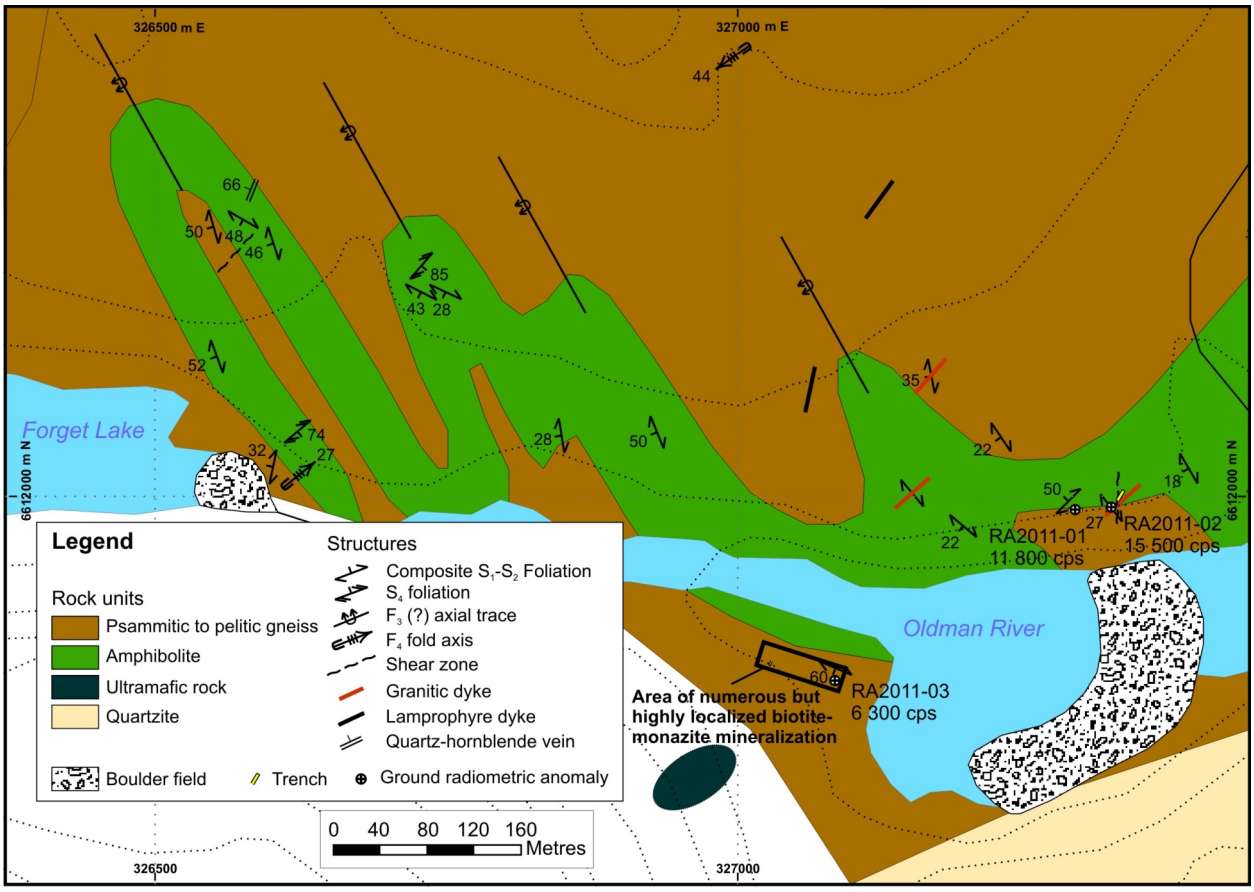

Figure 10 – Geological setting of the Oldman River monazite occurrence. In contrast to the Alces Lake occurrence, biotite-monazite–rich mineralization is hosted by strongly migmatized Murmac Bay group psammopelitic gneiss structurally above a generally south-dipping, 40 m thick amphibolite layer and ~150 m from the contact with quartzite.

Murmac Bay group supracrustal rocks. Rich monazite mineralization in euhedral crystals measuring up to 7 mm in diameter is known to occur in biotite segregations within white pegmatites that cut amphibolite at location 22 (Table 3, Figure 3) near the north end of Schaffer Lake (Normand, 2011a, 2011b) and "showing" 50-TT-62 of Goldfields Uranium Mines Ltd. (Robinson, 1955; location 164, Table 6 and Figure 6).

Type 2: Mineralization in which Monazite is Associated with an Ilmenite (±Fe Oxide)–Rich Paragenesis

Mineralization of this type is apparently very rare in Saskatchewan, and only two are known to exist. In one, the Kulyk Lake monazite occurrence, apatite forms an important part of the mineralization and is hosted by a granitic pegmatite. A description of this deposit follows in the "Type 3: Pegmatite-Associated Mineralization in which Monazite is Associated with Fe and Ti Oxides and Apatite" section. The other deposit, known as the Trans Canada REE-U zone no. 2 or Archie Lake REE showing in the Saskatchewan Geological Survey SMDI database, contains only minor to trace amounts of apatite and is thought to represent a syngenetic accumulation of detrital monazite, or paleoplacer (SME Assessment Files 74O05-NW-0038, -0046, -0053, and -0059; Harper, 1986, 1987; Smith and Cathro, 2010).

Archie Lake Monazite Occurrence (SMDI #1552; Location 21, Table 3 and Figure 3)

The Archie Lake occurrence is considered to represent one of the largest potential monazite resources in Saskatchewan, and has recently been evaluated by Niocorp Developments Ltd. (formerly Quantum Rare Earth Developments Corp). The deposit is located 110 km west-northwest of Stony Rapids, 50 km east-southeast of Uranium City, and 1.6 km northeast of Archie Lake in the Beaverlodge Domain. It was discovered during U prospecting in the Archie Lake area between 1968 and 1970, following ground verification of airborne radiometric anomalies (SMDI #1552). High-grade monazite mineralization in the deposit was reported from a horizon measuring up to 5 m in width, oriented parallel to the regional structural grain and traced for 600 m along strike (Harper, 1983, 1986).

Historical trenching and sampling of the mineralized horizon yielded 0.1% to 15.7% TREO, very low U_3O_8 and high Th values (SME Assessment Files 74O05-0038, -0046, -0053, and -0059). More recently, values up to 29.3 wt. % TREE were obtained from chip samples collected from old trenches on the deposit (Smith and Cathro, 2010), consistent with reports of monazite concentrations locally reaching 50 vol. % (Harper, 1983). In September 2010, Quantum Rare Earth Developments Corp. (now Niocorp Developments Ltd.) announced the mobilization of field crews for a fall 2011 drill program at the deposit. The results of this work had not been released prior to the writing of this report (Quantum Rare Earth Developments Corp., 2011).

The geology of the Archie Lake area was described most recently by Harper (1983, 1986) and Normand (2011a, 2011b). The Archie Lake occurrence is located at the western edge of the Eastern Plutonic complex of Ashton *et al.* (2006b) which is of probable Archean age, near the possibly fault-bounded (Ashton *et al.*, 2007a, Figure 2) contact with psammopelitic gneiss that likely belongs to the Murmac Bay group of Paleoproterozoic supracrustal rocks (Ashton *et al.*, 2007a). In the area of Nevins Lake, Normand (2013) proposed that Murmac Bay group rocks represent an overturned limb of a pre-D_4 fold and lie in fault contact to the east with the Eastern Plutonic complex.

Two rock units that correlate with the Eastern Plutonic complex of Ashton *et al.* (2006b) were described by Harper (1983, 1986) in the area of the Archie Lake deposit. They consist of garnet-feldspar gneiss (Harper's unit Fa) and hypersthene-feldspar gneiss (Harper's unit Fd). These units are probably equivalent to garnet-pyroxene granite (unit Egg) and pyroxene granite (Egp), respectively, that Ashton *et al.* (2006a) documented farther south. Both Harper (1983, 1986) and Ashton *et al.* (2006b) suggested an igneous origin (volcanic for Harper, 1986, and intrusive for Ashton *et al.*, 2006b) for the pyroxene-feldspar rocks and recognized that the more garnet-rich rocks, locally interlayered with rusty, cordierite-, sillimanite-, and graphite-bearing rocks, represent transitional rocks that may have formed from the mixing, through tectonic or other processes, of metasedimentary and igneous rocks. Cordierite, sillimanite, and graphite were not observed in 22 polished thin sections cut from 15 samples of the gneiss that host mineralization (Normand, unpublished data, 2012). This, however, would not be incompatible with a psammitic origin for the gneiss. A light grey, medium-grained, locally quartz-rich and garnetiferous granitic gneiss layer measuring ~65 m thick is present immediately to the west of the deposit, between the orthopyroxene+garnet feldspathic gneiss and the garnet-biotite-sillimanite-graphite psammopelitic gneiss farther west. Small lenses, <5 m thick, of this granitic gneiss are also present in orthopyroxene+garnet feldspathic gneiss in the area of the deposit. A red, medium- to coarse-grained, quartz-poor leucogranitoid rock is closely associated with, and cuts and incorporates fragments of, mineralized rock. It is not known if any relationship exists between this rock unit and similar brick red, quartz-poor, and feldspar-rich rocks present at the Alces Lake monazite occurrence.

Three phases of deformation that affected rocks in the Eastern Plutonic complex were recognized by Harper (1986). Evidence for the imprint of all three was observed in mineralized rock by Normand (2011a, 2011b). It is unclear, due to a lack of absolute age relationships, if first generation, east-striking isoclinal F_1 folds correlate with F_1-F_2 folds recognized to the west of the area (Bethune *et al.*, 2013). The second-generation, upright, northwest-trending axes and third-generation, upright, northeast-striking folds of Harper (1986), however, can be associated with the 1.93 to 1.94 Ga Taltson D_3 and 1.90 to 1.91 Ga Snowbird D_4 events of Bethune *et al.* (2013).

Based on the association of monazite with abundant ilmenite and zircon (Harper, pers. comm., 2011) and the stratabound nature of the mineralization, Harper (1983, 1986, 1987) proposed a syngenetic origin for the deposit. Heaman *et al.* (1999) suggested that an upper intercept U-Pb age of 2574 ±47 Ma obtained on discordant monazite from the deposit represents the original age of detrital monazite derived from erosion of Archean rocks. This age is significantly greater than the oldest age reported for the Murmac Bay group (2330 Ma; Ashton *et al.*, 2013), which, according to Normand (2011a, 2011b), occurs within 70 m to the west of the deposit. Unfortunately, no other U-Pb ages of any kind are available for rocks in the Eastern Plutonic complex. Within reported analytical uncertainties, the Archie Lake upper-intercept monazite age is indistinguishable from that of shielded monazite inclusions in garnet from an Archean diatexitic semipelite sampled 20 km east-southeast of the Archie Lake deposit (Bethune *et al.*, 2013), in the west-central plutonic rocks of Ashton *et al.* (2006b). Bethune *et al.* (2013) suggested an Archean metamorphic origin for this monazite that yielded a U-Pb SHRIMP age of 2566 ±8 Ma.

Mineralization at Archie Lake is relatively simple. The only REE mineral identified through preliminary examination of polished thin sections of the mineralization is monazite. Two broad types of monazite were recognized: 1) up to ~50 vol. % yellow-green, rounded crystals, measuring <600 µm in diameter, in semimassive lenses with variable proportions of ilmenite (up to 75 to 80 vol. % in some lenses, averaging 1 mm in diameter), zircon (<1 vol. %), and garnet in orthopyroxene+garnet+amphibole+biotite feldspar gneiss; and 2) red-brown, coarser crystals, measuring <1 mm, in biotite-rich fissure fillings associated with the red, quartz-poor, massive leucogranitoid rock. Based on bulk-rock geochemical data provided in Smith and Cathro (2010), the monazite mineralization at Archie Lake has similar negative Eu anomalies (Eu/Eu* of 0.07), but is depleted in U (U/Th of ~0.006) and HREE ((THREE+Y)/TREE = 0.6 to 1.0%) compared to monazite from biotite-rich mineralization elsewhere in the Beaverlodge and Zemlak domains.

Type 3: Pegmatite-Associated Mineralization in which Monazite is Associated with Fe and Ti Oxides and Apatite

Only one occurrence of this type is known to occur in the province: the Kulyk Lake monazite occurrence. The mineralization is not only unique to Saskatchewan, but appears to be unique globally for its mineralogy, its proportion of minerals, and its geological setting among Fe- and/or Fe-Ti oxide– and apatite-rich, intrusion-related or hydrothermal mineralization (*e.g.*, IOCG (or IOCG-like) deposits and nelsonites). The REE in these deposits are commonly contained in apatite and, where present, monazite usually occurs as fine inclusions in apatite and rarely (*e.g.*, Thor claim, Nevada; Garside, 1973) represents greater than a few modal percent of parageneses. Nelsonites are invariably associated with anorthosite and related rocks.

Kulyk Lake Monazite Occurrence (SMDI #0985; Location 74, Table 3 and Figure 3)

The occurrence was discovered in the Foster lakes area in the late 1960s by International Nuclear Corporation (SME Assessment Files 74A12-0005 and -0006) during U exploratory work. It is located on the eastern side of Kulyk Lake, about 122 km north-northwest of Missinipe and 65 km south of the Key Lake mine, in the Wollaston Domain.

According to Watkinson and Mainwaring (1976), and confirmed by McKeough *et al.* (2010, 2011a, 2011b) and McKeough and Lentz (2011), the occurrence consists of a small (<5 cm wide and 15 m long) vein/dyke with aplitic margins emplaced near the centre of an undeformed, <4 m wide, K-feldspar– and quartz-rich granitic pegmatite. The pegmatite intrudes calc-silicate paragneiss (McKeough *et al.*, 2011a, 2011b; McFarlane and McKeough, 2013b) of the Wollaston Supergroup (Yeo and Delaney, 2007), which forms part of the westernmost Trans-Hudsonian, 1.86 to 1.76 Ga fold belt (Annesley *et al.*, 2005; Yeo and Delaney, 2007; Schneider *et al.*, 2007).

The mineralogical composition of the phosphate-rich vein/dyke, provided by McKeough *et al.* (2011b) and McFarlane and McKeough (2013b), includes >50% subhedral to euhedral monazite (measuring 0.5 to 3 mm and averaging 2 mm, in diameter; Watkinson and Mainwaring, 1976), 30% apatite, 15% Fe-Ti oxides, <1% zircon, and trace feldspar. Quartz is absent. The ThO_2 concentrations in monazite, determined by electron microprobe analysis and reported by Watkinson and Mainwaring (1976), vary between 3.7 and 5.1 wt. %. McKeough *et al.* (2011b) reported 3 to 7 wt. % ThO_2. The SPI electron microprobe monazite standard AS1240-AB (SPI Supplies®, 2014)

from the locality is reported to contain 3.17 wt. % ThO_2 and <1.1 wt. % THREE+Y, but is enriched in Eu (1000 ppm) and shows a relatively small, negative Eu anomaly (Eu/Eu* = 0.46). Four bulk-sample analyses from the vein/dyke (SME Assessment File 74A11-0053) contain 7 to 22 wt. % TREE and present similar elevated Eu/Eu* values of 0.58 to 0.61 that are by far the highest among monazite-rich occurrences for which REE data are available in the province (Table 3). McFarlane and McKeough (2013b) reported lower Eu/Eu* values of 0.24 to 0.26. McKeough *et al.* (2011a, 2011b) suggested that the vein/dyke formed at a temperature between 750° and 850°C, based on quartz/mineral $\delta^{18}O$ fractionation thermometry. A temperature estimate of >850°C was reported by McFarlane and McKeough (2013b).

McKeough *et al.* (2011b) and McFarlane and McKeough (2013b) have shown that the monazite in the phosphate-rich vein/dyke is zoned with partially resorbed As-V–rich domains, dated at >1875 Ma, interpreted to represent possible authigenic monazite that grew in a metalliferous, pelitic sedimentary protolith of the basal Wollaston Supergroup (McFarlane and McKeough, 2013a, 2013b). McFarlane and McKeough (2013b) described a younger, *ca.* 1830 Ma overgrowth similar to monazite in the aplitic margin of the vein/dyke that they interpreted to have formed during emplacement. The proportion of older, inherited cores to that of overgrowth in the phosphate-rich vein/dyke was reported to be <20% by McFarlane and McKeough (2013b), suggesting that most of the monazite crystallized from a fluid (or melt). They reported Th concentrations in monazite, determined by laser-ablation inductively coupled plasma–mass spectrometry (LA-ICP-MS), of 2.2 to 4.4 wt. % (2.5 to 5.0 wt. % ThO_2) in core zones and 2.3 to 4.0 wt. % (2.6 to 4.6 wt. % ThO_2) in overgrowths.

The chemistry of monazite of authigenic origin, including the so-called grey monazites, was studied in detail by Rosenblum and Mosier (1983). Although their study confirmed systematically the long-recognized Eu-rich nature of those monazites, the vast majority of analyses presented in their study show ThO_2 concentrations below 1 wt. %, with a maximum value of 3.2 wt. %. An authigenic origin for older monazite cores at Kulyk Lake would make them exceptionally rich in Th compared to other localities (Cabella *et al.*, 2001) and merits further study.

The potential for discovery of large, economic, vein/dyke, Eu-rich monazite REE deposits in this area or beyond has yet to be demonstrated.

Allanite (±Apatite)–Dominant Mineralization (Saskatchewan Mineral Deposit Model A-22[17])

The most important allanite-rich mineralization includes allanite (±apatite)–dominant vein/dykes of alkaline affinity in the Hoidas Lake–Nisikkatch Lake area (Hogarth, 1957; Harvey *et al.*, 2002; Gunning and Card, 2005; Normand and McEwan, 2009; Normand *et al.*, 2009; Halpin 2010), and near 'Bear Lake' (unofficial name; Normand, 2010a, 2010b). They are located in the Zemlak Domain along a 40 km long corridor in hornblende orthogneiss (map unit Zgh in Ashton, 2009) that consist predominantly of 2.3 Ga granitoids and minor Archean granitoids injected by 1.9 Ga leucogranite. The corridor lies within 4 km of the Black Bay fault in the Hoidas Lake area and the transition to predominantly granodioritic to granitic gneiss (units Zghm and Zqf in Ashton, 2009; combination of 2.6 Ga and Arrowsmith granitoids) at its southernmost extremity (Figure 11). This narrow corridor is also characterized by the presence of abundant mafic dykes (Normand *et al.*, 2009) and mylonites, which suggest the presence of a deep-reaching structure that favoured intrusion and circulation of fertile, possibly mantle-derived melts and fluids. Although Koster (1965b) mentioned the existence of allanite showings extending as far north as Norwest Lake, 5 km northeast of Hoidas Lake, no reference was found to corroborate their location (SMDI #1614). Attempts to locate vein/dyke–type allanite occurrences at Norwest Lake during mapping in the area (Normand, 2010a, 2010b) were unsuccessful.

The potential for the discovery of economic allanite-rich deposits elsewhere in the province, and not necessarily of the same nature as those in the Hoidas Lake area, is difficult to evaluate due to a lack of detailed information on the mineralogy and geochemistry of the deposits where the mineral has been reported. Deposits that appear to be most interesting include: 1) the *Ox Lake allanite showing* (SMDI #1145; location 172, Table 6 and Figure 6), where allanite is reported to occur in a series of small shear zones, traced over a strike length of 243.8 m, that crosscut a second generation pegmatite dyke in Wollaston Group conglomerates; and 2) the *PIX U-Cu±Mo showing* (SMDI #0798; location 181, Table 6 and Figure 6), where allanite is reported to occur with radioactive minerals, chalcopyrite, pyrite, and molybdenite in north-striking, shallow-dipping lenticular veins. The mineralization occurs within the contact zone between graphitic biotite schist and granitic intrusive rocks. The veins are reported to measure up to 5.1 cm in width and 3.0 m in length, and are spaced 0.3 m apart. Sample assays of up to 0.27 wt. %

[17] See http://www.er.gov.sk.ca/depositmodels.

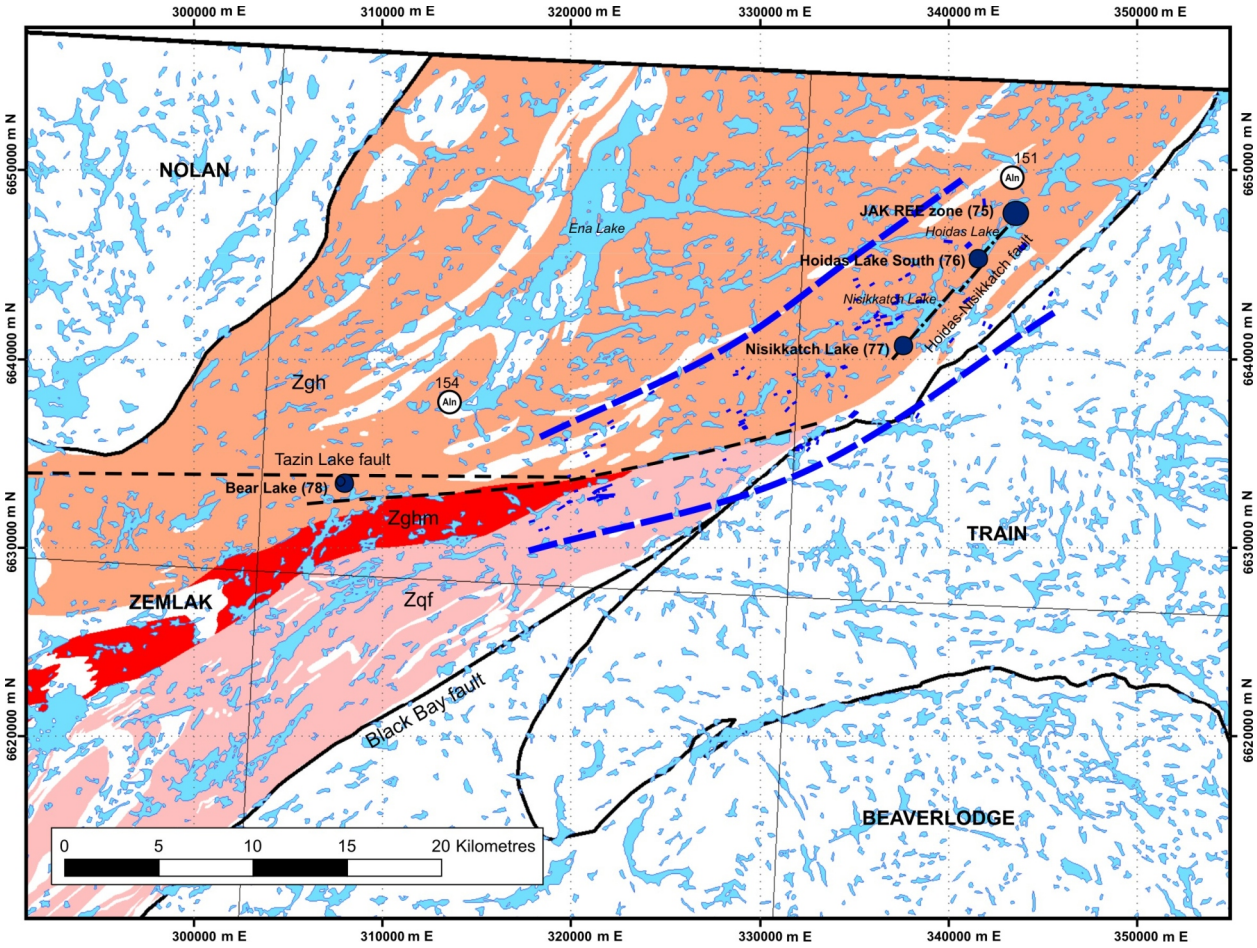

Figure 11 – Simplified geology of the area of the Hoidas Lake and Bear Lake allanite-apatite vein/dyke mineralization. It is generally held that mineralization at Hoidas Lake is late and related to the Black Bay fault. Examination of the map shown here, however, suggests that control on the distribution of the deposits is along the transition between terrains composed predominantly of hornblende orthogneisses (unit Zgh) and those composed predominantly of granodioritic to granitic gneisses (units Zghm and Zqf) and containing rocks of the Murmac Bay group. Abundant mafic dykes of various relative ages and compositions (thin solid blue lines within a thick dashed blue envelope) also follow this transition zone instead of the Black Bay fault. Recent U-Pb dating of centimetre-size zircon crystals from the JAK zone and titanite from the Bear Lake occurrence support this view. See text for a discussion of implications from radiometric-dating results.

U_3O_8 have been reported. A detailed description of the most significant occurrences in the Hoidas Lake–Nisikkatch Lake and Bear Lake areas is provided below.

Hoidas Lake–Nisikkatch Lake Alkaline Vein/Dykes (SMDI #1610, #1611, and #1612)

An uncommon type of allanite- and apatite-rich REE mineralization is located in an underexplored area between Hoidas Lake and Nisikkatch Lake near the extreme northwestern corner of Saskatchewan (locations 75, 76, and 77; Table 4 and Figures 4 and 11). The main REE-bearing occurrence at Hoidas Lake, the JAK zone, was discovered in 1950 by J. Lane, who was prospecting for U. Hogarth (1957) examined the allanite occurrences of the area shortly after their discovery and provided the first description of the mineral paragenesis. Following this, the REE mineralization received only sporadic attention until 1996, when Daren Resources Ltd. staked the JAK zone. Great Western Gold Corp. optioned the property from Daren Resources in 1999 after encouraging metallurgical tests of the REE mineralization were obtained. The JAK zone and other known REE-mineralized showings in the area have since been examined by Great Western Gold Corp., later renamed Great Western Minerals Group Ltd. (GWMG). The JAK zone, located on the northwest shore of Hoidas Lake, was traced over a strike length of approximately 750 m. Extensive drilling was completed on this zone between 2001 and 2008 by GWMG. A NI 43-101–compliant Resource estimate by Barr Engineering Company, released by GWMG on November 20, 2009 (Barr Engineering Company, 2009), established combined Measured and Indicated Resources of 2 560 835 t grading 2.027% TREE at a 1.5% cut-off grade for the JAK zone. Mineralization is reported to remain open at depth and along strike.

The REE are hosted by vein/dykes in tonalitic to granodioritic gneisses, which have possible equivalents in the area of Ena Lake dated at 2.32 to 2.33 Ga by Ashton *et al.* (2007b), and amphibolites of the Zemlak Domain. Most rocks show upper amphibolite–facies metamorphic mineral assemblages, although orthopyroxene-bearing granodioritic gneisses are preserved on the northeastern side of Oshowy Lake, suggesting that granulite-facies metamorphism may have prevailed at least locally. Granulite-facies metamorphism may have been more widespread in the area prior to retrograde amphibolite-facies replacement by hornblende and biotite. Rocks in the area show evidence for four phases of deformation (Harvey *et al.*, 2002; Gunning and Card, 2005; Normand and McEwan, 2009; Normand *et al.*, 2009; Normand, 2010a, 2010b), hereafter designated D_1, D_2, D_3, and D_4. Ashton *et al.* (2009) provided a synthesis of the timing of deformation events that affected the Beaverlodge and Zemlak domains. The earlier fabric is a pervasive, composite S_1-S_2 gneissosity that rarely shows F_2 folds. The S_3 fabric is heterogeneously developed, varying from imperceptible to the eye on bedrock exposures to a predominant, commonly mylonitic, northeast-striking foliation. Peak, upper amphibolite–grade metamorphism in the Ena Lake and Uranium City areas is attributed to D_1-D_2 and was accompanied by widespread emplacement of leucogranites at 1940 to 1920 Ma (Ashton *et al.*, 2005; Ashton *et al.*, 2007b; Ashton *et al.*, 2009). Deformation during this time has been attributed to the Taltson orogen (Ashton *et al.*, 2009). Ashton *et al.* (2009) reported D_3 (1910 to 1900 Ma) to be coincident with deformation associated with the Snowbird tectonic zone, and D_4 (1830 to 1820 Ma or younger) to be coeval with the Trans-Hudson Orogen.

The REE mineralization of the Hoidas Lake–Nisikkatch Lake area was interpreted by Harvey *et al.* (2002) to have been the result of metasomatism/metamorphism of a pyroxene-rich ultramafic to lamprophyric vein/dyke system. It was interpreted to have an alkaline igneous affinity by Gunning and Card (2005) and Halpin (2010). Individual vein/dykes have been traced on surface over a strike length of 425 m, are up to 15 m in thickness, and have been tectonically reactivated (Wardrop Engineering Inc., 2006; Halpin and Ansdell, 2008). They are zoned and comprise apatite-dominant sections that are slightly enriched in the HREE, including Y, and LREE-rich sections composed predominantly of silicates, including allanite, Ba-rich alkali feldspar, and Ca-rich clinopyroxene (Halpin, 2010). Four generations of apatite have been recognized, all of which typically are brecciated (Halpin and Ansdell, 2008; Halpin 2010). Monazite is present as an accessory mineral and, according to Halpin (2010), is mainly secondary in nature, most commonly replacing the earliest generation of apatite. Primary monazite is reported to be rare. Vein/dykes with sections composed of calcite, barite, quartz, and apatite were also reported by Hogarth (1957). The carbonate-rich portion of the dykes was interpreted to be hydrothermal in origin by Hogarth (1957). The deposit was classified by Woolley and Kjarsgaard (2008) as carbohydrothermal type. This particular association of silicate-, phosphate-, and carbonate-rich assemblages is uncommon. Allanite-, apatite-, and Ba-feldspar–rich mineralization, in part similar to that of the Hoidas Lake–Nisikkatch Lake area, occurs near Kasipatnam, India (Choudhuri and Banerji, 1976; Rao, 1976), in the Nolan's Bore deposit in Australia (Maas *et al.*, 2009; Huston *et al.*, 2011), and at Korsnäs, Finland (Papunen and Lindsjö, 1972; Frietsch *et al.*, 1979).

The REE-mineralized occurrences of the Hoidas Lake–Nisikkatch Lake area are concentrated along the Hoidas-Nisikkatch fault (Harvey *et al.*, 2002), which is located at the transition between a relatively low-strain region west of Hoidas and Nisikkatch lakes, and a high-strain zone characterized by discrete, strongly mylonitized to ultramylonitized zones, less than 50 m thick, that alternate eastward up to the Black Bay fault. The REE vein/dykes are hosted by granitoid rocks at the Hoidas Lake showings (locations 75 and 76, Table 4) and by gabbro at the Nisikkatch Lake occurrence (location 77, Table 4). At most locations, the vein/dykes appear unaffected by ductile deformation and were interpreted to have been emplaced after D_2 (Harvey *et al.*, 2002) and during D_3 (Gunning and Card, 2005). In the JAK zone, most of the REE-mineralized vein/dykes are oriented subparallel to the main regional composite S_1-S_2 foliation. A 2.5 cm thick allanite vein that strikes north-northeast near a historical trench (UTM zone 13, NAD 83, 343786 m E, 6648213 m N) north of the main JAK zone, however, was folded and is cut by the S_3 fabric. REE mineralization in GWMG's bulk-sampling test pit is hosted by a brecciated apatite-rich vein/dyke interpreted by the author to lie along a fault zone. Whereas vein/dykes in the JAK zone generally appear little affected by ductile deformation, folding and shearing of the vein/dykes at the Hoidas Lake South and Nisikkatch Lake occurrences is common (Normand *et al.*, 2009). At Hoidas Lake South, locally boudinaged vein/dykes oriented parallel to the regional gneissosity are strongly deformed and present evidence for two episodes of folding with subparallel axial-planar surfaces striking northeast. Earlier folding produced folds with axes plunging moderately to strongly northeast, and later folding produced folds with axes plunging moderately southwest. Emplacement of the vein/dykes was interpreted to have taken place before D_3 (Normand *et al.*, 2009).

Brown, translucent, elongated, euhedral zircon crystals, showing simple prism and dipyramid forms and measuring up to 2 cm in length, were collected from a 1 m thick mineralized vein/dyke in trench JK-2 (Normand *et al.*, 2009; GWMG's trench 8). The crystals are partly attached to large, altered amphibole and feldspar crystals, and project into very coarse allanite (Normand, 2010a, Figure 2C). All the observed crystals are slightly bent and fractured.

Examination under backscattered imaging mode using a scanning electron microscope (SEM) revealed that the zircon is veined by allanite and later barite, and is not zoned (Normand, 2010a, Figure 3). Thirty spot analyses with <5 ppm common lead were obtained in 2010 from LA-ICP-MS analysis of the zircon. The results define a discordant age with an upper intercept age of 2289.6 ±7.3 Ma. This grain was reanalyzed in 2013 on much cleaner surfaces, and similar old ages were obtained: identical U-Pb and $^{207}Pb/^{206}Pb$ ages of 2311 ±7 Ma (Appendix I). Because of their euhedral habit and *in situ* growth, the large zircon crystals are not believed to represent inherited or mantle-related megacrysts, which can be much older than their hostrock (Corfu *et al.*, 2003). Preliminary Hf isotope analyses by LA-ICP-MS on the same large zircon crystal that was dated (DuFrane, pers. comm., 2013) yielded a present-day $^{176}Hf/^{177}Hf$ value of ~0.28120, which corresponds to a present-day ε_{Hf} of approximately -55.8. Assuming that the zircon did crystallize at 2311 Ma, the initial ε_{Hf} would be approximately -4 (plus or minus about 3 epsilon units), and would indicate a strong crustal Hf component. The age reported above is thus interpreted to be coeval with emplacement of the vein/dyke. The 1870 Ma U-Pb SHRIMP age of monazite reported by Gunning and Card (2005) is tentatively interpreted to represent a late apatite recrystallization event during which the monazite was formed. Similarly young ages of between 1.9 and 1.78 Ga were reported by Pandur *et al.* (2013a, 2013b) from LA-ICP-MS, U-Pb dating of zircon, titanite, apatite, and monazite from the Hoidas Lake deposit. Pandur *et al.* (2013a, 2013b) interpreted these ages to be related to emplacement of the REE mineralization.

The 2311 Ma zircon age from the JAK zone is similar to the crystallization ages of numerous granitoid rocks in the Zemlak (Ashton *et al.*, 2007b) and Beaverlodge (Hartlaub *et al.*, 2007) domains. Given the age of the vein/dykes, and because the mineralized vein/dykes must have been emplaced after development of gneissosity (S_1 fabric?) and before D_3 deformation, it is possible that the gneissic fabric in rocks that host the Hoidas Lake, Nisikkatch Lake, and Bear Lake mineralization is an older, preserved fabric that was formed during the Arrowsmith orogeny (Berman *et al.*, 2005, 2013), and corresponds to the ill-defined 2.3 to 2.4 Ga D_1 metamorphic event recognized by Hartlaub (2004; see also Hartlaub *et al.*, 2007) and the 2343 ±7 Ma Arrowsmith event recognized by Bethune *et al.* (2013) in granitic gneiss of the Beaverlodge Domain.

The source of the Hoidas Lake–type alkaline vein/dykes may be connected, in part, to partial melting or devolatilization of metasomatized sub-continental lithospheric mantle or lower continental crust beneath the Rae Province (Cousens *et al.*, 2001; Morelli *et al.*, 2009) and possibly from portions of upper mantle underlying cratonic segments that have undergone multiple collision and subduction events. Other areas adjacent to deep-rooted faults in the northwestern part of the province may constitute potential targets for this type of REE mineralization. Mineralized lineaments, however, may not be responsive to ground or airborne radiometric surveys where bedrock is covered by even relatively thin (Gunning and Card, 2005) overburden. Till dispersal trains express poorly the signature of mineralization in the Hoidas Lake–Nisikkatch Lake area. Gunning and Card (2005) have shown that sampling needs to be virtually on top of the mineralization to obtain a signal. Similarly, biogeochemical investigations reported by Dunn and Hoffmann (1986) have shown that the REE dispersion halo expressed by vegetation is limited to the immediate vicinity of mineralized vein/dykes. Magnetic and electromagnetic surveys conducted by Great Western Minerals Group (SME Assessment File 74O13-NW-0023) have shown that vein/dykes are very low frequency electromagnetic (VLF-EM) conductors and magnetic lows. No high-density lake-bottom sediment geochemical tracer surveys for REE mineralization have been carried out to evaluate the response of allanite-rich vein/dyke mineralization in the Hoidas Lake–Nisikkatch Lake area.

Bear Lake Allanite-Apatite Occurrence (Location 78, Table 4 and Figures 4 and 11)

Allanite in the form of veins was first reported in the area by de Zoysa (1974). The occurrence was examined by Normand (2010a, 2010b), who observed allanite mineralization in a 125 m by 475 m area in mylonitized, pink leucogranite south of the Tazin Lake fault, 530 m northwest of Bear Lake and 1.5 km north-northeast of the northern end of McNutt Lake. The main mineralized occurrence consists of allanite-rich veins exposed in three trenches aligned parallel to the east-northeast–trending mylonitic foliation exhibited by the host leucogranite. The location of the trenches coincides with a foliation-parallel structural lineament that can be traced on SPOT satellite images for a strike length of ~1.5 km. Allanite vein sections measuring up to 12 cm thick were observed in blasted material adjacent to the larger trench. The early mineral paragenesis at this locality includes allanite, apatite, titanite, calcic amphibole, and traces of zircon. Quartz, purple fluorite, calcite, and epidote(-allanite) formed late. The latter are typically found as fracture filling over a large area south and north of the Tazin Lake fault.

Preliminary mineralogical and U-Pb isotopic dating work can be used to compare the Bear Lake and Hoidas Lake mineralization. LA-ICP-MS U-Pb isotopic analyses of titanite revealed two distinct, discordant age populations. These are interpreted to represent crystallization and alteration U-Pb ages with discordant upper intercepts at 2383 ±32 Ma and 1910 ±37 Ma, respectively (Appendix I). The two age populations are also well represented by

$^{207}Pb/^{206}Pb$ ages: 2264 to 2392 Ma and 1826 to 1924 Ma. Similarly, analyses of zircon yielded two more or less distinct groups of older and younger ages, with a younger, well-defined discordant population that yielded a U-Pb age of 1848 ±20 Ma and $^{207}Pb/^{206}Pb$ ages between 1803 and 1861 Ma and between 2072 and 2271 Ma. These data suggest that titanite and zircon partially resisted strain and resetting, probably because of their coarse, centimetre-scale size, imposed by the Taltson and Snowbird events. Gneissosity in the northern part of the Zemlak Domain may, at least locally, represent a preserved fabric developed during the Arrowsmith orogeny.

Electron microprobe analyses on material from the Bear Lake occurrence provide further evidence for an origin similar to that of allanite mineralization in the Hoidas Lake–Nisikkatch Lake area. Specifically, the distribution of Sr and Y in apatite, and HREE in titanite, are comparable to those reported by Halpin (2010) in the same minerals from the Hoidas Lake–Nisikkatch Lake area. Apatite from the Bear Lake occurrence is distinguished from that at Hoidas Lake, however, in having Nd as the predominant REE instead of Ce (median values of Ce/Nd are 0.63 and 1.51 for the Bear Lake (n = 26) and Hoidas Lake (n = 21) occurrences, respectively).

Mixed REE Mineralization in which THREE+Y(±Sc) Constitute >20% of the TREE

This class of mineralization includes U(±Th)–rich mineralization containing a sufficient amount of one or more minerals that contribute 20% or more THREE+Y to the contained TREE. Calculated values of the ratio (THREE+Y)/TREE from 5331 bulk rock analyses of samples originating from mixed REE mineralization containing greater than 1000 ppm U average 34% (77% of the data is greater than 20). This average value increases to 46% for samples containing greater than 1% U and to 62% for samples containing greater than 10% U. The more important HREE+Y–rich minerals reported from these deposits (not all necessarily associated together) include uraninite/pitchblende (reported to contain >10% REE in some granite/pegmatite–associated deposits; *e.g.*, Frondel, 1958), thorianite, thorite, brannerite, and coffinite. Xenotime, which typically contains ~50 wt. % REE (Y commonly dominates, followed by Dy and Er), fergusonite, pyrochlore-group minerals, and aeschynite-group minerals also occur locally, as well as apatite, titanite, and zircon that may contain appreciable concentrations of HREE and Y.

In Saskatchewan, U(±Th)– and THREE+Y(±Sc)–enriched, mixed REE mineralization comprise:

1) ***intrusion-associated U mineralization***, including intrusive phases, metasomatic/hybrid zones that resulted from melt/wallrock interaction, and subsolidus hydrothermal alteration zones[18] (Table 8; Figure 12);
2) ***vein-type U mineralization***, including impregnations in wallrock and cement in cataclasites and other types of brittle structure-associated mineralization infillings; Table 9; Figure 13), and;
3) ***unconformity-related U mineralization*** (Table 10; Figure 14).

Minerals in which U is an essential constituent, such as uraninite (including pitchblende) and coffinite, may contain major proportions of all REE (Frondel, 1958; Gerasimovskii, 1960; Fryer and Taylor, 1987; Pagel *et al.*, 1987; Förster, 1999). Eight-fold co-ordinated effective ionic radii very similar to that of U^{4+} for $HREE^{3+}$ and Y^{3+} (Shannon, 1976) allow for a range of ionic substitutions. This is illustrated in the complex formula of uraninite, generalized by the revised Janeczek and Ewing (1992) formula (Finch and Ewing, 1992):

$$\left(U^{4+}_{1-x-y-z-v}U^{6+}_{x}REE^{3+}_{y}M^{2+}_{z}\right)O_{2+x-(0.5y)-z}$$

Few data are available in the literature, however, concerning exchange reactions involving REE in uraninite. Heterovalent, coupled substitutions such as $U^{4+} + M^{2+} \leftrightarrow 2REE^{3+}$, similar to the exchange reaction between members of the monazite-cheralite series ($Th^{4+} + Ca^{2+} \leftrightarrow 2REE^{3+}$), may be important. Uraninite forms a solid solution with thorianite, ideally ThO_2, and complete solid solution between the two end-members (see Frondel, 1958, and references therein) is estimated to occur at temperatures above ~770°C based on theoretical thermodynamic considerations provided by Shuller *et al.* (2011). In Saskatchewan, uraninite from pegmatites in the Moore Lakes and Fraser Lakes areas (Annesley *et al.*, 2000; McKechnie, 2012; Mercadier *et al.*, 2013) contains >5 wt. %Th. Similarly, intrusion-associated U oxides contain the most REE. Up to 15 wt. % TREO (and 3.86 wt. % ThO_2) were reported by Frondel (1958) in uraninite from a pegmatite at Isaka, Japan. Uraninite from pegmatites in the Moore Lakes and Fraser Lakes areas contain >2 wt. % REE.

Shuller *et al.* (2011) noted that low-temperature U oxides worldwide contain less Th than is theoretically possible (12 wt. % Th permitted at 60°C on the calculated UO_2-rich limb of the solvus in the system UO_2-ThO_2) and attribute

[18] Some ill-defined occurrences assigned to category 1 may belong to category 2.

Table 8 – Mixed REE mineralization: intrusion-associated U.

Location #	Name	Category	SMDI #	Location[1]				References
				NTS Area	Easting	Northing	Domain	
204	Hill Lake area	Occurrences	near 1278	74N/08	316876	6599099	Beaverlodge	SME Assessment File 74N08-0162
205			none		316878	6599096		
206					316500	6598579		
207		Bedrock geochemical anomalies			315169	6596972		
208					317224	6596176		
209					318928	6599660		
210	Shearika Ridge	Bedrock geochemical anomaly	1590		419985	6595856	Train	SME Assessment File 74O09-0024
211	Davenport Lake	Occurrence	none	74O/09	432683	6618400		SME Assessment File 74O09-0023
212	East Addie Lake	Occurrence			432482	6618712		SME Assessment File 74O09-0024
213		Bedrock geochemical anomaly			431139	6617525		
—	n. r.	Bedrock geochemical anomaly	ins. dat.	n. r.	n. r.	n. r.	Wollaston	SME Assessment File 74A12-0014
214	Louise	Occurrence	none	74A/12	465978	6273523		SME Assessment File 74A12-0014
215	Eldorado dyke U-REE showing	Occurrence	0980	74A/11	470082	6274795		Mawdsley (1957); McKeough and Lentz (2011)
		Bedrock geochemical anomaly			470082	6274795		
216	Nate	Bedrock geochemical anomaly	none		486424	6277649		Brown (2011)
217	Red October	Occurrences		74A/14	474269	6304668		SME Assessment File 74A14-0049
218					474343	6304779		
219	Fraser Lakes area (zone A)	Occurrence		74H/02	500656	6320181		SME Assessment File 74H02-0045
220		Bedrock geochemical anomalies			500496	6320188		
221					500674	6320108		
222	Fraser Lakes area (zone B)	Developed U prospect with Resources	1122, 1127		503160	6321758		
223					504147	6322674		
224					504093	6322654		
225	Walker River area	Occurrences	none		508614	6330268		SME Assessment File 74H02-0043
226					509342	6327428		SME Assessment File 74H02-0045
227		Bedrock geochemical anomaly			500747	6322302		SME Assessment File 74H02-0043
228	Alexander Lake area	Occurrences			522726	6339166		SME Assessment File 74H02-0045
229					518524	6337004		SME Assessment File 74H02-0043
230		Bedrock geochemical anomalies			521398	6338093		SME Assessment File 74H02-0043
231					518345	6336967		SME Assessment File 74H02-0045
232	Way Lake area	Bedrock geochemical anomaly		74H/07	528068	6350642		SME Assessment File 74H02-0043

Table 8 (continued) – Mixed REE mineralization: intrusion-associated U.

Location #	Name	Sample #	Source of Data	U (wt. %)	Th (wt. %)	Sc (ppm)	La (ppm)	Ce (ppm)	Dy (ppm)	Y (ppm)	Yb (ppm)	Eu/Eu*	La_N/Yb_N	TREE (wt. %)	(THREE+Y)/TREE (%)	(THREE+Y)/U	(THREE+Y)/Th	U/Th
204	Hill Lake area	MG131	SME Assessment File 74N08-0162	0.56	0.0788	21	1084	<1	164	893	70	ins. dat.	10.7	0.284	48	0.24	1.7	7.14
205		MG132		0.32	0.1467	11	1773	<1	223	1120	74	ins. dat.	16.6	0.422	42	0.55	1.2	2.19
206		RD313		0.21	0.0834	7	929	1778	136	704	49	ins. dat.	13.1	0.416	27	0.52	1.3	2.56
207		DT106		0.09	0.0184	9	189	392	58	327	44	ins. dat.	3.0	0.118	43	0.56	2.8	4.93
208		JF269		0.01	0.1587	25	<1	<1	120	318	10	ins. dat.	ins. dat.	0.182	39	5.40	0.4	0.08
209		MG093		0.07	0.0807	3	1245	<1	136	547	41	ins. dat.	20.8	0.271	36	1.41	1.2	0.85
210	Shearika Ridge	OM471	SME Assessment File 74O09-0024	<~ 0.6	0.1720	ins. dat.	ins. dat.	49	86	299	31	ins. dat.	ins. dat.	0.064	83	ins. dat.	0.31	ins. dat.
211	Davenport Lake	WM342	SME Assessment File 74O09-0023	0.68	0.1530	525	199	694	534	1420	193	0.01	0.7	0.421	66	0.41	1.8	4.46
212	East Addie Lake	RD272	SME Assessment File 74O09-0024	0.13	0.0446	ins. dat.	ins. dat.	63	199	732	83	ins. dat.	ins. dat.	0.135	90	0.93	2.74	2.96
213		RD269		0.02	0.0516	ins. dat.	ins. dat.	59	65	395	58	ins. dat.	ins. dat.	0.069	88	3.92	1.17	0.30
—	n. r.	5042	SME Assessment File 74A12-0014	0.01	0.0319	47	92	188	37.6	415	117	0.30	0.5	0.104	64	11.63	2.08	0.18
214	Louise	5137	SME Assessment File 74A12-0014	0.02	0.2650	39	66	213	93.2	912	334	0.41	0.1	0.193	81	10.29	0.59	0.06
215	Eldorado dyke U-REE showing	25	McKeough and Lentz (2011)	0.01	0.0035	n. r.	101	312	109	608	69	0.28	1.0	0.176	57	14.49	28.5	1.97
		21		0.42	0.0720	n. r.	98	306	86	415	53	0.21	1.3	0.147	50	0.17	1.0	5.86
216	Nate	JBJLR002	Brown (2011)	0.08	0.4350	n. r.	n. r.	32	n. r.	335	88.6	ins. dat.	ins. dat.	0.066	84	0.70	0.13	0.18
217	Red October	JBELR063	SME Assessment File 74A14-0049	1.93	0.1800	169	74	491	246	1140	157	0.33	0.3	0.306	64	0.10	1.1	10.72
218		AGELR008		1.34	0.1420	133	208	614	200	826	144	0.34	1.0	0.276	54	0.11	1.1	9.44
219	Fraser Lakes area (zone A)	WA08-O-2003	SME Assessment File 74H02-0045	0.01	0.1070	49	661	1370	122	1000	110	0.10	4.2	0.438	34	14.73	1.4	0.10
220		WA08-O-1006		0.01	0.0316	53	41	95	52	592	153	0.63	0.2	0.110	83	13.84	2.9	0.21
221		WA08-O-0005		0.01	0.0464	6	499	1040	54	361	42	0.12	8.2	0.277	21	7.83	1.3	0.16
222	Fraser Lakes area (zone B)	WA08-B-0048		0.06	0.0744	31	287	663	71	630	158	0.09	1.3	0.242	43	1.78	1.4	0.79
223		WA08-O-0033		0.39	0.2380	19	234	512	49	295	27	0.08	6.0	0.154	31	0.12	0.2	1.64
224		WA08-O-2039		0.33	0.2860	18	487	992	57	303	27	0.08	12.5	0.262	20	0.16	0.2	1.15
225	Walker River area	WA0709011	SME Assessment File 74H02-0043	0.05	0.1930	15	1390	3670	479	2230	225	0.09	4.3	1.174	34	7.39	2.0	0.28
226		WA08-O-0010	SME Assessment File 74H02-0045	0.04	0.2520	7	1970	4640	350	2740	342	0.04	4.0	1.386	30	11.00	1.7	0.15
227		WA0709004	SME Assessment File 74H02-0043	0.02	0.0136	6	2	17	87.6	258	108	0.05	0.0	0.064	90	2.41	4.2	1.76
228	Alexander Lake area	WA08-O-2056	SME Assessment File 74H02-0045	0.21	0.0760	11	292	770	161	1700	416	0.26	0.5	0.390	68	1.26	3.5	2.76
229		WA0706038	SME Assessment File 74H02-0043	0.11	0.3880	20	1470	2530	110	882	112	0.22	9.1	0.608	22	1.20	0.3	0.28
230		WA07B2023	SME Assessment File 74H02-0043	0.00	0.0104	6	101	247	69.9	535	68	0.59	1.0	0.130	62	89.80	7.8	0.09
231		WA08-O-2006	SME Assessment File 74H02-0045	0.02	0.1320	18	43	230	83	617	77	0.17	0.4	0.142	66	3.99	0.7	0.18
232	Way Lake area	WA07B1009	SME Assessment File 74H02-0043	0.01	0.0275	2	363	811	45.5	294	25	0.03	10.2	0.226	21	5.36	1.8	0.33

[1] All location co-ordinates given in UTM Zone 13N, NAD 83.
Abbreviations: ins. dat., insufficient data; n. r., not reported.

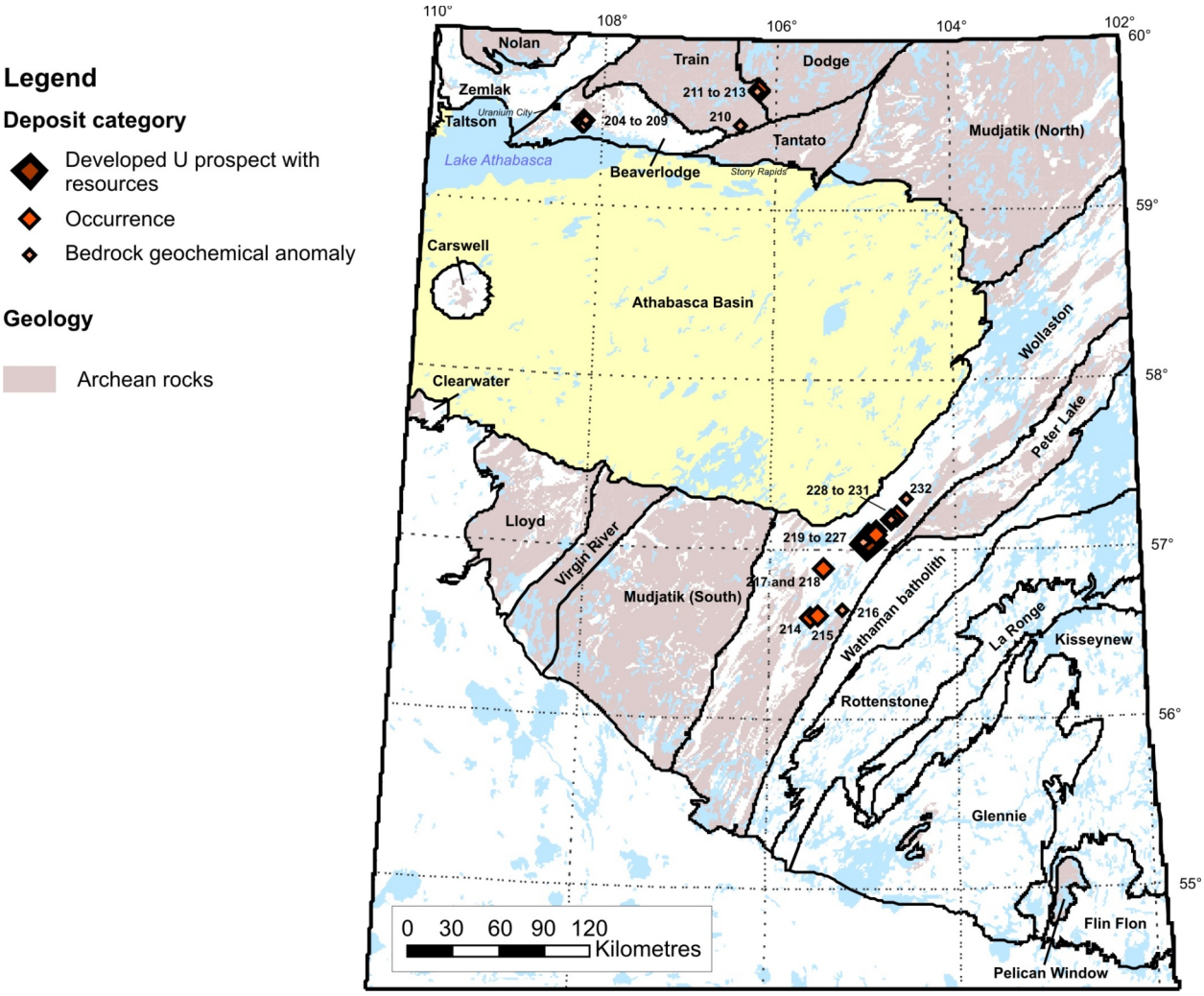

Figure 12 – Location of intrusion-associated U, mixed REE mineralization from which sample REE analyses have yielded >500 ppm THREE+Y, representing >20% of the total contained REE. Refer to Table 8 for details on sample locations and chemistry. Mineralization may be represented by REE-bearing U oxides (±thorite, pyrochlore,* etc.*) occurring as magmatic phases in granitic pegmatites (*e.g.*, Fraser Lakes area; locations 219 to 224, Table 8; SME Assessment File 74H02-0045; McKechnie* et al.*, 2012b) and by biotite-rich and calc-silicate reaction zones at the contact between granitic pegmatites and hostrock (*e.g.*, Eldorado dyke; McKeough* et al.*, 2010, 2013; McKeough and Lentz, 2011).

this to the very low Th solubility under the physicochemical conditions that prevail in hydrothermal fluids that deposit U oxide. U is mobile under oxidizing conditions and, by contrast with Th, which occurs exclusively in the tetravalent state in nature, is preferentially removed from source regions and reprecipitated in Th-depleted hydrothermal deposits at low temperature (Langmuir, 1978; Langmuir and Herman, 1980; Bailey and Ragnarsdottir, 1994; Neck *et al.*, 2003; Hazen *et al.*, 2009; Cuney, 2009, 2010; Bali *et al.*, 2011). The available data show that hydrothermal U oxides present in vein-type and unconformity-associated mineralization in Saskatchewan are generally much poorer in Th (less than ~2 wt. %), generally contain less REE (less than ~2 wt. %), and show higher Eu/Eu* values than uraninite from intrusion-associated mineralization (Figures 15 and 16). These data also show that there are no consistent differences in (THREE+Y)/TREE ratios between high- and low-temperature mineralization.

Elevated concentrations of Sc are present in some vein-type mineralization, particularly in examples located near the northern shore of Lake Athabasca, and in the most U- or P-enriched zones of some unconformity-associated U mineralization, such as McArthur River (up to 683 ppm; SME Assessment File 74H-0048), West Bear (up to 674 ppm; SME Assessment File 74H16-SE-0079), Cigar Lake (up to 500 ppm; SME Assessment File 74I02-0024), and Millennium (up to 564 ppm; SME Assessment File 74H12-0043). Minerals that *may* contain significant (≥50 ppm) Sc (excluding minerals that contain essential Sc) and are likely to contribute anomalies to bulk-rock

Table 9 – Mixed REE mineralization: vein-type U.

Location #	Name	Category	SMDI #	Location[1]				References
				NTS Area	Easting	Northing	Domain	
233	Cayzor mine area	Closed U mine	1404	74N/10	294457	6610281	Zemlak	SME Assessment Files 74N10-SE-0533 and -0537
234	Don Lake deposit	U prospect	1393		296960	6613170		SME Assessment File 74N10-SE-0533
					296960	6613170		
235	Pitch-Ore Uranium Mines Ltd., Orb claims, zone 6A	U prospect	1451		286400	6612870		SME Assessment File 74N10-0549; Beck (1969)
236	Rock dump on north side of Shaft Lake	Closed U mine (Eagle?)	(1360?)		n. r. (SMDI 1360:300978)	n. r. (SMDI 1360: 6610291)	Beaverlodge	Uranium City Resources Inc. (2005)
237	Emar Lake (RRK DDH 07RB1-004)	Occurrence	none	74N/09	308085	6609812		SME Assessment File 74N09-0354
238	Hab mine area	U prospect	none		306814	6614494		SME Assessment File 74N09-0356
239		Closed U mine	1289		n. r. (SMDI 1289:307322)	n. r. (SMDI 1289: 6614401)		SME Assessment File 74N09-NW-0351
240	Ace-Fay U mine	Closed U mine	1285		304141	6607593		Beck (1969)
241	Gunnar mine area	Closed U mine	1206	74N/07	279963	6589289		SME Assessment File 74N07-0335
					279963	6589289		
242					278054	6590246		SME Assessment File 74N07-NW-0333
243					278693	6590474		
244	Nicholson Bay mine, #1 zone	Closed U mine	1264	74N/08	305483	6595839		Peiris (1991)
	Nicholson Bay mine, #4 zone							
	Nicholson Bay mine, #2 zone							Sibbald (1988)
245	Eldorado Nuclear Ltd., radioactive A zone	U prospect	1274		307972	6595465		
246	MacIntosh Bay	Occurrences	1278 (see SME assessment file 74N08-0162)		311732	6598714		SME Assessment File 74N08-0162
247					311730	6598701		
248					311730	6598717		
249					311729	6598707		
250	Felix Bay	Occurrences	none		319740	6598131		
251					319742	6598145		
252	Adair Bay	Occurrences	none	74N/05	340587	6589842		
253					340569	6589858		
254					340571	6589874		
255	Gaitwin uranium zone A (Fall occurrence of CanAlaska)	Occurrences	1567		352950	6589270		
256					352955	6589273		
257					352991	6589345		
258					352902	6589327		
259					352916	6589307		
260					352914	6589307		
261					352941	6589279		
262					352922	6589284		
263					352913	6589326		
264					352914	6589302		
265					352922	6589301		
266					352903	6589315		
267					352909	6589316		
268					352906	6589331		
269	Bradley Lake area	Occurrence	1593	74O/08	437571	6595528	Tantato	SME Assessment File 74O09-0023
		Bedrock geochemical anomalies			437571	6595528		
270					437741	6595544		
271					437560	6595523		
272	Hook Lake	Occurrences	2016	74H/07	527282	6347098	Wollaston	SME Assessment File 74H02-0043
273					527325	6346997		SME Assessment File 74H02-0040

Table 9 (continued) – Mixed REE mineralization: vein-type U.

Location #	Name	Sample #	Source of Data	U (wt. %)	Th (wt. %)	Sc (ppm)	La (ppm)	Ce (ppm)	Dy (ppm)	Y (ppm)	Yb (ppm)	Eu/Eu*	La_N/Yb_N	TREE (wt. %)	(THREE+Y)/TREE (%)	(THREE+Y)/U	(THREE+Y)/Th	U/Th
233	Cayzor mine area	14171	SME Assessment File 74N10-SE-0533	3.97	<0.0001	11	453	1840	74	818	18	0.66	18	0.467	25	0.0299	>1186	>39700
		14168		19.20	<0.0001	6	906	383	12	146	4	ins. dat.	153	0.204	24	0.0026	>496	>192000
		50902	SME Assessment File 74N10-SE-0537	2.15	0.0103	9	329	1400	38	318	15	0.57	15	0.304	16	0.0225	5	209
234	Don Lake deposit	14170	SME Assessment File 74N10-SE-0533	9.00	0.0035	77	247	675	86	680	42	1.04	4	0.261	41	0.0119	31	2571
		14161		3.39	0.0097	21	277	999	50	489	21	0.65	9	0.260	27	0.0209	7	349
235	Pitch-Ore Uranium Mines Ltd., Orb claims, zone 6A	123622	SME Assessment File 74N10-0549	0.34	n. r.	14	n. r.	n. r.	n. r.	640	n. r.	ins. dat.	ins. dat.	ins. dat.	ins. dat.	ins. dat.	ins. dat.	ins. dat.
236	Rock dump on north side of Shaft Lake	801633	Uranium City Resources Inc. (2005)	9.50	n. r.	n. r.	n. r.	n. r.	n. r.	1240	n. r.	ins. dat.	ins. dat.	ins. dat.	ins. dat.	ins. dat.	ins. dat.	ins. dat.
237	Emar Lake (RRK DDH 07RB1-004)	RB1-D010	SME Assessment File 74N09-0354	1.92	0.0022	15	63	582	n. r.	422	n. r.	ins. dat.	ins. dat.	ins. dat.	ins. dat.	ins. dat.	ins. dat.	879
238	Hab mine area	826327	SME Assessment File 74N09-0356	0.23	0.0022	14	776	1340	110	589	29	ins. dat.	18	>0.40	<25	0.4503	46	101
239		801622	SME Assessment File 74N09-NW-0351	2.53	0.0111	15	152	351	70	535	20	0.66	5	0.173	46	0.0315	7	228
240	Ace-Fay U mine	Average of 49 analyses of Ace-Fay ore	Beck (1969; table 5.3)	10.68	0.1320	n. r.	n. r.	n. r.	n. r.	470	n. r.	ins. dat.	ins. dat.	ins. dat.	ins. dat.	ins. dat.	ins. dat.	ins. dat.
241	Gunnar mine area	MH032	SME Assessment File 74N07-0335	4.43	0.0259	6	385	974	207	1430	47	0.23	5.64	0.470	47	0.0500	9	171
		MH033		1.40	0.0103	5	70	170	74	348	23	0.34	2.14	0.109	55	0.0426	6	136
242		888540 (GU-171R)	SME Assessment File 74N07-NW-0333	17.90	0.0099	14	<1	1030	138	799	33	ins. dat.	ins. dat.	0.304	36	0.0062	11	1808
243		888539		0.35	0.0040	40	17	96	55	330	18	0.33	0.66	0.067	72	0.1407	12	86
244	Nicholson Bay mine, #1 zone	8730_42	Peiris (1991)	0.22	0.00004	156	90	118	191	507	47	0.90	1.33	0.168	66	0.5165	2789	5399
	Nicholson Bay mine, #4 zone	8730_15		0.27	0.000012	193	1	6	166	361	40	0.85	0.02	0.090	89	0.2948	6681	22664
245	Nicholson Bay mine, #2 zone	none	Sibbald (1988)	0.69	0.0089	n. r.	n. r.	n. r.	n. r.	2644	n. r.	ins. dat.	ins. dat.	ins. dat.	ins. dat.	ins. dat.	ins. dat.	78
	Eldorado Nuclear Ltd., radioactive A zone	none		3.17	0.0429	n. r.	n. r.	n. r.	n. r.	696	n. r.	ins. dat.	ins. dat.	ins. dat.	ins. dat.	ins. dat.	ins. dat.	74
		none		4.60	0.0687	n. r.	n. r.	n. r.	n. r.	568	n. r.	ins. dat.	ins. dat.	ins. dat.	ins. dat.	ins. dat.	ins. dat.	67
246	MacIntosh Bay	RD317	SME Assessment File 74N08-0162	3.04	0.0008	44	117	591	264	815	84	ins. dat.	0.97	0.268	57	0.0504	191	3798
247		JR457		0.64	0.0011	69	60	242	225	600	77	ins. dat.	0.54	0.170	68	0.1823	109	600
248		GS053		1.02	0.0010	32	30	207	156	365	45	ins. dat.	0.47	0.123	62	0.0745	74	995
249		GS051		1.20	0.0013	24	57	200	93	301	26	ins. dat.	1.52	0.096	57	0.0456	43	947
250	Felix Bay	DT091		8.68	0.0011	233	58	287	683	1292	285	ins. dat.	0.14	0.396	76	0.0348	275	7893
251		DT093		3.63	0.0009	82	30	132	265	580	93	ins. dat.	0.23	0.162	76	0.0342	136	3984
252	Adair Bay	FT056		3.40	0.0066	60	44	68	190	694	118	1.06	0.26	0.195	74	0.0422	22	515
253		FT057		4.50	0.0068	56	119	120	143	572	70	0.78	1.19	0.186	63	0.0261	17	662
254		AM206		2.18	0.0053	77	87	110	50	230	26	0.60	2.30	0.088	53	0.0213	9	411
255	Gaitwin uranium zone A (Fall occurrence of Canalaska)	CH210		1.34	0.0016	23	32	48	23	92	11	0.80	2.09	0.040	51	0.0151	13	838
256		CH209		2.29	0.0028	24	45	67	39	170	16	0.82	1.96	0.069	53	0.0160	13	818
257		MG118		2.47	0.0074	14	109	316	170	597	141	1.19	0.54	0.225	58	0.0529	18	334
258		MG115		3.22	0.0108	132	77	213	350	824	140	1.15	0.38	0.301	68	0.0634	19	298
259		MG112		2.59	0.0027	20	26	34	83	314	34	0.90	0.54	0.097	68	0.0254	24	959
260		CH214		27.20	0.0288	49	258	12	825	2570	329	0.90	0.54	0.854	69	0.0218	21	944
261		CH211		38.50	0.0485	80	310	1	1210	3980	500	0.91	0.43	1.257	71	0.0231	18	794
262		CH212		49.40	0.0576	98	452	1	1540	5110	633	0.92	0.49	1.602	71	0.0230	20	858
263		CH216		7.50	0.0065	25	53	15	231	832	89	0.92	0.41	0.252	71	0.0238	27	1154
264		MG113		19.70	0.0127	53	128	119	719	2320	289	1.02	0.31	0.721	72	0.0262	41	1551
265		CH213		38.50	0.0446	84	315	1	1340	4310	570	0.97	0.38	1.338	72	0.0250	22	863
266		CH215		3.51	0.0036	50	31	49	170	612	69	1.14	0.31	0.173	73	0.0359	35	975
267		MG111		1.52	0.0015	58	17	32	85	322	36	1.20	0.33	0.087	73	0.0422	43	1013
268		CH217		43.70	0.0482	460	115	1	2560	6560	1020	1.09	0.08	2.133	75	0.0367	33	907
269	Bradley Lake area	OM389	SME Assessment File 74O09-0023	1.40	<0.0001	12	42	261	133	1090	27	1.00	1.06	0.242	66	0.1141	>1598	>14000
		OM385		0.61	<0.0001	10	19	122	41	409	9	0.88	1.48	0.105	57	0.0991	>599	>6050
270		TR006		2.99	0.0115	<1	51	834	55	550	17	0.58	2.04	0.250	36	0.0298	7.8	260.00
271		JR325		0.25	0.0003	7	157	433	48	358	17	1.03	6.59	0.164	35	0.2239	188.4	841.67
272	Hook Lake	WA07B2002	SME Assessment File 74H02-0043	48.90	0.8260	0.5	1910	13000	1440	8140	1400	0.33	0.94	3.17	42	0.0270	2	59
273		WA60-726	SME Assessment File 74H02-0040	40.90	0.7340	0.5	0.5	14300	1200	7510	1420	0.32	0.00	4.09	41	0.0410	2	56
		WA6B-001		33.90	0.3820	0.5	861	8110	975	5090	967	0.31	0.62	2.47	38	0.0274	2	89

[1] All location co-ordinates given in UTM Zone 13N, NAD 83.
Abbreviations: DDH, diamond-drill hole; ins. dat., insufficient data; n. r., not reported.

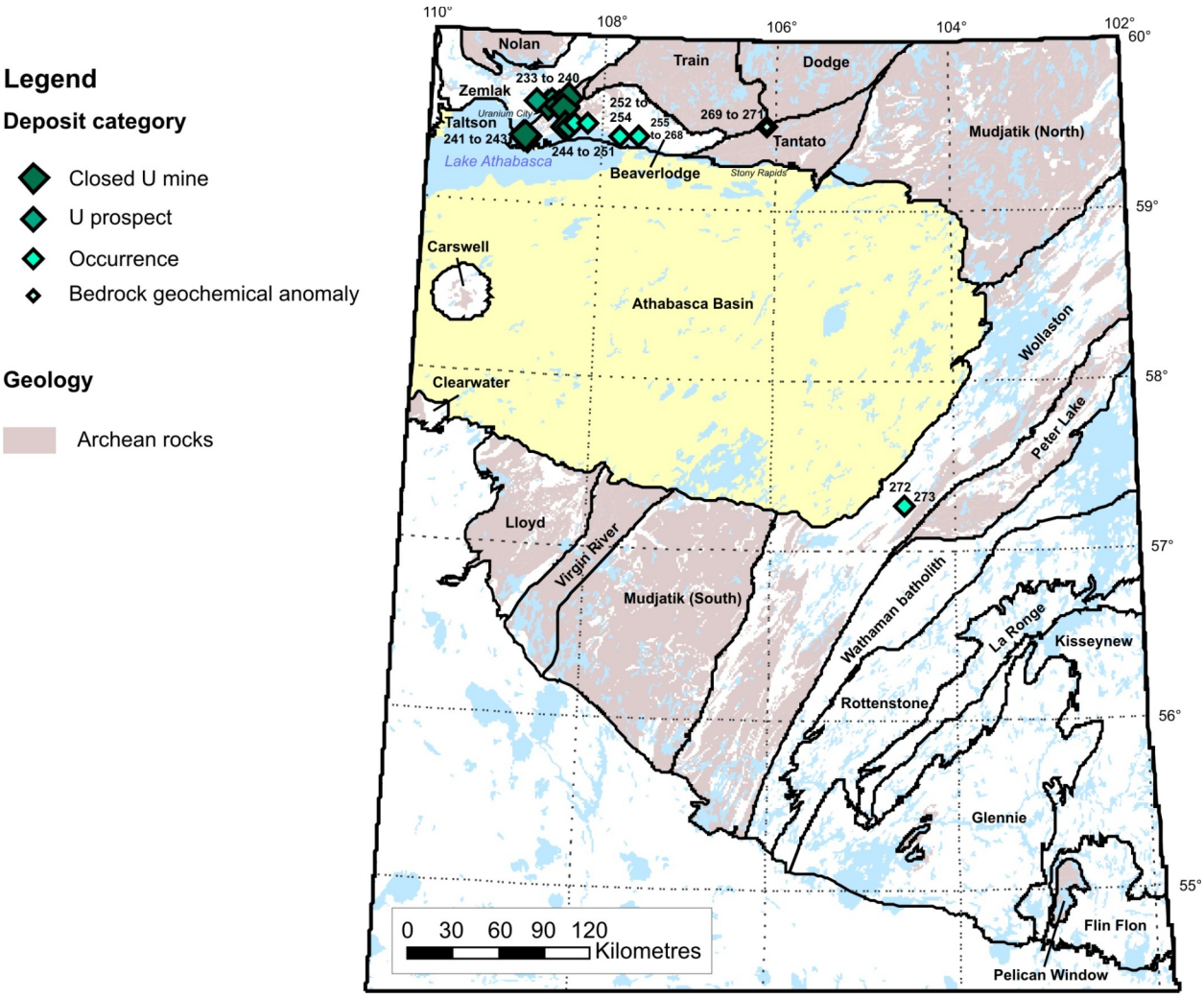

Figure 13 – Location of vein-type U, mixed REE mineralization from which sample REE analyses have yielded >500 ppm THREE+Y, representing >20% of the total contained REE. Refer to Table 9 for details on sample locations and chemistry.

analyses are numerous, including clinopyroxene, amphibole, biotite, Mn-rich garnet, epidote, Ti-rich oxides, Nb-Ta–bearing oxides, V-rich minerals, wolframite, cassiterite, beryl (see bazzite), xenotime (1 to 2 wt. % with pretulite; Bernhard *et al.*, 1998), zircon (up to 10 wt. % Sc_2O_3; Bea, 1996; Breiter at al., 2006), and APS minerals (up to 0.8 and 0.3 wt. % Sc_2O_3 in crandallite and goyazite, respectively; Frondel *et al.*, 1968). Sc oxide concentrations of 0.15 to 0.22 wt. % in pegmatitic and hydrothermal uraninite from India and France have been reported by Sankaran *et al.* (1970), and up to 0.25 wt. % in thorogummite inclusions in allanite from the Kingman pegmatite, Mojave Province, Nevada, has been reported by Brown (2010).

The minerals that host Sc in Saskatchewan U deposits have not been determined. Good correlations between Sc and U, Sc and Y, and Sc and heavy lanthanides, and the lack of correlation between Sc and P, and between Sc and Sr suggest that Sc is contained in U minerals at McArthur River. Similar Shannon effective ionic radii for U^{6+} and Sc^{3+} suggest that there may be substitution between these cations. Likely candidates to contain the Sc at West Bear include APS minerals, apatite, and zircon. The correlations of Sc with U and HREE are poor, but they are good with P, Sr, and Zr. The place of Sc in unconformity-related U mineralization of the Athabasca Basin is discussed in further detail in the "Unconformity-Related U Mineralization (<1.7 Ga)" section.

Intrusion-Associated Mineralization (Table 8; Figure 12)

The vast majority of the intrusive rocks that host REE mineralization in Saskatchewan are granitic. Silica-undersaturated, alkaline varieties are rare, having been recorded only from the miaskitic Lyle Lake nepheline syenite

Table 10 – Mixed REE mineralization: unconformity-related U.

Location #	Name	Category	Type	SMDI #	Location[1]			References
					NTS Area	Easting	Northing	
274	Midwest	Developed U prospect with Reserves	Polymetallic	1720	74I/08	555148	6465359	SME Assessment File 74I08-0069
275						555147	6465360	
276						555147	6465363	
277	McClean Lake (Caribou Lake)	Developed U prospect with Resources	Polymetallic	2754	64L/05	569045	6459444	SME Assessment File 64L05-SW-0157
278	Dawn Lake (Collins Creek zone, or Tamarack)	Developed U prospect with Resources	Polymetallic	near 1716, 1717	64L/05	562695	6458579	SME Assessment File 74I01-0114
279						563157	6458699	
280						563202	6458705	
281	Horseshoe	Developed U prospect with Resources	Monometallic	1722	64L/04	574297	6446821	SME Assessment File 64L04-0130
282						574177	6446861	
283	Cigar East	Developed U prospect without Reserves/ Resources	Polymetallic	none	74I/02	528162	6436703	SME Assessment File 74I02-0083
284						528269	6436722	
285	West Bear	Developed U prospect with Reserves	Polymetallic	1146	74H/16	555925	6415302	SME Assessment File 74H16-SE-0079
286						555866	6415286	
287						555866	6415289	
288						555844	6415268	
289	McArthur River (P2 North)	Operating U mine	Monometallic	2533	74H/14	495125	6402525	SME Assessment File 74H-0048
290	Read Lake	Occurrences	Polymetallic	2165	74H/14	487847	6402323	SME Assessment Files74H14-0073 and 74H-0065
291						487852	6402387	SME Assessment File 74H14-0073
292						487779	6402410	
293						487766	6402429	
294	Centennial	Occurrence	Monometallic	2737, 2758	74G/12	345581	6386050	SME Assessment File 74G12-SE-0042
295	Millenium	Developed U prospect with Resources	Monometallic	2742	74H/12	461858	6375528	SME Assessment File 74H12-0043
296	Wheeler River (Phoenix zone discovery hole)	Developed U prospect with Resources	Monometallic	near 2156, 2159, 2162	74H/11	477159	6374104	SME Assessment File 74H06-0142
297	Moore Lakes	Developed U prospect without Reserves/ Resources	Polymetallic	near 2458, 2740	74H/06	492425	6363945	SME Assessment File 74H06-NE-0128
298						492423	6363949	
299	P-Patch	Developed U prospect with Resources	Monometallic	2371	74H/04	465172	6340618	SME Assessment File 74H04-0117
300						465267	6340625	
301	Shea Creek (Anne, Kianna)	Developed U prospects with Resources	Weak polymetallic	2730, 2752	74K/04	234828	6463076	SME Assessment File 74K04-0031
302						234745	6463063	SME Assessment File 74K04-0042
303						234475	6463578	SME Assessment File 74K04-0041
304						234483	6463678	SME Assessment File 74K04-0037
305	Smart Lake	Occurrence	Polymetallic	none	74F/13	208949	6418996	SME Assessment File 74F13-0056

Table 10 (continued) – Mixed REE mineralization: unconformity-related U.

Location #	Name	DDH #	Sample #	Hostrock	Source of Data	P_2O_5 (wt. %)	Sr (ppm)	U (wt. %)	Th (wt. %)	Sc (ppm)	La (ppm)	Ce (ppm)	Pr (ppm)	Nd (ppm)	Sm (ppm)	Eu (ppm)	Gd (ppm)	Tb (ppm)	Dy (ppm)	Y (ppm)
274	Midwest	MW659	MW659_1SEL_05	Sandstone	SME Assessment File 74I08-0069	0.310	19	14.00	0.0239	88	279	1	434	288	187	27	133	89	301	1120
			MW659_1SEL_06	Sandstone		0.510	24	19.00	0.0400	118	393	1	485	1	157	24	32	115	363	831
275		MW660	MW660_1SEL_05	Sandstone		0.770	20	16.70	0.0287	31	1	1	397	1	137	19	31	88	263	693
			MW660_1SEL_20	Sandstone		1.100	2760	2.16	0.0099	54	665	1620	202	1050	244	33	289	52	249	1470
276		MW662	MW662_1BAS_14	Basement		0.210	29	3.38	0.0028	131	50	102	164	705	189	62	218	53	206	1390
277	McClean Lake (Caribou Lake)	S-728	S728MN18	Sandstone	SME Assessment File 64L05-SW-0157	0.032	48	27.5	<d. l.	297	<d. l.	251	<d. l.	<d. l.	<d. l.	<d. l.	<d. l.	<d. l.	396	1130
			S728MN21	Sandstone		0.135	29	20.2	<d. l.	178	<d. l.	518	<d. l.	<d. l.	<d. l.	<d. l.	<d. l.	<d. l.	295	911
			S728MN22	Sandstone		0.042	38	29.0	<d. l.	240	<d. l.	131	<d. l.	<d. l.	<d. l.	<d. l.	<d. l.	<d. l.	382	1100
			S728MN23	Sandstone		0.031	32	23.0	<d. l.	230	<d. l.	122	<d. l.	<d. l.	<d. l.	<d. l.	<d. l.	<d. l.	345	1020
			S728MN25	Sandstone		0.075	40	35.0	<d. l.	344	<d. l.	174	<d. l.	<d. l.	<d. l.	<d. l.	<d. l.	<d. l.	453	1290
278	Dawn Lake (Collins Creek zone, or Tamarack)	Q8-138	10586	Basement	SME Assessment File 74I01-0114	0.399	41	57.50	0.1970	346	<1	<1	<1	1190	171	<0.2	25	<0.3	988	2030
			10587	Basement		0.442	45	22.60	0.0905	112	<1	<1	<1	558	83	5	59	<0.3	417	1080
279		Q8-158	11599	Sandstone		1.120	821	43.00	0.0421	190	2550	1460	<1	2400	<0.5	78	657	<0.3	430	983
280		Q8-162	11744	Sandstone		<0.002	350	32.10	<0.0001	98	1090	328	<1	273	10	48	418	140	461	1030
			11745	Sandstone		<0.002	423	43.50	<0.0001	152	1410	362	<1	362	12	65	578	205	680	1510
281	Horseshoe	HU-016	HU-16 204.8	Basement	SME Assessment File 64L04-0130	0.227	158	18.8	0.00005	25	0.5	701	101	452	109	44	325	1830	250	980
			HU-16 206	Basement		0.101	151	6.9	0.00005	10	0.5	278	21	129	30	18	112	671	82	316
			HU-16 207.4	Basement		0.235	181	10.3	0.00005	15	0.5	802	67	356	55	26	194	1000	95	526
			HU-16 212.85	Basement		0.235	579	10.5	0.00005	7	0.5	236	15	105	6	14	80	975	36	127
282		HU-100	65727	Basement		<0.002	584	16.0	0.00005	83	795	486	0.5	765	31	35	258	0.15	172	356
283	Cigar East	WC-244	WC-244_2BAS_01	Basement	SME Assessment File 74I02-0083	1.930	103	65.00	<0.0001	186	<1	840	1210	362	94	56	1240	5470	880	2470
			WC-244_2BAS_02	Basement		1.620	120	52.00	<0.0001	138	<1	537	941	149	36	35	916	4340	516	1470
			WC-244_1BAS_27	Basement		0.156	108	32.80	<0.0001	97	<1	821	581	241	30	29	738	2830	401	1210
284		WC-245	WC-245_1BAS_01	Basement		0.226	352	0.71	0.0313	23	210	323	43	164	44	11	78	71	45	343
			WC-245_2BAS_01	Basement		0.433	163	8.23	0.0285	92	<1	592	288	1170	513	108	791	813	468	2880
285	West Bear	UEX-024	05UEX024G002	n. s.	SME Assessment File 74H16-SE-0079	0.276	337	0.35	0.0073	<1	26	31	9	42	15	3	45	13	96	1210
286		UEX-026	05UEX026G021	n. s.		0.233	181	0.23	0.0037	24	40	97	9	52	34	12	167	58	369	1520
			05UEX026G022	n. s.		0.562	568	0.26	0.0037	31	113	193	20	118	70	28	392	132	816	3260
287		UEX-031	05UEX031G015	n. s.		0.291	220	0.94	0.0001	34	124	249	1	95	39	15	191	72	400	1820
288		UEX-035	05UEX035G018	n. s.		0.355	200	0.88	0.0006	27	46	214	1	53	30	14	182	67	388	2050
289	McArthur River (P2 North)	MAC204	48917	n. s.	SME Assessment File 74H-0048	0.300	225	57.24	0.0010	659	51	162	30	210	215	92	610	175	1093	2567
			48918	n. s.		0.200	176	56.99	0.0012	683	58	138	27	180	189	82	541	161	989	2269
			48919	n. s.		0.200	316	55.20	0.0016	631	34	196	24	155	186	78	518	154	967	1900
		MAC222	229030	n. s.		0.200	121	65.80	0.0630	414	6	10	14	140	189	73	672	184	1085	2934
		MAC236	369138	n. s.		0.200	102	57.24	0.0363	239	71	15	16	152	179	67	549	168	1027	2288
290	Read Lake	REA-107	15551	Basement	SME Assessment File 74H14-0073	0.891	2210	0.29	0.0256	22	177	459	62	306	68	13	99	15	102	638
			15552	Basement		0.725	97	5.45	0.0206	95	<1	72	8	118	126	31	206	51	297	1380
291		REA-107-2	15700	Sandstone		2.950	5080	1.24	0.0260	46	63	470	129	919	252	51	250	52	240	967
292		REA-112-1	15854	Sandstone		0.040	328	5.17	0.0127	45	79	<1	<1	237	18	13	238	4	91	212
293		REA-112-2	15887	Sandstone		0.920	739	13.20	0.0200	102	85	<1	<1	770	93	32	564	<1	100	198
294	Centennial	VR-018	04VR018G113	Sandstone	SME Assessment File 74G12-SE-0042	0.080	171	2.5	0.0050	2	192	462	62	399	101	27	110	22	114	233
			04VR018G152	Basement		0.100	275	2.8	0.0090	16	66	167	<1	175	13	11	86	13	80	334
			04VR018G153	Basement		0.140	402	10.7	0.1290	26	<1	419	447	457	119	8	70	38	243	689
			04VR018G154	Basement		0.050	308	15.2	0.1850	27	<1	324	604	415	107	<0.2	<0.5	9	79	417
			04VR018G157	Basement		0.220	674	13.7	0.1660	49	<1	283	540	383	102	<0.2	<0.5	14	129	245
295	Millenium	CX-055-9	6482	Basement	SME Assessment File 74H12-0043	<0.002	60	31.10	0.1700	535	<1	<1	324	<1	<0.5	20	125	<0.3	330	807
			6486	Basement		<0.002	27	35.90	0.1880	564	<1	<1	346	<1	<0.5	22	146	<0.3	416	993
			6487	Basement		<0.002	27	32.20	0.1700	500	<1	<1	305	<1	<0.5	22	173	<0.3	406	1020
			6488	Basement		<0.002	10	42.10	0.2120	363	<1	<1	406	<1	<0.5	28	213	<0.3	534	1280
			6489	Basement		<0.002	40	24.50	0.1390	543	<1	<1	235	<1	<0.5	15	117	<0.3	317	790
296	Wheeler River (Phoenix zone discovery hole)	WR-249	S51917	Sandstone	SME Assessment File 74H06-0142	0.170	308	0.9	0.0067	3	46	79	11	117	23	5	32	8	32	95
			S51919	Sandstone		0.310	262	2.2	0.0147	17	55	81	16	211	47	18	126	35	158	570
			S51920	Sandstone		0.320	706	1.7	0.0115	7	65	123	23	230	54	13	78	19	67	198
			S51921	Sandstone		0.350	886	0.7	0.0048	3	43	77	14	132	35	7	51	10	37	132
			G106555	Sandstone		0.239	527	0.4	0.0012	2	26	83	14	114	35	8	40.8	9.3	33	114
297	Moore Lakes	ML-101	ML101C-129	Sandstone	SME Assessment File 74H06-NE-0128	0.668	290	0.08	0.0046	32	<1	619	206	1520	614	110	680	151	822	2630
			ML101S-134	Basement		0.480	68	2.47	0.0069	19	46	298	69	186	61	20	207	49	337	2080
			ML101S-136	Basement		0.462	67	2.67	0.0071	15	65	296	64	135	52	17	173	44	315	1700
			ML101S-141	Basement		0.340	220	0.33	0.0023	34	96	170	28	103	35	12	156	45	293	1850
298		ML-104	ML104S-131	Basement		0.315	228	0.10	0.0032	31	115	272	33	187	73	17	161	39	258	1690
299	P-Patch	P94	P94_1BAS_11	Basement	SME Assessment File 74H04-0117	0.05	1310	7.21	0.0220	63	147	4	1	334	92	13	148	76	258	533
			P94_1BAS_12	Basement		0.04	456	8.27	0.0257	41	198	14	1	373	86	8	115	57	161	358
			P94_1BAS_14	Basement		0.06	123	3.98	0.0141	47	92	8	1	192	47	7	79	36	123	282
			P94_1BAS_20	Basement		0.12	391	5.96	0.0131	24	135	1	1	284	64	5	73	36	80	209
300		P110	P110_1BAS_54	Basement		0.01	48	4.51	0.0273	24	78	47	1	333	53	9	120	26	106	310
301	Shea Creek (Anne, Kianna)	SHE109-1 (Anne)	33	Basement	SME Assessment File 74K04-0031	0.359	409	5.46	0.0030	27	134	263	<1	218	158	33	366	69	341	2380
		SHE109-2 (Anne)	45	Basement		0.225	339	6.74	<0.0001	131	680	935	<1	1090	268	82	393	73	299	1020
302		SHE122-1 (Anne)	715.5 (m)	Basement	SME Assessment File 74K04-0042	0.200	724	25.60	0.0780	93	661	463	<1	1670	330	78	648	251	569	1940
		SHE122-1 (Anne)	716 (m)	Basement		<0.002	220	31.60	0.0870	299	796	257	<1	1690	307	76	627	270	469	1640
303		SHE115-8 (Kianna)	664.2 (m)	Sandstone	SME Assessment File 74K04-0041	1.020	255	37.30	<0.0001	156	<1	1950	<1	<1	387	139	506	574	580	1120
304		SHE114-11 (Kianna)	691.9 (m)	Sandstone	SME Assessment File 74K04-0037	3.83	7990	3.4	0.0103	235	161	403	161	629	555	222	1630	483	3090	18300
		SHE114-9 (Kianna)	686.5 (m)	Sandstone		8.31	<1	12.6	0.0711	585	779	1920	<1	1500	490	222	1440	434	2750	14600
		SHE114-11 (Kianna)	691.4 (m)	Sandstone		6.72	<1	27	<0.0001	822	668	1690	142	1290	636	301	1250	354	2260	10400
305	Smart Lake	SMT-08-05	12710	Basement	SME Assessment File 74F13-0056	0.36	24	0.09	0.0065	475	<1	36	5	44	46	31.7	228	88	617	2350
			12714	Basement		2.61	734	0.07	0.0009	11	255	633	67	315	59	27.3	207	55	337	2770
			12709	Basement		0.23	23	0.04	0.0050	540	<1	11	<1	20	26	20	140	57	407	1460
			12713	Basement		0.30	56	0.01	0.0008	20	<1	33	3	22	9	10.7	87	24	158	1300
			12715	Basement		4.83	1780	0.06	0.0063	18	633	1330	138	631	103	18.2	70	11	78	570

[1] All location co-ordinates given in UTM Zone 13N, NAD 83.
Substantial proportions of the HREE and Y in samples from locations 304 and 305 may be contained in xenotime.
Abbreviations: DDH, diamond-drill hole; <d. l., less than detection limit; ins. dat., insufficient data; n. r., not reported; n. s., not specified.

Table 10 (continued) – Mixed REE mineralization: unconformity-related U.

Location #	Name	DDH #	Sample #	Hostrock	Source of Data	Ho (ppm)	Er (ppm)	Tm (ppm)	Yb (ppm)	Lu (ppm)	Eu/Eu*	La_N/Yb_N	TREE (wt. %)	THREE+Y (wt. %)	(THREE+Y)/TREE (%)	(THREE+Y)/U	(THREE+Y)/Th	U/Th
274	Midwest	MW659	MW659_1SEL_05	Sandstone	SME Assessment File 74I08-0069	76	144.0	n. r.	79	n. r.	0.50	2.44	0.316	0.197	62	0.0141	8.24	586
			MW659_1SEL_06	Sandstone		89	182.0	n. r.	105	n. r.	0.68	2.59	0.278	0.174	63	0.0092	4.35	475
275		MW660	MW660_1SEL_05	Sandstone		81	157.0	n. r.	79	n. r.	0.61	0.01	0.195	0.141	72	0.0084	4.92	582
			MW660_1SEL_20	Sandstone		49	78.7	n. r.	55	n. r.	0.38	8.42	0.606	0.227	38	0.1053	22.98	218
276		MW662	MW662_1BAS_14	Basement		43	118.0	n. r.	126	n. r.	0.92	0.27	0.343	0.222	65	0.0656	79.14	1207
277	McClean Lake (Caribou Lake)	S-728	S728MN18	Sandstone	SME Assessment File 64L05-SW-0157	<d. l.	<d. l.	n. r.	159	12	ins. dat.	ins. dat.	0.195	0.170	87	0.0062	ins. dat.	ins. dat.
			S728MN21	Sandstone		<d. l.	<d. l.	n. r.	113	8	ins. dat.	ins. dat.	0.185	0.133	72	0.0066	ins. dat.	ins. dat.
			S728MN22	Sandstone		<d. l.	<d. l.	n. r.	156	13	ins. dat.	ins. dat.	0.178	0.165	93	0.0057	ins. dat.	ins. dat.
			S728MN23	Sandstone		<d. l.	<d. l.	n. r.	139	10	ins. dat.	ins. dat.	0.164	0.151	93	0.0066	ins. dat.	ins. dat.
			S728MN25	Sandstone		<d. l.	<d. l.	n. r.	188	15	ins. dat.	ins. dat.	0.212	0.195	92	0.0056	ins. dat.	ins. dat.
278	Dawn Lake (Collins Creek zone, or Tamarack)	Q8-138	10586	Basement	SME Assessment File 74I01-0114	<0.4	990.0	n. r.	265	n. r.	ins. dat.	ins. dat.	0.566	0.430	76	0.0075	14.72	292
			10587	Basement		<0.4	395.0	n. r.	102	n. r.	0.19	ins. dat.	0.270	0.206	76	0.0091	8.24	250
279		Q8-158	11599	Sandstone		<0.4	454.0	n. r.	92	n. r.	ins. dat.	19.25	0.910	0.269	30	0.0063	2.64	1021
280		Q8-162	11744	Sandstone		38	<0.2	n. r.	90	n. r.	0.77	8.39	0.393	0.222	57	0.0069	>2224.60	>321000
			11745	Sandstone		79	<0.2	n. r.	137	n. r.	0.77	7.13	0.540	0.325	60	0.0075	>3254.30	>435000
281	Horseshoe	HU-016	HU-16_204.8	Basement	SME Assessment File 64L04-0130	27	35.7	n. r.	49	n. r.	0.66	0.01	0.490	0.354	72	0.0188	7081.60	376000
			HU-16_206	Basement		10	17.1	n. r.	20	n. r.	0.82	0.02	0.170	0.125	73	0.0181	2491.40	138000
			HU-16_207.4	Basement		15	24.4	n. r.	19	n. r.	0.67	0.02	0.318	0.190	60	0.0184	3799.20	206000
			HU-16_212.85	Basement		2	0.1	n. r.	11	n. r.	1.11	0.03	0.161	0.125	77	0.0119	2490.40	210000
282		HU-100	65727	Basement		37	593.0	n. r.	41	n. r.	0.81	13.46	0.357	0.149	42	0.0093	2984.10	320000
283	Cigar East	WC-244	WC-244_2BAS_01	Basement	SME Assessment File 74I02-0083	<0.4	21.6	n. r.	244	n. r.	0.29	ins. dat.	1.289	1.038	81	0.0160	>10381.20	>650000
			WC-244_2BAS_02	Basement		<0.4	<0.2	n. r.	134	n. r.	0.26	ins. dat.	0.907	0.741	82	0.0143	>7411.00	>520000
			WC-244_1BAS_27	Basement		12	61.5	n. r.	105	n. r.	0.26	ins. dat.	0.706	0.539	76	0.0164	>5386.60	>328000
284		WC-245	WC-245_1BAS_01	Basement		8	16.8	n. r.	19	n. r.	0.58	7.49	0.138	0.059	43	0.0837	1.89	23
			WC-245_2BAS_01	Basement		71	156.0	n. r.	112	n. r.	0.51	ins. dat.	0.796	0.540	68	0.0656	18.94	289
285	West Bear	UEX-024	05UEX024G002	n. s.	SME Assessment File 74H16-SE-0079	24	57.1	n. r.	37	n. r.	0.34	0.48	0.161	0.149	92	0.4222	20.36	48
286		UEX-026	05UEX026G021	n. s.		58	113.0	n. r.	84	n. r.	0.39	0.33	0.261	0.238	91	1.0311	64.37	62
			05UEX026G022	n. s.		126	245.0	n. r.	185	n. r.	0.40	0.42	0.570	0.518	91	1.9636	140.11	71
287		UEX-031	05UEX031G015	n. s.		69	127.0	n. r.	88	n. r.	0.44	0.97	0.329	0.278	85	0.2975	2781.90	9350
288		UEX-035	05UEX035G018	n. s.		72	138.0	n. r.	84	n. r.	0.43	0.38	0.334	0.300	90	0.3415	499.22	1462
289	McArthur River (P2 North)	MAC204	48917	n. s.	SME Assessment File 74H-0048	151	339.7	44	247	25	0.72	0.14	0.601	0.534	89	0.0093	523.81	56118
			48918	n. s.		139	299.0	38	218	22	0.73	0.18	0.535	0.476	89	0.0083	389.98	46710
			48919	n. s.		126	281.2	35	201	20	0.72	0.12	0.487	0.428	88	0.0078	264.21	34077
		MAC222	229030	n. s.		143	297.9	31	161	17	0.55	0.02	0.596	0.560	94	0.0085	8.89	1045
		MAC236	369138	n. s.		132	279.0	33	178	18	0.60	0.27	0.517	0.474	92	0.0083	13.06	1578
290	Read Lake	REA-107	15551	Basement	SME Assessment File 74H14-0073	21	42.0	n. r.	34	n. r.	0.47	3.65	0.203	0.096	47	0.3377	3.76	11
			15552	Basement		51	95.1	n. r.	72	n. r.	0.59	ins. dat.	0.251	0.218	87	0.0400	10.60	265
291		REA-107-2	15700	Sandstone		39	90.5	n. r.	69	n. r.	0.61	0.63	0.359	0.176	49	0.1418	6.76	48
292		REA-112-1	15854	Sandstone		37	<0.2	n. r.	26	n. r.	0.36	2.13	0.096	0.062	65	0.0120	4.89	407
293		REA-112-2	15887	Sandstone		58	<0.2	n. r.	34	n. r.	0.33	1.75	0.193	0.099	51	0.0075	4.93	660
294	Centennial	VR-018	04VR018G113	Sandstone	SME Assessment File 74G12-SE-0042	12	40.4	n. r.	19	n. r.	0.78	6.92	0.179	0.058	32	0.0231	11.54	500
			04VR018G152	Basement		7	34.5	n. r.	13	n. r.	0.74	3.49	0.100	0.058	58	0.0207	6.43	311
			04VR018G153	Basement		<0.4	<0.2	n. r.	63	n. r.	0.23	ins. dat.	0.255	0.111	43	0.0104	0.86	83
			04VR018G154	Basement		<0.4	<0.2	n. r.	47	n. r.	ins. dat.	ins. dat.	0.200	0.055	28	0.0036	0.30	82
			04VR018G157	Basement		<0.4	<0.2	n. r.	48	n. r.	ins. dat.	ins. dat.	0.174	0.044	25	0.0032	0.26	83
295	Millenium	CX-055-9	6482	Basement	SME Assessment File 74H12-0043	<0.4	<0.2	n. r.	91	n. r.	ins. dat.	ins. dat.	0.170	0.137	81	0.0044	1.00	183
			6486	Basement		<0.4	<0.2	n. r.	113	n. r.	ins. dat.	ins. dat.	0.204	0.169	83	0.0047	1.08	191
			6487	Basement		<0.4	14.6	n. r.	110	n. r.	ins. dat.	ins. dat.	0.205	0.175	85	0.0054	1.21	189
			6488	Basement		<0.4	8.5	n. r.	142	n. r.	ins. dat.	ins. dat.	0.261	0.221	84	0.0052	1.23	199
			6489	Basement		<0.4	5.5	n. r.	87	n. r.	ins. dat.	ins. dat.	0.157	0.133	85	0.0054	1.13	176
296	Wheeler River (Phoenix zone discovery hole)	WR-249	S51917	Sandstone	SME Assessment File 74H06-0142	5	0.1	n. r.	9	n. r.	0.60	3.75	0.046	0.018	40	0.0200	2.78	139
			S51919	Sandstone		25	27.9	n. r.	38	n. r.	0.65	1.01	0.141	0.100	71	0.0464	6.78	146
			S51920	Sandstone		11	0.4	n. r.	13	n. r.	0.61	3.41	0.089	0.040	45	0.0238	3.47	146
			S51921	Sandstone		6	3.7	n. r.	7	n. r.	0.52	4.02	0.056	0.026	46	0.0379	5.30	140
			G106555	Sandstone		5	6.1	n. r.	6	n. r.	0.61	3.00	0.049	0.022	45	0.0560	18.47	330
297	Moore Lakes	ML-101	ML101C-129	Sandstone	SME Assessment File 74H06-NE-0128	128	283.0	n. r.	206	n. r.	0.51	ins. dat.	0.797	0.501	63	5.9501	108.91	18
			ML101S-134	Basement		58	138.0	n. r.	119	n. r.	0.49	0.27	0.367	0.301	82	0.1218	43.59	358
			ML101S-136	Basement		51	124.0	n. r.	115	n. r.	0.50	0.39	0.315	0.254	81	0.0951	35.76	376
			ML101S-141	Basement		56	135.0	n. r.	117	n. r.	0.43	0.57	0.310	0.266	86	0.8072	115.82	143
298		ML-104	ML104S-131	Basement		44	102.0	n. r.	58	n. r.	0.45	1.36	0.305	0.237	78	2.3926	74.02	31
299	P-Patch	P94	P94_1BAS_11	Basement	SME Assessment File 74H04-0117	46	0.2	n. r.	52	n. r.	0.35	1.96	0.170	0.113	66	0.0156	5.12	328
			P94_1BAS_12	Basement		32	0.2	n. r.	33	n. r.	0.25	4.21	0.144	0.076	53	0.0092	2.97	322
			P94_1BAS_14	Basement		20	0.2	n. r.	25	n. r.	0.34	2.58	0.091	0.057	63	0.0144	4.06	282
			P94_1BAS_20	Basement		18	0.2	n. r.	15	n. r.	0.23	6.19	0.092	0.044	47	0.0073	3.33	455
300		P110	P110_1BAS_54	Basement		21	0.2	n. r.	23	n. r.	0.33	2.36	0.113	0.062	55	0.0136	2.25	165
301	Shea Creek (Anne, Kianna)	SHE109-1 (Anne)	33	Basement	SME Assessment File 74K04-0031	82	146.0	n. r.	75	n. r.	0.41	1.25	0.426	0.350	82	0.0640	102.70	1606
		SHE109-2 (Anne)	45	Basement		70	85.5	n. r.	66	n. r.	0.76	7.18	0.506	0.207	41	0.0310	>2074.93	>67400
302		SHE122-1 (Anne)	715.5 (m)	Basement	SME Assessment File 74K04-0042	153	<0.2	n. r.	114	n. r.	0.50	4.01	0.688	0.375	55	0.0147	4.84	330
		SHE122-1 (Anne)	716 (m)	Basement		161	<0.2	n. r.	98	n. r.	0.51	5.61	0.639	0.334	52	0.0106	3.84	364
303		SHE115-8 (Kianna)	664.2 (m)	Sandstone	SME Assessment File 74K04-0041	<0.4	<0.2	n. r.	100	n. r.	0.95	ins. dat.	0.536	0.300	56	0.0081	>2999.36	>373000
304		SHE114-11 (Kianna)	691.9 (m)	Sandstone	SME Assessment File 74K04-0037	554	1280	n. r.	825	n. r.	0.66	0.14	2.829	2.638	93	0.7760	256.16	330
		SHE114-9 (Kianna)	686.5 (m)	Sandstone		512	1190	n. r.	707	n. r.	0.74	0.76	2.654	2.186	82	0.1735	30.74	177
		SHE114-11 (Kianna)	691.4 (m)	Sandstone		394	868	n. r.	607	n. r.	1.01	0.76	2.086	1.643	79	0.0609	>16434.00	>270000
305	Smart Lake	SMT-08-05	12710	Basement	SME Assessment File 74F13-0056	148	390	n. r.	442	n. r.	0.77	ins. dat.	0.443	0.429	97	4.5737	66.07	14
			12714	Basement		89	212	n. r.	138	n. r.	0.67	1.28	0.516	0.384	74	5.8287	426.14	73
			12709	Basement		99	267	n. r.	325	n. r.	0.80	ins. dat.	0.283	0.278	98	6.3793	55.50	9
			12713	Basement		44	110	n. r.	89.2	n. r.	0.76	ins. dat.	0.189	0.182	96	16.5718	227.86	14
			12715	Basement		21	54.2	n. r.	43	n. r.	0.62	10.19	0.370	0.087	23	1.5735	13.74	9

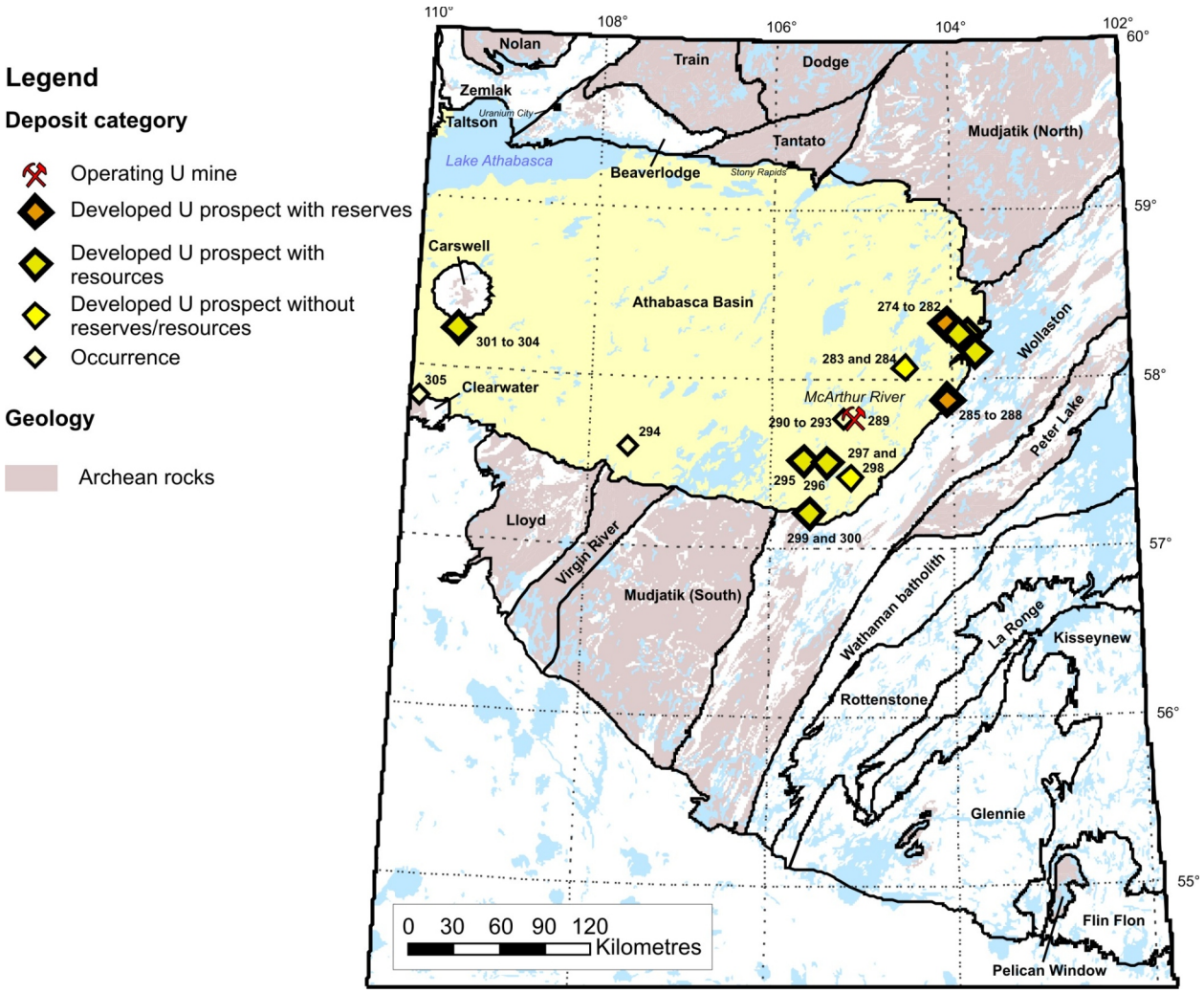

Figure 14 – Location of unconformity-related U, mixed REE mineralization from which sample REE analyses have yielded >500 ppm THREE+Y, representing >20% of the total contained REE. Refer to Table 10 for details on sample locations and chemistry.

(Peter Lake Domain; Quirt, 1992), and contain small proportions of REE-bearing minerals (maximum 285 ppm La+Ce). Elsewhere in the province, the REE-mineralized intrusive rocks are represented by granitic pegmatites. The pegmatites rarely exceed a few metres in thickness, contain white or pink feldspars or both, are generally free of muscovite, contain widely variable quartz and ferromagnesian mineral proportions, are rarely zoned, and have sharp or diffuse contacts with the wallrock. A large proportion of the pegmatites cut upper amphibolite– to granulite-facies metasedimentary rocks. The predominant metal association is REE, Th, and U, occasionally with elevated Nb (2110 ppm, Walker River area, SME Assessment File 74H02-0043, location 225 in Table 8 and Figure 12; 6940 ppm, Davenport Lake, SME Assessment File 74O09-0023, location 211 in Table 8 and Figure 12) but generally low Mo concentrations, although pegmatites in areas where REE may abound can contain elevated concentrations of the metal (*e.g.*, 6670 ppm Mo and 80 ppm TREE, Fraser Lakes area; SME Assessment File 74H02-0043). The characteristics of most pegmatites best match the abyssal, REE, allanite-monazite-uraninite subtype of Ercit (2005), or the abyssal, REE, monazite-allanite type AB of Černý and Ercit (2005).

The concentration of REE has not been reported for most of the pegmatite-hosted deposits/occurrences listed in the SMDI or reported in assessment files. In most cases, the described occurrence of an REE-bearing mineral, commonly as an accessory phase present in unspecified proportions, is the only indication of the presence of these metals. Although REE may be present in no more than trace amounts at some localities, evaluation of the REE potential for most is not possible at the present. When reported, the paragenetic position of the REE mineralogy with respect to pegmatite emplacement is frequently not well documented in the available literature. The REE-bearing

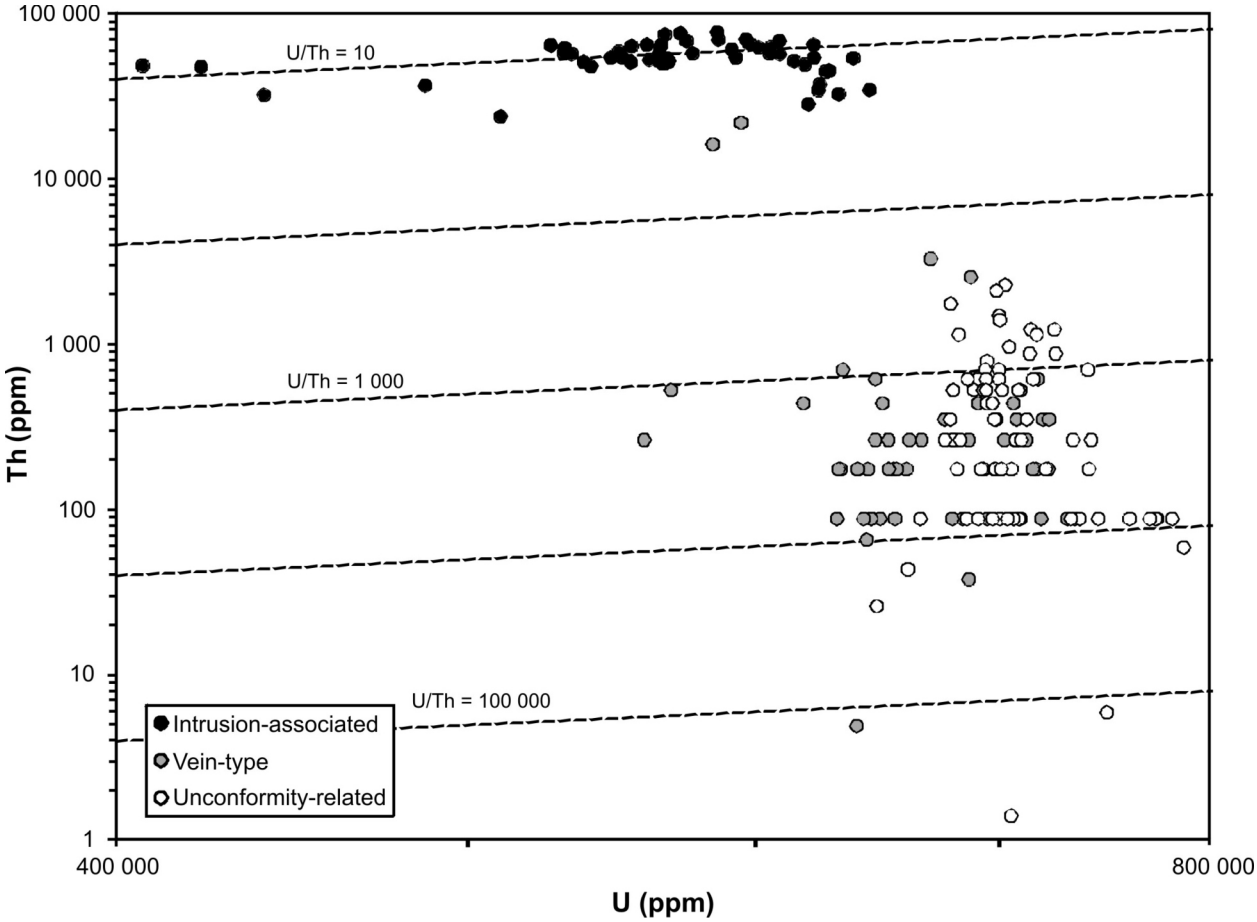

Figure 15 – Log-log plot of the relationship between U and Th concentrations in U oxides from intrusion-associated, vein-type, and unconformity-associated U mineralization. U oxides from unconformity-associated and vein-type mineralization have similar Th concentrations, although those from unconformity-associated mineralization tend to be more U rich. Some data points clustered in rows at low Th concentrations (80 to 200 ppm) are near the detection limit (typically 100 ppm ThO_2) for low-precision electron microprobe analysis. Sources of data for U-oxide compositions from intrusion-associated mineralization: Annesley* et al. *(2000) (Moore Lakes: electron microprobe); McKechnie* et al. *(2012b) and Mercadier* et al. *(2013) (Moore Lakes and Fraser Lakes: electron microprobe). Sources of data for U-oxide compositions from vein-type mineralization: Dieng (2012) (Ace, Fay, and Gunnar mines: electron microprobe); Mercadier* et al. *(2013) (Hook Lake: electron microprobe). Sources of data for U-oxide compositions from unconformity-associated mineralization: Fayek (1996) (Cigar Lake, McArthur River, Key Lake, Sue zone, and Eagle Point North: electron microprobe, inductively coupled plasma–mass spectrometry); Beshears (2010) (Millennium: electron microprobe); Ng (2012) (McArthur River: electron microprobe).

minerals may have crystallized from a melt during emplacement of pegmatites, may have formed through metasomatic reaction between melt or volatiles and wallrock, or may have precipitated from a hydrothermal solution and not be related to the emplacement of the pegmatite at all. In those cases where insufficient data are available, REE mineralization was tentatively assigned an intrusion-associated origin. At certain locations, field descriptions and geochemical analyses of the mineralization cutting granitic pegmatites allow determination of a hydrothermal origin for the mineralization unrelated to pegmatite emplacement. An example of this is given by the Bradley occurrence (locations 269 to 271, Table 9), where U-rich veins that cut, and are restricted to, pegmatite show geochemical characteristics (U/Th >100, elevated Eu/Eu*) that suggest they are not related to pegmatite emplacement. Granitic pegmatite–associated deposits worldwide have rarely been mined for REE, and when this has been the case, the production was limited. Perhaps the most interesting mineralization of this class in Saskatchewan, value-wise, is that dominantly enriched in U or Ta. The minerals that host the REE in this mineralization are typically enriched in the HREE, such as U minerals, and minerals of, for example, the pyrochlore supergroup, the aeschinite group, or the fergusonite group, so they might offer economic potential as a secondary source of HREE. U- and REE-enriched pegmatites appear to be particularly abundant in migmatized metasedimentary rocks from all major pre-Athabasca basins. They are most commonly encountered in the Wollaston, Beaverlodge, Zemlak, and Glennie domains. Not all U mineralization associated with granitoid intrusive rocks, however, contains appreciable

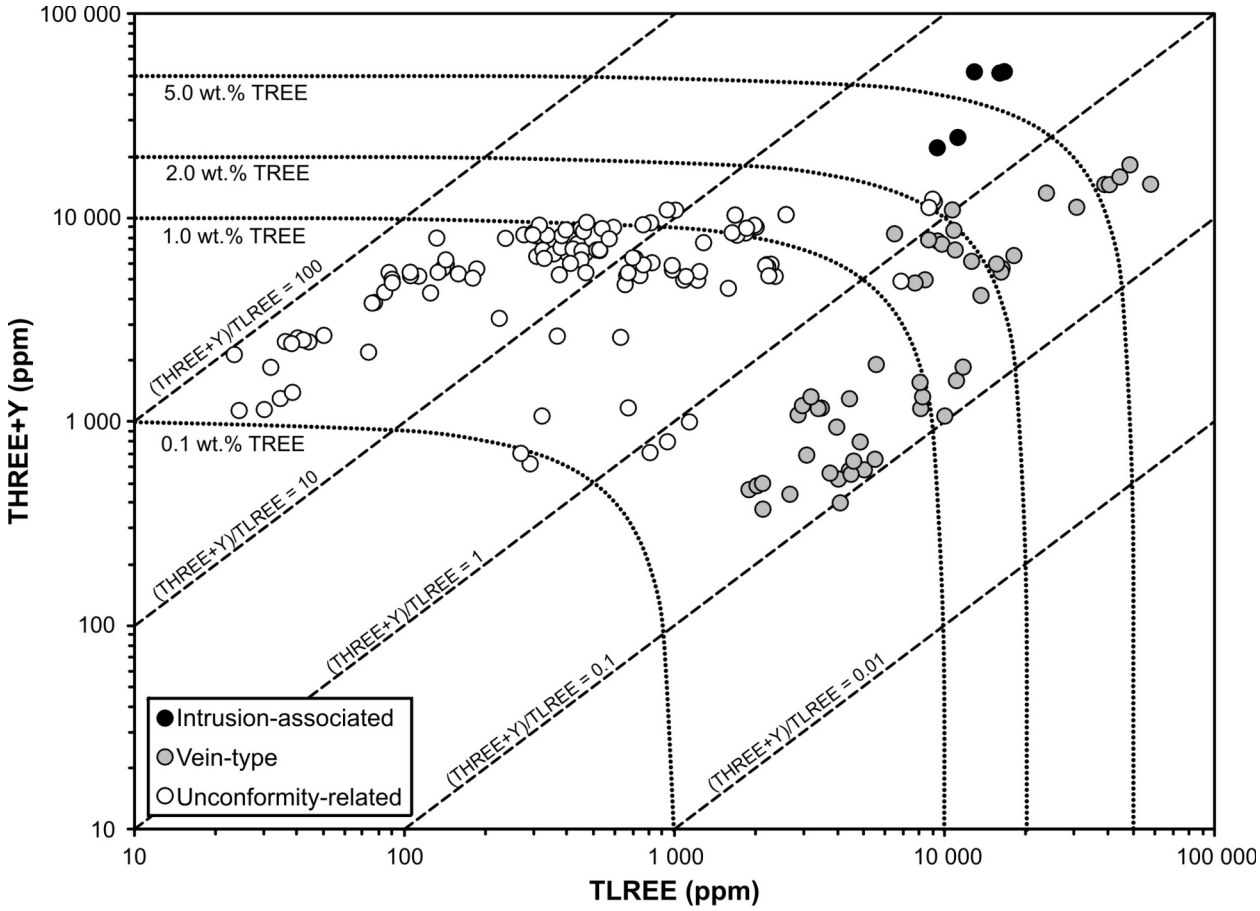

Figure 16 – Log-log plot of the relationship between LREE and THREE+Y concentrations in U oxides from intrusion-associated, vein-type, and unconformity-associated U mineralization. Available data indicate that U oxides: 1) from intrusion-associated mineralization contain 3 to 7 wt. % TREE with (THREE+Y)/TLREE ratios between 2 and 5; 2) from vein-type mineralization contain widely variable TREE concentrations of between 0.2 to 7.2 wt. % with relatively low (THREE+Y)/TLREE ratios between 0.1 and 1.3; and 3) from unconformity-associated mineralization contain 0.1 to 2.1 wt. % TREE and show the greatest THREE+Y enrichment ((THREE+Y)/TLREE ratios between 0.7 and 92.5). Sources of data for U-oxide compositions from intrusion-associated mineralization: Mercadier* **et al.** *(2013) (Moore Lakes and Fraser Lakes: SIMS and LA-ICP-MS). Sources of data for U-oxide compositions from vein-type mineralization: Dieng (2012) (Ace, Fay, and Gunnar mines: LA-ICP-MS); Mercadier* **et al.** *(2013) (Hook Lake: SIMS and LA-ICP-MS). Sources of data for U-oxide compositions from unconformity-associated mineralization: Fayek (1996) (Cigar Lake, McArthur River, Key Lake, Sue zone, and Eagle Point North: ICP-MS); Bonhoure (2007) and Bonhoure* **et al.** *(2007) (Shea Creek and McArthur River: SIMS); Mercadier (2008) (Millennium and Eagle Point: SIMS). Abbreviations: ICP-MS, inductively coupled plasma–mass spectrometry; LA-ICP-MS, laser-ablation inductively coupled plasma–mass spectrometry; SIMS, secondary-ion mass spectrometry.

REE concentrations. For example, there is no REE enrichment accompanying U mineralization in Si-Na metasomatites associated with quartz monzonite in the Grease River area (SME Assessment File 74O09-0023). Where pegmatites are enriched in HREE and Y, this enrichment is correlated with increased U concentrations. This is illustrated in the U vs. Dy diagram in Figure 17, where the data separate into a clear population of points that projects toward magmatic uraninite compositions obtained from pegmatites in the Moore Lakes area (Annesley *et al.*, 2000) and the Fraser Lakes area (McKechnie *et al.*, 2012b; Mercadier *et al.*, 2013), and a more dispersed population of points that extends to lower U/Dy ratios defined by monazite compositions. The importance of monazite in controlling part of the REE budget of the pegmatites is further suggested by the Th and Ce abundances illustrated in Figure 18. Electron microprobe analyses of uraninite, thorite, Nb oxide, and monazite from the Fraser Lakes area, provided by McKechnie *et al.* (2012b), and bulk-rock geochemical data from locations across the province suggest that uraninite, Th-U silicates, and monazite could be the most important minerals controlling HREE+Y concentrations in most uraniferous pegmatites in Saskatchewan.

Exploration drilling of the intrusion-associated U mineralization in the Fraser Lakes area enabled JNR Resources Inc. to delineate a U-Th-REE deposit, named the Fraser Lakes zone B (locations 222 to 224, Table 8 and Figure 12),

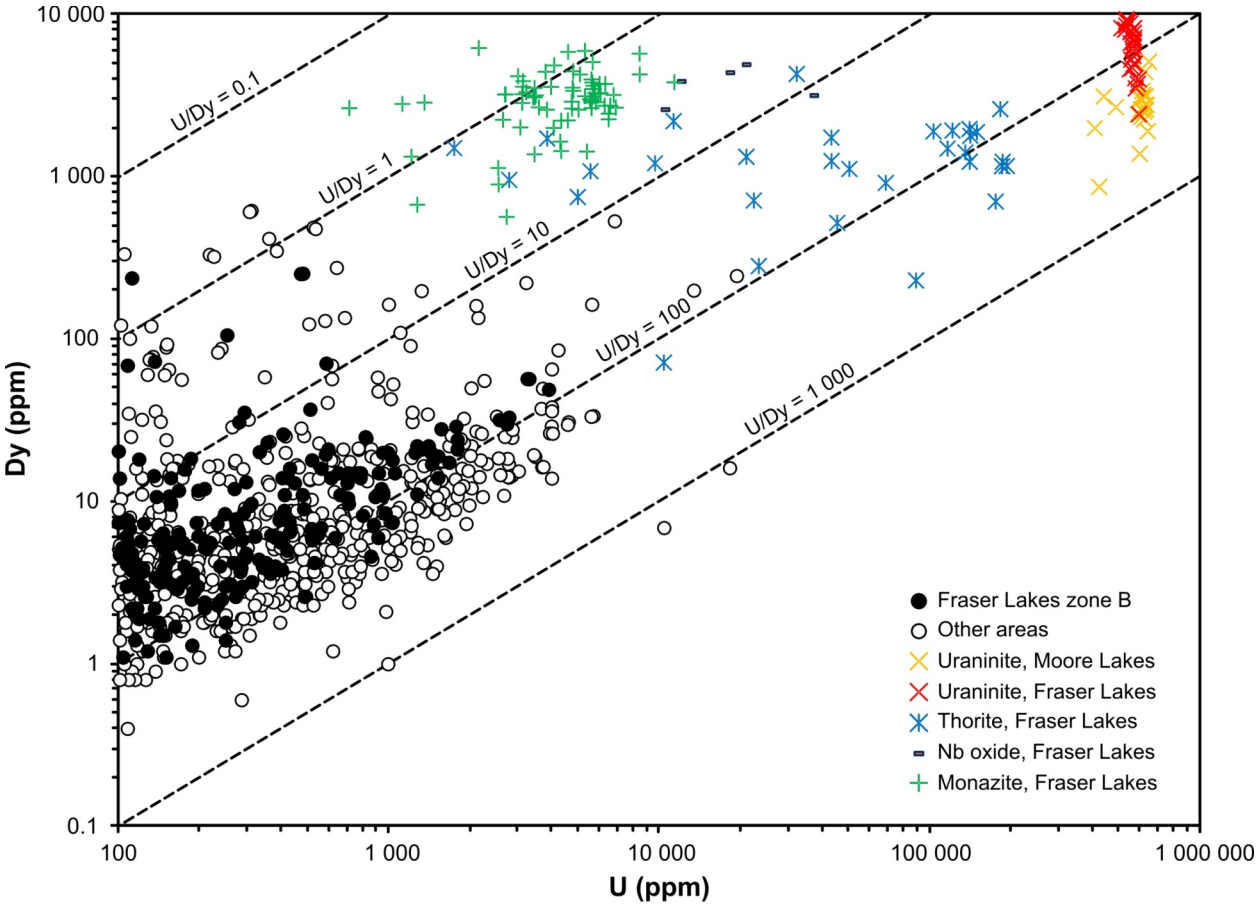

Figure 17 – Log-log plot of the relationship between U and Dy concentrations in intrusion-associated U mineralization.

for which a Resource estimate was published in a NI 43-101–compliant technical report in 2012 (Armitage and Sexton, 2012). The document reports an Inferred Resource estimate, based on a 0.01% U_3O_8 cut-off grade, of 10 354 926 t grading 0.03% U_3O_8 (or 254 ppm U), 0.023% ThO_2 (or 202 ppm Th), 0.02% La_2O_3 (or 171 ppm La), 0.06% Ce_2O_3 (or 512 ppm Ce), 0.001% Yb_2O_3 (or 8.8 ppm Yb), and 0.007% Y_2O_3 (or 55.1 ppm Y). Converting oxide to metal concentrations, U/Th, U/La, U/Ce, U/Yb, U/Y, and Th/Ce ratios of 1.3, 1.5, 0.5, 29.0, 4.6, and 0.4, respectively, were obtained.

Mineralization in the Fraser Lakes area is hosted by pegmatites intruded into folded Wollaston Group metasedimentary rocks of Proterozoic age near the contact with underlying Archean gneiss (McKechnie *et al.*, 2012b). Two types of mineralized pegmatites were reported to be present in the area by McKechnie *et al.* (2012b): group A, containing uraninite, uranoan thorite, zircon, and traces of coffinite and allanite; and group B, containing monazite, uranoan thorite, zircon, and rare xenotime, pyrochlore, and allanite (classified in this report under "Monazite-Dominant Mineralization"; see Table 3). Group A pegmatites differ from those of group B in being more quartz rich and biotite poor. Only the group A pegmatites were successfully dated and it was suggested that they were generated during decompression melting of Wollaston Group metasedimentary rocks, during peak Trans-Hudsonian metamorphic conditions at *ca.* 1.85 to 1.80 Ga, where peraluminous melt was channelled during deformation along the Archean basement–Proterozoic cover interface and collected along regional fold noses (McKechnie *et al.*, 2012a).

Electron microprobe, secondary-ion mass spectrometer (SIMS), and laser-ablation inductively coupled plasma–mass spectrometer (LA-ICP-MS) analyses presented in Mercadier *et al.* (2013) show that uraninite in the pegmatites of the Fraser Lakes area averages 8.1 to 8.4 wt. % Th and 2.2 to 3.4 wt. % Y, and contains up to 3.5 wt. % lanthanides. The data of Mercadier *et al.* (2013) show that the THREE+Y concentrations constitute >53% of the TREE contained in the uraninite. The calculated Eu/Eu* values are very low (<0.03), a feature that can be attributed to consumption of Eu by early-crystallizing plagioclase during solidification of the pegmatite melt.

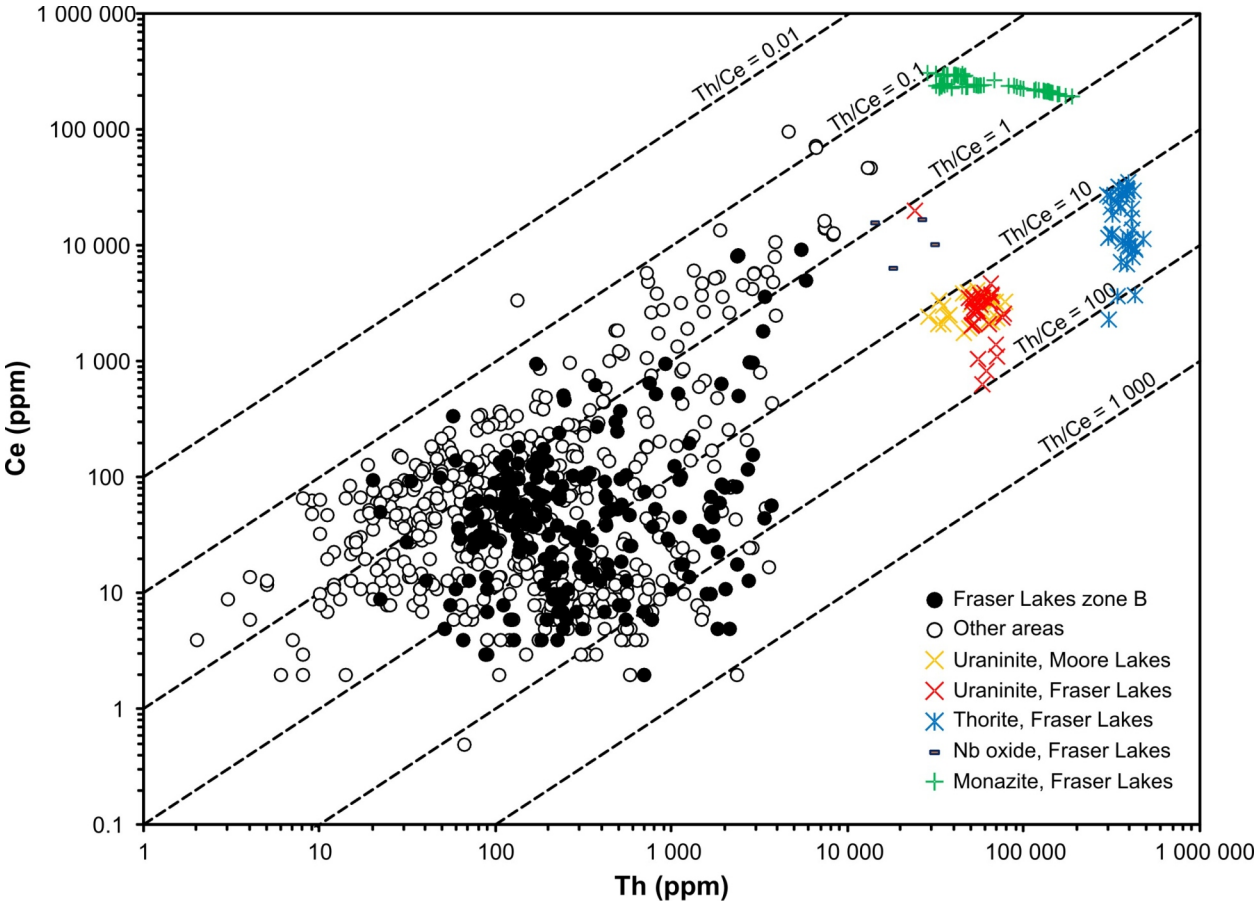

Figure 18 – Log-log plot of the relationship between Th and Ce concentrations in intrusion-associated U mineralization.

Robinson (1955) reported the occurrence of pyrochlore-microlite (betafite according to Koeppel, 1968), allanite, uraninite, uranothorite, and cyrtolite (metamict, U-REE–rich variety of zircon) in a granitic pegmatite on the north side of Viking Lake (SMDI #1345; location 167, Table 6 and Figure 6), 20 km east of Uranium City in the Beaverlodge Domain. At this location, there is a transition between regionally metamorphosed upper amphibolite– and granulite-facies rocks. No bulk-sample REE data are available. Fergusonite was also reported to occur in the same area (Christie, 1953; Robinson, 1955; Rowe, 1958), but the exact location is unknown.

REE–bearing minerals have not been reported from occurrences of U-Th-Nb-Ta–enriched mineralization in biotite-rich zones of granitic pegmatites near 'Tinco Lake' (unofficial name) and Cup Lake in the southern Mudjatik Domain. A grab sample of biotite-rich material, collected from a 1.5 m wide pegmatite 1 km northwest of Tinco Lake, assayed up to 0.50% Nb_2O_5 and 0.08% Ta_2O_5 (SME Assessment File 74B02-0005, ground anomaly 101, sample 17426B). Field spectrometric measurements from this location indicated 0.06% eU_3O_8 and 1.5% $eThO_2$ (SMDI #1028; SME Assessment File 74B02-0005). Near the south end of the westernmost arm of Cup Lake, a sample collected from another biotite-rich pegmatite lens, 15 cm wide and 7.6 m long, cutting calcsilicate gneiss assayed 0.12% Nb_2O_5, 0.07% Ta_2O_5, and 0.036% U_3O_8 (SMDI #1618; SME Assessment File 74B02-0005). In addition, Cup Lake Uranium Ltd. documented radioactive, coarse-grained, biotite-rich rocks from bedrock exposures and float, some containing round patches of a black mineral with dull lustre that was not identified, on the northwest side of Cup Lake (SME Assessment File 74B02-NW-0003). In one instance (no. 4 "showing"), the occurrence of radioactive, biotite-rich rock was traced over a strike length of more than 30 m ("several hundred feet"). U was not detected by chemical analysis, and radioactivity was attributed to Th. Analyses for Nb or Ta were not reported. Many U-Th-Nb-Ta–rich minerals, such as pyrochlore, fergusonite, euxenite, polycrase, samarskite, and aeschynite, contain appreciable or essential concentrations of HREE+Y. Deposits containing economic concentrations of these minerals in metaluminous to peraluminous granitic pegmatites have, however, rarely been encountered and are only of historical interest.

Vein-Type U Mineralization (Older than 1.70 Ga) (Table 9, Figure 13)

Analytical data for REE from vein-type U deposits in Saskatchewan are comparatively scarce. The available data are mostly for a small proportion of the deposits in the Uranium City historical U-producing district, for which a review was presented in Normand (2013). Other locations of vein-type U mineralization for which bulk-sample REE data are available in the Beaverlodge Domain include 'MacIntosh Bay' (unofficial name), Felix Bay, Adair Bay, and the Gaitwin U zone A (SMDI #1567; SME Assessment File 74N08-0162). Bulk-sample REE data for vein-type U mineralization are also available for the Bradley Lake occurrence (SMDI #1593; SME Assessment File 74O09-0023) in the Tantato Domain and the Hook Lake occurrence (SMDI #2016; SME Assessment Files 74H02-0024, -0040, and -0043) in the Wollaston Domain. Geochemical data and descriptions for the above examples are presented in Table 9, and their locations are shown in Figure 13.

U mineralization in the Uranium City general area reportedly developed over a long period of time, culminating at *ca.* 1850 Ma according to Dieng *et al.* (2013), and paragenetic sequences comprising six to seven stages have been documented (Robinson, 1955; Sassano *et al.*, 1972; Tremblay, 1978; Dieng, 2012). Historical production of 25 142 t U between 1953 and 1982 is reported to have been largely supplied (>90%) by the Ace, Fay, Verna, and, to a lesser extent, Gunnar mines (Sibbald *et al.*, 1991). U grades were low in the deposits, averaging between 0.1 and 0.2 wt. % U. REE were not produced because their concentrations were considered too low (Beck, 1969). However, U oxides in some of the district's deposits have long been known, or suspected, to contain significant REE concentrations. Alcock (1936) reported 2 wt. % REE in a sample from the No. 1 zone of the Nicholson mine (Robinson, 1955; location 244, Table 9 and Figure 13), which consisted chiefly of altered pitchblende, chalcopyrite, and limonite. Partial analysis of a biotite concentrate from the Hacker zone (SMDI #1275) in Fish Hook Bay was reported by Robinson (1955) to contain 6.47% U and 0.19 wt. % Th+REE. An average of 12.59 wt. % U_3O_8 and 470 ppm Y was reported by Beck (1969, Table 5.3, column D) for 49 X-ray fluorescence (XRF) analyses of Ace-Fay ore. U-rich samples (>0.3 wt. % U) containing anomalous Y concentrations (>100 ppm, up to 2644 ppm) were reported by Sibbald (1988) to occur in the Eldorado Radioactive occurrence 45-SH-10 (SMDI #1272), the Eldorado Radioactive A zone (SMDI #1274), and the Joe occurrence, all in Fish Hook Bay. Peiris (1991) analyzed massive and botryoidal pitchblende from the Nicholson mine by neutron activation and obtained up to 158 ppm Eu, 440 ppm Tb, 410 ppm Yb, and 60 ppm Lu (LREE were not reported due to analytical interferences).

More recently, Dieng (2012) obtained electron microprobe and LA-ICP-MS analyses of brannerite and several generations of U oxides from the Ace, Fay, and Gunnar deposits. His results show that the brannerite contains between 0.02 and 0.52 wt. % Y+Tb and that the U oxides, all generations included, contain between 0.21 and 3.53 wt. % TREE, of which the proportion of THREE+Y varies between 3 and 57% of the TREE (higher proportions of THREE+Y tend to occur in the U oxides containing the most REE). Normand (2013) showed that variations in concentration of many of the REE and U in rock samples from the Uranium City area correlate positively where U is present in concentrations exceeding 0.2 wt. % (average U grade of the Ace-Fay deposit). This observation is attributed to a threshold value above which the abundance of REE-bearing U minerals becomes sufficient to cause an increase in REE concentrations above those in the rocks that host U mineralization. Thus, the problem appears to be not so much the lack of REE in the U ore minerals but the lack of abundance of those minerals. The discovery of higher grade and large tonnage mineralization in the Uranium City district in the future may stimulate further research into the recovery of REE from the U ores.

A number of occurrences of vein-type U mineralization were analyzed for REE by CanAlaska Uranium Ltd. as part of their Poplar project, focussed along the northern shore of Lake Athabasca (SME Assessment File 74N08-0162), and are briefly described here. At MacIntosh Bay (locations 246 to 249, Table 9 and Figure 13), the mineralization is reported to consist of a vein, 2 cm wide, >40 m in strike length, and cutting metapelite, quartzite, and minor pegmatite, from which analyses returned up to 3 wt. % U and 1532 ppm THREE+Y (representing 57% of the TREE). Another sample assayed 0.64 wt. % U and 1159 ppm THREE+Y (representing 68% of the TREE), as well as 34.3 g/t Au. At Felix Bay (locations 250 and 251, Table 9 and Figure 13), samples of metapelite and pegmatites cut by 1 to 10 mm wide mineralized veinlets of unknown strike length returned up to 8.68 wt. % U and 3023 ppm THREE+Y (representing 76% of the TREE). A sample containing 3.63 wt. % U and 1421 ppm THREE+Y also contained 46.94 g/t Au. From the Adair Bay area (locations 252 to 254, Table 9 and Figure 13), two samples of mineralized amphibolite (samples FT056 and FT057, Table 9) assayed, respectively, 3.4 wt. % U and 1435 ppm THREE+Y (representing 74% of the TREE), and 4.5 wt. % U, 1174 ppm THREE+Y (representing 63% of the TREE), 3.8 g/t Au, 1.5 g/t Pt, and 0.8 g/t Pd. At the Gaitwin Uranium zone A (renamed the Fall showing by CanAlaska Uranium Ltd.) on the Natukam Peninsula (locations 255 to 268, Table 9 and Figure 13), U mineralization occurs in short (<50 m in strike length), thin (<1 cm wide) veins, the thickest of which are associated with north-northwest–striking fault zones. Pitchblende and secondary yellow U minerals were identified in the

veins, from which samples assayed up to 49.4 wt. % U and 1.13 wt. % THREE+Y (representing 71% of the TREE). U/Th ratios >400, elevated Eu/Eu* (normally associated with hydrothermal U oxides), and generally low La_N/Yb_N characterize samples from CanAlaska's Poplar project. The mineral that hosts the REE at most of these occurrences was not specified, but it is reasonable to assume that U minerals contain them, at least in part. The calculated (THREE+Y)/U values of the samples are fairly constant, averaging ~0.04 irrespective of TREE and U concentrations (see Table 9), and further suggesting that one phase carries most of the REE.

At the Bradley Lake occurrence (locations 269 to 271, Table 9 and Figure 13; SME Assessment File 74O09-0023), located near the southern edge of the Grease River shear zone in the Tantato Domain and 30 km northwest of Stony Rapids, pitchblende mineralization was reported to occur in fractures oriented perpendicular to the edge of, and restricted to within, a leucogranitic pegmatite intruded into mylonitic biotite-rich pelitic paragneiss. The fractures, measuring 0.2 to 0.8 cm wide, were traced up to several metres, but the density of their distribution was not reported. Chemical analyses of mineralized samples from the locality returned up to 2.99 wt. % U and 892 ppm THREE+Y (representing 36% of the TREE). Calculated bulk-sample La_N/Yb_N values are closest to those calculated for samples from localities in the Uranium City area.

Elevated REE concentrations of up to 1.4 wt. % TREE were reported by Agip Canada Ltd. (locations 272 and 273, Table 9 and Figure 13; SME Assessment File 74H02-0024) from a 6 by 1.5 m, arcuate, fault-hosted uraninite-rich vein located near Hook Lake in the Wollaston Domain, 65 km southeast of the McArthur River mine. Drilling by the company failed to intersect the mineralization at depth. The locality was re-examined recently by JNR Resources Inc. as part of their Way Lake project (SME Assessment Files 74H02-0040 and -0043), and assay results from the vein confirmed earlier reports of elevated REE concentrations. Three samples containing between 33.9 and 48.9 wt. % U also contained >2.5 wt. % TREE, including 0.9 to 1.6 wt. % THREE+Y (representing 38 to 42% of the TREE). Calculated U/Th values for these samples are lower than those obtained from other localities of vein-type U mineralization. Electron microprobe, SIMS, and LA-ICP-MS analyses presented in Mercadier *et al.* (2013) show that uraninite in the Hook Lake vein averages 2.1 to 2.8 wt. % Th and 0.6 to 1.0 wt. % Y, and surprisingly elevated lanthanide concentrations of up to 6.6 wt. % (mainly LREE). Mercadier *et al.* (2013) suggested that the elevated Th and REE concentrations in the uraninite from this locality reflect elevated temperature conditions during emplacement, which is consistent with U-Pb isotopic ages determined for the mineral (1805 ±11 Ma) that coincide with thermal peak (1.82 to 1.81 Ga) to post–thermal peak (1.81 to 1.72 Ga) events related to the evolution of the Trans-Hudson Orogen.

Globally, the vein-type U mineralization presents lower THREE+Y enrichments ((THREE+Y)/TREE (%)) than the intrusion-associated U mineralization of equivalent U concentrations (Figure 19). No significant extent has been demonstrated for the vein systems discussed in this section, except those in the Uranium City area. U mineralization hosted by a vein-and-fault Riedel system at the historical Nisto mine (SMDI #1621; Normand, 2013), located ~14 km northeast of the community of Black Lake near the western shore of Black Lake, should be tested for REE.

Unconformity-Related U Mineralization (<1.7 Ga) (Table 10, Figure 14)

There are many comprehensive studies on various aspects of the unconformity-related U deposits located in the Athabasca Basin. For an excellent overview, the reader is referred to Jefferson *et al.* (2007). Some examples of more recent, specialized studies discussing deposit age, the dynamics of fluid flow in the Athabasca Basin, physicochemical controls on mineralization, origin of fluids, and deposit genesis are Alexandre *et al.* (2009a, 2009b, 2010), Cloutier *et al.* (2010, 2011), Richard *et al.* (2010, 2011), Mercadier *et al.* (2011a, 2011b, 2012), and Chi *et al.* (2013). The discussion that follows is focussed on a general assessment of the distribution of REE in the unconformity-related U mineralization of the Athabasca Basin.

The world-class unconformity-related U deposits of the Athabasca Basin are variably classified, from a geological setting or geochemical perspective, as basement- or sandstone-hosted (further distinguished as located at the unconformity or 'perched' in sandstone above the unconformity), complex polymetallic or simple monometallic types, and ingress (ore-forming fluids derived from the Athabasca Basin) or egress (ore-forming fluids derived from basement rocks) types. REE enrichment in unconformity-related deposits of the Athabasca Basin was recognized by a number of exploration companies and investigators in the early 1980s (Harper, 1987, and references therein). According to Jefferson *et al.* (2007), the more REE-rich deposits include those that are characterized by a complex, polymetallic mineral paragenesis. Whereas this appears to be verified *on average* for mineralization containing less than 1000 ppm U, the relationships between U and TREE in monometallic and polymetallic deposits at U concentrations above 1000 ppm show considerable overlap (Figure 20), making a distinction in REE enrichments between the two types based upon diversity of metal content unreliable. The locations of 15 mineralized areas that

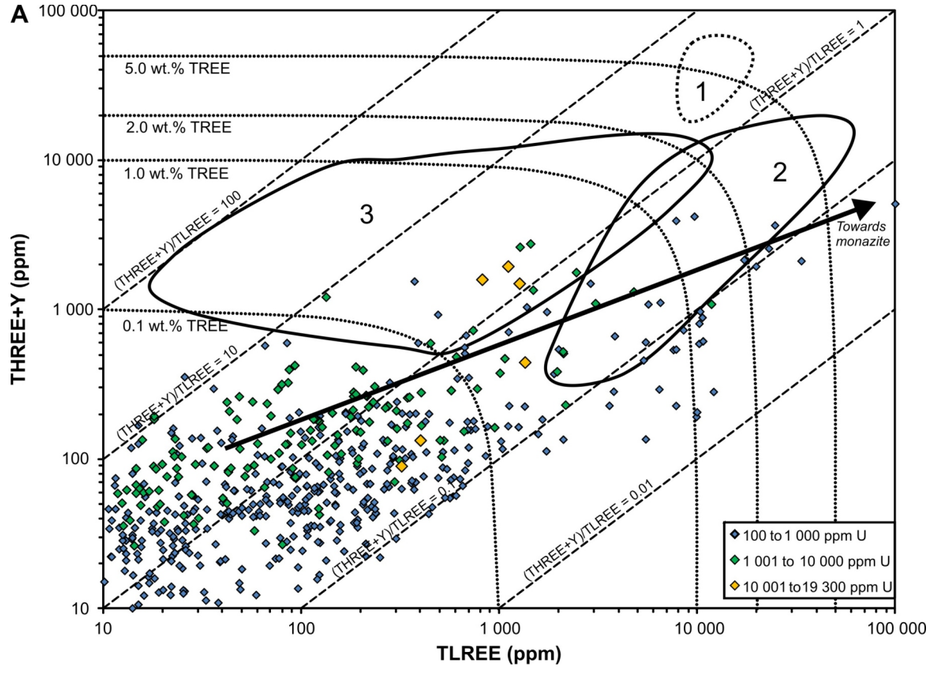

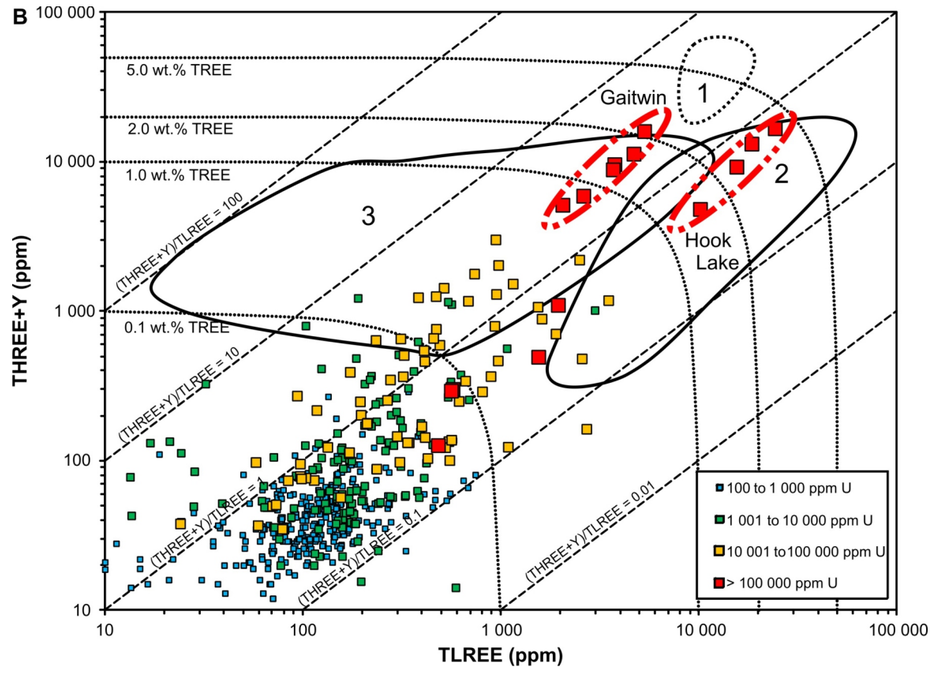

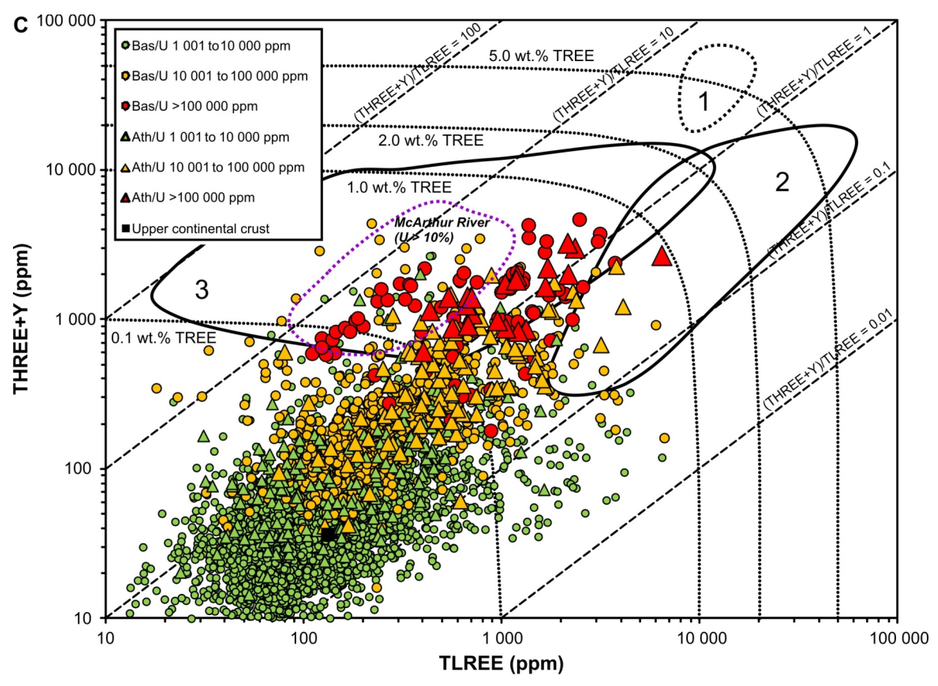

***Figure 19** – Log-log plots of the relationships between TLREE and THREE+Y concentrations in U mineralization of Saskatchewan: a) intrusion-associated b) vein-type, and c) unconformity-related of the Athabasca Basin. Contoured areas numbered 1, 2, and 3 represent the ranges in TLREE and THREE+Y concentrations reported from U oxides in intrusion-associated, vein-type, and unconformity-related U mineralization, respectively. Areas in part B with thick orange dashed-dotted outlines contain samples from the Gaitwin and Hook Lake occurrences; area in part C with purple dotted outline contains samples from the McArthur River deposit with >10 wT. % U. See captions of Figures 15 and 16 for sources of data. Abbreviations: Bas, basement host; Ath, Athabasca Group sediment host.*

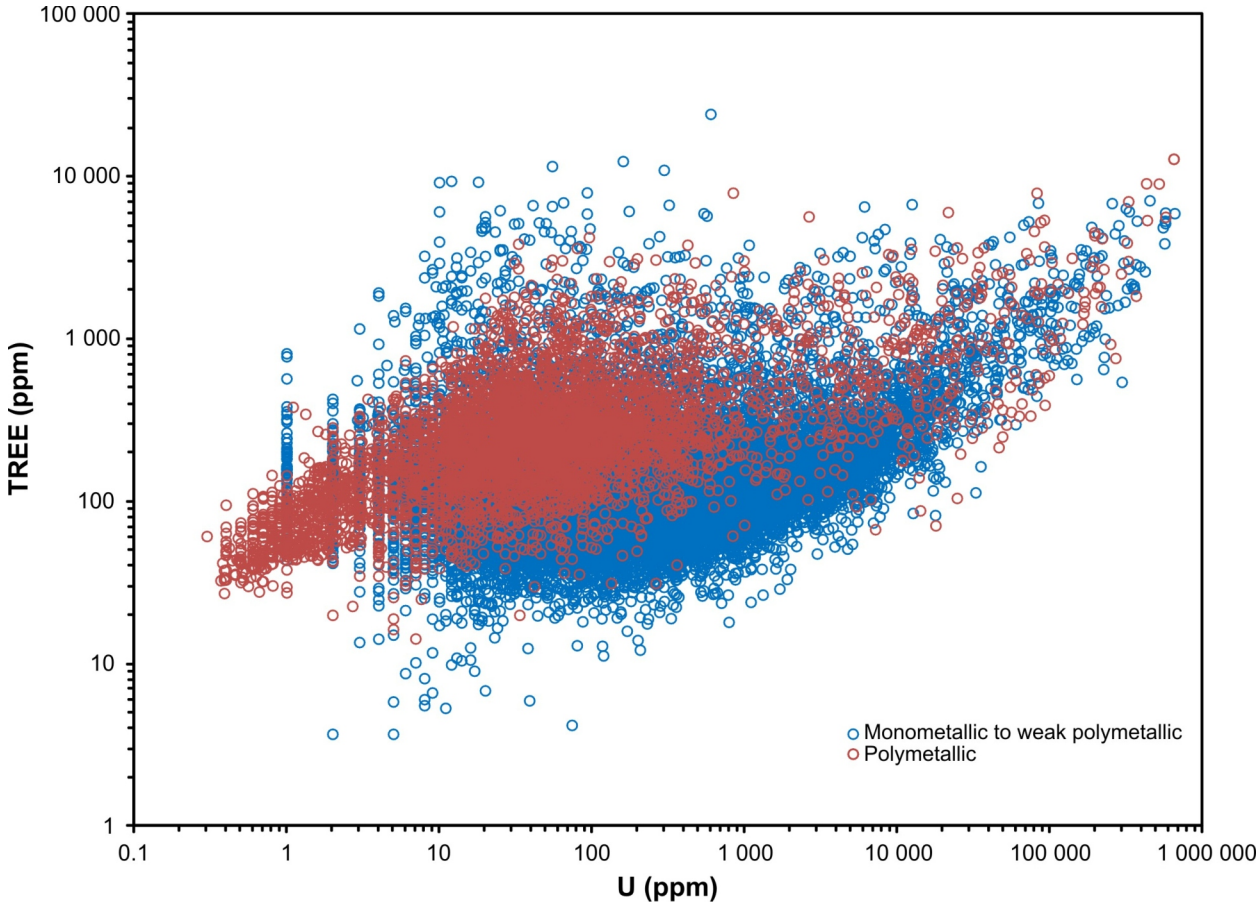

Figure 20 – Log-log plot of the relationship between U and TREE concentrations in monometallic to weakly polymetallic, and polymetallic unconformity-related mineralization of the Athabasca Basin. The data (n = 22,973) presented in this diagram were compiled from selected drill-core sections (selective or systematic sampling) and bulk-rock geochemical U and REE analyses (total digestion, ICP or fluorimetric) obtained from twelve deposits or areas. Data from monometallic or weak polymetallic deposits are represented by Horseshoe (n = 15,941; complete database from SME Assessment File 64L04-0130), McArthur River (n = 41; data from SME Assessment File 74H-0048), Millennium (n = 36; selected data from SME Assessment File 74H12-0043), P-Patch (n = 59; selected data from SME Assessment File 74H04-0110), Phoenix (n = 70; selected data from SME Assessment File 74H06-0142, discovery hole), and Shea Creek (n = 1,796; selected and complete data from SME Assessment Files 74K04-NE-0031, -0041, and -0042). Data from polymetallic deposits are represented by Cigar East (n = 90; selected data from SME Assessment Files 74I02-0083, -0084, and -0087), Midwest Lake (n = 34; selected data from SME Assessment File 74I08-0069), Moore Lakes (n = 679; complete database from SME Assessment File 74H06-NE-0128), Read Lake (n = 439; complete database from SME Assessment File 74H14-0073), Tamarack (n = 24; selected data from SME Assessment Files 64L05-0180 and 74I01-0114), and West Bear (n = 3,764; selected data and complete database from SME Assessment Files 74H16-SE-0079 and 74H16-0093, respectively). Although the compiled dataset varies in completeness and quality of analyses, the overall effects of the lower quality and incomplete data (e.g., some REE may not have been analyzed or detection limits may vary according to the technique used) during manipulation of the database is believed to be minimal and should not affect significantly the conclusions reached in the data analysis presented in this study.

qualify as TREE or THREE+Y occurrences are shown in Figure 14, and geochemical data for selected diamond-drill core samples are presented for each in Table 10.

REE in the U deposits of the Athabasca Basin are hosted by a variety of diagenetic or hydrothermal minerals, and include mainly U oxides and silicates, APS minerals, and accessory apatite, xenotime, and monazite (Quirt *et al.*, 1991; Fayek, 1996; Fayek and Kyser, 1997; Gaboreau *et al.*, 2007; Cloutier *et al.*, 2009, 2010, 2011; Mercadier *et al.*, 2011a, 2011b). Other pre-diagenetic or pre-ore minerals of magmatic, metamorphic, or detrital origin that are expected to contribute minor or trace amounts of lanthanides, Y, and Sc in basement or Athabasca Group rocks and may be present in trace to major proportions include garnet, titanite, phyllosilicates, Ti and Fe oxides, apatite, allanite, monazite and xenotime (see Fayek and Kyser, 1997).

U oxides, which form the major part of the ore (or mineralization) of the deposits, commonly contain elevated REE concentrations. Fayek (1996) reported 1.18 wt. % TREE in a third-generation uraninite from the Cigar Lake deposit,

41.9% of which comprises THREE+Y, including 953 ppm Dy; and 0.71 wt. % TREE in uraninite from the McArthur River mine, 90% of which comprises THREE+Y, including 1386 ppm Dy. Similar results for uraninite from the McArthur River deposit were reported by Bonhoure *et al.* (2007). U and REE concentrations in U oxides were compiled from eight unconformity-related deposits (Fryer and Taylor, 1987; Reyx and Ruhlman, 1993; Fayek and Kyser, 1997; Bonhoure *et al.*, 2007; Mercadier, 2008; Beshears, 2010; Mercadier *et al.*, 2011a; Ng, 2012). Statistical data for U, Th, and REE are presented in Table 11. Highlights from this analysis are: Y is by far the most abundant REE (median 3622 ppm; n = 183), followed by Dy (median 780 ppm; n = 127) and Er (median 248 ppm; n = 116); the calculated median TREE, TLREE, and THREE+Y concentrations are 6886, 448, and 5967 ppm, respectively (n = 116). Consistent with the relative magnitude of the latter numbers, the calculated median values for (THREE+Y)/TREE percentage and La_N/Yb_N are 94% and 0.1, respectively (n = 116); the median of the arithmetically calculated Eu/Eu* values is 1.3 (n = 39).

U mineralization in the Athabasca Basin displays extreme variations in (THREE+Y)/TREE that converge to above ~75% as U concentrations increase toward those equivalent to 100% U oxide (Figure 21). Such variations are obviously the result of dilution of HREE+Y–rich U oxides in hostrocks that contain variable proportions of different minerals (see above) that, in turn, contain different REE concentrations and are characterized by different (THREE+Y)/TREE percentages. Locally abundant APS minerals likely contribute a very significant LREE component to the U ores (or mineralization), as suggested by data presented in Figure 22. APS minerals in the unconformity-related U deposits are represented mainly by solid solutions among the end members florencite ($LREEAl_3(PO_4)_2(OH)_6$), crandallite ($CaAl_3(PO_4)_2(OH)_5•(H_2O)$), goyazite ($SrAl_3(PO_4)_2(OH)_5•(H_2O)$), and svanbergite ($SrAl_3(PO_4)(SO_4)(OH)_6$) of the alunite supergroup of minerals (Gaboreau *et al.*, 2007; Bayliss *et al.*, 2010; Cloutier *et al.*, 2011). Reported REE concentrations in the APS minerals vary from <1 to 20 wt. % TLREO or greater in the Wheeler River area (Cloutier *et al.*, 2010), and in the Eagle Point (Mercadier *et al.*, 2011a) and Anne deposits (Gaboreau *et al.*, 2007).

Examination of the relationships between U concentrations and TREE, TLREE, THREE+Y, and Dy concentrations, illustrated in Figure 23, provide further evidence that most of the variation in (THREE+Y)/TREE percentage values displayed by the geochemical data in unconformity-related U deposits is due to the mixing of variable proportions of LREE-rich minerals, which obscure the signature of U oxides. Two populations of data points, especially well represented by samples obtained from Athabasca Group siliciclastic rocks, are readily apparent in Figure 23. The first population, characterized by low U/REE ratios and U concentrations mainly below 100 ppm, defines a comparatively nonmineralized group in which the U and REE variations are attributed to the presence of variable proportions of igneous, metamorphic, detrital, diagenetic, and hydrothermal REE-bearing and relatively U-poor minerals (*e.g.*, monazite, xenotime, APS minerals, zircon, apatite). The second population, characterized by elevated U/REE ratios, defines a mineralized group in which the U and REE variations are attributed to the presence of variable proportions of various generations of REE-bearing U oxides and silicates. The data presented in Figures 23A, C, and D for TREE, THREE+Y, and Dy, respectively, show a good correspondence with a theoretical maximum limit in U/REE ratios imposed by U oxides. This is not the case, however, for the majority of the TLREE data shown in Figure 23B, and can be explained either by a nonrepresentative TLREE distribution in the dataset of U oxide compositions used here or by the systematic presence of significant amounts of other LREE-rich phases in the U ores.

The McArthur River and Cigar Lake deposits are the richest U deposits in the world, with proven reserve grades of 24.18 and 22.31 wt. % U_3O_8, respectively (or 23.3 and 21.5 wt. % UO_2). Such ores containing ~20 wt. % uraninite would contain in excess of 200 ppm Dy (calculated from data in Table 11), competing favourably in terms of grade with much-sought-after REE mineralization associated with alkaline intrusions, which contain resource Dy grades in the range 200 to 300 ppm (*e.g.*, Strange Lake, Thor Lake, Kipawa). No REE resource estimates are available for deposits in the Athabasca Basin. Based on the REE content of U ore minerals contained in the Athabasca Basin unconformity-related U deposits, Fayek and Kyser (1997) estimated that a total of approximately 5000 t REE was contained in the ensemble of unconformity-related U deposits known at this time. This estimate should be taken as a minimum, however, as it does not take into account the presence of other REE-rich minerals. A revised estimate of the REE contained in the unconformity-related U deposits of the Athabasca Basin can be calculated by first considering data presented in Figure 23. TREE, TLREE, THREE+Y, and Dy concentrations were separated into 11 groups with the U concentration ranges: 101 to 200 ppm, 201 to 500 ppm, 501 to 1 000 ppm, 1 001 to 2 000 ppm, 2 001 to 5 000 ppm, 5 001 to 10 000 ppm, 10 001 to 30 000 ppm, 30 001 to 50 000 ppm, 50 001 to 100 000 ppm, 100 001 to 300 000 ppm, and >300 000 ppm. Univariant statistical analysis was performed on each group of data and the results are presented in graphical form in Figure 24, where they can be compared to calculated contributions from U oxides in Table 12.

Table 11 – Results of univariant statistical analysis of REE concentrations in uranium oxides of unconformity-related uranium mineralization of the Athabasca Basin.

	U (ppm)	Th (ppm)	La (ppm)	Ce (ppm)	Pr (ppm)	Nd (ppm)	Sm (ppm)	Eu (ppm)	Gd (ppm)	Tb (ppm)	Dy (ppm)	Y (ppm)	Ho (ppm)	Er (ppm)	Tm (ppm)	Yb (ppm)	Lu (ppm)	TREE (ppm)	TLREE (ppm)	THREE (ppm)	THREE+Y (ppm)	(THREE+Y)/ TREE (%)	Eu/Eu* (arithmetic)	La_N/Yb_N
N	184	70	116	117	116	116	116	116	39	71	127	183	59	116	59	116	114	116	116	116	116	116	39	116
Minimum	665883.7	1.4	0.2	1.7	0.4	2.6	11.3	4.6	20	10	37	393.7199	9	14	2	2	0.9	917	23.3	80	140	14.79915	0.4167543	0.00303008
Maximum	781095.5	2284.904	3017	3638	2410	1958	2871	1062	2431	5721	6450	9405	3931	3332	3110	3165	2238	41696	10256	31440	31440	98.93041	1.58538	40.50383
Sum	1.31E+08	33442.57	19501.5	35378.11	11689.6	37664.9	25965.9	15067.1	9828.7	18357.6	112106.2	676940.6	11972.6	34176.1	6865.9	21355	5086.5	865853.7	127297.2	228560.5	738556.5	10230	45.46229	114.0481
Mean	709617.9	477.7511	168.1164	302.377	100.7724	324.6974	223.844	129.8888	252.0179	258.5577	882.726	3699.129	202.9254	294.6216	116.3712	184.0948	44.61842	7464.256	1097.39	1970.349	6366.866	88.18962	1.1657	0.983173
Standard error	1895.481	59.37822	50.9443	63.26538	24.78066	41.34184	29.23672	14.10085	69.71766	97.30288	58.35833	163.0493	71.18386	31.58198	58.46011	29.97306	21.22002	477.6271	182.142	293.7951	343.1446	1.225404	0.04576507	0.3761295
Variance	6.61E+08	246804.1	301057.3	468293.4	71233.39	198261.1	99155.13	23064.75	189561.6	672217.4	432523.3	4865067	298961.4	115700.9	201637.5	104212.6	51332.99	2.65E+07	3848382	1.00E+07	1.37E+07	174.1872	0.08168322	16.41092
Standard deviation	25711.55	496.7938	548.6869	684.3197	266.8958	445.2652	314.8891	151.8708	435.3867	819.8887	657.665	2205.69	546.7736	340.1484	449.0406	322.8198	226.5678	5144.202	1961.729	3164.27	3695.78	13.198	0.2858028	4.051039
Median	701672.5	263.6428	15.5	76	25.65	145	141	99	110.4	96	780	3622.223	92.7	248	24.6	157	13	6885.5	447.5	1528.55	5966.5	93.51257	1.2647	0.1044286
25^{th} percentile	691535.2	87.88093	2.825	25.5	7.5	45.3	62.05	29.25	73.9	72.1	564.9	1797	62.3	150.175	18	27	8	5301.475	162.425	1056.275	4874.025	82.72375	1.017435	0.03950946
75^{th} percentile	725340.7	637.1368	82.25	217	85.75	467	243.4	146.5	162.4	124.6	1177	4876	133	352.5	32	233.25	19.125	8870	995.5	2167.75	8324.975	97.0762	1.368723	0.2753143
Skewness	0.9125239	1.73337	4.683661	3.532401	6.414645	2.344257	5.573516	2.997279	3.783941	5.544341	4.948354	0.5521507	5.977012	6.713443	5.750727	7.330891	8.624115	3.093973	3.376188	7.686833	2.652797	-2.461944	-1.02847	8.429135
Kurtosis	0.2866638	3.113227	21.5003	11.85453	50.37101	5.467592	43.48805	12.77425	16.7099	32.30293	40.39115	-0.516496	38.93046	56.71719	35.80713	64.78831	80.30293	17.03782	11.34683	67.69977	17.30977	8.646285	0.3834167	80.34183
Geometric mean	709164	260.2393	17.65388	80.27936	25.47546	132.3367	126.3866	74.19522	133.7147	96.58028	704.6673	2981.725	90.30689	213.3793	24.59899	95.51849	11.46697	6054.988	427.8044	1378.774	5245.2	86.6261	1.121318	0.1279655
Sources of the data*	1, 2, 3, 4	1, 3, 5	2, 5, 6, 7, 8	2, 4, 5, 6, 7, 8	2, 5, 6, 7, 8	2, 5, 6, 7, 8	2, 5, 6, 7, 8	2, 5, 6, 7, 8	5, 7, 8	2, 5, 6, 7, 8	2, 5, 6, 7, 8	3, 4, 5, 6, 8	2, 5, 6, 8	2, 4, 5, 6, 8	2, 5, 6, 8	2, 4, 5, 6, 8	2, 5, 6, 8	Calculated	Calculated	Calculated	Calculated	Calculated	Calculated	Calculated

* 1, Beshears (2010); 2, Mercadier et al. (2011); 3, Ng (2012); 4, Reyx and Ruhlman (1993); 5, Fayek (1996); 6, Bonhoure (2007); 7, Fryer and Taylor (1987); 8, Mercadier (2008).

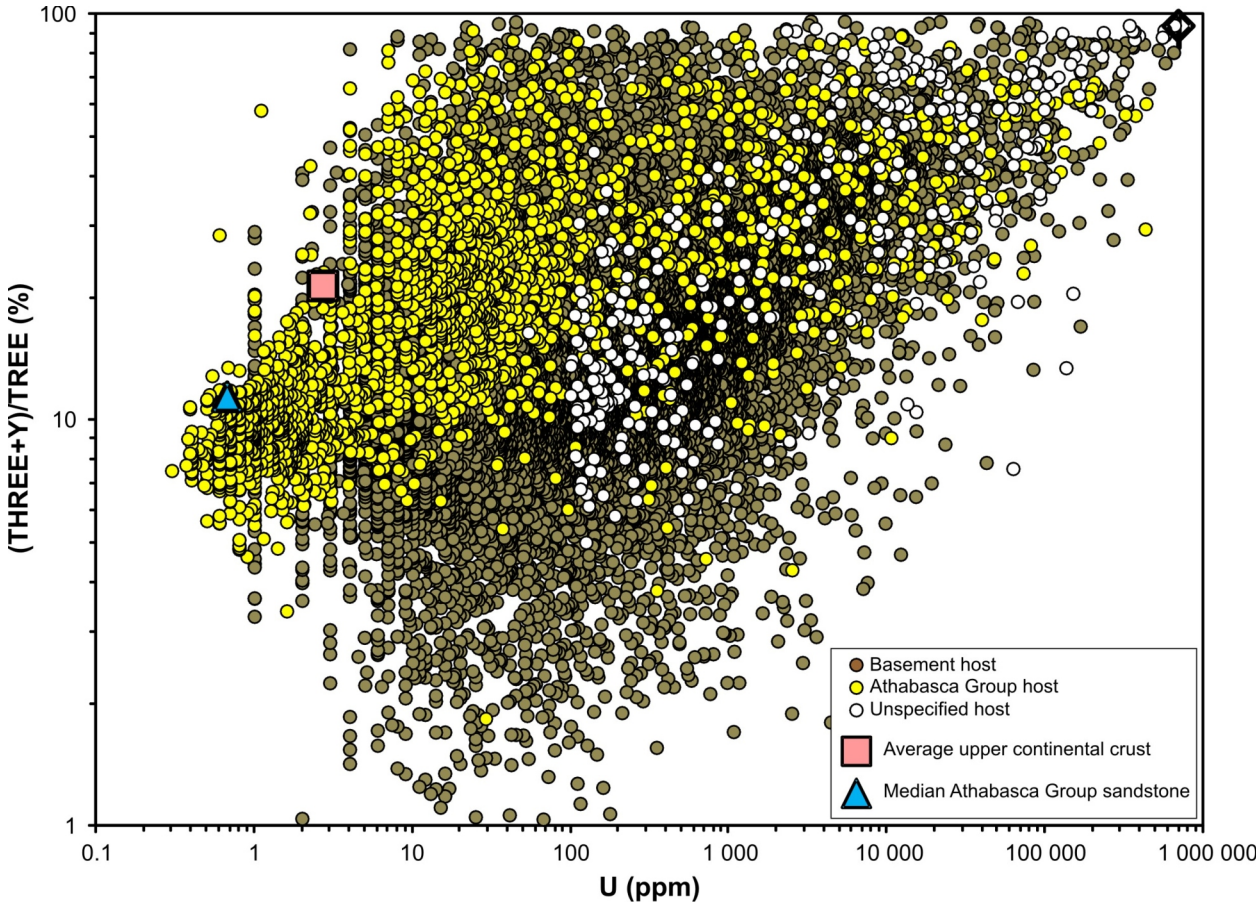

Figure 21 – Log-log plot of the relationship between U concentration and (THREE+Y)/TREE percentage in 22 973 diamond-drill core samples obtained from 12 unconformity-related U deposits of the Athabasca Basin. Values for average upper continental crust (pink filled square) from Rudnick and Gao (2003) and median for Athabasca Group sandstones (blue filled triangle) calculated from data in Card* et al. *(2011), Card and Bosman (2012), and Bosman and Card (2012) are shown for reference. Open black diamond symbol with black vertical bar in upper right corner of plot represents median U and (THREE+Y)/TREE(%) values and the 25th to 75th percentiles of the (THREE+Y)/TREE (%) distributions, respectively, for U oxides presented in Table 11. Basement rocks show a much wider diversity in (THREE+Y)/TREE percentage compared to rocks from the Athabasca Basin, presumably due to a greater variety of minerals in the former. See text for discussion.

The calculations result in relatively modest estimates of Dy and THREE+Y contents, about a hundredth of those contained in, for example, the Thor Lake (Nechalacho) deposit of Avalon Rare Metals Inc. Despite this, several advantages may play in favour of profitable recovery of REE from the unconformity-related U deposits of the Athabasca Basin. Intensive and continued exploration for U in the Athabasca Basin will probably contribute to a continuous, albeit small, supply of ore; mining and milling infrastructures are already in place, permits for radioactive substance storage (Th) have been obtained, and solvent extraction circuits at the Key Lake and McClean Lake mills to recover U (International Atomic Energy Agency, 1993; Areva Resources Canada Inc., 2014; Cameco Corp., 2014) employ methods similar to those used to recover REE (Gupta and Krishnamurthy, 2005). Metals contained in the U ores, such as Mo, Ni, Co, and, by inference, possibly the REE, are separated during the purification process of U at the Key Lake and McClean Lake mill facilities and discarded to tailing ponds. Studies have shown that recovery of Ni and Co from tailings is technically feasible but that economic viability of the process would be strongly dependent on the market for these metals (International Atomic Energy Agency, 1993; Perron, 1996; Cameco Corp., 2002).

Although Y was extracted and marketed as a byproduct of U exploitation from the Denison mine in the Elliot Lake district in the 1970s and 1980s (International Atomic Energy Agency, 1993; Cochrane and Hwozdyk, 2007), no publicly available documentation reports on the feasibility of REE recovery and marketing from U ores of the Athabasca Basin. No data are publicly available on REE concentrations in solutions along the solvent extraction

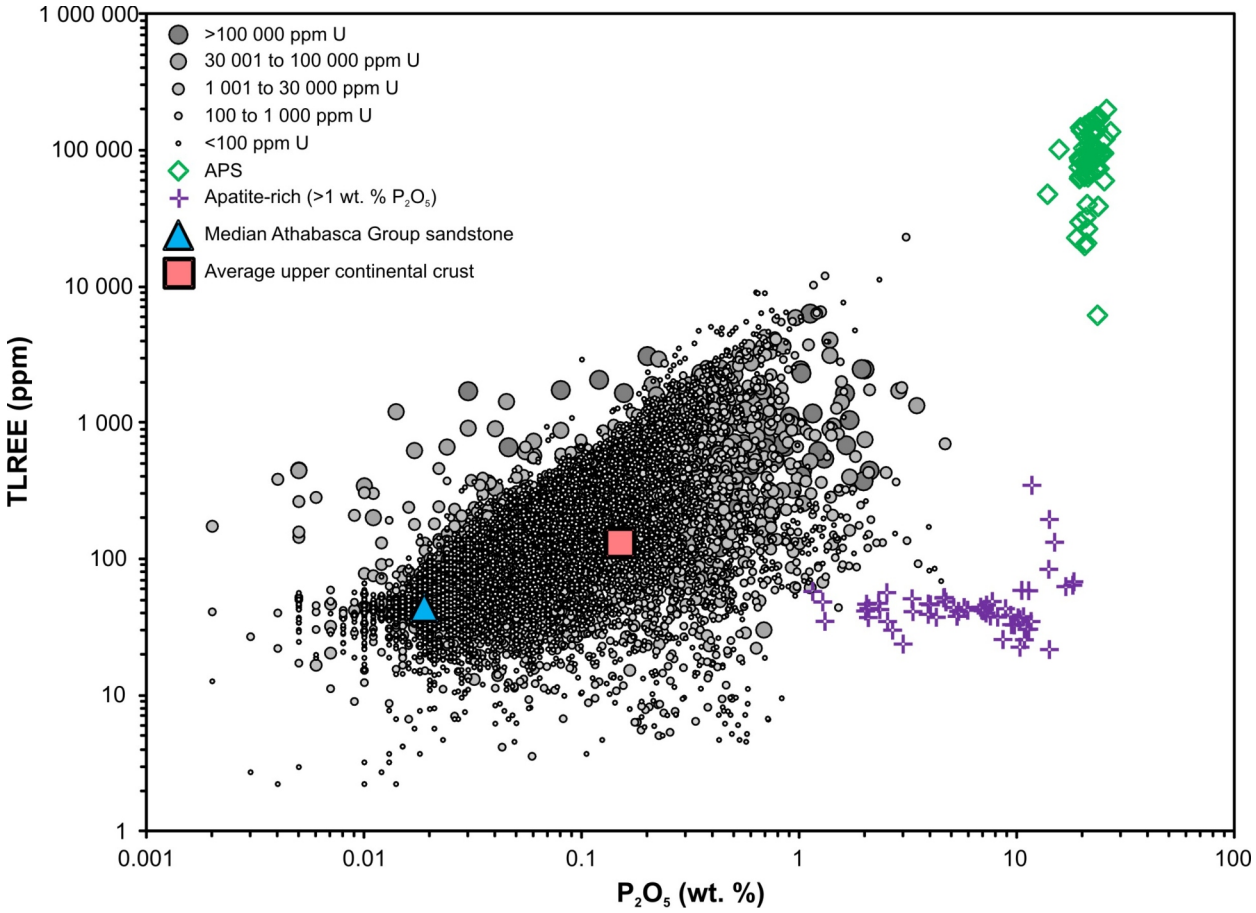

Figure 22 – Log-log plot of the relationship between P_2O_5 and TLREE concentrations in 22 835 diamond-drill core samples obtained from 10 unconformity-related U deposits of the Athabasca Basin. The data suggest that aluminum phosphate-sulphate (APS) minerals (open green diamond symbols) exercise a strong control on the distribution of TLREE in samples containing <30 000 ppm U. Data from Gaboreau* et al. *(2007), Cloutier* et al. *(2009, 2010, 2011), and Mercadier* et al. *(2011a). The role of apatite in controlling TLREE distribution appears to be marginal (blue cross symbols represent apatite-rich samples from the Wolverine Point Formation). Data from Card* et al. *(2011), Card and Bosman (2012), Bosman and Card (2012), and SME Assessment File 74O01-0028.

circuits and solid separates, in calcined yellowcake at the exit of the Key Lake and McClean Lake mill facilities, or in tailings. The feasibility of adding a supplementary solvent-extraction system for profitable recovery of the REE in the mills and production of high-purity metal oxides remains to be demonstrated. At the present time, prospects for economic recovery of REE from U ores of the Athabasca Basin are uncertain.

Sc is another REE of interest that occurs in anomalous concentrations in many U deposits of the Athabasca Basin. Sc is one of the most valuable of the REE. Depending on purity, Gambogi (2013) reported 2011 to 2012 selling prices per kilogram Sc_2O_3 of US$900 (99.0000% purity) to US$5900 (99.9995% purity). Prices as high as US$7100/kg for 99.95% Sc_2O_3 were reported recently (HEFA Rare Earth Canada Co. Ltd., 2013). As a result, the metal is in low demand and is used principally in aluminum alloys for aerospace components and sporting equipment. In 2012, worldwide Sc consumption did not exceed 10 t (Gambogi, 2013). In the event of a sharp drop in price for this commodity, Raade (2003) forecasted immediate demand for large-scale production of Sc alloys.

According to Rudnick and Gao (2003), the abundance of Sc in the upper continental crust is 14 ppm, close to the abundances of Nb (12 ppm) and Pb (17 ppm). REE more abundant than Sc in the upper continental crust are Ce (63 ppm), La (31 ppm), and Y (21 ppm). As discussed briefly in the "General Considerations" section, Sc tends to be dispersed in Al- and Fe-rich minerals in the upper continental crust and is rarely concentrated in amounts sufficient to form an essential constituent of minerals. Sc is the least soluble of the REE in aqueous solutions. Differences in solubility products between $Sc(OH)_{3\,(s)}$, $ScF_{3\,(s)}$, and $ScPO_{4\,(s)}$, and other solid trivalent REE hydroxides, fluorides, and phosphates, of three to 12 orders of magnitude at 25°C (Speight, 2005; Wood and Samson, 2006; Shkol'nikov, 2009) serve to illustrate this characteristic of Sc. It is usually a byproduct of the mining

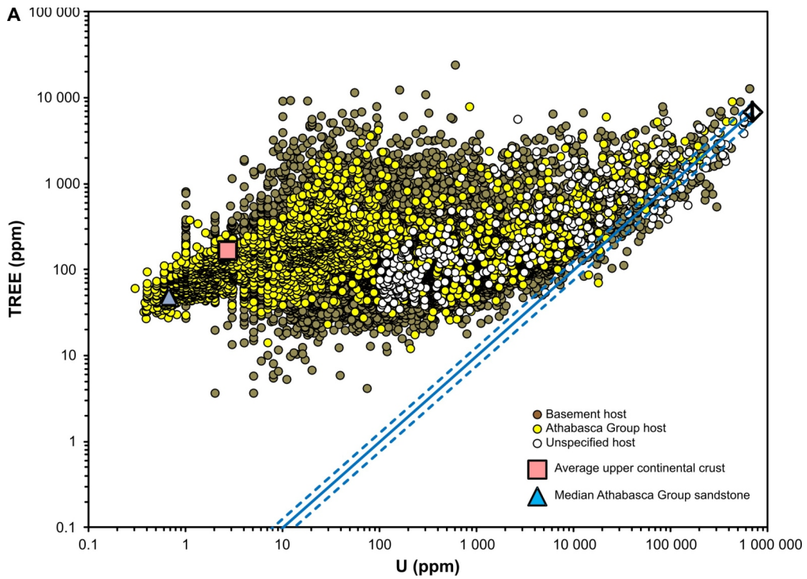

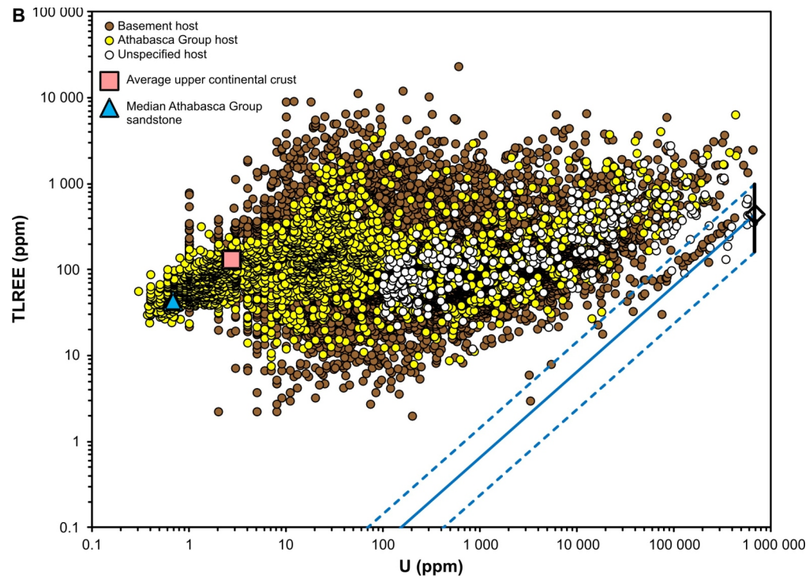

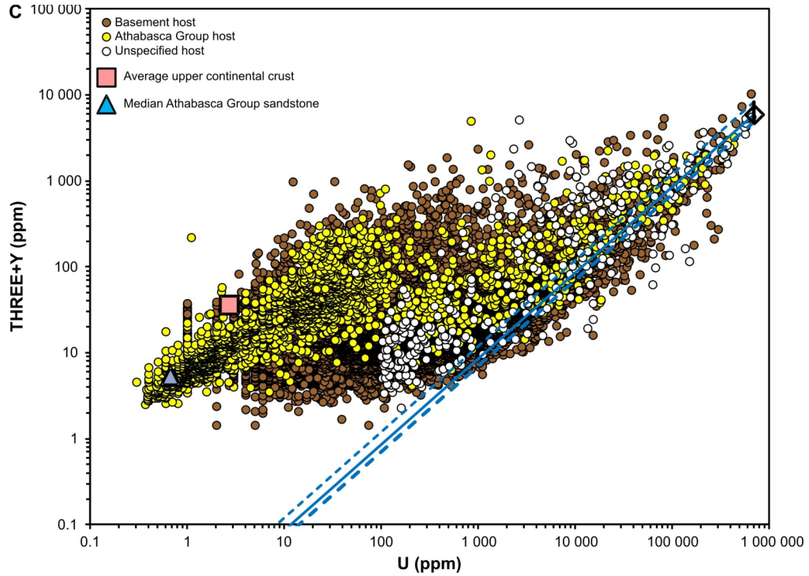

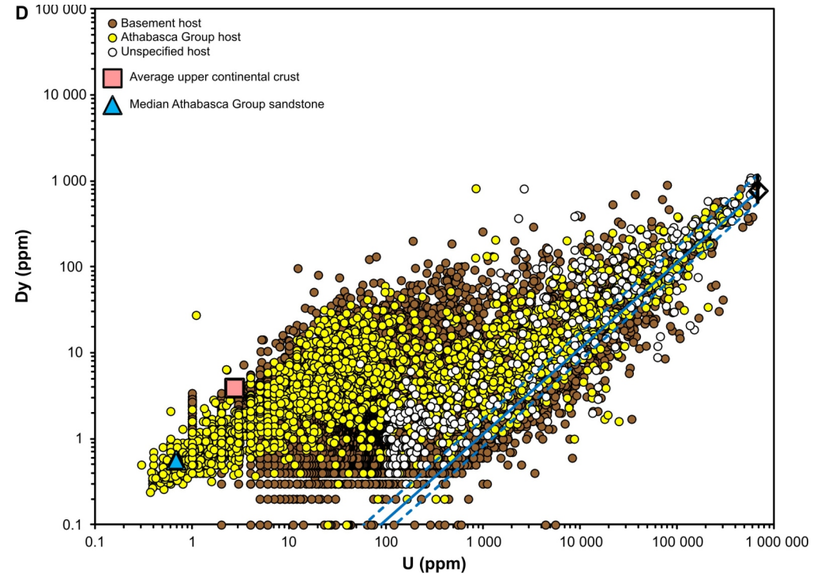

Figure 23 – Log-log plots of the relationships between U and a) TREE (n = 22 949), b) TLREE (n = 22 949), c) THREE+Y (n = 22 947), and d) Dy (n = 23 465) concentrations in basement- and Athabasca Group sediment–hosted mineralized and nonmineralized, sonic or diamond-drill core sections obtained by different companies during examination of unconformity-related U deposits of the Athabasca Basin. The bulk-rock geochemical U and REE data illustrated in the diagrams were compiled for 13 deposits, namely Caribou Lake (SME Assessment File 64L05-SW-0157), Cigar East (SME Assessment Files 74I02-0083, -0084, and -0087), Horseshoe (SME Assessment File 64L04-0130), McArthur River (SME Assessment Files 74H-0048 and 74H14-0077), Midwest Lake (SME Assessment File 74I08-0069), Millennium (SME Assessment File 74H12-0043), Moore Lakes (SME Assessment File 74H06-NE-0128), Phoenix zone discovery hole (SME Assessment File 74H06-0142), P-Patch (SME Assessment File 74H04-0117), Read Lake (SME Assessment File 74H14-0073), Shea Creek (SME Assessment Files 74K04-NE-0031, and 74K04-0041 and -0042), Tamarack (SME Assessment Files 74I01-0114 and 64L05-0180), and West Bear (SME Assessment Files 74H16-0079 and -0093). The data in the diagrams concentrate into two populations: non–U-mineralized samples characterized by low U/REE ratios and U-mineralized samples characterized by elevated U/REE ratios. TLREE concentrations are much less dependent on variations in U concentrations than THREE+Y (or Y, or Dy, or any other HREE considered individually) concentrations are. Note that a significant proportion of the samples in the database containing >0.5 wt. % TLREE are non–U mineralized and show U/TLREE ratios <0.5 (31 out of 35). Black, open diamond symbols with vertical black lines represent median compositions with ranges between the 25th and 75th percentiles of the distributions for the data presented in Table 11. Solid and dashed blue lines represent theoretical compositions (median compositions and compositions that lie between the 25th and 75th percentiles referred to above) along U oxide dilution trends with U- and REE-free matrixes. See text for further discussion.

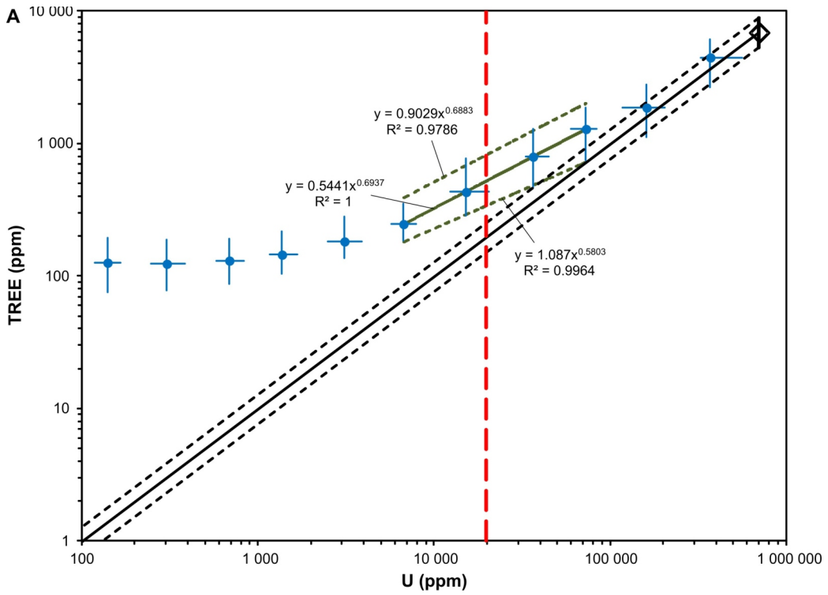

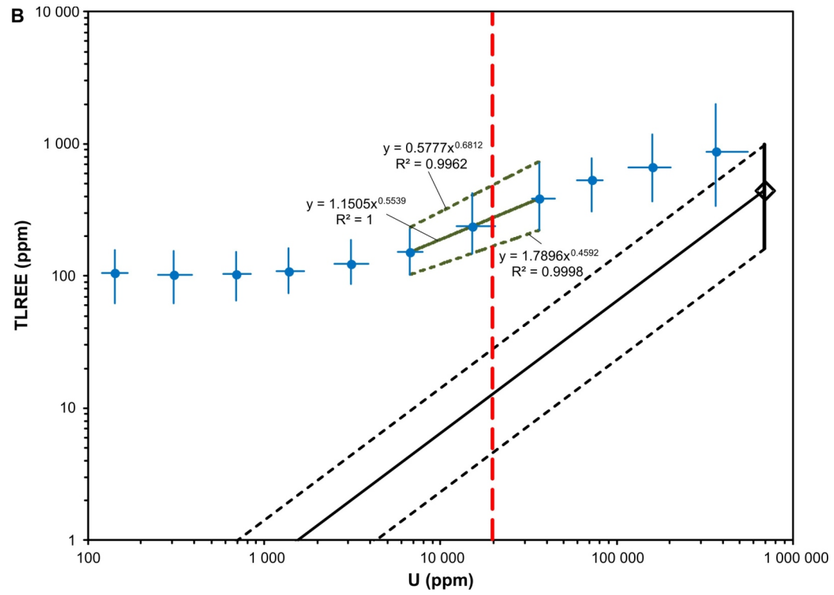

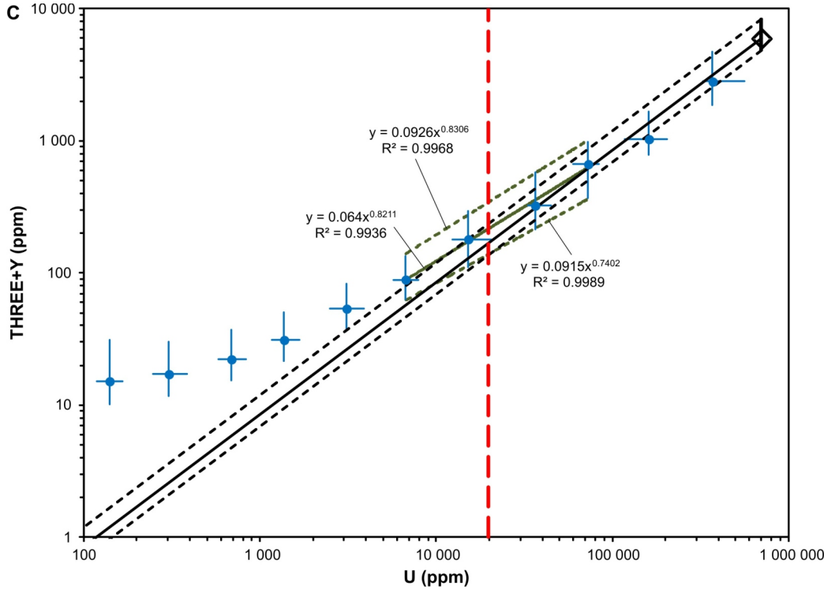

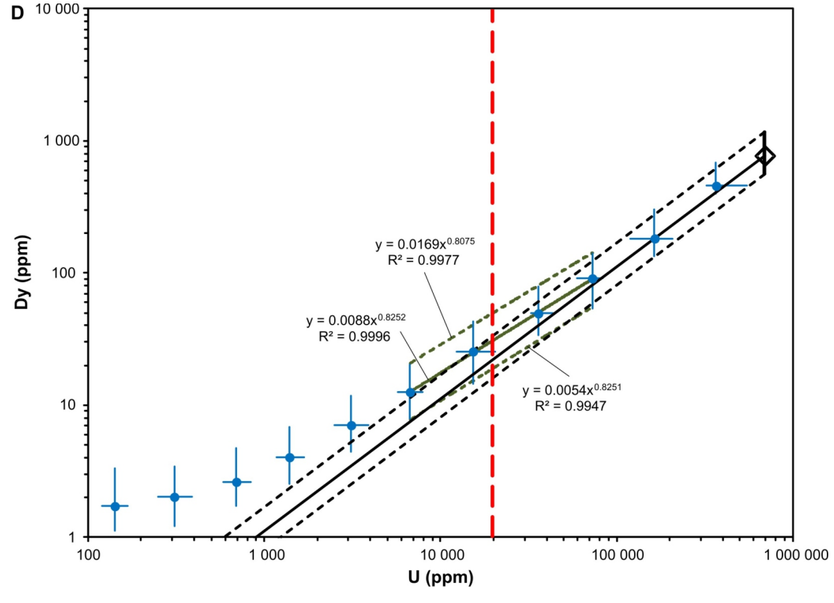

Figure 24 – Log-log plots of U versus TREE (A), TLREE (B), THREE+Y (C), and Dy (D) concentrations, showing the medians (thin black solid lines) and 25th and 75th percentile distribution envelopes (thin short-dashed black lines; 95% confidence level) within groups defined by the following ranges in U concentration: 101 to 200 ppm, 201 to 500 ppm, 501 to 1 000 ppm, 1 001 to 2 000 ppm, 2 001 to 5 000 ppm, 5 001 to 10 000 ppm, 10 001 to 30 000 ppm, 30 001 to 50 000 ppm, 50 001 to 100 000 ppm, 100 001 to 300 000 ppm, and >300 000 ppm. Also shown are the calculated median composition of U oxides from unconformity-related U deposits in the Athabasca Basin (diamond symbol crossed by thick vertical solid line that defines the 25th to 75th percentile distribution envelope of REE concentrations given in Table 11) and the average grade of the deposits (thick vertical red dashed line at 1.97 wt. % U; Jefferson et al., 2007, Table 1). The diagrams show that median THREE+Y and Dy bulk-rock concentrations are statistically similar to those that could be attributed to U oxides in ores grading 1.97 wt. % U. Median TREE and TLREE bulk-rock concentrations are, however, significantly higher than those that could be attributed exclusively to U oxides in ores grading 1.97 wt. % U. Considering the data compiled in this study, and the estimated 29 811 000 t averaging 1.97 wt. % U, a TREE content of between 10 000 and 24 000 t is estimated from these figures to be contained in the ensemble of the Athabasca Basin unconformity-related U deposits (see Table 12).

Table 12 – Approximations of the TREE, TLREE, THREE+Y, and Dy contents of unconformity-related U deposits of the Athabasca Basin.

		From median	From 25th percentile distribution	From 75th percentile distribution
U/REE ratios in uranium oxides calculated from data given in Table 11[1].	U/TREE	102	132	79
	U/TLREE	1568	4319	705
	U/(THREE+Y)	118	142	85
	U/Dy	899	1242	596
Calculated mass of contained REE in unconformity-related uranium deposits of the Athabasca Basin obtained by dividing the total U content estimate of 587 063 tonnes provided in Jefferson *et al.* (2007, Table 1) by the calculated U/REE ratios of U oxides given above.	TREE (t)	5762	4436	7422
	TLREE (t)	374	136	833
	THREE+Y (t)	4985	4130	6943
	Dy (t)	653	473	985
Calculated mass of contained REE in unconformity-related uranium deposits of the Athabasca Basin obtained using the equation: ppm REE[2] x (29 811 000[3] / 1 000 000).	TREE (t)	15457	10062	24316
	TLREE (t)	8203	5002	14503
	THREE+Y (t)	6408	4117	10185
	Dy (t)	918	563	1479

[1] Median U concentration of 701 584.3 ppm used to obtain all calculated ratios.
[2] Solution to equations in Figures 24a, b, c, and d, obtained using U = 19 700 ppm (average U grade of unconformity-related uranium deposits in the Athabasca Basin; Jefferson *et al.* , 2007, Table 1).
[3] Total tonnage of U ore contained in unconformity-related uranium deposits of the Athabasca Basin estimated by Jefferson *et al.* (2007, Table 1).

of other metals. Under some circumstances, the metal is concentrated in residual deposits, such as laterites developed on ultramafic and other rock types (Naumov, 2008; Van Huet *et al.*, 2010).

The presence of Sc-rich minerals is also well documented in association with granitic rocks, including miarolitic granites and granitic pegmatites (Wise *et al.*, 1998; Gramaccioli *et al.*, 1999; Černý and Chapman, 2001; Segalstad and Raade, 2003; Kristiansen, 2009), some topaz rhyolites and granites (Frondel, 1970; Scott *et al.*, 1998), and thortveitite ($Sc_2Si_2O_7$)–bearing fluorite mineralization (Shawe, 1976; Foord *et al.*, 1993). Only very small amounts of Sc have been extracted from such deposits in the past. Eudialyte group, apatite group, and other minerals are reported to contain significant Sc concentrations at some localities in alkaline plutonic rocks (Liferovich *et al.*, 1998; Tice, 2009; Gambogi, 2013). In recent years, production of Sc has been reported as a byproduct material from China, Kazakhstan, Russia, and Ukraine (Raade, 2003; Cardarelli, 2008; Gambogi, 2013). REE ore tailings in the Bayan Obo REE deposit are reported to contain up to 163 ppm Sc, where the metal is contained in magnetite, hematite, bastnäsite-(Ce), parisite-(Ce), monazite-(Ce), riebeckite, aegirine, phlogopite, biotite, and apatite (Shimazaki *et al.*, 2007). The only present-day mining operation dedicated to the production of Sc is the Zhovti Vody mine in Ukraine (Laznicka, 2010), which holds 775 t of proven reserves of Sc in V-Sc–rich aegirine–alkali amphibole–bearing ores grading 105 ppm Sc (Nechaev *et al.*, 2002; Cardarelli, 2008).

There are no reported analyses of Sc in minerals from any type of deposit in Saskatchewan. Elevated concentrations of the metal, however, were identified by companies from analysis of mineralized diamond-drill core during evaluation of numerous unconformity-related U deposits of the Athabasca Basin, including the West Bear deposit (up to 674 ppm Sc; SME Assessment File 74H16-SE-0079), the McArthur River mine (up to 659 ppm Sc; SME Assessment File 74H-0048), the Millennium deposit (up to 635 ppm Sc; SME Assessment File 74H12-0043), the Cigar Lake and Cigar East deposits (up to 500 and 189 ppm, respectively; SME Assessment Files 74I02-0024 and -0083), the Caribou Lake pod (up to 365 ppm Sc; SME Assessment File 64L05-SW-0157), the Collins Creek (now Tamarack) deposit (up to 346 ppm Sc; SME Assessment File 74I01-0114), and deposits in the Shea Creek area (up to 299 ppm Sc at the Anne deposit (SME Assessment File 74K04-0042) and up to 822 ppm at the Kianna deposit (SME Assessment File 74K04-0037)). Elevated Sc concentrations are reported both for samples cored from basement rocks and for samples cored from Athabasca Basin sedimentary rocks.

In nonmineralized Athabasca Basin siliciclastic sedimentary rocks, the variation in Sc concentrations is dependant mainly on the concentrations of TiO_2 (and Nb, Ta), Al_2O_3 (and V), P_2O_5, and, to a lesser extent, Zr, suggesting distribution principally among Ti oxides, clay minerals, APS minerals, and zircon. Similar to other REE, Sc concentrations display a general increase from sandstone and conglomerate to siltstone and mudstone. Values range between 0.05 and 34 ppm (median 0.4 ppm, n = 1206; data from Card *et al.* (2011), Card and Bosman (2012), Bosman and Card (2012)). Owing to the wide variation of rock types below and surrounding the Athabasca Basin, wide variations in Sc concentrations are expected to be encountered in nonmineralized rocks. In 5495 samples of basement rocks (U =20 ppm), reported Sc concentrations vary between 0.001 and 68 ppm, and a median

concentration of 2 ppm was calculated. The calculated median concentrations reported above are significantly lower than the value of 14 ppm reported by Rudnick and Gao (2003) for average upper continental crust.

As mentioned above and in the "Mixed REE Mineralization in which THREE+Y(±Sc) Constitute >20% of the TREE" section, the minerals that host Sc in unconformity-related U deposits of the Athabasca Basin remain to be determined. Graphical and statistical analysis of the U and Sc diamond-drill core geochemical data included in SME assessment files suggest that U-rich minerals probably host significant concentrations of Sc. This is shown in the plots in Figure 25 using selected REE geochemical diamond-drill data for the McArthur River deposit from SME Assessment Files 74H-0048 and 74H14-0077. Figure 25A shows that the U/Sc ratios calculated from the database attain a plateau in samples containing greater than approximately 50 000 ppm U. This suggests that at least one U-rich phase controls the distribution of Sc in this interval of U concentration. Statistical analysis of 33 Sc-REE–rich samples containing >50 000 ppm U returned the following: median U/Sc is 1128, U/Sc at the 25th percentile distribution is 892, and U/Sc at the 75th percentile distribution is 1567. Assuming that the main U-rich phase that holds Sc is uraninite, and using an intermediate U concentration in uraninite from the McArthur River deposit of 749 421 ppm calculated using data in Fayek (1996), an estimated Sc concentration of between 466 and 818 ppm is calculated for the U oxides.

The estimated Sc concentrations are significantly lower than published data on Sc concentrations in uraninite derived from pegmatite-hosted or vein-type deposits (978 to 1434 ppm; Sankaran *et al.*, 1970), and, by analogy with other REE, this may be related, at least in part, to the lower formation temperatures of unconformity-related deposits of the Athabasca Basin. Examination of Figure 25Bb shows that the distribution of sample data is consistent with mixing of the hypothetical Sc-rich U oxide with basement and Athabasca Group rocks. Figure 25B also suggests that, due to the low estimated Sc concentrations in U oxides from the Athabasca Basin, increases in Sc concentrations contributed by U-rich minerals in mineralized rocks are expected to be perceptible only where the mass proportion of these minerals in the rocks is above approximately 5 to 10%. Assuming Sc at McArthur River is held in uraninite and using total U Reserve and Resource figures published for the deposit (172 129.5 t), it is estimated that 110 to 193 t Sc (168 to 296 t Sc_2O_3) are contained in the deposit, which could represent a valuable byproduct (potentially worth more than US$1.0 billion in the purest oxide form at current market prices).

The relationships between U and Sc observed at McArthur River appear to hold for the ensemble of the unconformity-related U deposits of the Athabasca Basin. This is shown in Figures 26 and 27, where the relationship between U and Sc concentrations using 23 014 analyses from 13 deposits is displayed. Similar to what is observed in Figure 25a, U and Sc concentrations appear in Figure 26 to become interdependent in basement- and Athabasca Group–hosted mineralization where U concentrations exceed ~50 000 ppm. In order to test this, the database was separated into the following 14 intervals of U concentration: 101 to 200, 201 to 500, 501 to 1 000, 1 001 to 2 000, 2 001 to 5 000, 5 001 to 10 000, 10 001 to 20 000, 20 001 to 30 000, 30 001 to 50 000, 50 001 to 70 000, 70 001 to 100 000, 100 001 to 200 000, 200 001 to 300 000, and >300 000 ppm. Univariant statistical analysis was carried out on samples in each group for U and Sc concentrations and U/Sc ratios. The results are displayed in graphical form in Figure 27. The calculated U/Sc ratios attain a near-plateau with minimal Sc dispersion in samples containing greater than approximately 50 000 ppm U, comparable to what is observed using the more limited dataset from the McArthur River deposit. Statistical analysis of the 270 samples containing >50 000 ppm U returned the following:

Figure 25 – Log-log plot of the relationships between U concentration and U/Sc ratio (A), and U and Sc concentrations (B) in 190 diamond-drill geochemical analyses from the McArthur River unconformity-related U deposit (selected from SME Assessment Files 74H-0048 and 74H14-0077). In (A), open red circles represent U-rich and Sc-REE–poor samples that were not taken into account in the statistical analysis discussed in the text. The dotted vertical red line corresponds to the reported U grade of ore Reserves of the McArthur River deposit. Solid and dash-dotted horizontal red lines in the upper right part of the diagram correspond to the median and the 25th and 75th percentile U/Sc values within the interval of U concentrations 50 000 ppm (indicated by the short full red vertical line) and greater. The alignment of points on the left side of the diagram is produced as an artifact of the relatively elevated detection limit for Sc of 1 ppm in sample analyses compiled from SME Assessment File 74H14-0077. In (b), the open black diamond with vertical black line represents the calculated median composition of an hypothetical U oxide with ranges in Sc concentrations between the 25th and 75th percentiles of the data considered. See text for details. Solid and dashed blue lines represent theoretical compositions (median compositions and compositions that lie between the 25th and 75th percentiles referred to above) along dilution trends between hypothetical U oxides and U- and Sc-free matrixes. Dash-dotted blue line represents a mixing line between hypothetical U oxides and the average Proterozoic cratonic shale composition reported in Condie (1993). Dash–double dotted blue line represents a mixing line between hypothetical U oxides and the calculated median composition of 1206 samples of Athabasca Group siliciclastic rocks (data from Card* **et al.**, *2011; Card and Bosman, 2012; Bosman and Card, 2012). The mixing lines constrain reasonably well the distribution of the data and, in the case of the more Sc-rich case, converge with the hypothetical U oxide dilution trend at ~50 000 ppm U.

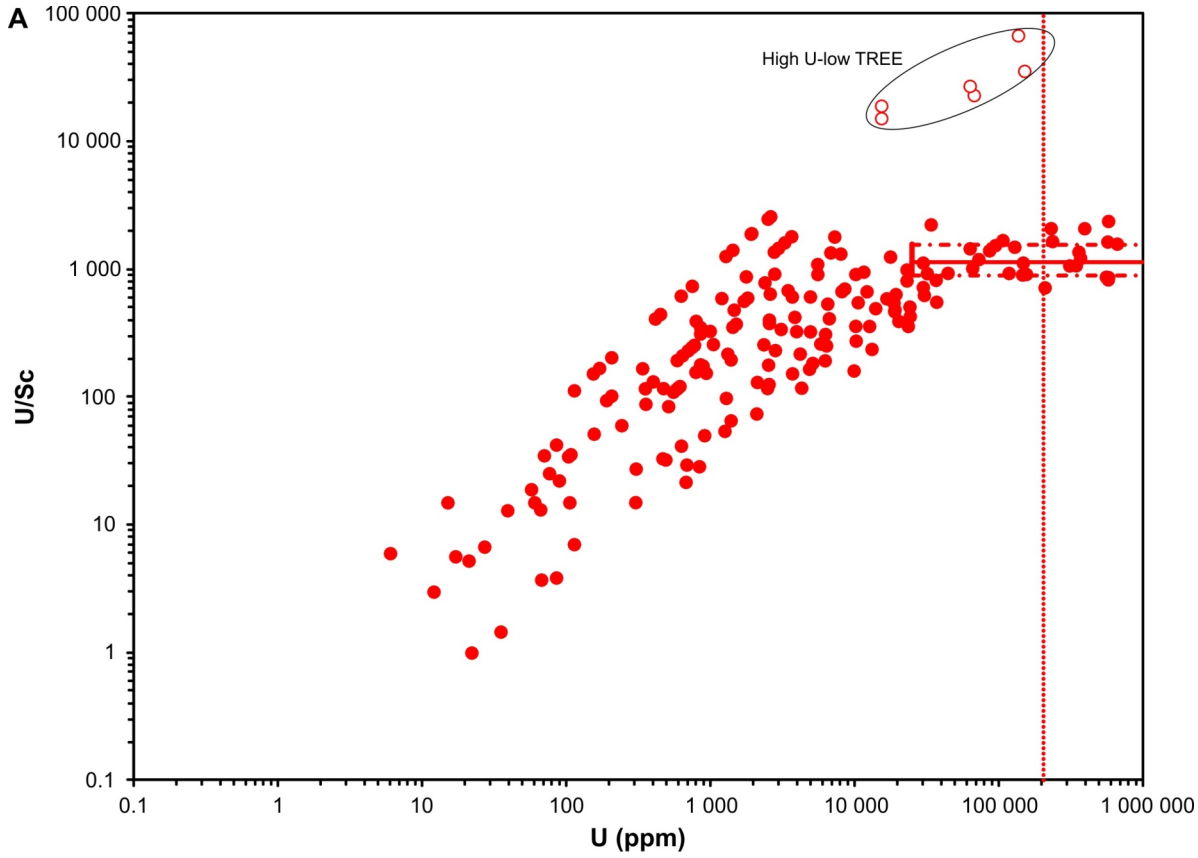
A
High U-low TREE
U/Sc
U (ppm)
100 000
10 000
1 000
100
10
1
0.1
0.1
1
10
100
1 000
10 000
100 000
1 000 000

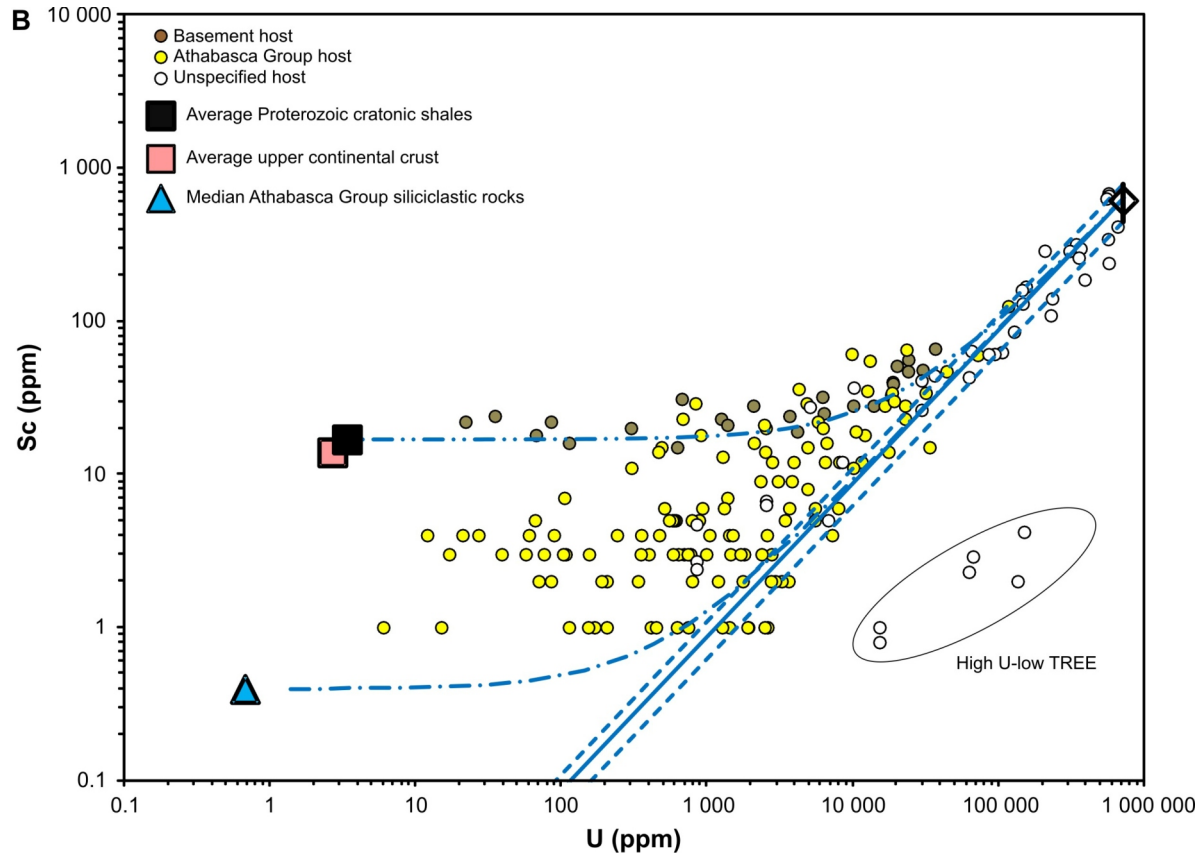
B
Basement host
Athabasca Group host
Unspecified host
Average Proterozoic cratonic shales
Average upper continental crust
Median Athabasca Group siliciclastic rocks
High U-low TREE
Sc (ppm)
U (ppm)
10 000
1 000
100
10
1
0.1
0.1
1
10
100
1 000
10 000
100 000
1 000 000

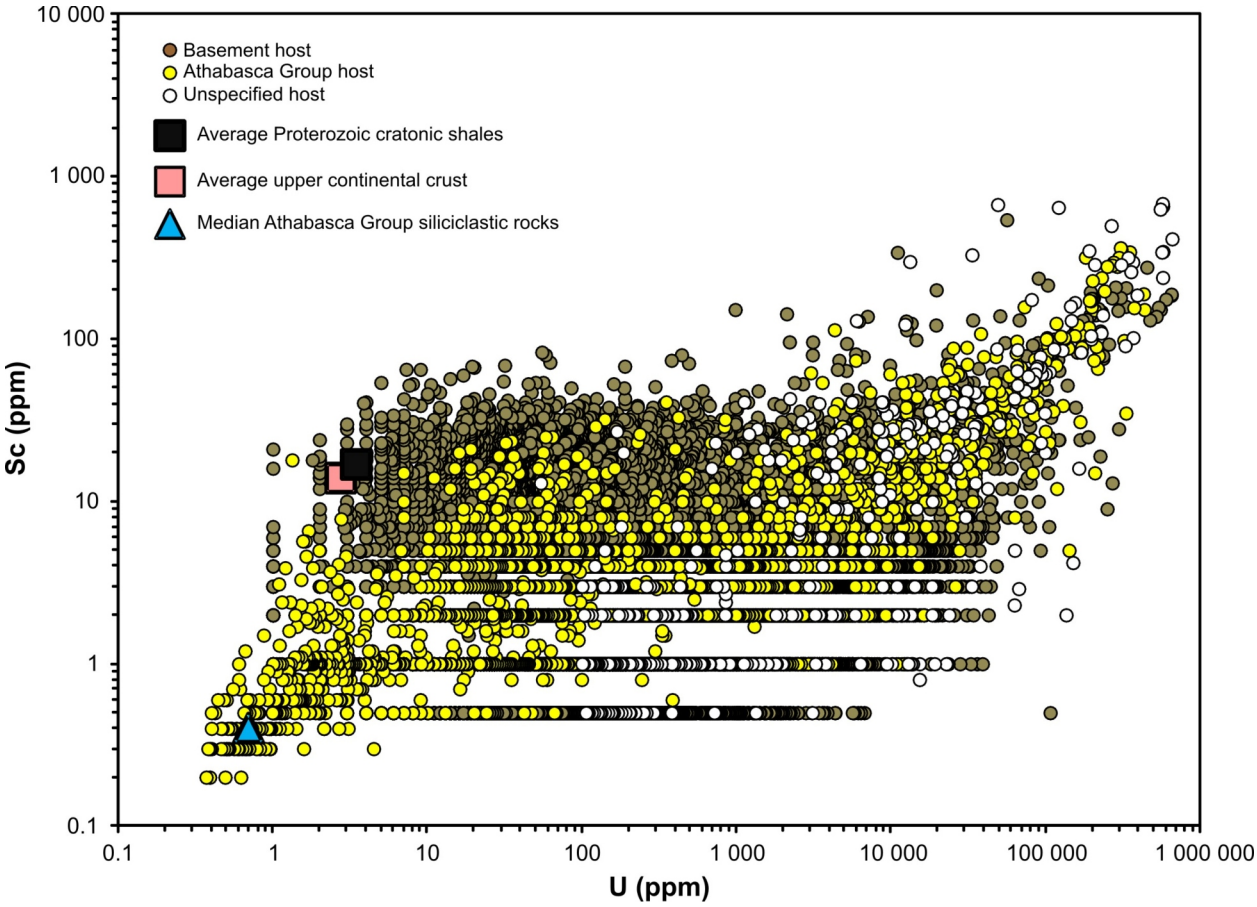

Figure 26 – Log-log plot of the relationship between U and Sc concentrations in 23 014 core samples obtained from 13 unconformity-related U deposits of the Athabasca Basin: Caribou Lake (SME Assessment File 64L05-SW-0157), Cigar East (SME Assessment Files 74I02-0083, -0084, and -0087), Cigar Lake (SME Assessment File 74I02-0038), Horseshoe (SME Assessment File 64L04-0130), McArthur River (SME Assessment Files 74H-0048 and 74H14-0077), Midwest Lake (SME Assessment File 74I08-0069), Moore Lakes (SME Assessment File 74H06-NE-0128), Phoenix (SME Assessment File 74H06-0142), P-Patch (SME Assessment File 74H04-0117), Read Lake (SME Assessment File 74H14-0073), Shea Creek area (SME Assessment Files 74K04-NE-0031, and 74K04-0041 and -0042), Tamarack (SME Assessment Files 74I01-0114 and 64L05-0180), and West Bear (SME Assessment Files 74H16-0079 and -0093). Similar to other REE, the data form two groups: a nonmineralized group characterized by low U/Sc ratios and a mineralized group characterized by elevated U/Sc ratios.

median U/Sc is 1,637, U/Sc at the 25th percentile distribution is 1,251, and U/Sc at the 75th percentile distribution is 3,118.

Assuming again that the main U-rich phase that holds Sc is uraninite, and using the median U concentration of uraninite from Table 11 of 701 673 ppm, an estimated Sc concentration of between 225 and 561 ppm is calculated for the U oxides. This calculated range of concentrations is roughly similar to those calculated for the McArthur River deposit. Employing a similar approach to the one used above to calculate other REE contents[19] in the ensemble of the unconformity-related U deposits of the Athabasca Basin, the U/Sc ratios given above and the U content estimate of 587 063 t provided in Jefferson *et al.* (2007, Table 1) were used to provide a rough estimate of the Sc content. Results suggest between 188 and 469 t, although the U content estimate in Jefferson *et al.* (2007)[20] is now exceeded due to recent discoveries of new deposits.

Mineralization in which THREE+Y Constitute >90% of the TREE

REE deposits in which the proportions of HREE and Y represent more than 90% of the contained TREE are very rare. They are the expression of mineralization in which the composition of REE minerals is dominated by HREE

[19] Sc was not included in these calculations.
[20] Includes past production at the time of publication.

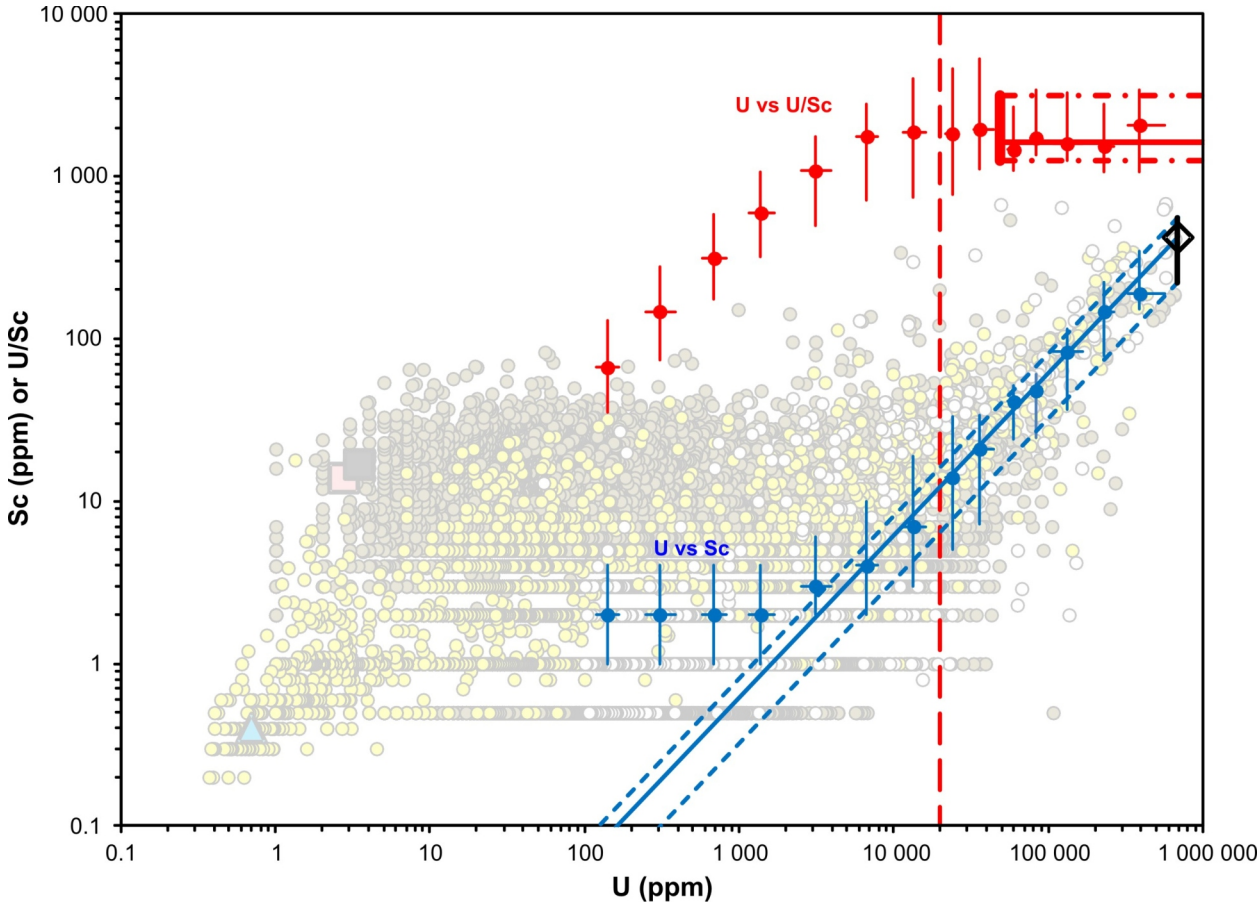

Figure 27 – Log-log plot of U versus Sc, showing statistically derived median and 25th and 75th percentiles for U and Sc concentrations or U/Sc ratios from the data referred to in the caption of Figure 26. See text for details. Vertical-axis units for red-filled symbols (medians within a given interval of U concentrations) and associated vertical thin red lines (25th to 75th percentile ranges within a given interval of U concentrations), and horizontal thick solid red (median within the interval of U concentrations >50 000 ppm) and dash-dotted red lines (associated 25th to 75th percentiles) are U/Sc. Vertical-axis units for the rest of the symbols are Sc (ppm). Blue-filled circles and associated horizontal and vertical thin blue lines represent medians within a given interval of U concentrations and the 25th to 75th percentiles within this interval, respectively. Open black diamond with vertical black line represents the estimated median and 25th to 75th percentile range of Sc concentrations, respectively, of an hypothetical U oxide containing 701 673 ppm U. Solid and dashed blue lines represent theoretical compositions (median compositions and compositions that lie between the 25th and 75th percentiles referred to above) along dilution trends between hypothetical U oxides and U- and Sc-free matrixes. The vertical dashed red line corresponds to the average U grade (1.97 wt. %) of unconformity-related U deposits of the Athabasca Basin given in Jefferson* et al. *(2007, Table 1). Diamond-drill core analytical data points from Figure 26 appear translucent in the background for reference.

and Y. REE-rich minerals likely to produce such HREE+Y–rich mineralization, potentially in economic concentrations, are not numerous, the main one being xenotime-(Y). Xenotime-(Y) is an orthophosphate mineral of general formula $(Y,HREE)PO_4$ that typically contains ~60 wt. % $THREO+Y_2O_3$ and may contain substantial concentrations (up to a few wt. %) of U and/or Th. The more abundant HREE in xenotime are, in general, Dy, Er, and Yb. The larger LREE are present only in very low concentrations in the more compact structure of xenotime, where HREE and Y occur in eight-fold co-ordination with respect to oxygen (Miyawaki and Nakai, 1996).

Xenotime is a comparatively rare mineral, much rarer than monazite. It seldom occurs in more than trace amounts in a wide variety of rock types that usually contain more abundant LREE-rich minerals. It is also reported as a rare accessory mineral in granitic pegmatites and alpine fissure veins. Percentage concentrations of xenotime in rocks are reported, however, from several locations, including, for example, in biotite-rich segregations in gneiss in the Music Valley area, Riverside County, California (Evans, 1964) and the Central City district, Colorado (Young and Sims, 1961); in biotite-magnetite-amphibole–rich layers in metamorphosed siliciclastic sedimentary rocks at Olserum, Sweden (Reed, 2013); as hydrothermal mineralization in basal conglomerates of the Paleoproterozoic Killi Killi

Formation, Australia (Gardner Range project of Quantum Resources Limited, 2013); and in hydrothermal xenotime breccias at the Wolverine HREE deposit, Western Australia (Browns Range project of Northern Minerals Limited, 2013).

In Saskatchewan, exceptionally rich xenotime mineralization was discovered during U exploration in the Athabasca Basin at a number of locations, including the McClean Lake U deposits (Wallis *et al.*, 1983; location 310, Table 13 and Figure 28) where the mineral locally yields up to 10 wt. % Y_2O_3 in clay-rich zones. The larger xenotime occurrences, however, appear to be spatially dissociated from the U mineralization. Two of the better known examples in the province are the MAW REE zone, hosted by sandstones of the Manitou Falls Formation in the Wheeler River area (SMDI #2160; location 309, Table 13 and Figure 28), and a group of occurrences discovered by Marlin Oil in 1980 in Otherside River formation sandstones of the Douglas River–Beatty River area (SMDI #2141, #2142, and #2143; locations 306, 307, and 308, Table 13 and Figure 28). Marlin Oil's REE occurrences have been worked most recently by Great Western Minerals Group Ltd. (GWMG) to evaluate the economic potential of the area. Bulk-rock REE distributions are very similar at both locations, where the xenotime occurs as a very fine grained (*i.e.*, 30 to 40 µm in diameter in the Douglas River–Beatty River area; SME Assessment File 74K03-0024) and averaging <5 µm in diameter in the MAW REE zone (Hanly, 2001)) phase in the interstices of detrital quartz and in silicified zones. Whereas the Beatty River area xenotime occurs in zones that are conformable to bedding within the sandstone (SME Assessment File 74K-0015), it is hosted by highly altered, fractured, and brecciated sandstone in the MAW Rare Earth zone (Knox, 1985, 1986; Quirt *et al.*, 1991).

Owing to the very fine grained and disseminated nature of the mineralization, xenotime is reported to be virtually impossible to identify in the field (Hanly, 2001). The mineralogy tends to be fairly simple and there are no reported associations with reliable indicator minerals that may extend away from mineralized zones and be used as pathfinders. Except perhaps for silicification, there are no dependable alteration types associated with xenotime mineralization, and no useful geochemical tracer has been identified. For instance, there is no particular enrichment in Ni-Co-Cu-Zn-Ti-V-Zr or other trace elements other than those contained in xenotime; tourmaline (B) is absent in the Douglas River–Beatty River area, and APS minerals (Sr, Ba) are weakly developed in the MAW REE zone and relatively common throughout the Athabasca Basin. A good suggestion for the presence of the mineral may be a radioactive response obtained using a gamma-ray field spectrometer (SME Assessment File 74K-0015). According to electron microprobe data (Hanly, 2001), xenotime from the MAW REE zone contains up to 0.5 wt. % U+Th. APS minerals, which may contain up to ~2 wt. % U+Th (Cloutier *et al.*, 2009, 2010, 2011; Mercadier *et al.*, 2011a), can occur with xenotime, thus adding to the difficulty in determining the presence of xenotime. U/Th ratios are, however, distinct in both phases: U/Th is >1.1 (1.1 to 18.1) in xenotime from the MAW zone; the median U/Th value is 0.15 (0.006 to 26.825) in a population of 26 microprobe analyses of APS minerals reported in Fayek and Kyser (1997), Cloutier *et al.* (2009, 2010, 2011) and Mercadier *et al.* (2011a), with the lowest values observed for APS minerals occurring outside the perimeter of U deposits. Calculated U/Th ratios from bulk-rock geochemical data in Table 13 range from 0.01 to 73.68, with a median value of 2.3 (25th percentile at 1.0; 75th percentile at 4.7; n = 55), similar to those obtained from xenotime. Apatite-rich beds in the Wolverine Point formation are also radioactive and, based on seven bulk-rock analyses presented in Card and Bosman (2012) that show >10 wt. % P_2O_5, they contain between 41 and 207 ppm U and between 3 and 8 ppm Th. Calculated U/Th ratios using these data vary between 12 and 63, and average 29. The apatite-rich beds have distinctly higher U/Th signatures than do xenotime-rich rocks. Nitric acid and ammonium molybdate reagents can be used in the field to verify the presence of apatite in Athabasca Group sediments where the phosphate content is greater than 1000 ppm (Oakes, 1938; Barrie, 1965). Access to a portable XRF spectrometer would allow confirmation of the presence of anomalous REE directly in the field. The age of the mineralization in the MAW REE zone and in the Douglas River–Beatty River area, and the temperature and pressure at which the mineralization formed, remain unknown.

Hanly and Hagni (2002) postulated that the Y and HREE were derived largely from earlier U mineralization in an area close to the MAW REE zone, implying that depositional mechanisms for the REE mineralization were not related to, and were different from, those responsible for the formation of the unconformity-related U deposits. Quirt *et al.* (1991) and Barker (2007), on the other hand, suggested that the MAW REE zone may represent the distal halo of a hydrothermal system responsible for the U mineralization. This could be verified by chemical analysis of fluid inclusions that, in U deposits, contain up to 2.8×10^{-3} mol/L U (Richard *et al.*, 2011).

In the mid-1980s, Union Oil Company of Canada Ltd. provided a drill-estimated indicated resource for the MAW REE zone of 462 664 t averaging 0.21% Y_2O_3 (Knox, 1985, 1986; see Table 1). Using bulk-rock geochemical data for samples in Table 13 containing <0.3 wt. % Y, linear regression between Y and Tb, Dy, Ho, Er, Tm, Yb, and Lu resulted in calculated R^2 values of better than 0.96. Applying the calculated linear-regression equations to

Table 13 – HREE-dominant mineralization: diagenetic-hydrothermal, sandstone-hosted xenotime.

Location #	Name	Category	SMDI #	Location[1]			Sample #	DDH #
				NTS Area	Easting	Northing		
306	Helipad #1 (Douglas River area)	Occurrences	2143	74K03	50 m west of historical area 2S occurrence		n. r.	n. a.
	Helipad #2 (Douglas River area)						n. r.	n. a.
	Area 2S yttrium showing (Douglas River area); Marline South of Great Western Minerals Group Ltd. (GWMG), 5 m south of historical area 2S trench				241883	6457943	n. r.	n. a.
307	Area 11 yttrium showing (Beatty River area)	n. a. (presence of elevated REE has not been confirmed)	2142	74K04	213075	6451702	n. r.	n. a.
308	Area 10 yttrium showing (Beatty River area)	Occurrence	2141		215883	6449638	*DRT-85-1-21	n. a.
							*DRT-85-1-22	n. a.
							*DRT-85-1-11	n. a.
							*DRT-85-1-35	n. a.
							*DRT-85-1-29	n. a.
							*DRT-85-1-26	n. a.
							*DRT-85-1-36	n. a.
							*DRT-85-1-15	n. a.
							*DRT-85-1-10	n. a.
							*DRT-85-1-34	n. a.
							*DRT-85-1-14	n. a.
							*DRT-85-1-19	n. a.
							*DRT-85-1-24	n. a.
							*DRT-85-1-30	n. a.
							*DRT-85-1-28	n. a.
							*DRT-85-1-33	n. a.
							*DRT-85-1-18	n. a.
							*DRT-85-1-12	n. a.
							*DRT-85-1-32	n. a.
							*DRT-85-1-8	n. a.
							*DRT-85-1-27	n. a.
							*DRT-85-1-23	n. a.
							*DRT-85-1-6	n. a.
							*DRT-85-1-13	n. a.
							*DRT-85-1-39	n. a.
							*DRT-85-1-5	n. a.
							*DRT-85-1-7	n. a.
							*DRT-85-1-25	n. a.
							*DRT-85-1-20	n. a.
							*DRT-85-1-31	n. a.
							202610	n. a.
							202609	n. a.
							202611	n. a.
							202617	n. a.
							202619	n. a.
							202613	n. a.
							202608	n. a.
							202618	n. a.
							202616	n. a.
							202615	n. a.
							202923	n. a.
							202614	n. a.
							202612	n. a.
							202924	n. a.
							202922	n. a.
309	MAW REE zone (and Wheeler River area)	Developed prospect with Resources	2160	74H06	472592	6369679	MAW-1	n. a.
							MAW-2	n. a.
							MAW-3	n. a.
							MAW-4	n. a.
							MAW-5	n. a.
							MAW-6	n. a.
							MAW-7	n. a.
							MAW-8	n. a.
							MAW-9	n. a.
							RA-1-83	n. a.
							RA-2-83	n. a.
							RA-3-83	n. a.
							RA-4-83	n. a.
							RA-5-83	n. a.
							RA-6-83	n. a.
							RA-7-83	n. a.
							90114	n. a.
							90110	n. a.
							90109	n. a.
							85 3A	85-3A
							8556	85-5
							84416	84-4
							84118	84-1
							85311	85-3
							85213	85-2
							32 1 00B	n. a.
							32 1 00A	n. a.
							ZM6D 1037	ZM-10
							ZM6D 1038	ZM-10
							G104636	84-02
							G105916	ZK-20
							G104634	84-02
							G103230	ZK-11
							G103303	ZQ-09
							G105706	ZK-12
							G104632	84-07
							G103302	ZQ-09
							G104635	84-02
							ZQ-08-36	ZQ-08
							G100402	WR-208
							S50132	WR-206
							ZM-10-363	ZM-10
							ZM-4-362	ZM-04
							85-2-65	85-02
							S50130	WR-206
							S50227	WR-211
							85-6-110	85-06
							ZM-4-368	ZM-04
							ZM-14-380	ZM-14
							ZQ-08-18	ZQ-08
							S50143	WR-207
							G100400	WR-208
							ZM-4-350	ZM-04
							85-5-35	85-05
							S50229	WR-211
							S50131	WR-206
310	McClean Lake uranium deposits	Occurrence	1718, 1719, 1780, 2529	64L05	568130 (JEB)	6467748 (JEB)	n. r.	n. a.
311	Riou/Black Lake area	Bedrock geochemical anomaly	3378, 3379 (near)	74P04	454117	6560505	BL68-281.0	BL68
312		Occurrence	2728, 3374 (near)		446057	6549868	BL02-105	BL02
313	Hocking Lake area	Occurrence	none	74J16	432540	6536875	9629	C.L.G.-D5
314		Bedrock geochemical anomaly			437538	6537861	SL11-725	S.L.G.-D11

[1] All location co-ordinates given in UTM Zone 13N, NAD 83.
*ICP fusion
Abbreviations: ins. dat., insufficient data; n. a., not applicable (surface samples); n. r., not reported.

Table 13 (continued) – HREE-dominant mineralization: diagenetic-hydrothermal, sandstone-hosted xenotime.

Source of Data	TREE (wt. %)	THREE+Y (wt. %)	(THREE+Y)/TREE (%)	P_2O_5 (wt. %)	Sr (ppm)	La (ppm)	Dy (ppm)	Y (ppm)	Dy/Y	Yb (ppm)	La_N/Yb_N	Eu/Eu*	Sc (ppm)	U (ppm)	Th (ppm)	U/Th
Great Western Minerals Group Ltd. (2011)	2.31 (TREO)	2.29 (THREO+Y)	99.19 (THREO+Y)/TREO (%)	n. r.	n. r.	n. r.	n. r.	n. r.	ins. dat.	n. r.	ins. dat.	ins. dat.	n. r.	n. r.	n. r.	ins. dat.
	1.04 (TREO)	1.02 (THREO+Y)	98.18 (THREO+Y)/TREO (%)	n. r.	n. r.	n. r.	n. r.	n. r.	ins. dat.	n. r.	ins. dat.	ins. dat.	n. r.	n. r.	n. r.	ins. dat.
	4.04 (TREO)	3.99 (THREO+Y)	98.85 (THREO+Y)/TREO (%)	n. r.	n. r.	n. r.	n. r.	n. r.	ins. dat.	n. r.	ins. dat.	ins. dat.	n. r.	n. r.	n. r.	ins. dat.
SME assessment file 74K-0015	n. r.	n. r.	n. r.	n. r.	n. r.	n. r.	n. r.	n. r.	ins. dat.	n. r.	ins. dat.	ins. dat.	n. r.	n. r.	n. r.	ins. dat.
SME assessment file 74K-0015	6.28	6.28	99.94	4.61	n. r.	5	7840	49300	0.159	1440	0.002	ins. dat.	n. r.	n. r.	3	ins. dat.
	5.04	5.03	99.80	4.18	n. r.	5	6630	39800	0.167	570	0.006	ins. dat.	n. r.	n. r.	3	ins. dat.
	4.07	4.06	99.75	3.57	n. r.	5	5240	32100	0.163	700	0.005	ins. dat.	n. r.	n. r.	3	ins. dat.
	1.00	1.00	99.15	1.98	n. r.	15	1310	7840	0.167	135	0.077	ins. dat.	n. r.	n. r.	3	ins. dat.
	0.85	0.84	99.03	1.31	n. r.	5	1100	6560	0.168	76.4	0.045	ins. dat.	n. r.	n. r.	11	ins. dat.
	0.71	0.70	98.44	1.46	n. r.	5	970	5500	0.176	52.1	0.066	ins. dat.	n. r.	n. r.	4	ins. dat.
	0.74	0.73	98.41	1.98	n. r.	25	930	5800	0.160	141	0.123	ins. dat.	n. r.	n. r.	8	ins. dat.
	0.67	0.66	98.83	1.07	n. r.	10	810	5070	0.160	180	0.038	ins. dat.	n. r.	n. r.	3	ins. dat.
	0.45	0.44	96.85	0.76	n. r.	20	606	3358	0.180	89.4	0.155	ins. dat.	n. r.	n. r.	3	ins. dat.
	0.47	0.47	99.04	1.06	n. r.	9	650	3590	0.181	73	0.085	ins. dat.	n. r.	n. r.	3	ins. dat.
	0.34	0.34	98.11	0.51	n. r.	11	381	2598	0.147	120	0.063	ins. dat.	n. r.	n. r.	3	ins. dat.
	0.32	0.31	97.69	0.56	n. r.	8	435	2388	0.182	67.1	0.083	ins. dat.	n. r.	n. r.	6	ins. dat.
	0.28	0.27	96.99	1.06	n. r.	12	388	2120	0.183	31.3	0.265	ins. dat.	n. r.	n. r.	5	ins. dat.
	0.25	0.23	92.58	1.03	n. r.	16	292	1791	0.163	37.5	0.295	ins. dat.	n. r.	n. r.	6	ins. dat.
	0.29	0.28	98.36	0.53	n. r.	7	380	2193	0.173	57.8	0.084	ins. dat.	n. r.	n. r.	3	ins. dat.
	0.27	0.26	97.16	1.19	n. r.	15	340	2010	0.169	57	0.182	ins. dat.	n. r.	n. r.	3	ins. dat.
	0.22	0.20	92.24	1.70	n. r.	18	273	1531	0.178	40	0.312	ins. dat.	n. r.	n. r.	5	ins. dat.
	0.21	0.20	95.10	0.63	n. r.	11	275	1504	0.183	51.7	0.147	ins. dat.	n. r.	n. r.	3	ins. dat.
	0.21	0.20	93.90	0.59	n. r.	10	282	1556	0.181	13.6	0.509	ins. dat.	n. r.	n. r.	9	ins. dat.
	0.19	0.18	96.42	0.46	n. r.	11	225	1386	0.162	62.9	0.121	ins. dat.	n. r.	n. r.	3	ins. dat.
	0.21	0.20	96.80	0.55	n. r.	8	263	1558	0.169	39.9	0.139	ins. dat.	n. r.	n. r.	3	ins. dat.
	0.19	0.19	95.66	0.84	n. r.	9	259	1441	0.180	15.9	0.392	ins. dat.	n. r.	n. r.	3	ins. dat.
	0.17	0.16	93.80	0.82	n. r.	36	195	1193	0.163	51.3	0.486	ins. dat.	n. r.	n. r.	9	ins. dat.
	0.17	0.16	96.43	0.49	n. r.	11	200	1254	0.159	56.5	0.135	ins. dat.	n. r.	n. r.	3	ins. dat.
	0.18	0.17	94.88	1.49	n. r.	17	219	1360	0.161	38.5	0.306	ins. dat.	n. r.	n. r.	10	ins. dat.
	0.12	0.11	92.97	0.64	n. r.	10	154	820	0.188	14.8	0.468	ins. dat.	n. r.	n. r.	3	ins. dat.
	0.06	0.05	79.05	0.57	n. r.	11	56	344	0.163	12.1	0.629	ins. dat.	n. r.	n. r.	4	ins. dat.
	0.05	0.03	68.64	0.77	n. r.	13	46	248	0.185	4.7	1.915	ins. dat.	n. r.	n. r.	9	ins. dat.
	0.07	0.06	91.27	0.44	n. r.	8	77	481	0.160	22.5	0.246	ins. dat.	n. r.	n. r.	4	ins. dat.
	0.06	0.06	85.81	0.87	n. r.	10	78	438	0.178	9.4	0.737	ins. dat.	n. r.	n. r.	8	ins. dat.
SME assessment file 74K03-0024	7.14	7.13	99.90	5.14	1700	<20	10000	45100	0.222	850	ins. dat.	ins. dat.	34	220	60	3.67
	5.12	5.11	99.82	3.80	2020	<20	7100	35700	0.199	1020	ins. dat.	ins. dat.	36	140	30	4.67
	4.76	4.75	99.69	3.98	4310	<20	6480	31400	0.206	1020	ins. dat.	ins. dat.	38	140	30	4.67
	4.12	4.11	99.71	3.32	2710	<20	5570	27900	0.200	830	ins. dat.	ins. dat.	34	80	20	4.00
	3.63	3.62	99.81	2.73	2240	<20	4940	24400	0.202	530	ins. dat.	ins. dat.	24	120	20	6.00
	3.44	3.44	99.80	2.96	3570	<20	4710	24100	0.195	710	ins. dat.	ins. dat.	28	80	<20	>4.00
	2.93	2.91	99.45	2.74	4860	30	3840	19900	0.193	600	0.035	ins. dat.	20	150	80	1.88
	2.90	2.88	99.59	2.41	2900	<20	3990	19000	0.210	300	ins. dat.	ins. dat.	6	70	20	3.50
	2.82	2.81	99.65	2.77	4820	<20	3910	18800	0.208	490	ins. dat.	ins. dat.	22	90	<20	>4.50
	2.46	2.45	99.80	2.06	2220	<20	3390	17000	0.199	460	ins. dat.	ins. dat.	29	60	<20	>3.00
	1.58	1.57	99.49	1.76	3710	<20	2040	11100	0.184	440	ins. dat.	ins. dat.	23	40	<20	>2.00
	1.15	1.14	99.39	1.33	3250	<20	1500	7880	0.190	240	ins. dat.	ins. dat.	9	30	<20	>1.50
	0.94	0.93	98.83	1.30	3760	<20	1220	6270	0.195	130	ins. dat.	ins. dat.	5	40	<20	>2.00
	0.06	0.06	92.06	0.52	2660	<20	70	400	0.175	20	ins. dat.	ins. dat.	<2	<20	<20	ins. dat.
	0.06	0.06	88.71	1.11	6150	<20	70	390	0.179	<20	ins. dat.	ins. dat.	<2	<20	<20	ins. dat.
SME assessment file 74H-0051	ins. dat.	ins. dat.	ins. dat.	0.04	n. r.	n. r.	520	2720	0.191	105	ins. dat.	ins. dat.	n. r.	n. r.	n. r.	ins. dat.
	ins. dat.	ins. dat.	ins. dat.	0.04	n. r.	n. r.	600	3020	0.199	110	ins. dat.	ins. dat.	n. r.	n. r.	n. r.	ins. dat.
	ins. dat.	ins. dat.	ins. dat.	0.06	n. r.	n. r.	1150	6280	0.183	210	ins. dat.	ins. dat.	n. r.	n. r.	n. r.	ins. dat.
	ins. dat.	ins. dat.	ins. dat.	0.01	n. r.	n. r.	140	790	0.177	26	ins. dat.	ins. dat.	n. r.	n. r.	n. r.	ins. dat.
	ins. dat.	ins. dat.	ins. dat.	0.04	n. r.	n. r.	200	1140	0.175	41	ins. dat.	ins. dat.	n. r.	n. r.	n. r.	ins. dat.
	ins. dat.	ins. dat.	ins. dat.	0.02	n. r.	n. r.	80	480	0.167	14	ins. dat.	ins. dat.	n. r.	n. r.	n. r.	ins. dat.
	ins. dat.	ins. dat.	ins. dat.	0.01	n. r.	n. r.	100	640	0.156	21	ins. dat.	ins. dat.	n. r.	n. r.	n. r.	ins. dat.
	ins. dat.	ins. dat.	ins. dat.	0.02	n. r.	n. r.	100	550	0.182	18	ins. dat.	ins. dat.	n. r.	n. r.	n. r.	ins. dat.
	ins. dat.	ins. dat.	ins. dat.	0.03	n. r.	n. r.	180	1130	0.159	31	ins. dat.	ins. dat.	n. r.	n. r.	n. r.	ins. dat.
SME assessment file 74H06-NW-0080	4.42	4.40	99.57	0.3	n. r.	<60	4100	36400	0.113	1100	0.000	0.385	n. r.	220	6	36.67
	2.47	2.46	99.61	0.12	n. r.	10	2800	19900	0.141	600	0.011	0.192	n. r.	420	5.7	73.68
	0.50	0.49	99.30	0.13	n. r.	6.7	490	4000	0.123	110	0.041	0.199	n. r.	9.1	1.4	6.50
	0.06	0.05	93.08	<0.01	n. r.	8.1	6	500	0.013	2	3.242	0.423	n. r.	16.4	1.4	11.71
	1.84	1.84	99.67	0.49	n. r.	9	2000	14600	0.137	400	0.015	0.175	n. r.	41.2	6.1	6.75
	1.78	1.77	99.44	0.24	n. r.	10	1900	14300	0.133	370	0.018	0.246	n. r.	70.4	2.6	27.08
	8.17	8.16	99.79	0.51	n. r.	<70	6800	67600	0.101	1700	0.000	0.192	n. r.	160	3	53.33
MacDougall (1990)	0.51	0.51	98.77	0.02	n. r.	8.4	352	4270	0.082	91	0.063	ins. dat.	7.98	3.7	2.9	1.28
	0.12	0.12	98.41	0.03	n. r.	5.4	128	991	0.129	34	0.107	ins. dat.	4.4	4.4	1.9	2.32
	0.03	0.03	92.60	0.03	n. r.	6.2	20	218	0.090	8	0.562	ins. dat.	3.53	10	2.5	4.00
Hanly (2001)	0.10	0.09	96.42	0.085	25	8	109	681	0.160	25	0.214	0.303	5	3.9	1	3.90
	0.16	0.13	82.46	0.182	203	70	139	945	0.147	38	1.247	0.657	9	15.8	14	1.13
	0.03	0.03	91.61	0.036	27	7	37	222	0.164	9	0.523	0.265	2	3.1	1	3.10
	0.03	0.02	86.21	0.032	21	9	27	167	0.162	7	0.900	0.754	4	3.4	1	3.40
	0.02	0.01	62.99	0.036	68	21	15	99	0.152	5	3.175	0.375	2	1.3	5	0.26
	0.06	0.05	93.93	0.051	27	9	61	390	0.155	13	0.486	0.318	2	3.9	1	3.90
	0.03	0.02	89.37	0.027	18	7	32	169	0.189	7	0.711	0.152	1	2.2	1	2.20
	0.06	0.06	97.69	0.056	17	7	80	415	0.193	17	0.283	0.207	2	3.8	1	3.80
	0.22	0.20	92.56	0.191	151	36	192	1490	0.129	40	0.620	0.492	4	58.1	20	2.91
	0.05	0.04	79.47	0.067	37	5	44	257	0.170	6	0.586	0.383	2	2900	71	40.85
SME assessment file 74H06-0136	0.08	0.08	99.13	0.065	26	0.5	95	560	0.170	26	0.013	0.325	2	6	4	1.50
	0.05	0.04	87.07	0.068	65	13	54	279	0.195	14	0.655	0.370	1	1	5	0.20
	0.03	0.03	97.85	0.038	23	2	41	239	0.172	12	0.118	0.410	2	4	2	2.00
	0.04	0.02	63.40	0.132	424	61	27	156	0.174	12	3.347	0.247	1	2	86	0.02
	0.02	0.02	93.02	0.023	22	5	19	106	0.180	5	0.709	0.420	0.5	2	2	1.00
	0.02	0.01	60.68	0.088	254	36	16	85	0.189	7	3.711	0.221	1	1	72	0.01
	0.02	0.01	85.02	0.028	29	12	15	94	0.161	4	2.041	0.662	0.5	1	1	1.00
	0.01	0.01	86.31	0.023	27	9	13	77	0.169	4	1.458	0.405	1	1	2	0.50
	0.01	0.01	91.33	0.016	18	4	11	62	0.177	3	0.825	0.451	1	7	1	7.00
SME assessment file 74H11-0115	0.11	0.11	98.18	0.072	15	5	129	805	0.160	29	0.119	0.304	2	8	2	4.00
	0.11	0.10	92.63	0.096	63	17	112	745	0.150	20	0.593	0.504	2	7	5	1.40
	0.14	0.08	55.18	0.258	627	176	91	545	0.168	22	5.418	0.563	8	81	84	0.96
	0.07	0.07	91.18	0.073	58	15	71	488	0.145	13	0.779	0.451	1	9	5	1.80
	0.10	0.07	65.74	0.131	359	79	64	484	0.132	14	3.785	0.353	1	5	2	2.50
	0.06	0.06	93.90	0.048	27	10	66	451	0.147	16	0.415	0.312	2	3	1	3.00
	0.06	0.05	88.10	0.07	59	15	58	370	0.157	12	0.865	0.649	1	8	7	1.14
	0.07	0.05	69.95	0.136	282	43	51	345	0.148	15	1.912	0.484	8	44	27	1.63
	0.05	0.04	91.09	0.046	37	10	49	331	0.147	14	0.479	0.425	1	1	8	0.13
	0.05	0.04	85.86	0.047	67	16	41	298	0.137	8	1.296	0.488	0.5	4	6	0.67
	0.04	0.03	79.01	0.045	60	21	31	238	0.132	9	1.681	0.519	0.5	9	6	1.50
	0.03	0.03	92.79	0.035	20	6	40	236	0.171	9	0.439	0.262	1	6	1	6.00
	0.04	0.03	64.99	0.081	146	28	33	184	0.177	10	1.924	0.443	1	75	10	7.50
	0.06	0.02	41.51	0.139	472	90	28	169	0.164	7	9.004	0.456	1	7	30	0.23
	0.03	0.02	82.71	0.033	55	12	24	176	0.134	6	1.458	0.465	0.5	6	3	2.00
	0.05	0.02	49.92	0.095	201	61	23	173	0.132	8	5.390	0.654	8	7	15	0.47
	0.05	0.02	49.36	0.094	248	55	25	161	0.152	7	5.757	0.494	2	22	11	2.00
	0.03	0.02	66.49	0.051	95	27	23	151	0.155	5	3.402	0.474	1	13	13	1.00
Wallis et al. (1983)	n. r.	n. r.	n. r.	n. r.	n. r.	n. r.	n. r.	78744	ins. dat.	n. r.	ins. dat.	ins. dat.	n. r.	n. r.	n. r.	ins. dat.
SME assessment file 74P04-0041	0.11	0.06	54.39	0.24	765	105	60	450	0.133	26.6	3.95	ins. dat.	4	<2	9	<0.22
SME assessment file 74P04-SW-0035	ins. dat.	ins. dat.	ins. dat.	0.41	1352	45	n. r.	1467	ins. dat.	n. r.	ins. dat.	ins. dat.	n. r.	5.1	16	0.3
SME assessment file 74J16-NW-0018	0.15	0.14	96.46	0.257	836	8	158	1080	0.1463	15.3	0.362	0.328	<1	<2	5	<0.40
SME assessment file 74J16-NE-0019	0.09	0.08	94.92	0.082	92	10	80.4	611	0.13159	25.8	0.268	0.236	4	<2	10	<0.20

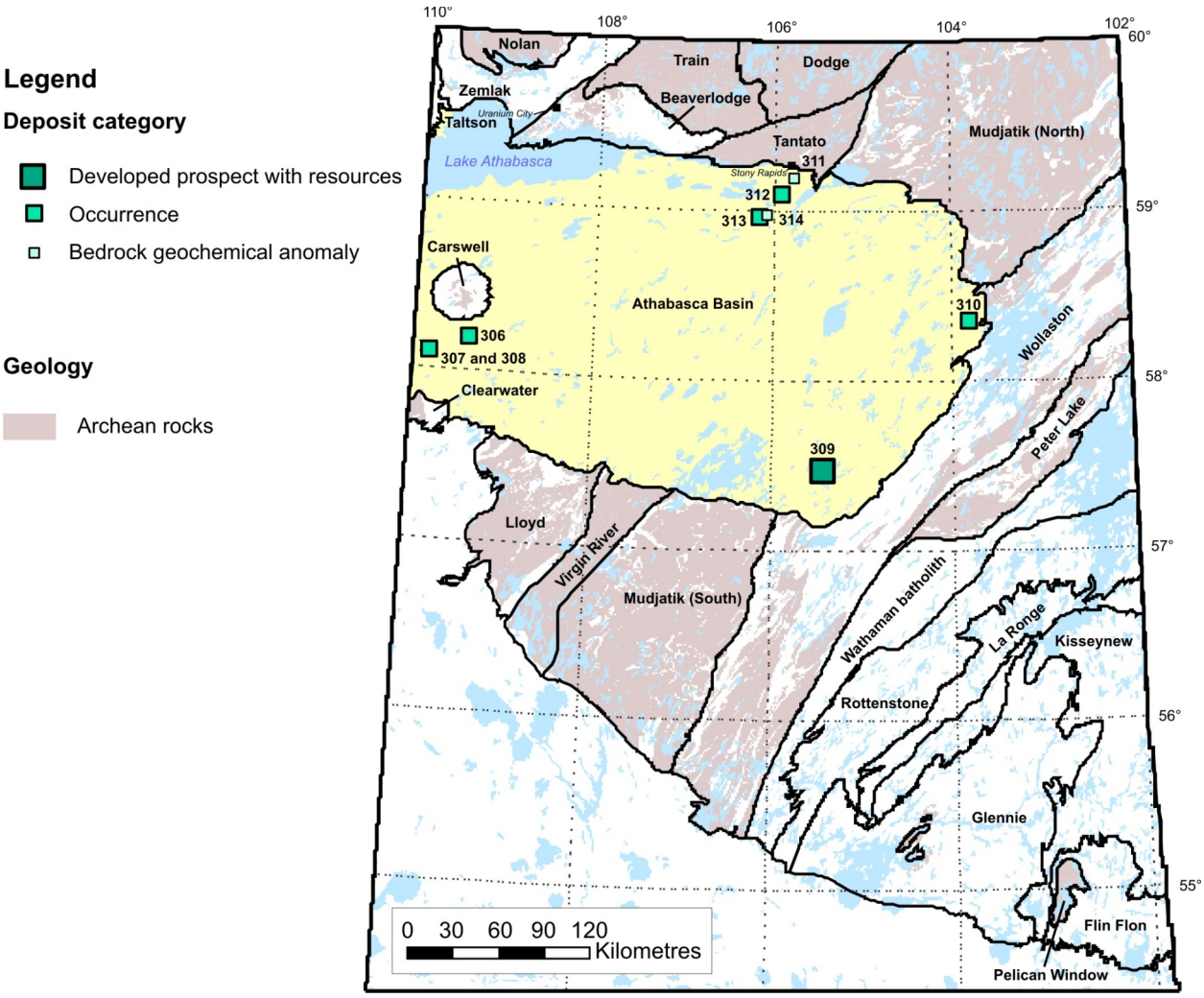

Figure 28 – Location of mineralization in which (THREE+Y)/TREE is predominantly >90%: diagenetic-hydrothermal sandstone-hosted xenotime occurrences in the Athabasca Basin.

extrapolate Tb, Dy, Ho, Er, Tm, Yb, and Lu concentrations at the average grade of 0.21% Y_2O_3 (1653.6 ppm Y), values of 37, 295, 45, 110, 12, 58, and 8 ppm, respectively, were obtained for these REE. Assuming a resource of 462 664 t, a rough estimate of the amounts of Tb_4O_7, Dy_2O_3, Ho_2O_3, Er_2O_3, Tm_2O_3, Yb_2O_3, Lu_2O_3, and Y_2O_3 potentially contained in the MAW REE zone is 20, 157, 24, 58, 6, 31, 4, and 972 t, respectively (1272 t total).

Indications of the presence of significant xenotime mineralization elsewhere in the Athabasca Basin are few. Elevated concentrations of HREE were encountered in a number of drill holes north of the Athabasca Basin in the area between Black Lake and Hocking Lake (locations 311 to 314, Table 13 and Figure 28). The best sample (BL02-105, selective sampling; location 312) contains an estimated 0.43 wt. % xenotime (calculated from bulk-rock chemical analyses). The xenotime occurs in strongly fractured and silicified sandstone not correlated with clay mineral content in close spatial relationship with the Platt Creek shear zone (SME Assessment Files 74P04-SW-0035, and 74P04-0041 and -0045). Significant proportions of APS minerals may be present and would dilute the HREE+Y proportion of the TREE to <70%.

Compositional data in Hanly (2001) obtained from electron microprobe analysis of xenotime from the MAW REE zone support a hydrothermal origin for xenotime at this locality (Figure 29). Knox (1985) suggested that mineralization in the MAW REE zone was formed during a late fracturing episode that overprinted an early fracture/brecciation/silicification event. According to Knox's (1985) proposed hypothesis, brittle deformation of the competent sandstone during this late, main mineralization event would have been accompanied by infiltration of Y(+HREE)–bearing fluids from which the REE were adsorbed onto clay minerals. A P-rich fluid would have

Figure 29 – Log-log plots showing compositional Dy_N vs Eu_N (A) and Gd_N vs Eu_N (B) relationships in xenotime from the MAW REE zone, using data from electron microprobe analyses provided in Hanly (2001). Dotted elliptical fields designate detrital-igneous, diagenetic, and hydrothermal sources proposed by Vallini (2006). Xenotime from the MAW REE zone shows elevated Eu_N values, typical of hydrothermal REE minerals formed from ligand-rich fluids at low temperatures and under comparatively elevated oxygen fugacities, as opposed to those grown from a melt in which Eu is present predominantly in the divalent state and fractionates into plagioclase feldspars during crystallization (Sverjenski, 1984; Wood, 1990; Bau, 1991).

subsequently reacted with the adsorbed REE to deposit xenotime, presumably after a strong dravitization event. Another possible mechanism that could be very effective in precipitating xenotime directly from solution is through mixing of the above-cited Y(+HREE)–bearing and P-rich fluids. REE solubility can be extremely elevated in phosphate-, carbonate-, and fluoride-free, and chloride- or sulphate-rich fluids (Williams-Jones *et al.*, 2012; Loges *et al.*, 2013; Figure 30). Inclusion fluids in quartz from unconformity-related U deposits contain up to 35 wt. % equivalent NaCl with molar Na/Ca ratios as low as 0.5 (Derome *et al.*, 2005; Richard *et al.*, 2010). APS minerals containing significant proportions of svanbergite in solid solution provide indirect evidence for the presence of sulphate in the fluids as well, although no information on its concentrations in fluid inclusions is available. Richard *et al.* (2011) estimated that the pH of the ore-forming fluids responsible for deposition of U in unconformity-related U deposits must have been between 2.5 and 4.5. Such acidic fluids are also efficient in enhancing REE solubility in hydrothermal fluids.

Preliminary calculations indicate that the solubility of crystalline YPO_4 in fluids saturated with hydroxylapatite at 25°C[21], pH values of 3 to 7, fixed activities of H_2O and Cl^- of 1, and activities of Ca^{2+} of 0.01, 0.10, and 1.00 is well below 1 ppm. Similarly, very low solubility of $CePO_4$ is obtained in such fluids. Retrograde (and stoichiometric) solubility of REE phosphates up to ~300°C (Wood, 2004; Cetiner *et al.*, 2005) suggests that low xenotime solubilities are probably maintained in apatite-saturated fluids up to those temperatures. The absence of monazite or rhabdophane, and relative scarceness of LREE-rich APS minerals in xenotime mineralization suggest that the mineralizing fluid was also poor in LREE. Where APS minerals are present with xenotime and apatite is absent, and considering the case where it is assumed that APS minerals and xenotime were formed simultaneously, the total dissolved P concentration in solution in equilibrium with those minerals is predicted to be elevated and that of Y very low (Figure 31). Reaction of an HREE+Y–rich and P-poor fluid circulating through fracture zones that cut rock types containing abundant phosphates, such as are documented in the upper parts of the Wolverine Point (1.60 to 1.64 Ga diagenetic apatite cement; Davis *et al.*, 2011) and Otherside formations, and in the Douglas Formation and the marine section of the Manitou Falls Formation (Ramaekers, 1980, 1990), in principle should lead to massive precipitation of xenotime. No xenotime mineralization has been reported in apatite-rich (*i.e.*, several percent) rocks of the Athabasca Group to this date. The number of samples of such apatite-rich rocks that were analyzed for Y and HREE is, however, extremely limited. This might indicate limited areal extent of xenotime mineralization, which could be localized in intensely fractured zones where flow of mineralizing fluids would have been concentrated.

[21] There are currently no widely available thermodynamic datasets that include properties for xenotime-(Y), other solid Y phases, and aqueous Y species at elevated temperatures.

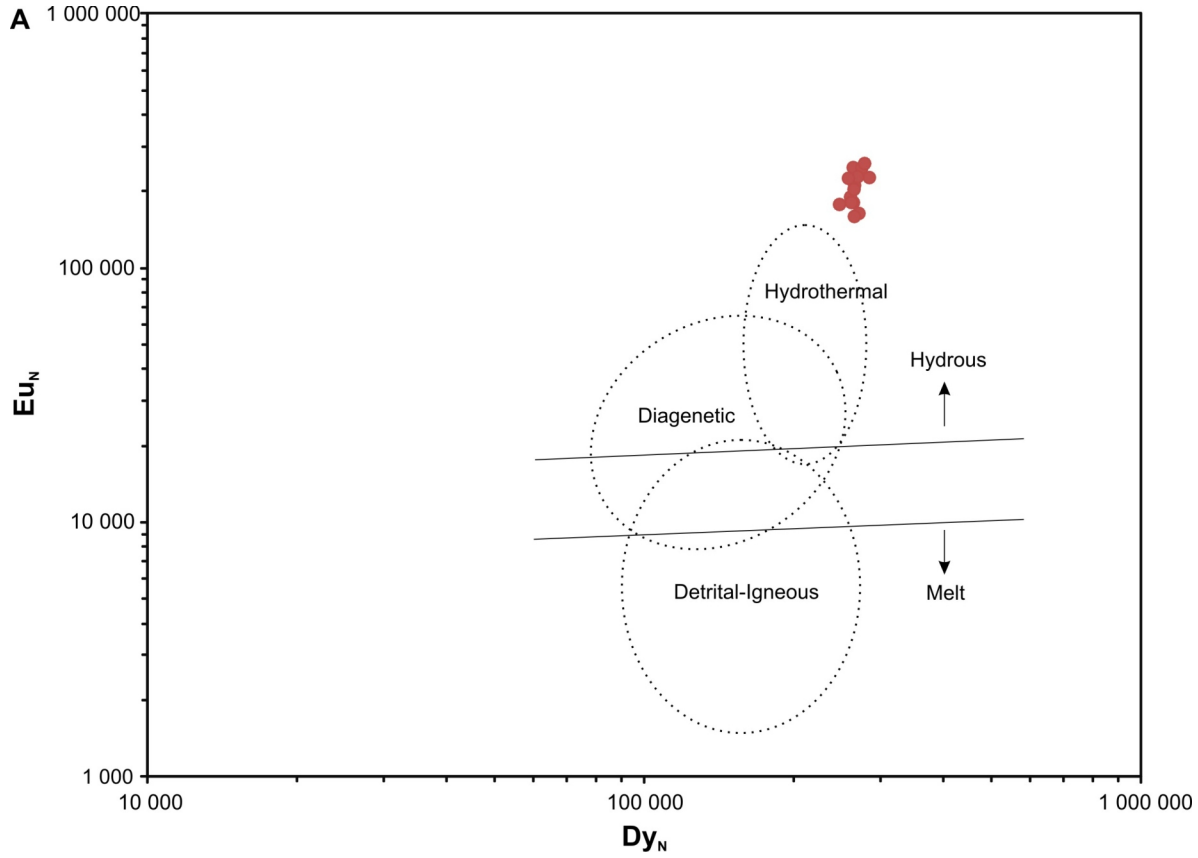
A
1 000 000
100 000
10 000
1 000
Eu$_N$
10 000
100 000
1 000 000
Dy$_N$
Hydrothermal
Hydrous
Diagenetic
Detrital-Igneous
Melt

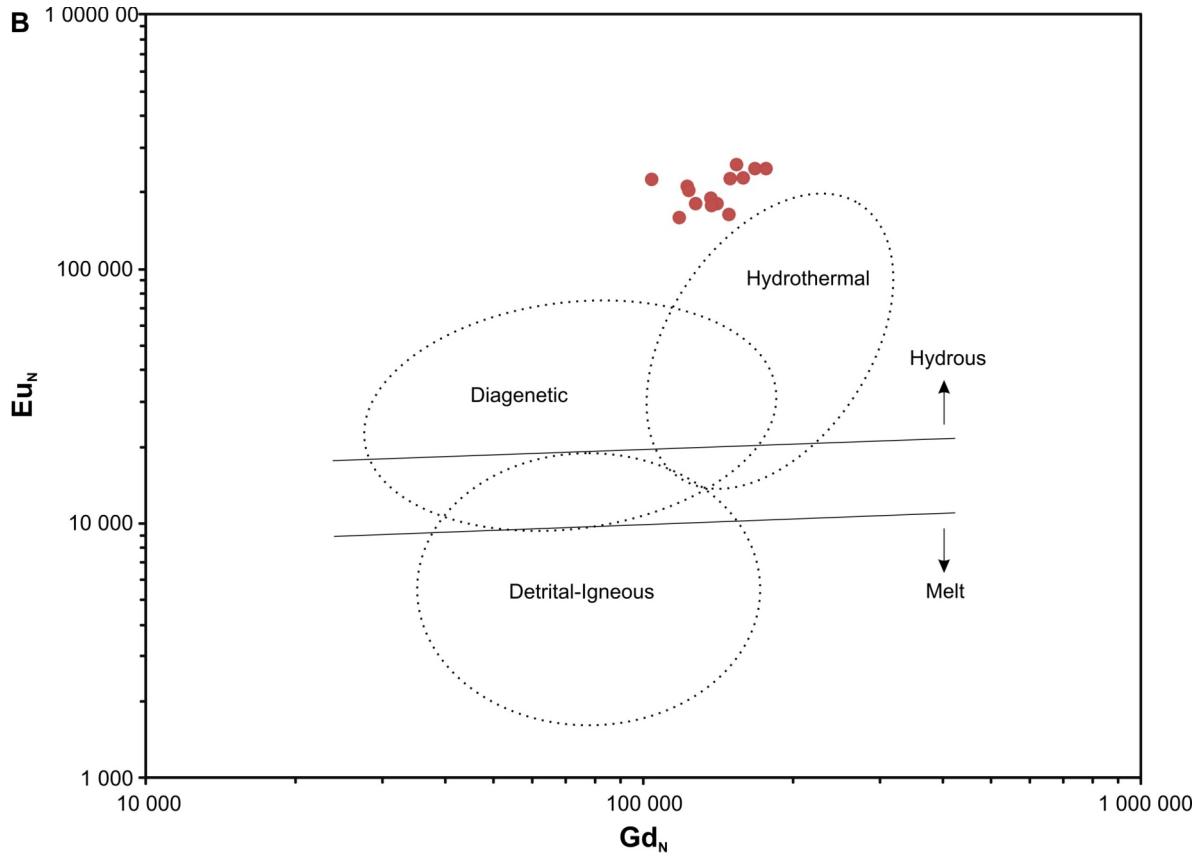
B
1 0000 00
100 000
10 000
1 000
Eu$_N$
10 000
100 000
1 000 000
Gd$_N$
Hydrothermal
Hydrous
Diagenetic
Detrital-Igneous
Melt

Summary and Conclusions

At the present time, the alkaline veins in the Hoidas Lake–Nisikkatch Lake area and the sandstone-hosted xenotime and unconformity-related U deposits of the Athabasca Basin offer the best potential for economic recovery of REE. The sandstone-hosted xenotime and unconformity-related U deposits of the Athabasca Basin are of particular interest for their elevated HREE and Sc concentrations. The Athabasca Basin sandstones represent an ideal target area for future exploration and discovery of new REE resources.

The economic importance of monazite occurrences associated with biotite-rich zones in high-grade metamorphosed sedimentary rocks is largely unknown. Monazite is not invariably present in such biotite-rich zones and xenotime, where reported, is never present in more than trace amounts. None of the zones reported appear to exceed 2 m in width. The maximum reported strike length of any individual zone is less than ~100 m. The vertical extent of group B granitic pegmatites in the Fraser Lakes zone B was demonstrated to be ~100 m (SME Assessment File 74H02-0044). Most commonly, the concentration of monazite in the biotite-rich zones is below 2 to 3% by volume of rock. Exceptionally elevated monazite concentrations, locally exceeding 20% by volume of rock, however, were observed at two occurrences. TREE grades obtained by analysis of three hand samples collected from highly radioactive zones at the Alces Lake occurrence varied between 13 and 29 wt. %. To date, the most extensive monazite mineralization recognized in Saskatchewan is the Archie Lake deposit of presumed detrital origin. The economic importance of this deposit, however, has not been demonstrated. Whereas spectacularly rich monazite mineralization is documented from the Kulyk Lake occurrence, the surface exposure is very small and it remains to be shown whether more of this mineralization lies concealed or the occurrence simply constitutes a scientific curiosity. Relatively little work has been undertaken in the area and no drilling has taken place at the occurrence.

Intrusion-associated, vein-type, and unconformity-related U deposits are of interest for their HREE+Y–enriched character, due mainly to the presence of REE-bearing U oxides. Because of their low to very low U grades, economic recovery of REE as a byproduct from intrusion-associated and vein-type deposits might be profitable only where very large tonnages are identified. Existing mining and processing infrastructure for unconformity-related, U-rich deposits in the Athabasca Basin offer potential for eventual recovery of the valuable heavier lanthanide elements, Y, and Sc.

Figure 30 – Log-log plots of pH versus* Σa*Y species, showing A) the solubility of the stable solid phases $Y(OH)_{3(s)}$ and $Y_2(CO_3)_3 \bullet H_2O_{(s)}$, and of metastable $YF_{3\,(s)}$, in the system Y-Cl-F-S-C-O-H; and B) the solubility of the stable solid phases $Y(OH)_{3\,(s)}$ and $YPO_{4(s)}$ in the system Y-Cl-F-S-C-P-O-H. Temperature and pressure were fixed at 25°C and 1 bar in all cases. Maximum* aF^-, aSO_4^{2-}, aCO_3^{2-}, *and* aPO_4^{3-} *in solution were fixed by saturation with fluorite, gypsum, calcite, and hydroxylapatite, respectively, at prescribed* aCa^{2+} *of 0.01, 0.10, and 1.00. A value for* aCl^- *of 1 was used in all calculations. The aqueous Y species considered in the calculations were Y^{3+}, $Y(OH)^{2+}$, YCl^{2+}, $YF_{3(aq)}$, YF_2^+, YF^{2+}, YSO_4^+, $Y(SO_4)_2^-$, $YPO_{4(aq)}$, $YHPO_4^+$, $YH_2PO_4^{2+}$, YCO_3^+, and $YHCO_3^{2+}$. Inspection of the diagrams shows that Y solid phase solubilities increase with increasing* aCa^{2+} *and concomitant decreases in* aF^-, aSO_4^{2-}, aCO_3^{2-}, *and* aPO_4^{3-} *(Le Chatelier's principle). Maximum solubilities are achieved in solutions containing only chloride and sulphate ligands (Y chloride and sulphate salts are highly soluble in water). The solubility of crystalline $YPO_{4\,(s)}$ (pure end-member xenotime-(Y) composition) is very low and is increasingly so with increasing total dissolved phosphate concentrations. In solutions saturated with hydroxylapatite, maximum total dissolved Y in solution is well below 1 ppm at pH values between 3 and 7. Thermodynamic data for solids and aqueous species used for calculation of the diagrams are from the thermo_minteq.dat dataset of* **The Geochemist Workbench** *(Bethke, 1996; Bethke and Yeakel, 2009;* **The Geochemist Workbench** *datasets available at http://www.gwb.com/). Deep-basinal, acidic, and calcium-rich brines (Frape* **et al.**, *2003; Kharaka and Hanor, 2003), such as those encountered in fluid inclusions from unconformity-related U deposits (Mercadier* **et al.**, *2010; Richard* **et al.**, *2011), would represent excellent candidates to accumulate (Cuney, 2008) and transport Y and HREE in the Athabasca Basin. Reaction of such REE-enriched fluids with pre-existing phosphates could be a very efficient mechanism for precipitating fine-grained xenotime from highly supersaturated solutions. Note that $Y(OH)_{3\,(s)}$ and $YF_{3\,(s)}$ phases are not reported to occur in nature. $Y_2(CO_3)_3 \bullet H_2O_{(s)}$ is close to tengerite $[Y_2(CO_3)_3 \bullet 2\text{-}3H_2O]$. The activity of $YPO_{4\,(s)}$ in natural xenotime is always <1, so calculated $YPO_{4\,(s)}$ solubilities shown in Figure 30b represent maximum estimates. The systems considered here are simplified and reflect only partially equilibrium, which would be expected to take place in natural systems where additional components (Na, Al, Si, etc.) allow formation of a large number of other minerals for which phase relations are largely unknown. Such naturally occurring solid phases, not included in the thermo_minteq.dat dataset or for which experimentally determined, fundamental thermodynamic properties are commonly lacking, include, for example, bastnäsite-(Y) $[YCO_3F]$, gagarinite-(Y) $[NaCaYF_6]$, and REE-rich fluorite $[(Ca, REE)F_{2+x}]$. Solubility relationships of Y in P-containing and P-free systems are, however, expected to be similar for data presented here and data that would be obtained from natural systems. The relative solubility of Y in P-containing and P-free systems at higher temperatures, corresponding to the thermal history of the Athabasca Basin, would also be expected to show similar large differences.

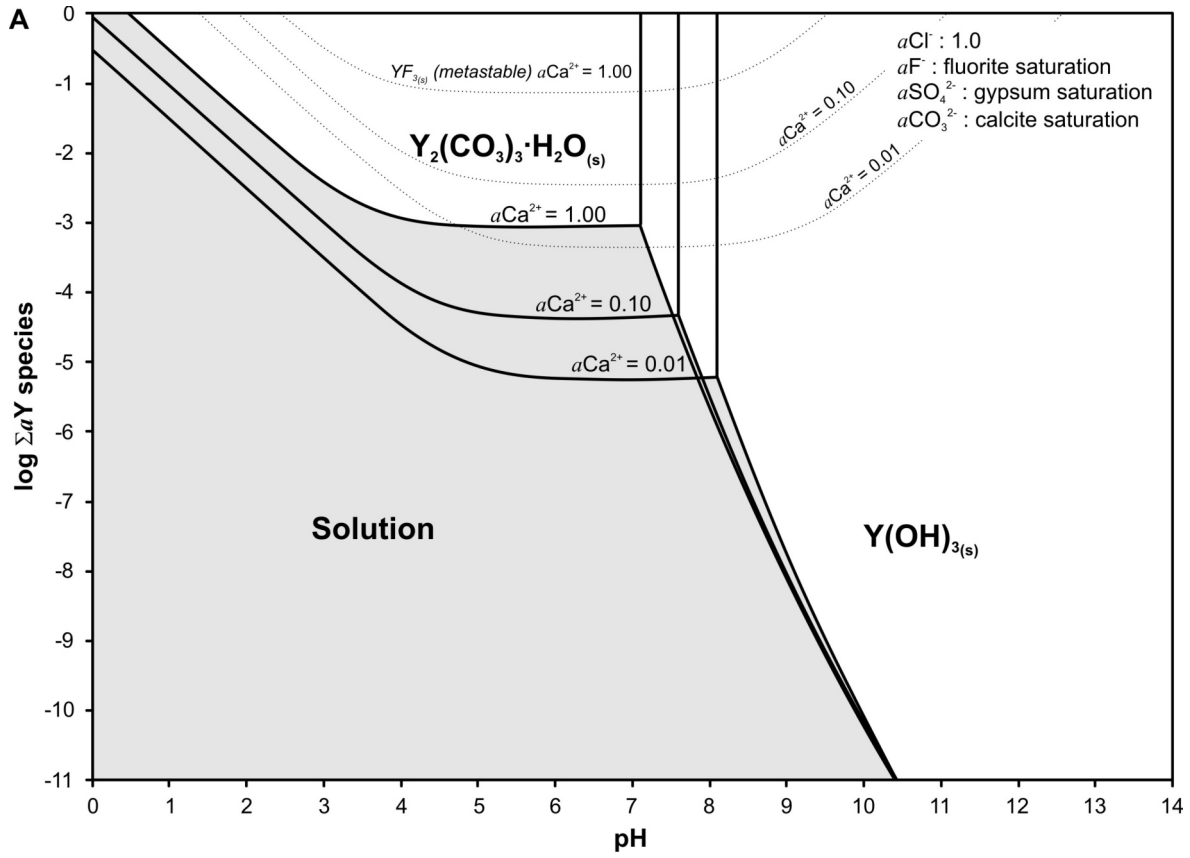
A
log ΣaY species
pH
aCl⁻ : 1.0
aF⁻ : fluorite saturation
aSO4 2- : gypsum saturation
aCO3 2- : calcite saturation
YF3(s) (metastable) aCa2+ = 1.00
Y2(CO3)3·H2O(s)
aCa2+ = 1.00
aCa2+ = 0.10
aCa2+ = 0.01
Solution
Y(OH)3(s)

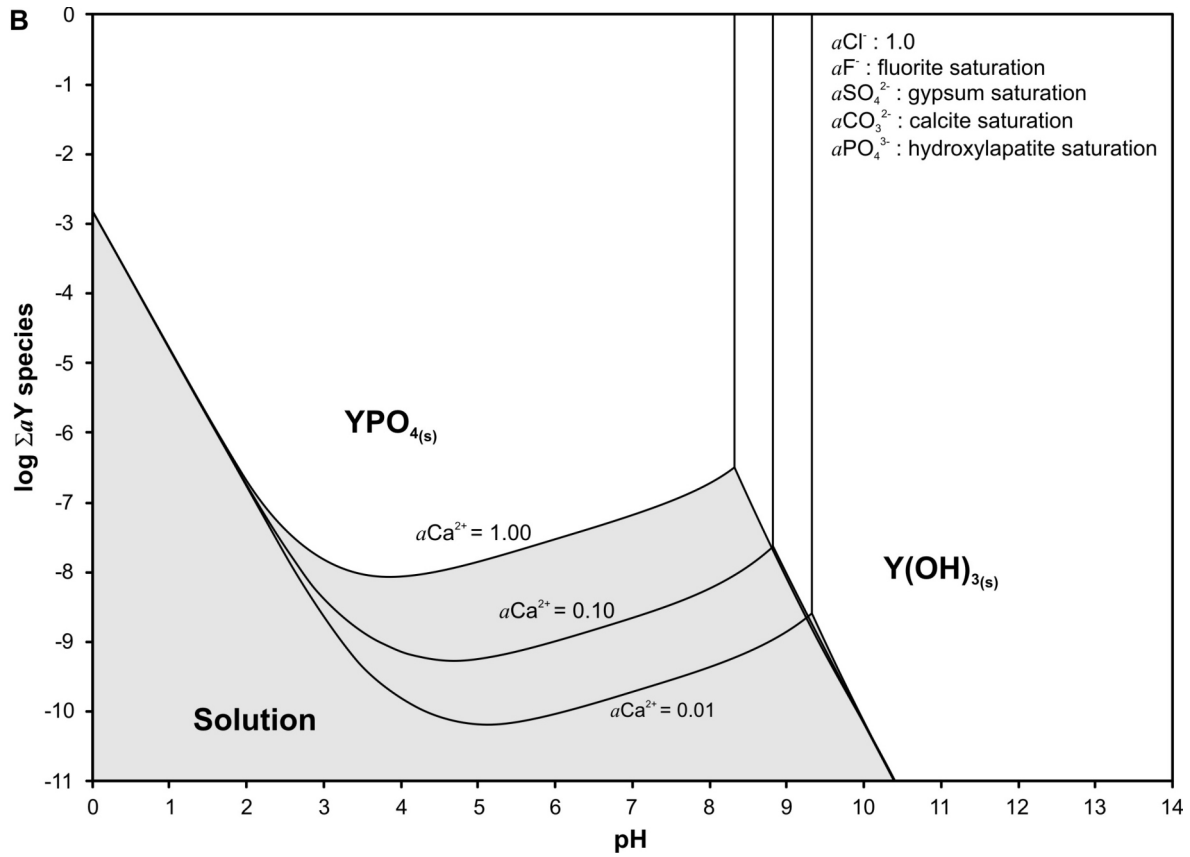
B
log ΣaY species
pH
aCl⁻ : 1.0
aF⁻ : fluorite saturation
aSO4 2- : gypsum saturation
aCO3 2- : calcite saturation
aPO4 3- : hydroxylapatite saturation
YPO4(s)
aCa2+ = 1.00
aCa2+ = 0.10
aCa2+ = 0.01
Solution
Y(OH)3(s)

Diagenetic-hydrothermal, sandstone-hosted xenotime deposits show the most dramatic HREE+Y enrichment of all REE deposits in Saskatchewan. To date, however, only subeconomic deposits of this type have been discovered in the Athabasca Basin. Factors limiting exploration for this type of deposit in the Athabasca Basin include extremely scarce exposures of bedrock, a poorly defined radiometric signature, and lack of associated distinctive alteration haloes and pathfinder elements. Nevertheless, existing documentation suggests that the Athabasca Basin, by its size and fluid-flow history, offers potential for the discovery of economic HREE+Y deposits. Apatite-rich occurrences, mostly in the Wolverine Point Formation, appear not to have been prospected as potential traps for HREE-bearing fluids circulating in tectonized areas to react and deposit xenotime.

Figure 31 – A) Log-log plot of **a**Y^{3+}**/a**Ce^{3+} ***versus*** **a**$H_3PO_{4\ (aq)}$***, showing the stability fields of monazite-(Ce), florencite-(Ce), and xenotime-(Y) in equilibrium with quartz and kaolinite (all pure end-members) at a temperature of 25°C and a pressure of 1 bar. Solid black lines represent equilibrium log*** **a**Y^{3+}**/a**Ce^{3+} ***and log*** **a**$H_3PO_{4\ (aq)}$ ***values between solid phases. Horizontal dashed grey lines show the values of log*** **a**$H_3PO_{4\ (aq)}$ ***at saturation with hydroxylapatite for values of log (*****a**Ca^{2+}**/a**H^{+2}***) of 4.0, 4.5, 5.0, and 5.5. The activity of*** Ca^{2+} ***in solution in equilibrium with florencite-(Ce) and xenotime-(Y) is predicted to be below*** $10^{-2.3}$ ***in the absence of hydroxylapatite. B) log-log plot of the sum of the activities of the contributing aqueous Y species as a function of log*** **a**$H_3PO_{4\ (aq)}$***, showing variations in*** $YPO_{4\ (s)}$ ***(xenotime-(Y)) solubility at fixed*** **a**Ca^{2+} ***of 0.01, 0.10, and 1.00 in aqueous solutions at a temperature of 25°C and a pressure of 1 bar in the system Y-Cl-F-S-C-P-O-H saturated with hydroxylapatite, fluorite, gypsum, and calcite. Maximum*** **a**F^-**,** **a**SO_4^{2-}**,** **a**CO_3^{2-}**, and** **a**PO_4^{3-} ***in solution are fixed by saturation with fluorite, gypsum, calcite, and hydroxylapatite, respectively, at the prescribed*** **a**Ca^{2+}***. Calculations predict that, at low*** **a**$Ca^{2,+}$ ***carbonate complexes predominate at low values of*** **a**$H_3PO_{4\ (aq)}$ ***and phosphate complexes predominate at elevated values of*** **a**$H_3PO_{4\ (aq)}$***. At elevated*** **a**Ca^{2+}***, chloride complexes are predicted to predominate at low values of*** **a**$H_3PO_{4\ (aq)}$***, and carbonate followed by phosphate complexes are predicted to predominate with increasing*** **a**$H_3PO_{4\ (aq)}$ ***at elevated values of*** **a**$H_3PO_{4\ (aq)}$***. Aqueous Y species considered:*** Y^{3+}***,*** $Y(OH)^{2+}$***,*** YCl^{2+}***,*** $YF_{3\ (aq)}$***,*** YF_2^+***,*** YF^{2+}***,*** YSO_4^+***,*** $Y(SO_4)_2^-$***,*** $YPO_{4\ (aq)}$***,*** $YHPO_4^+$***,*** $YH_2PO_4^{2+}$***,*** YCO_3^+***, and*** $YHCO_3^{2+}$***. Solid Y phases considered:*** $Y(OH)_{3\ (s)}$***,*** $YF_{3\ (s)}$***,*** $Y_2(CO_3)_3{\bullet}H_2O_{(s)}$***, and*** $YPO_{4\ (s)}$***. Activity of*** Cl^- ***was fixed at 1. Note low*** $YPO_{4\ (s)}$ ***solubility at all values of log*** **a**$H_3PO_{4\ (aq)}$***. Also note that the individual activity coefficients for the charged species at the ionic strength considered here can be significantly <1, so that the actual total solubilities of*** $YPO_{4\ (s)}$ ***(total Y molality represented by the sum of the individual molalities of the contributing Y aqueous species) are higher (by about. one order of magnitude). Thermodynamic data used for calculation of the diagrams: solubility product of florencite-(Ce) from Schwab* et al. *(1993) and all other solid phases and aqueous species from the thermo_minteq.dat dataset of* The Geochemist Workbench *(Bethke, 1996; Bethke and Yeakle, 2009; The Geochemist Workbench datasets available at http://www.gwb.com/).***

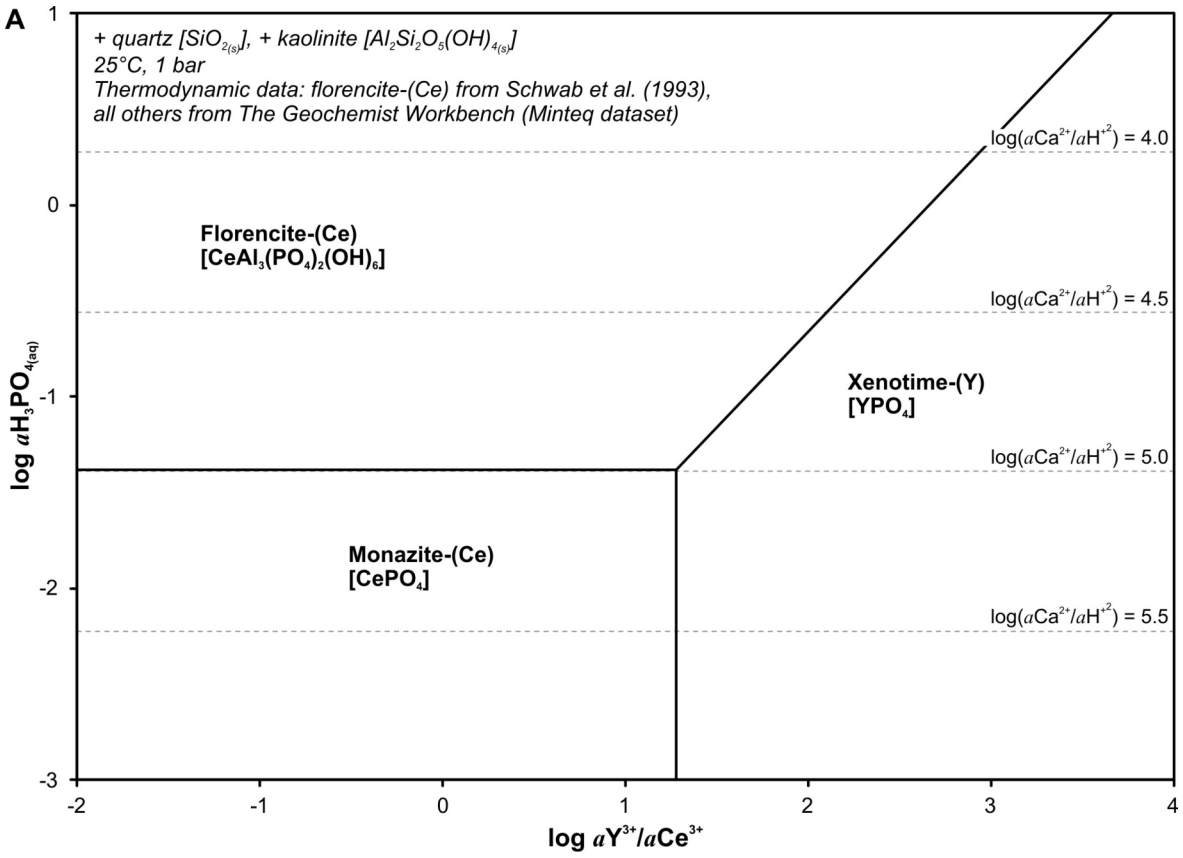
A
+ quartz [SiO2(s)], + kaolinite [Al2Si2O5(OH)4(s)]
25°C, 1 bar
Thermodynamic data: florencite-(Ce) from Schwab et al. (1993),
all others from The Geochemist Workbench (Minteq dataset)
log(aCa2+/aH+2) = 4.0
log(aCa2+/aH+2) = 4.5
log(aCa2+/aH+2) = 5.0
log(aCa2+/aH+2) = 5.5
Florencite-(Ce)
[CeAl3(PO4)2(OH)6]
Xenotime-(Y)
[YPO4]
Monazite-(Ce)
[CePO4]
log aH3PO4(aq)
log aY3+/aCe3+

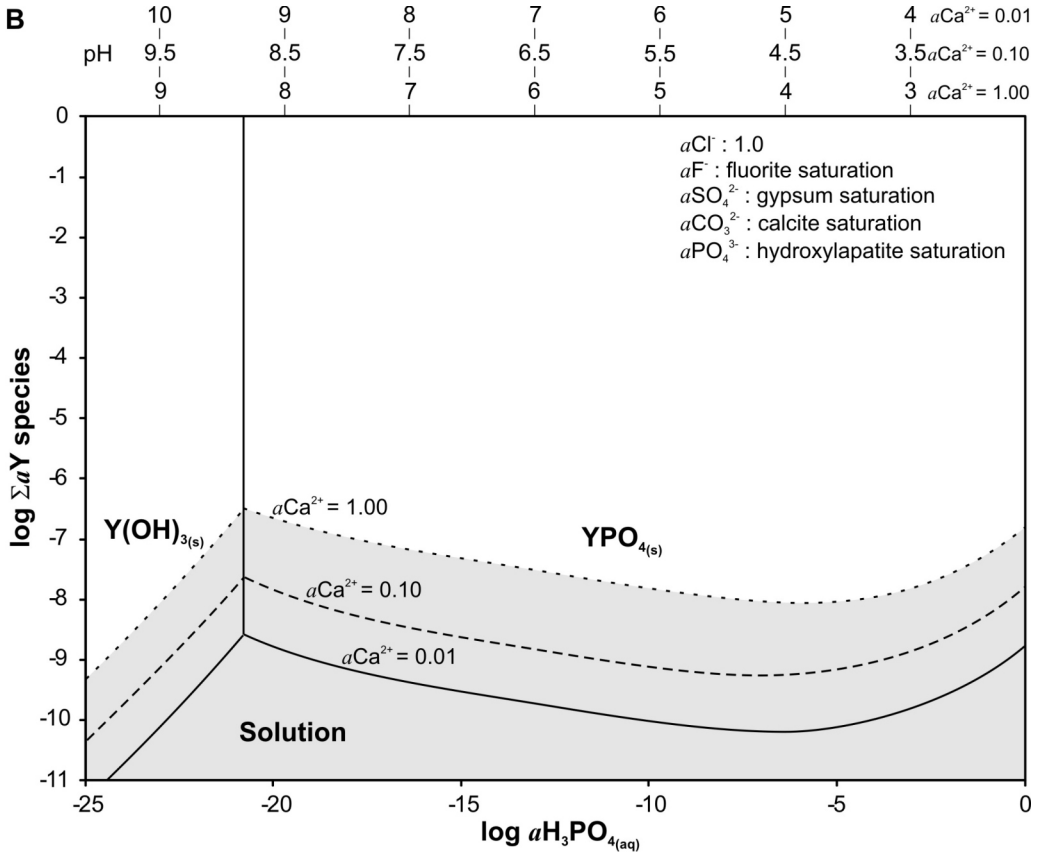
B
pH
aCa2+ = 0.01
aCa2+ = 0.10
aCa2+ = 1.00
aCl- : 1.0
aF- : fluorite saturation
aSO4 2- : gypsum saturation
aCO3 2- : calcite saturation
aPO4 3- : hydroxylapatite saturation
Y(OH)3(s)
YPO4(s)
Solution
log ΣaY species
log aH3PO4(aq)

For Further Information

To obtain further information on Saskatchewan occurrences of REE, use the *Saskatchewan Mineral Deposit Index* (SDMI; http://economy.gov.sk.ca/SMDI), or the *Geological Atlas of Saskatchewan* (http://www.infomaps.gov.sk.ca/website/SIR_Geological_Atlas/viewer.htm). Information can also be obtained by consulting the Saskatchewan Mineral Assessment Database (SMAD; http://economy.gov.sk.ca/smad). Information on all aspects of Saskatchewan's geology and mineral and petroleum resources is available at http://economy.gov.sk.ca/SGS.

References

Ague, J.J. (2011): Extreme channelization of fluid and the problem of element mobility during Barrovian metamorphism; Amer. Mineral., v96, p333-352.

Alcock, F.J. (1936): Geology of Lake Athabaska Region, Saskatchewan; Geol. Surv. Can., Mem. 196, 41p.

Aleinikoff, J.N. and Grauch, R.I. (1990): U-Pb geochronologic constraints on the origin of a unique monazite-xenotime gneiss, Hudson highlands, New York; Amer. J. Sci., v290, p522-546.

Alexandre, P., Kyser, K., and Jiricka, D. (2009a): Critical geochemical and mineralogical factors for the formation of unconformity-related uranium deposits: comparison between barren and mineralized systems in the Athabasca Basin, Canada; Econ. Geol., v104, p 413-435.

Alexandre, P., Kyser, K., and Layton-Matthews, D. (2010): REE concentrations in zircon and the origin of uranium in the unconformity-related U deposits in the Athabasca Basin, Canada; GeoCanada 2010 – Working with the Earth, Calgary, abstr., 4p, URL <http://www.cspg.org/documents/Conventions/Archives/Annual/2010/0214_GC2010_REE_Concentrations_in_Zircon.pdf>, accessed 27 Jan 14.

Alexandre, P., Kyser, K., Thomas, D., Polito, P., and Marlat, J. (2009b): Geochronology of unconformity-related uranium deposits in the Athabasca Basin, Saskatchewan, Canada and their integration in the evolution of the basin; Mineral. Dep., v44, p41-59.

Anders, E. and Grevesse, N. (1989). Abundances of the elements: meteoric and solar; Geochim. Cosmochim. Acta, v53, p197-214, doi: 10.1016/0016-7037(89)90286-X.

Andreoli, M.A.G., Hart, R.J., Ashwal, L.D., and Coetzee, H. (2006): Correlations between U, Th content and metamorphic grade in the Western Namaqualand Belt, South Africa, with implications for radioactive heating of the crust; J. Petrol., v47, p1095-1118.

Andreoli, M.A.G., Smith, C.B., Watkeys, M., Moore, J.M., Ashwal, L.D., and Hart, R.J. (1994): The geology of the Steenkampskraal monazite deposit, South Africa; implications for REE-Th-Cu mineralization in charnockite-granulite terranes; Econ. Geol., v89, p994-1016.

Annesley, I.R. and Madore, C. (1989): The Wollaston Group and its underlying Archean basement in Saskatchewan: 1989 fieldwork and preliminary observations; *in* Summary of Investigations 1989, Saskatchewan Geological Survey, Sask. Energy and Mines, Misc. Rep. 89-4, p87-91.

Annesley, I.R., Madore, C., Kusmirski, R.T., and Bonli, T. (2000): Uraninite-bearing granitic pegmatite, Moore Lakes, Saskatchewan – petrology and U-Th-Pb chemical ages; *in* Summary or Investigations 2000, Volume 2, Saskatchewan Geological Survey, Sask. Energy and Mines, Misc. Rep. 2000-4.2, CD-ROM, p201-211.

Annesley, I.R., Madore, C., and Portella, P. (2005): Geology and thermotectonic evolution of the western margin of the Trans-Hudson Orogen: evidence from the eastern sub-Athabasca basement, Saskatchewan; Can. J. Earth Sci., v42, p573-597.

Areva Resources Canada Inc. (2014): Site guide, McClean Lake operation; Areva Resources Canada Inc., URL <http://us.areva.com/home/liblocal/docs/Operations/Mining/McClean_Lake_Site_Guide2.pdf>, accessed 24 Feb 2014.

Armbruster, T., Bonazzi, P., Akasaka, M., Bermanec, V., Chopin, C., Gieré, R., Heuss-Assbichler, S., Liebscher, A., Menchetti, S., Pan, Y., and Pasero, M. (2006): Recommended nomenclature of epidote-group minerals; Eur. J. Mineral., v18, p551-567.

Armitage, A. and Sexton, A. (2012): Technical report on the resource estimate on the Way Lake uranium project, Fraser Lakes zone B, located in the Wollaston Group, east of the Athabasca Basin, northern Saskatchewan, NTS map sheets 74A/14, 74A/15, 74H/01, 74H/02, 74H/03, 74H/07 and 74H/08; NI 43-101–compliant technical report prepared by GeoVector Management Inc. for JNR Resources Inc., 55p, URL <http://www.sedar.com>, accessed 27 Jan 2014.

Ashton, K.E. (2009): Compilation Bedrock Geology, Tazin Lake, NTS Area 74N; Sask. Energy Resour., Map 246A, 1:250 000 scale.

Ashton, K.E., Card, C.D., Davis, W., and Heaman, L.M. (2007b): New U-Pb zircon age dates from the Tazin Lake map area (NTS 74N); *in* Summary of Investigations 2007, Volume 2, Saskatchewan Geological Survey, Sask. Ministry of Energy and Resources, Misc. Rep. 2007-4.2, CD-ROM, Paper A-11, 8p.

Ashton, K.E., Card, C.D., and Modeland, S. (2005): Geological reconnaissance of the northern Tazin Lake map area (NTS 74N), including parts of the Ena, Nolan, Zemlak, and Taltson domains, Rae Province; *in* Summary of Investigations 2005, Volume 2, Saskatchewan Geological Survey, Sask. Industry and Resources, Misc. Rep. 2005-4.2, CD-ROM, Paper A-1, 24p.

Ashton, K.E., Hartlaub, R.P., Bethune, K.M., Heaman, L.M., Rayner, N., and Niebergall, G.R. (2013): New depositional age constraints for the Murmac Bay group of the southern Rae craton, Canada; Precamb. Resear., v232, p70-88.

Ashton, K.E., Hartlaub, R.P., Heaman, L.M., Morelli, R.M., Card, C.D., Bethune, K., and Hunter, R. (2009): Post-Taltson sedimentary and intrusive history of the southern Rae Province along the northern margin of the Athabasca Basin, western Canadian Shield; Precamb. Resear., v175, p16-34.

Ashton, K.E., Knox, B,. and Bethune, K.M. (2006a): Bedrock geology of the western Fond-du-Lac area, south-central Beaverlodge Domain, Fond-du-Lac Project (part of NTS 74015 and 16), central sheet; 1:20 000-scale prelim. map *with* Summary of Investigations 2006, Volume 2, Saskatchewan Geological Survey, Sask. Industry and Resources, Misc. Rep. 2006-4.2.

Ashton, K.E., Knox, B., Bethune, K.M., and Marcotte, J. (2006b): Bedrock geology along the northern margin of the Athabasca Basin west of Fond-du-Lac (NTS 74O-5 and -6), south-central Beaverlodge Domain, Rae Province, Fond-du-Lac Project; *in* Summary of Investigations 2006, Volume 2, Saskatchewan Geological Survey, Sask. Industry and Resources, Misc. Rep. 2006-4.2, Paper A-1, 19p.

Ashton, K.E., Knox, B.R., Bethune, K.M., and Rayner, N. (2007a): Geochronological update and basement geology along the northern margin of the Athabasca Basin east of Fond-du-Lac (NTS 740/06 and 107), southeastern Beaverlodge– southwestern Tantato domains, Rae Province; *in* Summary of Investigations 2007, Volume 2, Saskatchewan Geological Survey, Sask. Ministry of Energy and Resources, Misc. Rep. 2007-4.2, CD-ROM, Paper A-9, 22p.

Ayers, J.C., Miller, C., Gorisch, B., and Milleman, J. (1999): Textural development of monazite during high-grade metamorphism: hydrothermal growth kinetics, with implications for U, Th-Pb geochronology; Amer. Mineral., v84, p1766-1780.

Bailey, E.H. and Ragnarsdottir, K.V. (1994): Uranium and thorium solubilities in subduction zone fluids; Earth Planet. Sci. Lett., v124, p119-129.

Bali, E., Audétat, A., and Keppler, H. (2011): The mobility of U and Th in subduction zone fluids: an indicator of oxygen fugacity and fluid salinity; Contrib. Mineral. Petrol., v161, p597-613.

Banks, D.A., Yardley, B.W.D., Campbell, A.R., and Jarvis, K.E. (1994): REE composition of an aqueous magmatic fluid: a fluid inclusion study from the Capitan Pluton, New Mexico, U.S.A.; Chem. Geol., v113, p259-272.

Barker, M. (2007): Structural analysis of the Maw zone: a sub-economic REE deposit; unpubl. B.Sc. thesis, St. Francis Xavier Univ., Antigonish, 82p.

Barr Engineering Company (2009): Form 43-101 – Mineral resource report on the Hoidas Lake rare earth project, Northern Mining District, Saskatchewan, NTS map area 74-O-13; NI 43-101–compliant technical report prepared for Great Western Minerals Group Ltd., Minneapolis, 20 Nov 2009, 69p., URL <http://www.sedar.com>, accessed 22 Jan 2014.

Barrie, J. (1965): Notes on some phosphate test procedures; Australia Department of National Development, Bureau of Mineral Resources, Geology and Geophysics, Record 1965/77.

Bau, M. (1991): Rare-earth element mobility during hydrothermal and metamorphic fluid-rock interaction and the significance of the oxidation state of europium; Chem. Geol., v93, p219-230.

Bayliss, P. and Levinson, A.A. (1988): A system of nomenclature for rare-earth mineral species: revision and extension; Amer. Mineral., v73, p422-423.

Bayliss, P., Kolitsch, U., Nickel, E.H., and Pring, A. (2010): Alunite supergroup: recommended nomenclature; Mineral. Mag., v74, p919-927.

Bea, F. (1996): Residence of REE, Y, Th and U in granites and crustal protoliths: implications for the chemistry of crustal melts; J. Petrol., v37, p521-552.

Beck, L.S. (1969): Uranium Deposits of the Athabasca Region; Sask. Miner. Resour., Rep. 126, 140p.

Berman, R.G. (1991): Thermobarometry using multi-equilibrium calculations: a new technique, with petrological applications; Can. Mineral., v29, p833-855.

_____ (2007): winTWQ (version 2.3): a software package for performing internally-consistent thermobarometric calculations; Geol. Surv. Can., Open File 5462, 41p, URL <http://geoscan.nrcan.gc.ca/starweb/geoscan/servlet.starweb?path=geoscan/fulle.web&search1=R=223425>. accessed 21 Feb 2014.

Berman, R.G., Pehrsson, S., Davis, W.J., Ryan, J.J., Qui, H., and Ashton, K.E. (2013): The Arrowsmith Orogeny: geochronological and thermobarometric constraints on its extent and tectonic setting in the Rae Craton, with implications for pre-Nuna supercontinent reconstruction; Precamb. Resear., v232, p44-69.

Berman, R.G., Sanborn-Barrie, M., Stern, R.A., and Carson, C.J. (2005): Tectonometamorphism at *ca.* 2.35 and 1.85 Ga in the Rae Domain, western Churchill Province, Nunavut, Canada: insights from structural, metamorphic and *in situ* geochronological analysis of the southwestern Committee Bay Belt; Can. Mineral., v43, p409-442.

Bernhard, F., Walter, F., Ettinger, K., Taucher, J., and Mereiter, K. (1998): Pretulite, $ScPO_4$, a new scandium mineral from the Styrian and Lower Austrian lazulite occurrences, Austria; Amer. Mineral., v83, p625-630.

Beshears, C.J. (2010): The geology and geochemistry of the Millennium uranium deposit, Athabasca Basin, Saskatchewan, Canada; unpubl. M.Sc. thesis, Univ. Manitoba, Winnipeg, 133p.

Bethke, C.M. (1996): Geochemical Reaction Modeling, Concepts and Applications; Oxford University Press, New York, 397p.

Bethke, C.M. and Yeakel, S. (2009): The Geochemist's Workbench®, Version 8.0: GWB Essentials Guide; Hydrogeology Program, Univ. Illinois, Urbana, 84p.

Bethune, K.M., Berman, R.G., Rayner, N., and Ashton, K.E. (2013): Structural, petrological and *in situ* U-Pb SHRIMP geochronological study of the western Beaverlodge Domain: implications for crustal architecture, multi-stage orogenesis and the extent of the Taltson Orogen in the SW Rae Craton, Canadian Shield; Precamb. Resear., v232, p89-118.

Blake, D.A.W. (1955): Oldman River Map Area, Saskatchewan; Geological Survey of Canada, Mem. 279, 52p.

Boatner, L.A. (2002): Synthesis, structure, and properties of monazite, pretulite, and xenotime; *in* Kohn, M.L., Rakovan, J. and Hughes, J.M. (eds.), Phosphates – Geochemical, Geobiological, and Materials Importance, Rev. Mineral. Geochem., v48, p87-121.

Bonhoure, J. (2007): Géochimie des Éléments de Terres Rares et du Plomb dans les Oxydes d'Uranium Naturels; unpubl. Ph.D. thesis, Nancy Univ., Nancy, 390p.

Bonhoure, J., Kister, P., Cuney, M., and Deloule, E. (2007): Methodology for rare earth element determinations of uranium oxides by ion microprobe; Geostand. Geoanalyt. Resear., v31, p209-225.

Bosman, S.A. and Card, C.D. (2012): Geochemical analyses of Athabasca Group drillholes in Saskatchewan (NTS 64L, 74F to 74K, and 74N to 74P) – supplementary to Data File Reports 24, 29, and 30; Sask. Ministry of the Economy, Data File Rep. 31, <http://economy.gov.sk.ca/DF31>, accessed 15 Jul 2014.

Breiter, K., Förster, H.-J., and Škoda, R. (2006): Extreme P-, Bi-, Nb-, Sc-, U- and F-rich zircon from fractionated perphosphorous granites: the peraluminous Podlesí granite system, Czech Republic; Lithos, v88, p15-34.

Brown, J.A. (2011): 2010 summary report for the Jenny Lakes uranium-REE project; Eagle Plains Resources, 12p.

Brown, T.J. (2010): Geology and geochemistry of the Kingman Feldspar, Rare Metals and Wagon Bow pegmatites; unpubl. M.Sc. thesis, University of New Orleans, New Orleans, 170p.

Bruns, J.J. (2011): Rare earth mineralization of southern Clark County, Nevada; unpubl. B.Sc. thesis, Calif. State Polytech. Univ., Pomona, 35p.

Budzyń, B., Harlov, D.E., Williams, M.L., and Jercinovic, M.J. (2011): Experimental determination of stability relations between monazite, fluorapatite, allanite, and REE-epidote as a function of pressure, temperature, and fluid composition; Amer. Mineral., v96, p1547-1567.

Cabella, R., Lucchetti, G., and Marescotti, P. (2001): Authigenic monazite and xenotime from pelitic metacherts in pumpellyite-actinolite-facies conditions, Sestri-Voltaggio zone, central Liguria, Italy; Can. Mineral., v39, p717-727.

Cameco Corp. (2002): Key Lake Operation Uranium Recycle Project Proposal; Cameco Corp., 292p.

_____ (2014): Key Lake virtual tour; Cameco Corp., URL <http://www.cameco.com/mining/key_lake/>, accessed 24 Feb 2014.

Canadian Securities Administrators (2011): NI 43-101 Standards of Disclosure for Mineral Projects, Form 43-101F1 Technical Report and Related Consequential Amendments; Canadian Institute of Mining, Metallurgy and Petroleum, URL <http://web.cim.org/standards/MenuPage.cfm?sections=177,181&menu=229>, accessed 17 Jan 2014.

Card, C.D. and Bosman, S.A. (2012): Geochemical analyses of Athabasca Group outcrops in Saskatchewan (NTS 64L, 74F to 74K, and 74N to 74P) – supplementary to Data File Report 29; Sask. Ministry of the Economy, Data File Rep. 30, <http://economy.gov.sk.ca/DF30>, accessed 15 Jul 2014.

Card, C.D., Bosman, S.A., Slimmon, W.L., Zmetana, D.J., and Delaney, G.D. (2011): Geochemical analyses of Athabasca Group outcrops in Saskatchewan (NTS 64L, 74F to 74K, and 74N to 74P); Sask. Ministry of the Economy, Data File Rep. 29, <http://economy.gov.sk.ca/DF29>, accessed 15 Jul 2014.

Cardarelli, F. (2008): Materials Handbook – A Concise Desktop Reference (Second Edition); Springer, New York, 1340p.

Carson, J.M., Holman, E.B., Shives, R.B.K., Ford, K.T., Ashton, K., and Slimmon, W.L. (2001): Tazin Lake area geophysical maps; Geol. Surv. Can., Open File 3952/Sask. Energy and Mines, Open File 2001-3, series of 10 geophysical maps at 1:250 000 scale.

Černý, P. and Chapman, R. (2001): Exsolution and breakdown of scandian and tungstenian Nb-Ta-Ti-Fe-Mn phases in niobian rutile; Can. Mineral., v39, p93-101.

Černý, P. and Ercit, T.S. (2005): The classification of granitic pegmatites revisited; Can. Mineral., v43, p2005-2026.

Cetiner, Z., Wood, S.A., and Gammons, C.H. (2005): The aqueous geochemistry of the rare earth elements, part XIV: the solubility of rare earth element phosphates from 23 to 150°C; Chem. Geol., v217, p147-169.

Chao, E.C.T., Back, J.M., and Minkin, J.A. (1992): Host-rock controlled epigenetic, hydrothermal metasomatic origin of the Bayan Obo REE-Fe-Nb ore deposit, Inner Mongolia, PRC; Appl. Geochem., v7, p443-458.

Cherniak, D.J., Watson, E.B., Grove, M., and Harrison, T.M. (2004): Pb diffusion in monazite: a combined RBS/SIMS study; Geochim. Cosmochim. Acta, v68, p829-840.

Chi, G., Bosman, S., and Card, C. (2013): Numerical modeling of fluid pressure regime in the Athabasca Basin and implications for fluid flow models related to the unconformity-type uranium mineralization; J. Geochem. Explor., v125, p8-19.

Choudhuri, R. and Banerji, K.C. (1976): On the occurrence, emplacement and origin of the apatite deposits of Kasipatnam in Visakhapatnam District, Andhra Pradesh; Proceedings of the Indian National Science Academy, ptA, v42, p387-406.

Christie, A.M. (1953): Goldfields–Martin Lake Map-Area, Saskatchewan; Geol. Surv. Can., Mem. 269, 126p.

Cloutier, J., Kyser, K., Olivo, G.R., and Alexandre, P. (2010): Contrasting patterns of alteration at the Wheeler River area, Athabasca Basin, Saskatchewan, Canada: insights into the apparently uranium-barren zone K alteration system; Econ. Geol., v105, p303-324.

Cloutier, J., Kyser, K., Olivo, G.R., Alexandre, P., and Halaburda, J. (2009): The Millennium uranium deposit, Athabasca Basin, Saskatchewan, Canada: an atypical basement-hosted unconformity-related uranium deposit; Econ. Geol., v104, p815-840.

Cloutier, J., Kyser, K., Olivo, G.R., and Brisbin, D. (2011): Geochemical, isotopic, and geochronologic constraints on the formation of the Eagle Point basement-hosted uranium deposit, Athabasca Basin, Saskatchewan, Canada and recent remobilization of primary uraninite in secondary structures; Mineral. Dep., v46, p35-56.

Cochrane, L.B. and Hwozdyk, L.R. (2007): Technical report on the Elliot Lake property, Elliot Lake district, Ontario, Canada; NI 43-101–compliant report prepared by Scott Wilson Roscoe Postle Associates Inc. for Denison Mines Corp., 94p, URL <http://www.sedar.com>, accessed 27 Jan 2014.

Condie, K.C. (1993): Chemical composition and evolution of the upper continental crust: contrasting results from surface samples and shales; Chem. Geol., v104, p1-37.

Corfu, F., Hanchar, J.M., Hoskin, P.W.O., and Kinny, P. (2003): Atlas of zircon textures; *in* Hanchar, J.H. and Hoskin, P.W.O. (eds.), Zircon, Rev. Mineral. Geochem., v53, p427-468.

Corliss, J.B., Dymond, J., Lyle, M., and Crane, K., (1978): The chemistry of hydrothermal mounds near the Galapagos Rift; Earth Planet. Sci. Lett., v40, p12-24.

Cousens, B.L., Aspler, L.B., Chiarenzelli, J.R., Donaldson, J.A., Sandeman, H.A., Peterson, T.D., and LeCheminant, A.N. (2001): Enriched Archean lithospheric mantle beneath western Churchill Province tapped during Paleoproterozoic orogenesis; Geol., v29, p827-830.

Crowley, J.L. and Ghent, E.D. (1999): An electron microprobe study of the U-Th-Pb systematics of metamorphosed monazite: the role of Pb diffusion versus overgrowth and recrystallization; Chem. Geol., v157, p285-302.

Cuney, M. (2008): Origin, nature and conditions of circulation of the fluids associated with the genesis of unconformity related uranium deposits; *in* Proceedings of XIII International Conference on Thermobarogeochemistry and IVth APIFIS Symposium, Volume 2, Russ. Mineral. Soc., DPI 2008-1-86-1, abstr., p151-155.

_____ (2009): The extreme diversity of uranium deposits; Mineral. Dep., v44, p3-9.

_____ (2010): Evolution of uranium fractionation processes through time: driving the secular variation of uranium deposit types; Econ. Geol., v105, p553-569.

Davidson, C.F. (1956): The economic geology of thorium; Min. Mag., v94, p197-208.

Davis, W.J., Gall, Q., Jefferson, C.W., and Rainbird, R.H. (2011): Fluorapatite in the Paleoproterozoic Thelon Basin: structural-stratigraphic context, *in situ* ion microprobe U-Pb ages, and fluid-flow history; Geol. Soc. Amer. Bull., v123, p1056-1073.

Derome, D., Cathelineau, M., Cuney, M., Fabre, C., Lhomme, T., and Banks, D.A. (2005): Mixing of sodic and calcic brines and uranium deposition at McArthur River, Saskatchewan, Canada: a Raman and laser-induced breakdown spectroscopic study of fluid inclusions; Econ. Geol., v100, p1529-1545.

de Zoysa, T.H. (1974): The Geology of the Ena Lake Area (West Half), Saskatchewan; Sask. Dep. Miner. Resour., Rep. 142, 26p.

Dieng, S. (2012): Fluid evolution and structural control on uranium deposits in successor basins in northern Canada and northern Australia; unpubl. Ph.D. thesis, Queen's Univ., Kingston, 277p.

Dieng, S., Kyser, K., and Godin, L. (2013): Tectonic history of the North American shield recorded in uranium deposits in the Beaverlodge area, northern Saskatchewan, Canada; Precamb. Resear., v224, p316-340.

Dollase, W.A. (1971): Refinement of the crystal structures of epidote, allanite and hancockite; Amer. Mineral., v56, p447-464.

Doran, R., Bouchard, A-M., Saucier, G., Rheault, M., Ayad, A.B., Knox, A., Lafleur, P-J., and Levaque, J-G. (2012): Preliminary economic assessment on Orbite Aluminae Inc. metallurgical grade alumina project, Quebec, Canada; NI 43-101–compliant revised technical report prepared by Roche/Genivar for Orbite Aluminae Inc., 332p, URL <http://www.sedar.com>, accessed 27 Jan 2014.

Dunn, C.E. and Hoffman, E. (1986): Multi-element study of vegetation from a zone of rare-earth rich allanite and apatite in northern Saskatchewan, Canada; Appl. Geochem., v1, p375-381.

Eagle Plains Resources Ltd. (undated a): Karin Lake project (U, REE); Eagle Plains Resources Ltd., information brochure.

_____ (undated b): Oreo property REE-U; Eagle Plains Resources Ltd. information brochure.

Ercit, T.S. (2002): The mess that is "allanite"; Can. Mineral., v40, p1411-1419.

_____ (2005): REE-enriched granitic pegmatites; *in* Linnen, R.L. and Sampson, I.M. (eds.), Rare-Element Geochemistry and Mineral Deposits, Geol. Assoc. Can., Short Course Notes, v17, p257-296.

Evans, J.R. (1964): Xenotime Mineralization in the Southern Music Valley Area, Riverside County, California; Calif. Div. Mines Geol., Spec. Rep. 79, 24p.

Fayek, M. (1996): Fluid events associated with gold, uranium, and REE deposits in the Proterozoic of northern Saskatchewan, Canada; unpubl. Ph.D. thesis, Univ. Sask., Saskatoon, 219p.

Fayek, M. and Kyser, K.T. (1997): Characterization of multiple fluid-flow events and rare-earth elements mobility associated with formation of unconformity uranium deposits in the Athabasca Basin, Saskatchewan; Can. Mineral., v35, p627-658.

Ferry, J.M. and Gerdes, M.L. (1998): Chemically reactive fluid flow during metamorphism; Ann. Rev. Earth and Planet. Sci., v26, p255-287.

Finch, R.J. and Ewing, R.C. (1992): The corrosion of uraninite under oxidizing conditions; J. Nucl. Mater., v190, p133-156.

Foord, E.E., Birmingham, S.D., Demartin, F., Pilati, T., Gramaccioli, C.M. and Lichte, F.E. (1993): Thortveitite and associated Sc-bearing minerals from Ravalli County, Montana; Can. Mineral., v31, p337-346.

Ford, R.B. (1955): Mineralogy of a uraninite-bearing pegmatite, Lac La Ronge, Saskatchewan; Econ. Geol., v50, p196-205.

Förster, H.-J. (1998): The chemical composition of REE-Y-Th-U-rich accessory minerals in peraluminous granites of the Erzgebirge-Fichtelgebirge region, Germany, part I: the monazite-(Ce)-brabantite solid solution series; Amer. Mineral., v83, p259-272.

_____ (1999): The chemical composition of uraninite in Variscan granites of the Erzgebirge, Germany; Mineral. Mag., v63, p239-252.

Frape, S.K., Blyth, A., Blomqvist, R., McNutt, R.H., and Gascoyne, M. (2003): Deep fluids in the continents, II: crystalline rocks; *in* Drever, J.I., Holland, H.D., and Turekian K.K. (eds.), Treatise on Geochemistry, Volume 5, Elsevier, Philadelphia, p541-580.

Fryer, B.J. and Taylor, R.P. (1987): Rare-earth element distributions in uraninites: implications for ore genesis; Chem. Geol., v63, p101-108.

Frietsch, R., Papunen, H., and Vokes, F.M. (1979): The ore deposits in Finland, Norway, and Sweden – a review; Econ. Geol., v74, p975-1001.

Friske, P.W.B., McCurdy, M.W., Day, S.J., Gross, H., Balma, R.G., Lynch, J.J., and Durham, C.C. (1994a): National geochemical reconnaissance lake sediment and water data, northeastern Saskatchewan (parts of NTS 64L, 64M, and 74P); Geol. Surv. Can., Open File 2857, 135 p., doi:10.4095/132667

_____ (1994b): National geochemical reconnaissance lake sediment and water data, northeastern Saskatchewan (parts of NTS 74N and 740); Geol. Surv. Can., Open File 2858, 125 p., doi:10.4095/125178

Frondel, C. (1958): Systematic Mineralogy of Uranium and Thorium; U.S. Geol. Surv., Bull. 1064, 400p.

_____ (1970): Scandium-rich minerals from rhyolite in the Thomas Range, Utah; Amer. Mineral., v55, p1058-1060.

Frondel, C., Ito, J., and Montgomery, A. (1968): Scandium content of some aluminum phosphates; Amer. Mineral., v53, p1223-1231.

Frost, B.R. and Frost, C.D. (2008): A geochemical classification for feldspathic igneous rocks; J. Petrol., v49, p1955-1969.

Fryer, B.J. and Taylor, R.P. (1987): Rare-earth element distributions in uraninites: implications for ore genesis; Chem. Geol., v63, p101-108.

Gaboreau, S., Cuney, M., Quirt, D., Beaufort, D., Patrier, P., and Mathieu, R. (2007): Significance of aluminum phosphate-sulfate minerals associated with U unconformity-type deposits: the Athabasca Basin, Canada; Amer. Mineral., v92, p267-280.

Gambogi, J. (2013): Scandium; U.S. Geol. Surv., Mineral Comm. Summ., January 2013, p140-141.

Garside, M. (1973): Radioactive Mineral Occurrences in Nevada; Nev. Bur. Mines Geol., Bull. 81, 121p.

Gent, M., Kletzel, A., and Guliov, P. (1995): Industrial mineral occurrences in the Precambrian of northern Saskatchewan, Map 2; Sask. Energy and Mines, Preliminary Geological Map, 95-4-(5.2), 1:1 000 000 scale, <http://economy.gov.sk.ca/Default.aspx?DN=f79f8c61-5869-43a2-b30d-00f4b2b3515d>, accessed 16 Jul 2014.

Gerasimovskii, V.I. (1960): Characteristic features of the mineralogy of uranium; Soviet J. Atomic Energy, v7, p570-577.

Gieré, R. and Sorensen, S.S. (2004): Allanite and other REE-rich epidote-group minerals; *in* Liebscher, A. and Franz, G. (eds.), Epidotes, Rev. Mineral. Geochem., v56, p431-493.

Gillerman, V.S. (2008): Geochronology of iron oxide-copper-thorium-REE mineralization in Proterozoic rocks at Lemhi Pass, Idaho, and a comparison to copper-cobalt ores, Blackbird Mining District, Idaho; Idaho Geol. Surv., final technical report to U.S. Geol. Surv., Mineral Resources External Research Program, Report 06HQGR0170, 148p.

Gramaccioli, C.M., Diella, V., and Demartin, F. (1999): An example of the role of complexes in the geochemistry of transition elements in pegmatites: the formation of scandium minerals; Can. Mineral., v37, p807-808.

Gramaccioli, C.M. and Segalstad, T.V. (1978): A uranium- and thorium-rich monazite from a south-alpine pegmatite at Piona, Italy; Amer. Mineral., v63, p757-761.

Gratz, R. and Heinrich, W. (1997): Monazite-xenotime thermobarometry: experimental calibration of the miscibility gap in the binary system $CePO_4$-YPO_4; Amer. Mineral., v82, p772-780.

Grauch, R.I. (1989): Rare earth elements in metamorphic rocks; *in* Lipin, B.R. and McKay, G.A. (eds.), Geochemistry and Mineralogy of Rare Earth Elements, Rev. Mineral., v21, p147-167.

Great Western Minerals Group Ltd. (2009): Great Western Minerals Group reports a 123% increase in the resource estimate at Hoidas Lake; Great Western Minerals Group Ltd., press release, 20 Nov 2009, URL <http://www.gwmg.ca/pdf/203301_2009-11-20_NR.pdf>, accessed 17 Jan 2014.

_____ (2011): Great Western Minerals Group discovers new showing at Douglas River: 2010 exploration results; Great Western Minerals Group Ltd., press release, 16 Jun 2011, URL <http://www.gwmg.ca/sites/default/files/press-releases/20110616%20GWMG%20Douglas%20River%202010%20Exploration%20Results.pdf>, accessed 24 Feb 2014.

_____ (2012): Great Western Minerals Group reports initial Steenkampskraal rare earth assays; Great Western Minerals Group Ltd., press release, 10 April 2012, URL <http://www.gwmg.ca/pdf/203435_2012-04-10_NR.pdf>, accessed 17 Jan 2014.

Gunning, M.H. and Card, C.D. (2005): Transects across the Black Bay shear none and Hoidas-Nisikkatch rare-element trend, northwest Saskatchewan; Sask. Industry and Resources, Open File Rep. 2004-2, CD-ROM, 40p.

Gupta, C.K. and Krishnamurthy, N. (2005): Extractive Metallurgy of Rare Earths; CRC Press, 504p.

Haapala, I., Ervamaa, P., Loefgren, A., and Ojanpera, P. (1969): An Occurrence of Monazite in Puumala, Eastern Finland; Geol. Soc. Finland, Bull. 41, p117-124.

Haar, L., Gallagher, J.S., and Kell, G.S. (1984): NBS/NRC Steam Tables: Thermodynamic and Transport Properties and Computer Programs for Vapor and Liquid States of Water in SI Units; Hemisphere Publishing Corporation, Washington, 320p.

Halpin, K.M. (2010): The characteristics and origin of the Hoidas Lake REE deposit; unpubl. M.Sc. thesis, Univ. Sask., Saskatoon, 173p.

Halpin, K.M. and Ansdell, K.M. (2008): The Hoidas Lake REE deposit, northern Saskatchewan: a complex apatite-allanite vein system; Geol. Assoc. Can.–Mineral. Assoc. Can., Jt. Ann. Meet., Québec, Abstr., v33, p68.

Hancox, P.J. and Jones, I. (2012): Resource estimate and technical report on the Steenkampskraal monazite property in the Western Cape Province, South Africa; NI 43-101–compliant report by prepared by Snowden for Great Western Minerals Group Ltd., 208p, URL <http://www.sedar.com>, accessed 27 Jan 2014.

Hanly, A.J. (2001): The mineralogy, petrology and rare earth element geochemistry of the MAW zone, Athabasca Basin, Canada; M.Sc. thesis, Univ. Missouri, Rolla, 168p.

Hanly, A.J. and Hagni, R.D. (2002): The petrology and rare earth element geochemistry of the Maw zone: an yttrium and heavy rare earth element enriched zone in the Athabasca basin, Canada; Geol. Assoc. Can.–Mineral. Assoc. Can., Jt. Ann. Meet., Saskatoon, Abstr., Vol. 27, p45.

Harper, C.T. (1983): Reconnaissance bedrock geology: Nevins–Forsyth lakes area (part of NTS 74 O); *in* Summary of Investigations 1983, Saskatchewan Geological Survey, Sask. Energy and Mines, Misc. Rep. 83-4, p5-15.

_____ (1986): Geology of the Nevins–Forsyth lakes area; Sask. Energy and Mines, Open File Rep. 86-4, 57p.

_____ (1987): Rare earth elements and their occurrence in northern Saskatchewan; *in* Summary of Investigations 1987, Saskatchewan Geological Survey; Sask. Energy and Mines, Misc. Rep. 87-4, p82-86.

Hartlaub, R.P (2004): Archean and Proterozoic evolution of the Beaverlodge Belt, Churchill Craton, Canada; unpubl. Ph.D. thesis, Univ. Alta., Edmonton, 189p.

Hartlaub, R.P., Heaman, L.M., Chacko, T., and Ashton, K.E. (2007): Circa 2.3-Ga magmatism of the Arrowsmith Orogeny, Uranium City region, western Churchill Craton, Canada; J. Geol., v115, p181-195.

Harvey, S.E., Young, I., and Billingsley, G. (2002): Geology of the Hoidas Lake area, Ena Domain, northwestern Saskatchewan; *in* Summary of Investigations 2002, Volume 2, Saskatchewan Geological Survey, Sask. Industry and Resources, Misc. Rep. 2002-4.2, CD-ROM, Paper C-2, 13p.

Hazen, R.M., Ewing, R.C., and Sverjensky, D.A. (2009): Evolution of uranium and thorium minerals; Amer. Mineral., v94, p1293-1311.

Heaman, I.M., Ashton, K.E., Hartlaub, R.P., and Harper, C.T. (1999): Preliminary U-Pb age constraints on the timing of the Clearwater Anorthosite Complex, metamorphism in the Train Lake Domain, and age of the Ourom Lake group; *in* Summary of Investigations 1999, Volume 1, Saskatchewan Geological Survey, Sask. Energy and Mines, Misc. Rep. 99-4.1, p137-139.

HEFA Rare Earth Canada Co. Ltd. (2013): Price quote, June 26, 2013; HEFA Rare Earth Canada Co. Ltd., URL <http://www.baotou-rareearth.com/quote.php>, accessed 26 Jan 2014.

Hetherington, C.J. and Harlov, D.E. (2008): Metasomatically induced formation of thorite and uraninite inclusions in xenotime and monazite from granite pegmatites, Hidra anorthosite massif, southwestern Norway: mechanics and fluid chemistry; Amer. Mineral., v93, p806-820.

Hogarth, D.D. (1957): The apatite bearing veins of Nisikkatch Lake, Saskatchewan; Can. Mineral., v6, p140-150.

Hogge, C., Klohn, M., and Broili, C. (2010): Thor REE project update, Clark County, Nevada, U.S.A.; technical report prepared for Elissa Resources Ltd. by BK Exploration Associates, 51p, URL <https://www.otciq.com/otciq/ajax/showFinancialReportById.pdf?id=60226>, accessed 24 Feb 2014.

Holland, T.J.B. and Powell, R. (1998): An internally consistent thermodynamic dataset for phases of petrological interest; J. Metamor. Geol., v16, p309-343.

Hornbrook, E.H.W. and Friske, P.W.B. (1988a): Regional lake sediment and water geochemical data, northwestern Saskatchewan; Geol. Surv. Can., Open File 1642, 100p.

_____ (1988b): Regional lake sediment and water geochemical data, northeastern Saskatchewan; Geol. Surv. Can., Open File 1643, 47 maps at 1:250 000 and 1:75 000 scale.

_____ (1988c): Regional lake sediment and water geochemical data, northern Saskatchewan; Geol. Surv. Can., Open File 1644, 120p.

Hoskin, P.W.O. and Schaltegger, U. (2003): The composition of zircon and igneous and metamorphic petrogenesis; *in* Hanchar, J.M. and Hoskin, P.W.O. (eds.), Zircon, Rev. Mineral. Geochem., v53, p27-62.

Huston, D.L., Maas, R., and Hussey, K.J. (2011): The Nolans Bore rare earth element-phosphorous-uranium-thorium deposit: geology, age and origin; *in* 11th Biennial Meeting SGA 2011 – Let's Talk Ore Deposits, Antofagasta, September 26 to 29, 2011, Proceedings Volume, abstr.

International Atomic Energy Agency (1993): Uranium Extraction Technology; Technical Report 359, 358p.

Janeczek, J. and Ewing, R.C. (1992): Dissolution and alteration of uraninite under reducing conditions; J. Nucl. Mater., v190, p157-173.

Janots, E., Brunet, F., Goffé, B., Poinssot, C., Burchard, M., and Cemič, L. (2007): Thermochemistry of monazite-(La) and dissakisite-(La): implications for monazite and allanite stability in metapelites; Contrib. Mineral. Petrol., v154, p1-14.

Janots, E., Engi, M., Berger, A., Allaz, J., Schwarz, J-O., and Spandler, C. (2008): Prograde metamorphic sequence of REE minerals in pelitic rocks of the central Alps: implications for allanite-monazite-xenotime phase relations from 250° to 610°C; J. Metamorph. Geol., v26, p509-526.

Jefferson, C.W., Thomas, D.J., Gandhi, S.S., Ramaekers, P., Delaney, G., Brisbin, D., Cutts, C., Portella, P., and Olson, R.A. (2007): Unconformity-associated uranium deposits of the Athabasca Basin, Saskatchewan, and Alberta; *in* Jefferson, C.W. and Delaney, G. (eds.), EXTECH IV: Geology and Uranium EXploration TECHnology of the Proterozoic Athabasca Basin, Saskatchewan and Alberta, Geol. Surv. Can., Bull. 588, p23-68 (*also* Saskatchewan Geological Society, Special Publication 17; Geological Association of Canada, Mineral Deposits Division, Special Publication 4).

Johnsen, O., Ferraris, G., Gault, R.A., Grice, J.D., Kampf, A.R., and Pekov, I.V. (2003): The nomenclature of eudialyte-group minerals; Can. Mineral., v41, p785-794.

Kharaka, Y.K. and Hanor, J.S. (2003): Deep fluids in the continents, I: sedimentary basins; *in* Drever, J.I., Holland, H.D., and Turekian K.K. (eds.), Treatise on Geochemistry, Volume 5, Elsevier, Philadelphia, p499-540.

Klimm, K., Blundy, J.D., and Green, T.H. (2008): Trace element partitioning and accessory phase saturation during H_2O-saturated melting of basalt with implications for subduction zone chemical fluxes; J. Petrol., v49, p523-553.

Knox, A. (1985): Geology and yttrium mineralization of the MAW zone, Wheeler River property, northern Saskatchewan; Union Oil Company of Canada Ltd., unpublished report, 89p.

_____ (1986): Results of the 1985 drilling program on the MAW zone and yttrium resource calculation, Wheeler River property, northern Saskatchewan; Union Oil Company of Canada Ltd., unpublished report, 60p.

Koeppel, V. (1968): Age and History of the Uranium Mineralization of the Beaverlodge Area, Saskatchewan; Geol. Surv. Can., Paper 67-31, 111p.

Korzhinskiy, D.S. (1955): Outline of metasomatic processes: *in* Fundamental Problems in the Study of Magmatogenic Ore Deposits, AN SSSR Press, Moscow, p335-453.

Koster, R. (1965a): The Geology of the Ena Lake Area (East Half), Saskatchewan; Sask. Dep. Miner. Resour., Rep. 91, 31p.

_____ (1965b): The Geology of the Dardier Lake Area (East Half), Saskatchewan; Sask. Dep. Miner. Resour., Rep. 101, 45p.

Kremer, P.D., Böhm, C.O., and Rayner, N. (2011): Far North Geomapping Initiative: bedrock geology of the Snyder Lake area, northwestern Manitoba (part of NTS 64N5); *in* Report of Activities 2011, Manit. Innov., Energy Mines, Manit. Geol. Surv., p6-17.

Kremer, P.D., Carlson, A.R., and Couëslan, C. (2010): Far North Geomapping Initiative: geological mapping in the Misty Lake area, Manitoba (parts of NTS 64K12, 13, 64N4); *in* Report of Activities 2010, Manit. Innov., Energy Mines, Manit. Geol. Surv., p50-61.

Kristiansen, R. (2009): A unique assemblage of scandium-bearing minerals from the Heftetjern-pegmatite, Tørdal, south Norway; Kongsberg Mineralsymposium 2009, Norsk Bergverksmuseum Skrift, v41, p75-104.

Lang, A.H., Griffith, J.W., and Steacy, H.R. (1962): Canadian Deposits of Uranium and Thorium (Second Edition); Geol. Surv. Can., Econ. Geol. Ser., no16, 324p.

Langmuir, D. (1978): Uranium solution-mineral equilibria at low temperatures with applications to sedimentary ore deposits; Geochim. Cosmochim. Acta, v42, p547-569.

Langmuir, D. and Herman, J.S. (1980): The mobility of thorium in natural waters at low temperatures; Geochim. Cosmochim. Acta, v44, p1753-1766.

Laznicka, P. (2010): Giant Metallic Deposits – Future Sources of Industrial Metals (Second Edition); Springer, New York, 950p.

Liferovich, R.P., Subbotin, V.V., Pakhomovsky, Y.A., and Lyalina, M.F. (1998): A new type of scandium mineralization in phoscorites and carbonatites of the Kovdor massif, Russia; Can. Mineral., v36, p971-980.

Linthout, K. (2007): Tripartite division of the system $2REEPO_4$-$CaTh(PO_4)_2$-$2ThSiO_4$, discreditation of brabantite, and recognition of cheralite as the name for members dominated by $CaTh(PO_4)_2$; Can. Mineral., v45, p503-508.

Loges, A., Migdisov, A.A., Wagner, T., Williams-Jones, A.E., and Markl, G. (2013): An experimental study of the aqueous solubility and speciation of Y(III) fluoride at temperatures up to 250°C; Geochim. Cosmochim. Acta, v123, p403-415, URL <http://dx.doi.org/10.1016/j.gca.2013.07.031>, accessed 27 Jan 2014.

Lund, K., Tysdal, R.G., Evans, K.V., Kunk, M.J., and Pillers, R.M. (2011): Structural controls and evolution of gold-, silver-, and REE-bearing copper-cobalt ore deposits, Blackbird district, east-central Idaho: epigenetic origins; Econ. Geol., v106, p585-618.

Maas, R., Huston, D., and Hussey, K. (2009): Isotopic constraints on the genesis of world-class REE-P-U-Th mineralization, Nolans Bore, central Australia (abstr.); 2009 Goldschmidt Conference, Geochim. Cosmochim. Acta Supplement, v73, pA809.

MacDougall, D.G. (1990): Rare earth element mineralization in the Athabasca Group – Maw zone; *in* Summary of Investigations 1990, Saskatchewan Geological Survey, Sask. Energy and Mines, Misc. Rep. 90-4, p103-105.

_____ (2002): Rare earth element and other mineral occurrences in the Phelps Lake region (NTS 64M); *in* Summary of Investigations 2002, Volume 2, Saskatchewan Geological Survey, Sask. Industry and Resources, Misc. Rep. 2002-4.2, CD-ROM, Paper B-1, 23p.

Mandarino, J.A. (1999): Fleischer's Glossary of Mineral Species (Eighth Edition); The Mineralogical Record Inc., 225p.

Marchenko, Y.Y. and Goncharova, Y.I. (1965): Part played by haloids in the formation and subsequent alteration of monazite of pneumatolytic to hydrothermal origin; Doklady Earth Sci., v155, p118-122.

Masau, M., Černý, P., Cooper, M.A., Chapman, R., and Grice, J.D. (2002): Monazite-(Sm), a new member of the monazite group from the Annie claim #3 granitic pegmatite, southeastern Manitoba; Can. Mineral., v40, p1649-1655.

Mawdsley, J.B. (1954): Radioactive, pronouncedly differentiated pegmatite sill, Lac La Ronge district, northern Saskatchewan; Econ. Geol., v49, p616-624.

_____ (1957): The Geology of the Middle Foster Lake Area, Northern Saskatchewan; Dep. Miner. Resour., Metallic and Industrial Minerals Branch, Geology Division, Rep. 26, 49p.

McCaig, A.M., Trilla, J., and Banks, D.A. (2000): Fluid mixing and recycling during Pyrenean thrusting: evidence from fluid inclusion halogen ratios; Geochim. Cosmochim. Acta, v64, p3395-3412.

McFarlane, C.R.M. and McKeough, M. (2013a): Anatexis of phosphatic metalliferous shales as an ingredient in unusual pegmatite-hosted monazite-apatite-ilmenite occurrences; Geol. Assoc. Can.–Mineral. Assoc. Can., Jt. Annu. Meet., Winnipeg, Abstr., Vol. 36, p140.

_____ (2013b): Petrogenesis of the Kulyk Lake monazite-apatite-Fe(Ti)-oxide occurrence revealed using in-situ LA-(MC)-ICP-MS trace element mapping, U-Pb dating, and Sm-Nd isotope systematic on monazite; Amer. Mineral., v98, p1644-1659.

McKechnie, C.L. (2012): The Fraser Lakes zone B U-Th-REE deposit and its host rocks: implications for pegmatite- and leucogranite-hosted U-Th-REE deposits in northern Saskatchewan, Canada; unpubl. M.Sc. thesis, Univ Sask., Saskatoon, 284p.

McKechnie, C.L., Annesley, I.R., and Ansdell, K.M. (2012a): Medium- to low-pressure pelitic gneisses of Fraser Lakes zone B, Wollaston Domain, northern Saskatchewan, Canada: mineral compositions, metamorphic p-t-t path, and implications for the genesis of radioactive abyssal granitic pegmatites; Can. Mineral., v50, p1669-1694.

_____ (2012b): Radioactive abyssal granitic pegmatites and leucogranites in the Wollaston Domain, northern Saskatchewan, Canada: mineral compositions and conditions of emplacement in the Fraser Lakes area; Can. Mineral., v50, p1637-1667.

McKeough, M. and Lentz, D. (2011): Paleoproterozoic late-tectonic granitic pegmatite-hosted U-Th±REE-Y-Nb mineralization, northern Saskatchewan: products of assimilation, fractional crystallization, and hybridization processes; *in* Summary of Investigations 2011, Volume 2, Saskatchewan Geological Survey, Sask. Ministry of Energy and Resources, Misc. Rep. 2011-4.2, Paper A-6, 21p, <http://economy.gov.sk.ca/SOI2011V2_A6>, accessed 16 Jul 2014.

McKeough, M., Lentz, D., and Brown, J. (2010): Geology and associated pegmatite- and vein-hosted uranium mineralization of the Kulyk, Eagle, and Karin lakes regions, Wollaston Domain, northern Saskatchewan; *in* Summary of Investigations 2010, Volume 2, Saskatchewan Geological Survey, Sask. Ministry of Energy and Resources, Misc. Rep. 2010-4.2, Paper A-6, 23p, <http://economy.gov.sk.ca/SOI2010V2_A6>, accessed 16 Jul 2014.

McKeough, M., Lentz, D., and McFarlane, C. (2011a): U-Th-Nb-REE-Y vein dyke mineralization at Kulyk Lake, northern Saskatchewan: petrogenesis of an immiscible P-Fe melt from a late tectonic NYF-pegmatite; Sask. Ministry of the Economy, Saskatchewan Geological Survey Open House 2011, abstr. vol., p15.

_____ (2011b): U-Th-Nb-REE-Y vein dyke mineralization at Kulyk Lake, northern Saskatchewan: petrogenesis of an immiscible P-Fe melt from a late tectonic NYF-pegmatite; Sask. Ministry of the Economy, Saskatchewan Geological Survey Open House 2011, oral presentation, URL <http://www.er.gov.sk.ca/Default.aspx?DN=c2967cf2-5d1b-40f4-8d8f-94e75efb46e4>, accessed 27 Jan 2014.

McKeough, M.A., Lentz, D.R., McFarlane, C.R.M., and Brown, J. (2013): Geology and evolution of pegmatite-hosted U–Th ± REE–Y–Nb mineralization, Kulyk, Eagle, and Karin Lakes region, Wollaston Domain, northern Saskatchewan, Canada: examples of the dual role of extreme fractionation and hybridization processes; J. Geosci., v58, p321-346.

Mercadier, J. (2008): Conditions de Genèse des Gisements d'Uranium Associés aux Discordances Protérozoïques et Localisés dans les Socles. Exemple du Socle du Basin d'Athabasca (Saskatchewan, Canada); unpubl. Ph.D. thesis, Institut National Polytechnique de Lorraine, 362p.

Mercadier, J., Annesley, I.R., McKechnie, C.L., Bogdan, T.S., and Creighton, S. (2013): Magmatic and metamorphic uraninite mineralization in the western margin of the Trans-Hudson Orogen (Saskatchewan, Canada): a uranium source for unconformity-related uranium deposits?; Econ. Geol., v108, p1037-1065.

Mercadier, J., Cuney, M., Cathelineau, M., and Lacorde, M. (2011a): U redox fronts and kaolinisation in basement-hosted unconformity-related U ores of the Athabasca Basin (Canada): late U remobilisation by meteoric fluids; Mineral. Dep., v46, p105-135.

Mercadier, J., Cuney, M., Lach, P., Boiron, M-C., Bonhoure, J., Richard, A., Leisen, M., and Kister, P. (2011b): Origin of uranium deposits revealed by their rare earth element signature; Terra Nova, v23, p264-269.

Mercadier, J., Richard, A., Boiron, M-C., Cathelineau, M., and Cuney, M. (2010): Migration of brines in the basement rocks of the Athabasca Basin through microfracture networks (P-Patch U deposit, Canada); Lithos, v115, p121-136.

Mercadier, J., Richard, A., and Cathelineau, M. (2012): Boron- and magnesium-rich marine brines at the origin of giant unconformity-related uranium deposits: $\delta^{11}B$ evidence from Mg-tourmalines; Geol., v40, p231-234.

Migdisov, A.A., Reukov, V.V., and Williams-Jones, A.E. (2006): A spectrophotometric study of neodymium(III) complexation in sulfate solutions at elevated temperatures; Geochim. Cosmochim. Acta, v70, p983-992.

Migdisov, A.A. and Williams-Jones, A.E. (2008): A spectrophotometric study of Nd(III), Sm(III) and Er(III) complexation in sulfate-bearing solutions at elevated temperatures; Geochim. Cosmochim. Acta, v72, p5291-5303.

Miyawaki, R. and Nakai, I. (1996): Crystal chemical aspects of rare earth minerals; *in* Jones, A.P., Wall, F., and Williams, C.T. (eds), Rare Earth Minerals: Chemistry, Origin and Ore Deposits, Chapman & Hall, London, p29-30.

Mogilevsky, P. (2007): On the miscibility gap in monazite-xenotime systems; Physics Chem. Minerals, v34, p201-214.

Montel, J-M. (1993): A model for monazite/melt equilibrium and application to the generation of granitic magmas; Chem. Geol., v110, p127-146.

Morelli, R.M., Hartlaub, R.P., Ashton, K.E., and Ansdell, K.M. (2009): Evidence for enrichment of subcontinental lithospheric mantle from Paleoproterozoic intracratonic magmas: geochemistry and U-Pb geochronology of Martin Group igneous rocks, western Rae Craton, Canada; Precamb. Resear., v175, p1-15.

Muecke, G.K. and Moller, P. (1988): The not-so-rare earths; Sci. Amer., v258, p72-77.

Naumov, A.V. (2008): Review of the world market of rare-earth metals; Russ. J. Non-Ferrous Metals, v49, p14-22.

Nechaev, S.V., Gursky, D.S., Bakarzhiev, A.Kh., Voinovsky, A.S., Isakov, L.V., and Makivchuk, O.F. (2002): Deposits of uranium, rare and rare-earth metals in the Ukrainian shield; Mineral. J. (Ukraine), v24, p5-20.

Nechayev, S.V. and Kononov, Y.V. (1965): New genetic type of rare-earth mineralization in Precambrian migmatites of European USSR; Internat. Geol. Rev., v7, p638-641.

Neck, V., Altmaier, M., Müller, R., Bauer, A., Fanghänel, T., and Kim, J.I. (2003): Solubility of crystalline thorium dioxide; Radiochim. Acta, v91, p253-262.

Ng, R. (2012): Geochemical and mineralogical evolution of the McArthur River zone 4 unconformity-related uranium ore body and application of iron oxidation state in clay alteration as indicator of uranium mineralization; unpubl. M.Sc. thesis, Queen's Univ., Kingston, 207p.

Normand, C. (2010a): Bedrock geology of the Oshowy Lake–Buchanan Lake area and investigation of the REE mineralization potential in the Ena Lake, Bear Lake and Alces Lake areas; *in* Summary of Investigations 2010, Volume 2, Saskatchewan Geological Survey, Sask. Ministry of Energy and Resources, Misc. Rep. 2010-4.2, Paper A-3, 23p, URL <http://economy.gov.sk.ca/SOI2010V2_A3>, accessed 16 Jul 2014.

_____ (2010b): Bedrock geology of the Oshowy Lake, Buchanan Lake, Ena Lake, Bear Lake and Alces Lake areas (parts of NTS 74N16, 74O13 and 74N09); 1:10 000- and 1:20 000-scale prelim. maps *with* Summary of Investigations 2010, Volume 2, Saskatchewan Geological Survey, Sask. Ministry of Energy and Resources, Misc. Rep. 2010-4.2, URL <http://economy.gov.sk.ca/Default.aspx?DN=3a743b94-c5ca-426d-9dc7-44a28e058c9b>, accessed 16 Jul 2014.

_____ (2011a): Investigation of the REE mineralization potential in the Forget Lake and Archie Lake areas, Beaverlodge Domain; the Miller Lake area, Train Domain; and the Bompas Lake–Upper Eva Lake area, Tantato and Mudjatik domains; *in* Summary of Investigations 2011, Volume 2, Saskatchewan Geological Survey, Sask. Ministry of Energy and Resources, Misc. Rep. 2011-4.2, Paper A-2, 24p, URL <http://economy.gov.sk.ca/SOI2011V2_A2>, accessed 16 Jul 2014.

_____ (2011b): Bedrock geology of the Forget Lake, Archie Lake, Miller Lake, Bompas Lake and Upper Eva Lake areas (parts of NTS 74O/09, 74O/05, 74O/10 and 74P/10); 1:20 000 scale prelim. maps *with* Summary of Investigations 2011, Volume 2, Saskatchewan Geological Survey, Sask. Ministry of Energy and Resources, Misc. Rep. 2011-4.2, URL <http://economy.gov.sk.ca/Default.aspx?DN=451f54b0-06b4-4bed-b67b-f29d7b2f92d2>, accessed 16 Jul 2014.

_____ (2012): Bedrock geology of the Nevins Lake area, Beaverlodge Domain (part of NTS 74O12); 1:10 000-scale prelim. map *with* Summary of Investigations 2012, Volume 2, Saskatchewan Geological Survey, Sask. Ministry of the Economy, Misc. Rep. 2012-4.2, URL <http://economy.gov.sk.ca/Default.aspx?DN=ac1824a6-5970-4f43-b7dd-80038ed5df44>, accessed 16 Jul 2014.

_____ (2013): Bedrock geology of the Nevins Lake area, central Beaverlodge Domain, and investigations of REE distribution in the historic Nisto mine, southeastern Tantato Domain, and in historic mines in the Uranium City area, Beaverlodge and Zemlak domains; *in* Summary of Investigations 2012, Volume 2, Saskatchewan Geological Survey, Sask. Ministry of the Economy, Misc. Rep. 2012-4.2, Paper A-4, 24p, URL <http://economy.gov.sk.ca/SOI2012V2_A4>, accessed 16 Jul 2014.

Normand, C. and McEwan, B. (2009): Geology of the Hoidas Lake–Nisikkatch Lake area (part of NTS 74O/13); 1:20 000-scale prelim. map *with* Summary of Investigations 2009, Volume 2, Saskatchewan Geological Survey, Sask. Ministry of Energy and Resources, Misc. Rep. 2009-4.2, URL <http://economy.gov.sk.ca/Default.aspx?DN=d69da818-a514-4cfb-aada-5aeca6d61fd1>, accessed 16 Jul 2014.

Normand, C., McEwan, B., and Ashton, K.E., (2009): Geology and REE mineralization of the Hoidas Lake–Nisikkatch Lake area revisited; *in* Summary of Investigations 2009, Saskatchewan Geological Survey, Sask. Ministry of Energy and Resources, Misc. Rep. 2009-4.2, Paper A-3, 17p, URL <http://economy.gov.sk.ca/SOI2009V2_A3>, accessed 16 Jul 2014.

Northern Minerals Limited (2013): Browns Range project; Northern Minerals Limited, URL <http://www.northernminerals.com.au/projects/browns-range.html>, accessed 24 Feb 2014.

Oakes, M.C. (1938): A field test for phosphates; Econ. Geol., v33, p.454-457.

Oelkers, E.H. and Poitrasson, F. (2002): An experimental study of the dissolution stoichiometry and rates of a natural monazite as a function of temperature from 50° to 230°C and pH from 1.5 to 10; Chem. Geol., v191, p73-87.

Overstreet, W.C. (1967): The Geologic Occurrence of Monazite; U.S. Geol. Surv., Prof. Pap. 530, 337p.

Pagel, M., Pinte, G., and Rotach-Toulhoat, N. (1987): The rare earth elements in natural uranium oxides; Monogr. Ser. Min. Dep., v27, p81.

Pandur, K., Ansdell, K., Pearson, J., Harper, C., Halpin, K., Creighton, S., Kontak, D., and McFarlane, C. (2013a): The Hoidas Lake vein-type rare earth element deposit: zonation, alteration, fluid evolution, and age constraints; Sask. Ministry of the Economy, Saskatchewan Geological Survey Open House 2013, abstr. vol., p16.

_____ (2013b): The Hoidas Lake vein-type rare earth elements deposit: zonation, alteration, fluid evolution, and age constraints; Sask. Ministry of the Economy, Saskatchewan Geological Survey Open House 2011, oral presentation, URL <http://economy.gov.sk.ca/Technical%20Session%202%20Overviews,%20Industrial%20Minerals,%20and%20Rare%20Metals>, accessed 24 Feb 2014.

Papunen, H. and Lindsjö, O. (1972): Apatite, monazite and allanite: three rare earth minerals from Korsnäs, Finland; Bull. Geol. Soc. Finland, v44, p123-129.

Peiris, E.P.W. (1991): Geology, geochemistry and petrography of the uranium–precious metal mineralization in the Nicholson Bay and Fish Hook Bay area in northern Saskatchewan; unpubl. M.Sc. thesis, Univ. Regina, Regina, 259p.

Pekov, I.V., Agakhanov, A.A., Boldyreva, M.M., and Grishin, V.G. (2005): Pautovite, $CsFe_2S_3$, a new mineral species from the Lovozero alkaline complex, Kola Peninsula, Russia; Can. Mineral., v43, p965-972.

Penniston-Dorland, S.C. and Ferry, J.M. (2005): Coupled dichotomies of apatite and fluid composition during contact metamorphism of siliceous carbonate rocks; Amer. Mineral., v90, p1606-1618.

Perron, L. (1996): Cobalt; *in* Canadian Minerals Yearbook, 1996, p23.1-23.16.

Poitrasson, F. (2004): Contrasted monazite and allanite crystalline lattice responses under hydrothermal alteration; Amer. Geophys. U., Spring Meet. 2004, abstr V22A-01.

Pourtier, E., Devidal, J-L., and Gibert, F. (2010): Solubility measurements of synthetic neodymium monazite as a function of temperature at 2 kbars, and aqueous neodymium speciation in equilibrium with monazite; Geochim. Cosmochim. Acta, v74, p1872-1891.

Price, J.R., Velbel, M.A., and Patino, L.C. (2005): Allanite and epidote weathering at the Coweeta Hydrologic Laboratory, western North Carolina, U.S.A.; Amer. Mineral., v90, p101-114.

Putnis, A. (2009): Mineral replacement reactions; *in* Oelkers, E.H. and Schott, J. (eds.), Thermodynamics and Kinetics of Water-Rock Interaction, Rev. Mineral. Geochem., v70, p87-124.

Pyle, J.M., Spear, F.S., Rudnick, R.L., and McDonough, W.F. (2001): Monazite-xenotime-garnet equilibrium in metapelites and a new monazite-garnet thermometer; J. Petrol., v42, p2083-2107.

Quantum Rare Earth Developments Corp. (2010): Quantum commences 2010 exploration program at the Archie Lake property; Quantum Rare Earth Developments Corp., press release, 6 Jul 2010, URL <http://www.quantumrareearth.com/index.php/press-releases/56-quantum-commences-2010-exploration-program-at-the-archie-lake-property>, accessed 16 Jul 2014.

_____ (2011): Quantum samples 3.32% TREO and confirms zones of parallel mineralization at Archie Lake; Quantum Rare Earth Developments Corp., press release, 16 Feb 2011, URL <http://www.marketwired.com/press-release/Geologix-Adopts-Shareholder-Rights-Plan-TSX-GIX-1565928.htm>, accessed 26 Feb 2014.

Quantum Resources Limited (2013): Gardner Range project: uranium-REE-gold-base metals; Quantum Resources Limited, URL <http://www.qur.com.au/gardnerrange/>, accessed 24 Feb 2014.

Quirt, D.H. (1992): Nepheline syenite from Lyle Lake, Peter Lake Domain; *in* Summary of Investigations 1992, Saskatchewan Geological Survey, Sask. Energy and Mines, Misc. Rep. 92-4, p158-167.

Quirt, D.H., Kotzer, T., and Kyser, T.K. (1991): Tourmaline, phosphate minerals, zircon and pitchblende in the Athabasca Group: Maw zone and McArthur River areas, Saskatchewan; *in* Summary of Investigations 1991, Saskatchewan Geological Survey, Sask. Energy and Mines, Misc. Rep. 91-4, p181-191.

Raade, G. (2003): Scandium; Chem. Eng. News, v81, p68.

Raade, G., Ferraris, G., Gula, A., Ivaldi, G., and Bernhard, F. (2002): Kristiansenite, a new calcium-scandium-tin sorosilicate from granite pegmatite in Tørdal, Telemark, Norway; Mineral. Petrol., v75, p89-99.

Ramaekers, P. (1980): Stratigraphy and tectonic history of the Athabasca Group (Helikian) of northern Saskatchewan; *in* Summary of Investigations 1991, Saskatchewan Geological Survey, Sask. Energy and Mines, Misc. Rep. 80-4, p99-106.

_____ (1990): Geology of the Athabasca Group (Helikian) in Northern Saskatchewan; Sask. Energy and Mines, Rep. 195, 49p.

Rao, A.T. (1976): Study of the apatite-magnetite veins near Kasipatnam, Visakhapatnam District, Andhra Pradesh, India; TMPM Tscher. Mineral. Petrograph. Mitteil., v23, p87-103.

Rare Earth Minerals PLC (2011): Follow-up rare earth samples from Canada; Rare Earth Minerals PLC, press release, 24 October 2011, URL <http://www.rareearthmineralsplc.com/index.php/news-detail/?rnsid=11013516>, accessed 16 Jul 2014.

Razafymahatratra, D. and Montel, J.M. (2011): La monazite des chaînes Anosyennes (S-E Madagascar): des gisements en place aux sables de plages à ilménite-zircon-monazite; Journées SGF dédiées à la Géologie et Métallogénie de Madagascar, 6 et 7 Décembre 2011, Société Géologique de France, 77 rue Claude Bernard, Paris.

Reed, G.C. (2013): Olserum REE deposit, southern Sweden; NI 43-101–compliant technical report prepared by Reed Leyton Consulting for Tasman Metals Limited, 84p.

Reyx, J. and Ruhlmann, F. (1993): Étude métallographique des différentes associations minérales et caractérisation chimique des minéraux uranifères du gisement de Cigar Lake (Saskatchewan, Canada); Can. J. Earth Sci., v30, p705-719.

Richard, A., Pettke, T., Cathelineau, M., Boiron, M-C., Mercadier, J., Cuney, M., and Derome, D. (2010): Brine-rock interaction in the Athabasca basement (McArthur River U deposit, Canada): consequences for fluid chemistry and uranium uptake; Terra Nova, v22, p303-308.

Richard, A., Rozsypal, C., Mercadier, J., Banks, D.A., Cuney, M., Boiron, M-C., and Cathelineau, M. (2011): Giant uranium deposits formed from exceptionally uranium-rich acidic brines; Nature Geosci., v5, p142-146.

Robinson, S.C. (1955): Mineralogy of Uranium Deposits, Goldfields, Saskatchewan; Geol. Surv. Can., Bull. 31, 128p.

Rogers, M.C. and Hart, C.N. (1995): Procedural guidelines for qualitative mineral potential evaluations by the Ontario Geological Survey; Ont. Geol. Surv., Open File Rep. 5929, 38p.

Rose, N.M. (1991): Dissolution rates of prehnite, epidote, and albite; Geochim. Cosmochim. Acta, v55, p3273-3286.

Rosenblum, S. and Mosier, E.L. (1983): Mineralogy and Occurrence of Europium-Rich Dark Monazite; U.S. Geol. Surv., Prof. Pap. 1181, 67p.

Rowe, R.B. (1958): Niobium (Columbium) Deposits of Canada; Geol. Surv. Can., Econ. Geol. Ser., no18, 108p.

Rudnick, R. L. and Gao, S. (2003): The composition of the continental crust; *in* Rudnick, R.L., Holland, H.D., and Turekian K.K. (eds.), Treatise on Geochemistry, Volume 3, Elsevier, Philadelphia, p1-64.

Sankaran, A.V., Bhattacharyya, T.K., and Dar, K.K. (1970): Rare-earths and other trace elements in uraninites; Geol. Soc. India J., v11, p205-216.

Sassano, G.P., Fritz, P., and Morton, R.D. (1972): Paragenesis and isotopic composition of some gangue minerals from the uranium deposits of Eldorado, Saskatchewan; Can. J. Earth Sci., v9, p141-157.

Sassier, C., Boulvais, P., Gapais, D., Capdevila, R., and Diot, H. (2006): From granitoid to kyanite-bearing micaschist during fluid-assisted shearing (Ile d'Yeu, France); Internat. J. Earth Sci. / Geolog. Rund., v95, p2-18.

Saucier, G., Roy, A., Casgrain, P., Côté, P., Thomassin, Y., Bilodeau, M., Cannus, Y., and Hayden, A. (2012): Preliminary Economic Assessment Study for Kipawa Project; NI 43-101 Report, Roche's Ref.: 061623.001-200, submitted to Matamec Explorations Inc., 162p.

Schaller, W.T. (1933): A large monazite crystal from North Carolina; Amer. Mineral., v18, p435-439.

Schaltegger, U., Pettke, T., Audetat, A., Reusser, E., and Heinrich, C.A. (2005): Magmatic-to-hydrothermal crystallization in the W-Sn mineralized Mole Granite (NSW, Australia), Part I: crystallization of zircon and REE-phosphates over three million years—a geochemical and U-Pb geochronological study; Chem. Geol., v220, p215-235.

Schandl, E.S. and Gorton, M.P. (2004): A textural and geochemical guide to the identification of hydrothermal monazite: criteria for selection of samples for dating epigenetic hydrothermal ore deposits; Econ. Geol., v99, p1027-1035.

Schneider, D.A., Heizler, M.T., Bickford, M.E., Wortman, G.L., Condie, K.C., and Perilli, S. (2007): Timing constraints of orogeny to cratonization: thermochronology of the Paleoproterozoic Trans-Hudson Orogen, Manitoba and Saskatchewan, Canada; Precamb. Resear., v153, p65-95.

Schwab, R.G., Gotz, C., Herold, H., and Oliveira, N.P. (1993): Compounds of the crandallite type—thermodynamic properties of Ca-phosphates, Sr-phosphates, Ba-phosphates, Pb-phosphates, La-phosphates, Ce-phosphates to Gd-phosphates and Ca-arsenates, Sr-arsenates, Ba-arsenates, Pb-arsenates, La-arsenates, Ce-arsenate; Neues Jahrb. Mineral. Monatsh., v12, p551-568.

Scott, P.W., Pascoe, R.D., and Hart, F.W. (1998): Columbite-tantalite, rutile and other accessory minerals from the St. Austell topaz granite, Cornwall; Proc. Ussher Soc., v9, pt3, p165-170.

Segalstad, T.V. and Raade, G. (2003): Scandium mineralizations in southern Norway—geological background for the field trip; Norsk Geol. Foren., Abstr. and Proc., no2, p57-86.

Shannon, R.D. (1976): Revised effective ionic radii and systematic studies of interatomic distances in halides and chalcogenides; Acta Cristallograph., A32, p751-767.

Shawe, D.R. (1976): Geology and Resources of Fluorine in the United States; U.S. Geol. Surv., Prof. Pap. 933, 99p.

Shchekina, T.I., Gramenitskiy, E.N., and Alferyeva, Ya.O. (2013): Leucocratic magmatic melts with the maximum fluorine concentrations: experiment and relations in nature; Petrol., v21, p454-470.

Shimazaki, H., Yang, Z., Miyawaki, R., and Shigeoka, M. (2007): Scandium-bearing minerals in the Bayan Obo Nb-REE-Fe deposit, Inner Mongolia, China; Resour. Geol., v58, p80-86.

Shkol'nikov, E.V. (2009): Thermodynamic characterization of the amphoterism of hydroxides and oxides of scandium subgroup elements in aqueous media; Russ. J. Appl. Chem., v82, p2098-2104.

Shubat, M.A. (1988): Scandium-Bearing Aluminium Phosphate Deposits of Utah; Utah Geol. Miner. Surv., Rep. of Invest. 209, 26p.

Shuller, L.C., Ewing, R.C., and Becker, U. (2011): Thermodynamic properties of $Th_xU_{1-x}O_2$ ($0 < x < 1$) based on quantum-mechanical calculations and Monte-Carlo simulations; J. Nucl. Mater., v412, p13-21.

Sibbald, T.I.I. (1988): Nicholson Bay uranium-gold-platinum group element deposit studies; *in* Summary of Investigations 1988; Saskatchewan Geological Survey, Sask. Energy and Mines, Misc. Rep. 88-4, p77-81.

Sibbald, T.I.I., Quirt, D.H., and Gracie, A.J. (1991): Uranium deposits of the Athabasca Basin, Saskatchewan (Field Trip 11); 8th IAGOD Symposium Field Trip Guidebook, Geol. Surv. Can., Open File 2166, 56p.

Siegfried, P. And Hall, M. (2012): NI 43-101 technical report and Mineral Resource estimate for area 4 of the Lofdal Rare Earth Element (REE) Project, Khorixas District, Republic of Namibia; prepared by The MSA Group (Pty) Ltd for Namibia Rare Earths Inc., 99p.

Skora, S. and Blundy, J. (2012): Monazite solubility in hydrous silicic melts at high pressure conditions relevant to subduction zone metamorphism; Earth Planet. Sci. Lett., v321-322, p104-114.

Smith, D.L. and Cathro, M.S. (2010): Technical report on the Archie Lake property north-west Saskatchewan; submitted to Butler Resource Corp., February 9, 2010, 52p, URL <http://www.sedar.com> (NioCorp Developments Ltd., 25 Feb 2010), accessed 27 Jan 2014.

Smyth, J.R., Jacobsen, S.D., and Hazen, R.M. (2000): Comparative crystal chemistry of dense oxide minerals; *in* Hazen, R.M. and Downs, R.T. (eds.), High-Temperature and High-Pressure Crystal Chemistry, Rev. Mineral. Geochem., v41, p157-186.

Snoke, A.W., McKee, E.H., and Stern, T.W. (1979) Plutonic, metamorphic and structural chronology in the northern Ruby Mountains, Nevada: a preliminary report; Geol. Soc. Amer., Abstr. Prog., v11, p520-521.

Sørensen, H. (1997): The agpaitic rocks—an overview; Mineral. Mag., v61, p485-498.

Sørensen, H. and Larsen, L.M. (2001): The hyper-agpaitic stage in the evolution of the Ilímaussaq alkaline complex, South Greenland; Geol. Greenland Surv., Bull. 190, p83-94.

Spear, F.S. and Pyle, J.M. (2002): Apatite, monazite, and xenotime in metamorphic rocks; *in* Kohn, M. L., Rakovan, J., and Hughes, J.M. (eds.),Phosphates: Geochemical, Geobiological, and Materials Importance, Rev. Mineral. Geochem., v48, p293-335.

_____ (2010): Theoretical modeling of monazite growth in a low-Ca metapelite; Chem. Geol., v273, p111-119.

Speight, J.G. (2005): Lange's Handbook of Chemistry (Sixteenth Edition); McGraw-Hill, London.

SPI Supplies® (2014): Monazite, Kulyk Lake, Saskatchewan, Canada; SPI Supplies®, Microanalysis Standard AS1240-AB andAS1245-AB, URL <http://www.2spi.com/catalog/standards/aweb/minerals/as124.shtml>, accessed 21 Feb 2014.

Svensen, H., Jamtveit, B., Banks, D.A., and Austrheim, H. (2001): Halogen contents of eclogite facies fluid inclusions and minerals: Caledonides, western Norway; J. Metamor. Geol., v19, p165-178.

Sverjensky, D.A. (1984): Europium redox equilibria in aqueous solution; Earth Planet. Sci. Lett., v67, p70-78.

Sverjensky, D.A., Shock, E.L., and Helgeson, H.C. (1997): Prediction of the thermodynamic properties of aqueous metal complexes to 1000°C and 5 kb; Geochim. Cosmochim. Acta, v61, p1359-1412.

Tao, F., Yuzhuo, Q., and Xiuhua, Q. (1996): Carbon and oxygen isotopic characteristics of REE-fluorocarbonate minerals and their genetic implications, Bayan Obo deposit, Inner Mongolia, China; Chin. J. Geochem., v15, p82-86.

Tarkhanov, A., Kulayev, A., Petrin, A., and Kozyr'kov, V. (1992): The Zheltorechensk vanadium-scandium deposit; Internat. Geol. Rev., v34, p496-502.

Teufel, S. and Heinrich, W. (1997): Partial resetting of the U-Pb isotope system in monazite through hydrothermal experiments: an SEM and U-Pb isotope study; Chem. Geol., v137, p273-281.

Tice, P. (2009): Mineralogy of eudialyte group minerals from the East Hill suite of the Mont Saint-Hilaire alkaline plutonic complex, including an alternative site-assignment algorithm and a proposed classification system; unpubl. M.Sc. thesis, Univ. New Orleans, New Orleans, 162p.

Tin, Q.D. (2007): Experimental studies on the behaviour of rare earth elements and tin in granitic systems; Ph.D. thesis, Instit. Geosci., Univ. Tuebingen, Tuebingen, 119p.

Touret, J.L.R. and Huizenga, J.-M. (2011): Fluids in granulites; *in* van Reenen, D.D., Kramers, J.D., McCourt, S., and Perchuk, L.L. (eds.), Origin and Evolution of Precambrian High-Grade Gneiss Terranes, with Special Emphasis on the Limpopo Complex of Southern Africa, Geol. Soc. Amer., Mem. 207, p25-37.

Tremblay, L.P. (1978): Geological setting of the Beaverlodge type of vein-uranium deposits and its comparison to that of the unconformity type; *in* Kimberley, M.M. (ed.), Uranium Deposits: Their Mineralogy and Origin, Mineral. Assoc. Can., Short Courses, v3, p431-456.

Tropper, P., Manning, C.E., and Harlov, D.E. (2011): Solubility of $CePO_4$ monazite and YPO_4 xenotime in H_2O and H_2O-NaCl at 800°C and 1 GPa: implications for REE and Y transport during high-grade metamorphism; Chem. Geol., v282, p58-66.

_____ (2013): Experimental determination of $CePO_4$ and YPO_4 solubilities in H_2O-NaF at 800°C and 1 GPa: implications for rare earth element transport in high-grade metamorphic fluids; Geofluids, v13, p372-380, doi:10.1111/gfl.12031.

Uranium City Resources Inc. (2005): Uranium City Resources (UCR: TSX-V) announces results from Eagle Lake uranium project, Uranium City mining district, northern Saskatchewan; Uranium City Resources Inc., press release, 2 Nov 2005.

Vallini, D.A. (2006): The formation of authigenic xenotime in Proterozoic sedimentary basins: petrography, age and geochemistry; unpubl. Ph.D. thesis, Univ. West. Australia, Crawley.

Van Huet, S., Jannink, A., Purcell, D.C., and Rangott, M. (2010): NI 43-101technical report on the Nyngan Gilgai scandium project, Jervois Mining Limited, Nyngan, New South Wales, Australia; NI 43-101–compliant technical report prepared for EMC Metals Corp. and Jervois Mining Limited, 50p, URL <http://www.sedar.com>, accessed 27 Jan 2014.

Vidale, R. (1983): Pore solution compositions in a pelitic system at high temperatures, pressures, and salinities; Amer. J. Sci., v283-A, p298-313.

Wallis, R.H., Saracoglu, N., Brummer, J.J., and Golightly, J.P. (1983): Geology of the McClean uranium deposits; *in* Cameron, E.M. (ed.), Uranium Exploration in Athabasca Basin, Saskatchewan, Canada, Geol. Surv. Can., Pap. 82-11, p71-110.

Walters, A. and Lusty, P. (2010): Rare Earth Elements; Brit. Geol. Surv., Commod. Prof., 45p.

Wardrop Engineering Inc. (2006): Technical report on the Hoidas Lake rare earth project, Saskatchewan; Wardrop Engineering Inc., Project 0539480100-REP-L0001-01, 69p URL <http://www.sedar.com> (Great Western Minerals Group Ltd., 29 Mar 2006), accessed 27 Jan 2014.

Watkinson, D.H. and Mainwaring, P.R. (1976): The Kulyk Lake monazite deposit, northern Saskatchewan; Can. J. Earth Sci., v13, p470-475.

Weill, D.F. and Drake, M.J. (1973): Europium anomaly in plagioclase feldspar: experimental results and semiquantitative model; Sci., v180, p1059-1060.

Whitney, D.L. and Evans, B.W. (2010): Abbreviations for names of rock-forming minerals; Amer. Mineral., v95, p185-187.

Williams-Jones, A.E., Migdisov, A.A., and Samson, I.M. (2012): Hydrothermal mobilisation of the rare earth elements—a tale of "ceria" and "yttria"; Elements, v8, p355-360.

Wing, B.A., Ferry, J.M., and Harrison, T.M. (2003): Prograde destruction and formation of monazite and allanite during contact and regional metamorphism of pelites: petrology and geochronology; Contrib. Mineral. Petrol., v145, p228-250.

Wise, M.A., Černý, P., and Falster, A.U. (1998): Scandium substitution in columbite-group minerals and ixiolite; Can. Mineral., v36, p673-680.

Wood, S.A. (1990): The aqueous geochemistry of the rare-earth elements and yttrium, 2: theoretical predictions of speciation in hydrothermal solutions to 350°C at saturation water vapor pressure; Chem. Geol., v88, p99-125.

_____ (2004): The hydrothermal geochemistry of the rare earth elements; The Gangue, no81, p1, 5-7.

Wood, S.A. and Samson, I.M. (2006): The aqueous geochemistry of gallium, germanium, indium and scandium; Ore Geol. Rev., v28, p57-102.

Woolley, A.R. and Kjarsgaard, B.A. (2008): Carbonatite occurrences of the world: map and database; Geol. Surv. Can., Open File 5796, 28p and 1 map, URL <http://geoscan.nrcan.gc.ca/starweb/geoscan/servlet.starweb?path=geoscan/downloade.web&search1=R=225115>, accessed 16 Jul 2014.

Wülser, P-A. (2009): Uranium metallogeny in the North Flinders Ranges region of South Australia; unpubl. Ph.D. thesis, Adelaide Univ., Adelaide, 179p.

Yakovenchuk, V.N., Pakhomovsky, Y.A., Men'shikov, Y.P., Ivanyuk, G.Y., Krivovichev, S.V., and Burns, P.C. (2003): Chlorbartonite, $K_6Fe_{24}S_{26}(Cl, S)$, a new mineral species from a hydrothermal vein in the Khibina massif, Kola Peninsula, Russia: description and crystal structure; Can. Mineral., v41, p503-511.

Yardley, B.W.D. (2013): The chemical composition of metasomatic fluids in the crust; *in* Metasomatism and the Chemical Transformation of Rock (Chapter 2 of Lecture Notes in Earth System Sciences), Springer-Verlag, Berlin-Heidelberg, p17-51.

Yeo, G.M. and Delaney, G., (2007): The Wollaston Supergroup, stratigraphy and metallogeny of a Paleoproterozoic Wilson cycle in the Trans-Hudson Orogeny, Saskatchewan; *in* Jefferson, C.W. and Delaney, G. (eds.), EXTECH IV: Geology and Uranium EXploration TECHnology of the Proterozoic Athabasca Basin, Saskatchewan and Alberta, Geol. Surv. Can., Bull. 588, p89-117 (*also* Saskatchewan Geological Society, Special Publication 17; Geological Association of Canada, Mineral Deposits Division, Special Publication 4).

Young, E.J. and Sims, P.K. (1961): Petrography and Origin of Xenotime and Monazite Concentrations, Central City District, Colorado; U.S. Geol. Surv., Bull. 1032-F, 38p.

Ziemann, M.A., Förster, H-J., Harlov, D., and Frei, D. (2005): Origin of fluorapatite-monazite assemblages in a metamorphosed, sillimanite-bearing pegmatoid, Reinbolt Hills, East Antarctica; Euro. J. Mineral., v17, p567-579.

Appendix I – Results of Zircon and Titanite U-Pb Isotopic Dating, Hoidas Lake and Bear Lake Allanite+Apatite–rich REE Mineralization

Laser-ablation inductively coupled plasma–mass spectrometry (LA-ICP-MS) was used to obtain crystallization ages of large zircon and titanite crystals in samples taken from the Hoidas Lake and Bear Lake allanite+apatite–rich REE mineralization (Normand, 2009, 2010a). Analytical work was performed by Andrew Dufrane at the Radiogenic Isotope Facility of the University of Alberta. Results are presented below.

Results of Zircon U-Pb Isotopic Dating, Hoidas Lake REE Deposit

Recent reanalysis of a large, euhedral zircon crystal from Hoidas Lake produced a slightly discordant $^{207}Pb/^{235}U$–$^{206}Pb/^{238}U$ age of 2311 ±6.6 Ma (calculated with lower intercept set at 0.0 Ma) on surfaces relatively clean from common Pb contamination (Table AI-1, Figure AI-1A). This age is virtually identical to the mean $^{207}Pb/^{206}Pb$ age of 2311 ±6.5 Ma (Figure AI-1B and C) calculated from the same analyses and similar to a previously obtained age of 2290 ±7 Ma on the same crystal (Normand, 2010a). Consistency between $^{207}Pb/^{235}U$–$^{206}Pb/^{238}U$ and $^{207}Pb/^{206}Pb$ ages suggests minimal or no Pb loss. See the "Allanite (±Apatite)–Dominant Mineralization (Saskatchewan Mineral Deposit Model A-22)" section of this report and Normand (2010a) for a description of the zircon occurrence and interpretation of the results.

Results of Zircon and Titanite U-Pb Isotopic Dating, Bear Lake Allanite+Apatite–Rich REE Occurrence

Preliminary U-Pb LA-ICP-MS isotopic analyses of zircon and titanite from the Bear Lake allanite+apatite occurrence (Normand, 2010a) were obtained to verify age relationships between the occurrence and similar mineralization at Hoidas Lake. The sample used for this purpose was composed mainly of primary titanite and apatite (approximately 50 and 14 wt. %, respectively, based on bulk-rock analysis of sample 10CN326-1; Normand, 2010a, Table 2) associated with lesser proportions of primary calcic amphibole and allanite, and traces of zircon. Titanite and apatite crystals are euhedral to subhedral and coarse-grained (up to 15 mm and 3 mm in diameter, respectively), and zircon crystals are euhedral, prismatic and measure <800 µm in length. The crystals were deformed during a late brittle episode, accompanied by the formation of paragenetically late allanite-epidote, quartz, calcite, and fluorite. Under the polarizing microscope, deformation textures in titanite correspond to localized mottled zones.

Isotopic data, obtained from LA-ICP-MA analysis of the material described above (300 µm thick polished section), are presented in Tables AI-2 and AI-3. U-Pb isotopic data for zircon (Table I-2) show a wide scatter on the concordia diagram presented on Figure AI-2A, with a subset showing well-defined discordant age intercepts of 9 ±79 and 1848 ±20 Ma (Figure AI-2B). The most prominent population of $^{207}Pb/^{206}Pb$ ages presented on the relative-probability plot in Figure I-2c corresponds closely to the upper intercept $^{207}Pb/^{235}U$–$^{206}Pb/^{238}U$ age of 1848 ±20 Ma for the same zircon population. This age may correspond to the time during which the paragenetically late allanite-epidote, quartz, calcite and fluorite assemblage formed, and, within error, may correspond to formation of monazite (1870 Ma U-Pb SHRIMP age; Gunning and Card, 2005), tentatively interpreted here to have taken place during an episode of apatite recrystallization at Hoidas Lake.

U-Pb isotopic data for titanite (Table AI-3) concentrate into two discordant populations on the concordia diagram presented on Figure AI-3A. The older discordant population gives lower and upper intercept $^{207}Pb/^{235}U$–$^{206}Pb/^{238}U$ ages of 511 ±320 Ma and 2383 ±32 Ma, respectively (Figure AI-3B), and the calculated mean $^{207}Pb/^{206}Pb$ age for this population is 2342 ±22 Ma. The younger discordant population gives lower and upper intercept $^{207}Pb/^{235}U$–$^{206}Pb/^{238}U$ ages of 407 ±490 Ma and 1910 ±37 Ma, respectively (Figure AI-3C), and the calculated mean $^{207}Pb/^{206}Pb$ age for this population is 1889 ±10 Ma. The younger discordant age population may represent new titanite growth from which Pb was subsequently lost, or could represent a disturbance of the U-Pb system in older grains.

Although, within the quoted errors, the U-Pb age obtained on zircon from Hoidas Lake and an older U-Pb age obtained on titanite from the Bear Lake occurrence may differ by 47 to 111 m.y., these ages suggest that allanite mineralization at both localities may have formed earlier than has been suggested by Gunning and Card (2005) and Pandur *et al.* (2013a, 2013b), and possibly just following peak Arrowsmith metamorphism, dated at 2.37 to 2.34 Ga in the Northwest Territories (Berman *et al.*, 2013). Veins at both localities cut hostrocks displaying penetrative

Table AI-1 – Hoidas Lake zircon U-Pb isotopic data.

Not common Pb corrected

Sample	^{206}Pb (cps)	^{204}Pb (cps)	$^{207}Pb/^{206}Pb$	2σ	$^{207}Pb/^{235}U$	2σ	$^{206}Pb/^{238}U$	2σ	ρ	$^{207}Pb^*/^{206}Pb^*$ age (Ma)	2σ error (Ma)	$^{207}Pb^*/^{235}U$ age (Ma)	2σ error (Ma)	$^{206}Pb^*/^{238}U$ age (Ma)	2σ error (Ma)	Discordance (%)	$^{238}U/^{206}Pb$	2σ	$^{207}Pb/^{206}Pb$	2σ
Standard																				
OG1-1	590428	128	0.29684	0.00440	28.84601	1.50526	0.70480	0.03526	0.959	3454	23	3448	50	3439	132	0.6	1.419	0.071	0.297	0.004
OG1-2	599263	88	0.29635	0.00443	29.72165	1.57663	0.72739	0.03702	0.959	3451	23	3478	51	3524	137	-2.7	1.375	0.070	0.296	0.004
OG1-3	466007	70	0.29576	0.00438	28.97425	1.47309	0.71051	0.03456	0.957	3448	23	3453	49	3460	129	-0.5	1.407	0.068	0.296	0.004
OG1-4	528516	53	0.29694	0.00440	28.91351	1.33616	0.70621	0.03091	0.947	3454	23	3451	44	3444	116	0.4	1.416	0.062	0.297	0.004
OG1-5	560241	33	0.29603	0.00441	28.88567	1.18824	0.70768	0.02713	0.932	3450	23	3450	40	3450	102	0.0	1.413	0.054	0.296	0.004
OG1-6	542528	112	0.29680	0.00441	28.88165	1.57870	0.70576	0.03712	0.962	3454	23	3450	52	3442	139	0.4	1.417	0.075	0.297	0.004
09CN101-1-1																				
RPT3	998280	9	0.14704	0.00219	9.07415	0.33654	0.44758	0.01520	0.915	2312	25	2346	33	2384	67	-3.8	2.234	0.076	0.147	0.002
RPT4	818820	12	0.14674	0.00219	8.89611	0.67618	0.43971	0.03277	0.981	2308	25	2327	67	2349	145	-2.1	2.274	0.170	0.147	0.002
RPT5	785453	13	0.14735	0.00219	9.37697	0.55871	0.46153	0.02663	0.968	2315	25	2376	53	2446	116	-6.8	2.167	0.125	0.147	0.002
RPT9	838811	21	0.14684	0.00220	8.71938	0.55228	0.43067	0.02651	0.972	2309	25	2309	56	2309	118	0.0	2.322	0.143	0.147	0.002
RPT6	768594	26	0.14681	0.00220	9.49964	0.48257	0.46929	0.02278	0.956	2309	25	2388	46	2480	99	-8.9	2.131	0.103	0.147	0.002
RPT2	869988	27	0.14749	0.00219	9.32830	0.51080	0.45872	0.02417	0.962	2317	25	2371	49	2434	106	-6.1	2.180	0.115	0.147	0.002
RPT10	892224	35	0.14627	0.00219	8.80567	0.44570	0.43662	0.02111	0.955	2303	26	2318	45	2336	94	-1.7	2.290	0.111	0.146	0.002
RPT8	644171	61	0.14513	0.00217	8.92714	0.52476	0.44612	0.02536	0.967	2289	26	2331	52	2378	112	-4.6	2.242	0.127	0.145	0.002
RPT1	888707	80	0.14678	0.00220	9.40038	0.48642	0.46450	0.02301	0.957	2309	25	2378	46	2459	100	-7.9	2.153	0.107	0.147	0.002
RPT15	809397	102	0.14868	0.00222	8.88224	0.43434	0.43329	0.02017	0.952	2331	25	2326	44	2321	90	0.5	2.308	0.107	0.149	0.002
RPT14	771732	112	0.14792	0.00221	8.85760	0.54254	0.43429	0.02580	0.970	2322	25	2323	54	2325	115	-0.2	2.303	0.137	0.148	0.002
RPT16	763969	128	0.14714	0.00221	8.91762	0.53166	0.43955	0.02536	0.968	2313	26	2330	53	2349	113	-1.8	2.275	0.131	0.147	0.002
RPT7	585493	147	0.14534	0.00232	8.96486	0.57720	0.44737	0.02791	0.969	2292	27	2334	57	2384	123	-4.8	2.235	0.139	0.145	0.002
RPT17	804090	165	0.14609	0.00222	8.64215	0.80380	0.42904	0.03937	0.987	2301	26	2301	81	2301	175	0.0	2.331	0.214	0.146	0.002
RPT13	807956	188	0.14913	0.00235	8.95026	0.43586	0.43528	0.02006	0.946	2336	27	2333	44	2329	89	0.3	2.297	0.106	0.149	0.002
NOT USED FOR AGE CALCULATIONS (PROBABLY Pb LOSS)																				
RPT18	818346	154	0.14353	0.00219	8.29970	0.45734	0.41938	0.02220	0.961	2270	26	2264	49	2258	100	0.7	2.384	0.126	0.144	0.002
RPT19	810918	157	0.13664	0.00211	7.42420	0.51884	0.39406	0.02686	0.975	2185	27	2164	61	2142	123	2.3	2.538	0.173	0.137	0.002
RPT11	613306	140	0.14330	0.00229	8.22538	0.44019	0.41629	0.02126	0.954	2268	27	2256	47	2244	96	1.2	2.402	0.123	0.143	0.002
CULLED (HIGH COMMON Pb)																				
~~RPT20~~	~~928068~~	~~809~~	~~0.15167~~	~~0.00406~~	~~8.32568~~	~~0.61077~~	~~0.39812~~	~~0.02719~~	~~0.931~~	~~2365~~	~~45~~	~~2267~~	~~64~~	~~2160~~	~~124~~	~~10.2~~	~~2.512~~	~~0.172~~	~~0.152~~	~~0.004~~
~~RPT12~~	~~603944~~	~~1013~~	~~0.15810~~	~~0.00757~~	~~9.90651~~	~~0.89552~~	~~0.45445~~	~~0.03485~~	~~0.848~~	~~2435~~	~~79~~	~~2426~~	~~80~~	~~2415~~	~~153~~	~~1.0~~	~~2.200~~	~~0.169~~	~~0.158~~	~~0.008~~

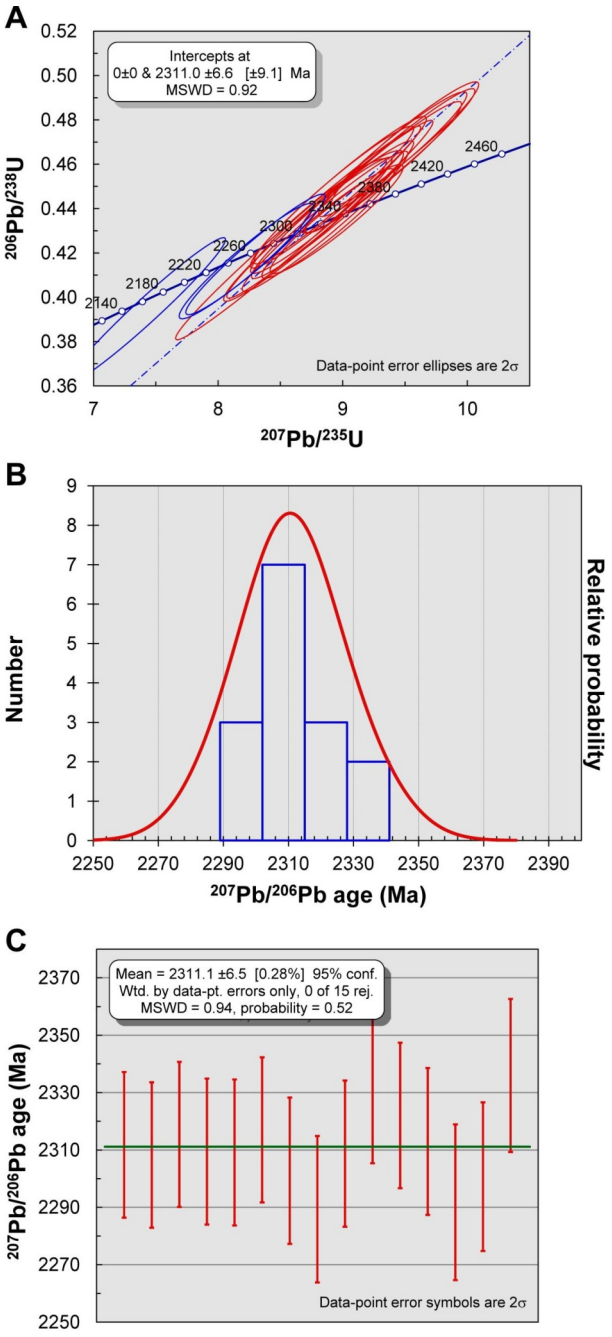

Figure AI-1 – Isotopic U-Pb LA-ICP-MS analytical results obtained on zircon from the Hoidas Lake REE deposit: A) U-Pb isotopic results shown on a concordia diagram; B) $^{207}Pb/^{206}Pb$ ages of the corresponding analyses shown on a relative probability plot; and C) $^{207}Pb/^{206}Pb$ ages of the corresponding analyses shown on an error-bar plot.

gneissosities that are traditionally assigned ages <1.94 Ga, based on similar rock fabrics and rock types occurring elsewhere in the same general area (Hartlaub, 2004; Ashton *et al.*, 2005, 2007a, 2007b, 2009, 2013; Hartlaub *et al.*, 2007; Bethune *et al.*, 2013). The possibility that the penetrative gneissosities at both localities might predate by a considerable margin Taltson events, and have been preserved and transposed at a later date parallel to regional structural grains, has not been evaluated in detail. Dating of deformation that produced gneissosities in rocks hosting the Hoidas Lake deposit and Bear Lake occurrence is critically needed to help shed light on these age discrepancies.

Table AI-2 – Bear Lake zircon U-Pb isotopic data.

Not common Pb corrected

Sample	^{206}Pb (cps)	^{204}Pb (cps)	^{207}Pb/^{206}Pb	2σ	^{207}Pb/^{235}U	2σ	^{206}Pb/^{238}U	2σ	ρ	^{207}Pb*/^{206}Pb* age (Ma)	2σ error (Ma)	^{207}Pb*/^{235}U age (Ma)	2σ error (Ma)	^{206}Pb*/^{238}U age (Ma)	2σ error (Ma)	Discordance (%)	^{238}U/^{206}Pb	2σ	^{207}Pb/^{206}Pb	2σ
Standard																				
OG1-1	493493	25	0.29708	0.00184	29.36182	1.40648	0.71682	0.03405	0.992	3455	10	3466	46	3484	127	-1.1	1.395	0.066	0.297	0.002
OG1-2	303195	10	0.29666	0.00180	28.71487	1.36592	0.70202	0.03312	0.992	3453	9	3444	46	3428	124	0.9	1.424	0.067	0.297	0.002
OG1-3	328665	14	0.29655	0.00180	29.01617	1.47837	0.70965	0.03590	0.993	3452	9	3454	49	3457	134	-0.2	1.409	0.071	0.297	0.002
OG1-4	467419	60	0.29860	0.00183	28.61252	1.33529	0.69498	0.03215	0.991	3463	9	3440	45	3402	121	2.3	1.439	0.067	0.299	0.002
10CN326-1.2																				
10CN3261.2-8D	229332	47	0.11024	0.00090	2.43257	0.17753	0.16004	0.01161	0.994	1803	15	1252	51	957	64	50.4	6.249	0.453	0.110	0.001
10CN3261.2-8C	273256	30	0.11131	0.00076	3.70258	0.20854	0.24125	0.01349	0.993	1821	12	1572	44	1393	70	26.1	4.145	0.232	0.111	0.001
10CN3261.2-5D	221478	40	0.11227	0.00084	3.10418	0.26231	0.20052	0.01688	0.996	1837	14	1434	63	1178	90	39.2	4.987	0.420	0.112	0.001
10CN3261.2-8E	278413	40	0.11257	0.00077	4.29673	0.32540	0.27684	0.02088	0.996	1841	12	1693	61	1575	105	16.3	3.612	0.272	0.113	0.001
10CN3261.2-5H	285602	39	0.11294	0.00104	2.58923	0.18189	0.16627	0.01158	0.991	1847	17	1298	50	992	64	49.9	6.014	0.419	0.113	0.001
10CN3261.2-5C	230882	35	0.11294	0.00083	2.52453	0.23608	0.16211	0.01511	0.997	1847	13	1279	66	969	83	51.1	6.169	0.575	0.113	0.001
10CN3261.2-8F	305807	45	0.11320	0.00077	4.76309	0.30687	0.30518	0.01955	0.994	1851	12	1778	53	1717	96	8.3	3.277	0.210	0.113	0.001
10CN3261.2-8H	264050	29	0.11379	0.00074	2.99076	0.21671	0.19063	0.01376	0.996	1861	12	1405	54	1125	74	43.0	5.246	0.379	0.114	0.001
10CN3261.2-8G	299142	46	0.11380	0.00074	4.42425	0.29573	0.28198	0.01876	0.995	1861	12	1717	54	1601	94	15.7	3.546	0.236	0.114	0.001
10CN3261.2-5B	296880	56	0.11908	0.00081	4.41790	0.28981	0.26909	0.01756	0.995	1942	12	1716	53	1536	89	23.5	3.716	0.242	0.119	0.001
10CN3261.2-5F	313405	36	0.12809	0.00098	4.62451	0.33012	0.26185	0.01858	0.994	2072	13	1754	58	1499	94	30.9	3.819	0.271	0.128	0.001
10CN3261.2-5G	264658	16	0.12836	0.00086	6.53067	0.46260	0.36899	0.02602	0.995	2076	12	2050	61	2025	121	2.9	2.710	0.191	0.128	0.001
10CN3261.2-3D	358514	82	0.12992	0.00100	3.70237	0.29472	0.20668	0.01637	0.995	2097	13	1572	62	1211	87	46.2	4.838	0.383	0.130	0.001
10CN3261.2-4E	570599	74	0.13355	0.00130	4.24566	0.30174	0.23057	0.01623	0.991	2145	17	1683	57	1337	84	41.6	4.337	0.305	0.134	0.001
10CN3261.2-2D	264654	68	0.13597	0.00164	4.38930	0.36614	0.23413	0.01933	0.989	2176	21	1710	67	1356	100	41.7	4.271	0.353	0.136	0.002
10CN3261.2-4D	560911	21	0.13672	0.00092	7.82356	0.51266	0.41501	0.02705	0.995	2186	12	2211	57	2238	122	-2.8	2.410	0.157	0.137	0.001
10CN3261.2-3B	341692	81	0.13921	0.00124	5.11502	0.50374	0.26648	0.02614	0.996	2217	15	1839	80	1523	132	35.1	3.753	0.368	0.139	0.001
10CN3261.2-5A	385258	51	0.13949	0.00091	4.44286	0.47374	0.23100	0.02459	0.998	2221	11	1720	85	1340	127	43.8	4.329	0.461	0.139	0.001
10CN3261.2-1B	654642	93	0.13982	0.00111	6.70245	0.42939	0.34767	0.02210	0.992	2225	14	2073	55	1923	105	15.7	2.876	0.183	0.140	0.001
10CN3261.2-4A	601112	85	0.14028	0.00104	4.98072	0.40704	0.25752	0.02096	0.996	2231	13	1816	67	1477	107	37.7	3.883	0.316	0.140	0.001
10CN3261.2-4B	422116	11	0.14358	0.00092	9.04554	0.62649	0.45692	0.03151	0.996	2271	11	2343	61	2426	138	-8.2	2.189	0.151	0.144	0.001
Culls																				
~~10CN3261.2-6A~~	~~744433~~	~~207~~	~~0.11352~~	~~0.00111~~	~~4.60120~~	~~0.35698~~	~~0.29397~~	~~0.02262~~	~~0.992~~	~~1856~~	~~18~~	~~1749~~	~~63~~	~~1661~~	~~112~~	~~11.9~~	~~3.402~~	~~0.262~~	~~0.114~~	~~0.001~~
~~10CN3261.2-6B~~	~~479717~~	~~168~~	~~0.09748~~	~~0.00129~~	~~1.30015~~	~~0.09995~~	~~0.09673~~	~~0.00732~~	~~0.985~~	~~1576~~	~~25~~	~~846~~	~~43~~	~~595~~	~~43~~	~~65.1~~	~~10.338~~	~~0.783~~	~~0.097~~	~~0.001~~
~~10CN3261.2-7A~~	~~573864~~	~~240~~	~~0.14574~~	~~0.00148~~	~~6.50491~~	~~0.60161~~	~~0.32372~~	~~0.02976~~	~~0.994~~	~~2297~~	~~17~~	~~2047~~	~~78~~	~~1808~~	~~143~~	~~24.4~~	~~3.089~~	~~0.284~~	~~0.146~~	~~0.001~~
~~10CN3261.2-7B~~	~~444838~~	~~396~~	~~0.10497~~	~~0.00164~~	~~3.68115~~	~~0.28749~~	~~0.25435~~	~~0.01946~~	~~0.980~~	~~1714~~	~~28~~	~~1567~~	~~61~~	~~1461~~	~~99~~	~~16.5~~	~~3.932~~	~~0.301~~	~~0.105~~	~~0.002~~
~~10CN3261.2-8A~~	~~324867~~	~~260~~	~~0.11015~~	~~0.00118~~	~~3.59308~~	~~0.24901~~	~~0.23657~~	~~0.01620~~	~~0.988~~	~~1802~~	~~19~~	~~1548~~	~~54~~	~~1369~~	~~84~~	~~26.6~~	~~4.227~~	~~0.289~~	~~0.110~~	~~0.001~~
~~10CN3261.2-8B~~	~~428367~~	~~220~~	~~0.11199~~	~~0.00083~~	~~4.17318~~	~~0.26882~~	~~0.27027~~	~~0.01729~~	~~0.993~~	~~1832~~	~~13~~	~~1669~~	~~51~~	~~1542~~	~~87~~	~~17.8~~	~~3.700~~	~~0.237~~	~~0.112~~	~~0.001~~
~~10CN3261.2-5E~~	~~557437~~	~~267~~	~~0.11453~~	~~0.00122~~	~~3.35745~~	~~0.29265~~	~~0.21261~~	~~0.01839~~	~~0.992~~	~~1873~~	~~19~~	~~1495~~	~~66~~	~~1243~~	~~97~~	~~36.9~~	~~4.704~~	~~0.407~~	~~0.115~~	~~0.001~~
~~10CN3261.2-4C~~	~~425663~~	~~157~~	~~0.12853~~	~~0.00145~~	~~4.35544~~	~~0.57331~~	~~0.24577~~	~~0.03223~~	~~0.996~~	~~2078~~	~~20~~	~~1704~~	~~103~~	~~1417~~	~~165~~	~~35.4~~	~~4.069~~	~~0.534~~	~~0.129~~	~~0.001~~
~~10CN3261.2-3C~~	~~478142~~	~~354~~	~~0.12435~~	~~0.00153~~	~~4.44842~~	~~0.27767~~	~~0.25946~~	~~0.01588~~	~~0.980~~	~~2020~~	~~22~~	~~1721~~	~~50~~	~~1487~~	~~81~~	~~29.5~~	~~3.854~~	~~0.236~~	~~0.124~~	~~0.002~~
~~10CN3261.2-3A~~	~~575731~~	~~254~~	~~0.12108~~	~~0.00107~~	~~2.88521~~	~~0.20763~~	~~0.17283~~	~~0.01234~~	~~0.992~~	~~1972~~	~~16~~	~~1378~~	~~53~~	~~1028~~	~~67~~	~~51.7~~	~~5.786~~	~~0.413~~	~~0.121~~	~~0.001~~
~~10CN3261.2-1C~~	~~607586~~	~~174~~	~~0.14004~~	~~0.00112~~	~~8.23648~~	~~0.57787~~	~~0.42656~~	~~0.02973~~	~~0.993~~	~~2228~~	~~14~~	~~2257~~	~~62~~	~~2290~~	~~133~~	~~-3.3~~	~~2.344~~	~~0.163~~	~~0.140~~	~~0.001~~
~~10CN3261.2-2A~~	~~601721~~	~~139~~	~~0.14404~~	~~0.00127~~	~~8.05545~~	~~0.57650~~	~~0.40559~~	~~0.02881~~	~~0.992~~	~~2276~~	~~15~~	~~2237~~	~~63~~	~~2195~~	~~131~~	~~4.2~~	~~2.466~~	~~0.175~~	~~0.144~~	~~0.001~~
~~10CN3261.2-2B~~	~~570275~~	~~216~~	~~0.13230~~	~~0.00168~~	~~4.29835~~	~~0.31133~~	~~0.23564~~	~~0.01680~~	~~0.985~~	~~2129~~	~~22~~	~~1693~~	~~58~~	~~1364~~	~~87~~	~~39.8~~	~~4.244~~	~~0.303~~	~~0.132~~	~~0.002~~
~~10CN3261.2-2C~~	~~571632~~	~~151~~	~~0.12451~~	~~0.00271~~	~~3.57752~~	~~0.35111~~	~~0.20839~~	~~0.01994~~	~~0.975~~	~~2022~~	~~38~~	~~1545~~	~~75~~	~~1220~~	~~106~~	~~43.4~~	~~4.799~~	~~0.459~~	~~0.125~~	~~0.003~~
~~10CN3261.2-1A~~	~~875926~~	~~536~~	~~0.12079~~	~~0.00242~~	~~4.08456~~	~~0.37256~~	~~0.24526~~	~~0.02182~~	~~0.976~~	~~1968~~	~~35~~	~~1651~~	~~72~~	~~1414~~	~~112~~	~~31.3~~	~~4.077~~	~~0.363~~	~~0.121~~	~~0.002~~

Table AI-3 – Bear Lake titanite U-Pb isotopic data.

Common Pb corrected

Sample	^{206}Pb (cps)	^{204}Pb (cps)	^{207}Pb/^{206}Pb	2σ	^{207}Pb/^{235}U	2σ	^{206}Pb/^{238}U	2σ	ρ	^{207}Pb*/^{206}Pb* age (Ma)	2σ error (Ma)	^{207}Pb*/^{235}U age (Ma)	2σ error (Ma)	^{206}Pb*/^{238}U age (Ma)	2σ error (Ma)	Discordance (%)	^{238}U/^{206}Pb	2σ	^{207}Pb/^{206}Pb	2σ
Standards																				
K1	357800	148	0.05773	0.00212	0.69615	0.02932	0.08746	0.00179	0.486	519	79	536	17	541	11	-4.2	11.433	0.234	0.058	0.002
K2	363788	127	0.05830	0.00208	0.69803	0.03112	0.08684	0.00232	0.600	541	76	538	18	537	14	0.8	11.516	0.308	0.058	0.002
K3	339612	160	0.05709	0.00219	0.67237	0.02907	0.08542	0.00171	0.463	495	82	522	18	528	10	-7.0	11.707	0.234	0.057	0.002
K4	322088	141	0.05736	0.00219	0.66507	0.03087	0.08409	0.00222	0.570	505	82	518	19	520	13	-3.1	11.892	0.315	0.057	0.002
KHAN5	291350	554	0.05883	0.00362	0.68063	0.04480	0.08391	0.00197	0.356	561	129	527	27	519	12	7.7	11.917	0.279	0.059	0.004
KHAN6	348312	158	0.05698	0.00216	0.66504	0.02866	0.08465	0.00174	0.478	491	81	518	17	524	10	-7.0	11.813	0.243	0.057	0.002
KHAN7	293802	345	0.05787	0.00294	0.66727	0.03695	0.08363	0.00184	0.397	525	108	519	22	518	11	1.4	11.958	0.263	0.058	0.003
KHAN8	404946	221	0.05664	0.00216	0.65606	0.02913	0.08400	0.00192	0.515	478	82	512	18	520	11	-9.2	11.905	0.272	0.057	0.002
10CN326-1.2																				
10CN326 T11	473830	1686	0.11162	0.00527	4.61985	0.26996	0.30019	0.01033	0.589	1826	83	1753	48	1692	51	8.3	3.331	0.115	0.112	0.005
10CN326 T28	403952	1990	0.11343	0.00655	4.49729	0.29535	0.28755	0.00901	0.477	1855	101	1730	53	1629	45	13.8	3.478	0.109	0.113	0.007
10CN326 T30	462571	1355	0.11395	0.00490	4.97865	0.28902	0.31688	0.01235	0.671	1863	76	1816	48	1774	60	5.5	3.156	0.123	0.114	0.005
10CN326 T29	477054	1965	0.11473	0.00576	4.79148	0.29767	0.30290	0.01109	0.589	1876	88	1783	51	1706	55	10.3	3.301	0.121	0.115	0.006
10CN326 T22	450210	1705	0.11488	0.00557	4.75669	0.31201	0.30030	0.01326	0.673	1878	85	1777	54	1693	65	11.2	3.330	0.147	0.115	0.006
10CN326 T21	502885	2251	0.11494	0.00601	4.58004	0.33614	0.28899	0.01489	0.702	1879	91	1746	59	1636	74	14.6	3.460	0.178	0.115	0.006
10CN326 T26	390002	1094	0.11509	0.00498	5.09799	0.31716	0.32125	0.01436	0.719	1881	76	1836	51	1796	70	5.2	3.113	0.139	0.115	0.005
10CN326 T7	390530	1866	0.11515	0.00650	5.03342	0.38132	0.31704	0.01601	0.667	1882	98	1825	62	1775	78	6.5	3.154	0.159	0.115	0.007
10CN326 T10	419844	1413	0.11517	0.00532	5.02451	0.34781	0.31641	0.01631	0.744	1883	81	1823	57	1772	79	6.7	3.160	0.163	0.115	0.005
10CN326 T6	502068	1782	0.11525	0.00531	4.98877	0.40257	0.31394	0.02081	0.821	1884	81	1817	66	1760	101	7.5	3.185	0.211	0.115	0.005
10CN326 T1	542500	1996	0.11531	0.00534	5.23642	0.31402	0.32935	0.01254	0.635	1885	81	1859	50	1835	61	3.0	3.036	0.116	0.115	0.005
10CN326 T8	393430	1456	0.11585	0.00564	4.67959	0.43627	0.29295	0.02329	0.853	1893	85	1764	75	1656	115	14.2	3.414	0.271	0.116	0.006
10CN326 T2	535200	1073	0.11602	0.00424	5.27459	0.28249	0.32973	0.01290	0.730	1896	64	1865	45	1837	62	3.6	3.033	0.119	0.116	0.004
10CN326 T9	424060	1156	0.11624	0.00487	5.06754	0.26941	0.31619	0.01034	0.615	1899	74	1831	44	1771	50	7.7	3.163	0.103	0.116	0.005
10CN326 T23	462520	3206	0.11650	0.00836	5.23093	0.42791	0.32566	0.01279	0.480	1903	124	1858	67	1817	62	5.2	3.071	0.121	0.116	0.008
10CN326 T4	497776	1849	0.11657	0.00547	5.51790	0.31810	0.34329	0.01151	0.582	1904	82	1903	48	1903	55	0.1	2.913	0.098	0.117	0.005
10CN326 T24	454212	1153	0.11682	0.00471	5.10330	0.37400	0.31685	0.01939	0.835	1908	71	1837	60	1774	94	8.0	3.156	0.193	0.117	0.005
10CN326 T27	427415	1243	0.11688	0.00500	4.83620	0.28772	0.30009	0.01240	0.694	1909	75	1791	49	1692	61	12.9	3.332	0.138	0.117	0.005
10CN326 T3	473082	825	0.11711	0.00419	5.60983	0.34094	0.34741	0.01706	0.808	1913	63	1918	51	1922	81	-0.6	2.878	0.141	0.117	0.004
10CN326 T25	421420	2136	0.11777	0.00668	5.19924	0.36337	0.32018	0.01307	0.584	1923	98	1852	58	1791	63	7.9	3.123	0.127	0.118	0.007
10CN326 T5	485845	1240	0.11783	0.00469	5.54629	0.28867	0.34139	0.01146	0.645	1924	70	1908	44	1893	55	1.8	2.929	0.098	0.118	0.005
10CN1026 T39	383006	3047	0.14299	0.00944	6.38919	0.49890	0.32407	0.01352	0.534	2264	110	2031	66	1810	65	23.0	3.086	0.129	0.143	0.009
10CN326 T15	371474	802	0.14369	0.00517	7.72713	0.44065	0.39002	0.01725	0.776	2272	61	2200	50	2123	80	7.7	2.564	0.113	0.144	0.005
10CN1026 T36	357709	2623	0.14527	0.00895	6.63336	0.51408	0.33117	0.01556	0.606	2291	102	2064	66	1844	75	22.4	3.020	0.142	0.145	0.009
10CN1026 T35	390803	1950	0.14530	0.00707	7.59185	0.50602	0.37896	0.01726	0.684	2291	81	2184	58	2071	80	11.2	2.639	0.120	0.145	0.007
10CN1026 T33	427446	1594	0.14877	0.00613	7.40971	0.52594	0.36122	0.02088	0.814	2332	69	2162	62	1988	98	17.1	2.768	0.160	0.149	0.006
10CN326 T19	415439	1819	0.14889	0.00666	7.87424	0.58857	0.38356	0.02296	0.801	2333	75	2217	65	2093	106	12.1	2.607	0.156	0.149	0.007
10CN326 T18	347459	384	0.14890	0.00477	8.17932	0.58733	0.39839	0.02560	0.895	2333	54	2251	63	2162	117	8.7	2.510	0.161	0.149	0.005
10CN1026 T34	390157	1744	0.14948	0.00672	7.87626	0.48554	0.38215	0.01612	0.684	2340	75	2217	54	2086	75	12.7	2.617	0.110	0.149	0.007
10CN1026 T31	467997	1343	0.14949	0.00554	8.49147	0.41319	0.41196	0.01301	0.649	2340	62	2285	43	2224	59	5.9	2.427	0.077	0.149	0.006
10CN326 T13	417232	352	0.15121	0.00463	8.56024	0.46859	0.41058	0.01862	0.829	2360	51	2292	49	2218	85	7.1	2.436	0.110	0.151	0.005
10CN326 T14	403881	314	0.15313	0.00467	8.92184	0.39785	0.42256	0.01374	0.729	2381	51	2330	40	2272	62	5.4	2.367	0.077	0.153	0.005
10CN1026 T32	418535	5127	0.15320	0.01310	6.44026	0.65224	0.30489	0.01656	0.536	2382	139	2038	85	1716	81	31.8	3.280	0.178	0.153	0.013
10CN1026 T37	378355	4228	0.15340	0.01229	6.74200	0.58006	0.31875	0.01002	0.365	2384	130	2078	73	1784	49	28.8	3.137	0.099	0.153	0.012
10CN326 T20	396186	310	0.15376	0.00470	9.04341	0.50410	0.42656	0.01989	0.837	2388	51	2342	50	2290	89	4.9	2.344	0.109	0.154	0.005
10CN326 T17	438252	476	0.15405	0.00479	8.88687	0.37288	0.41840	0.01180	0.672	2391	52	2326	38	2253	53	6.8	2.390	0.067	0.154	0.005
10CN326 T16	337477	250	0.15413	0.00476	8.69044	0.45917	0.40893	0.01754	0.812	2392	52	2306	47	2210	80	9.0	2.445	0.105	0.154	0.005
			Model 1 Solution (±95% conf.) without [with] decay-const. errs on 21 points Lower intercept: 407 ±490 Ma Upper intercept: 1910 ±37 [±38] Ma MSWD = 0.22, Probability of fit = 1.000									Model 1 Solution (±95% conf.) without [with] decay-const. errs on 16 points Lower intercept: 511 ±320 Ma Upper intercept: 2383 ±32 [±33] Ma MSWD = 1.11, Probability of fit = 0.34									
~~10CN326 T12~~	~~272692~~	~~1555~~	~~0.13116~~	~~0.00793~~	~~5.98067~~	~~0.40926~~	~~0.33071~~	~~0.01061~~	~~0.469~~	~~2114~~	~~102~~	~~1973~~	~~58~~	~~1842~~	~~51~~	~~14.8~~	~~3.024~~	~~0.097~~	~~0.131~~	~~0.008~~
~~10CN1026 T40~~	~~309325~~	~~2641~~	~~0.13461~~	~~0.01016~~	~~5.71481~~	~~0.45883~~	~~0.30791~~	~~0.00841~~	~~0.340~~	~~2159~~	~~126~~	~~1934~~	~~67~~	~~1730~~	~~41~~	~~22.6~~	~~3.248~~	~~0.089~~	~~0.135~~	~~0.010~~
~~10CN1026 T38~~	~~337960~~	~~6312~~	~~0.17496~~	~~0.01932~~	~~6.36076~~	~~0.74634~~	~~0.26367~~	~~0.01047~~	~~0.338~~	~~2606~~	~~173~~	~~2027~~	~~98~~	~~1509~~	~~53~~	~~47.1~~	~~3.793~~	~~0.151~~	~~0.175~~	~~0.019~~

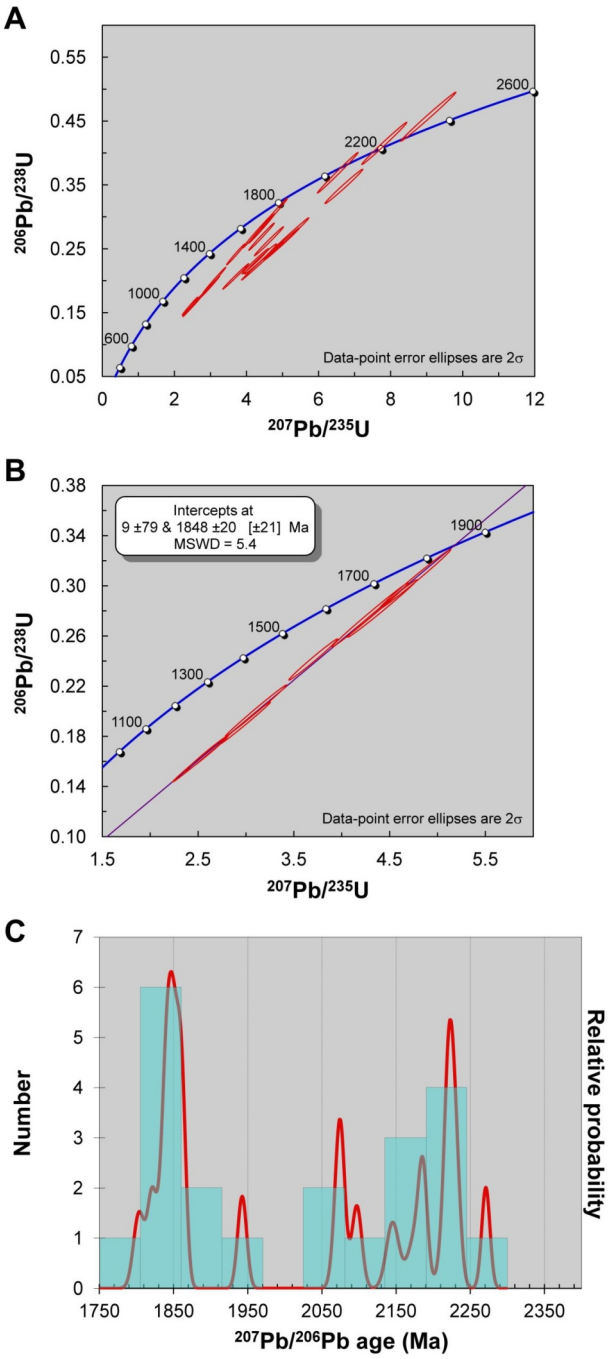

Figure AI-2 – Isotopic U-Pb LA-ICP-MS analytical results obtained on zircon from the Bear Lake REE occurrence: A) U-Pb isotopic results shown on a concordia diagram; B) subset population of discordant data from (a) showing a well-defined upper intercept age of 1848 ±20 Ma; and C) relative probability plot of $^{207}Pb/^{206}Pb$ ages.

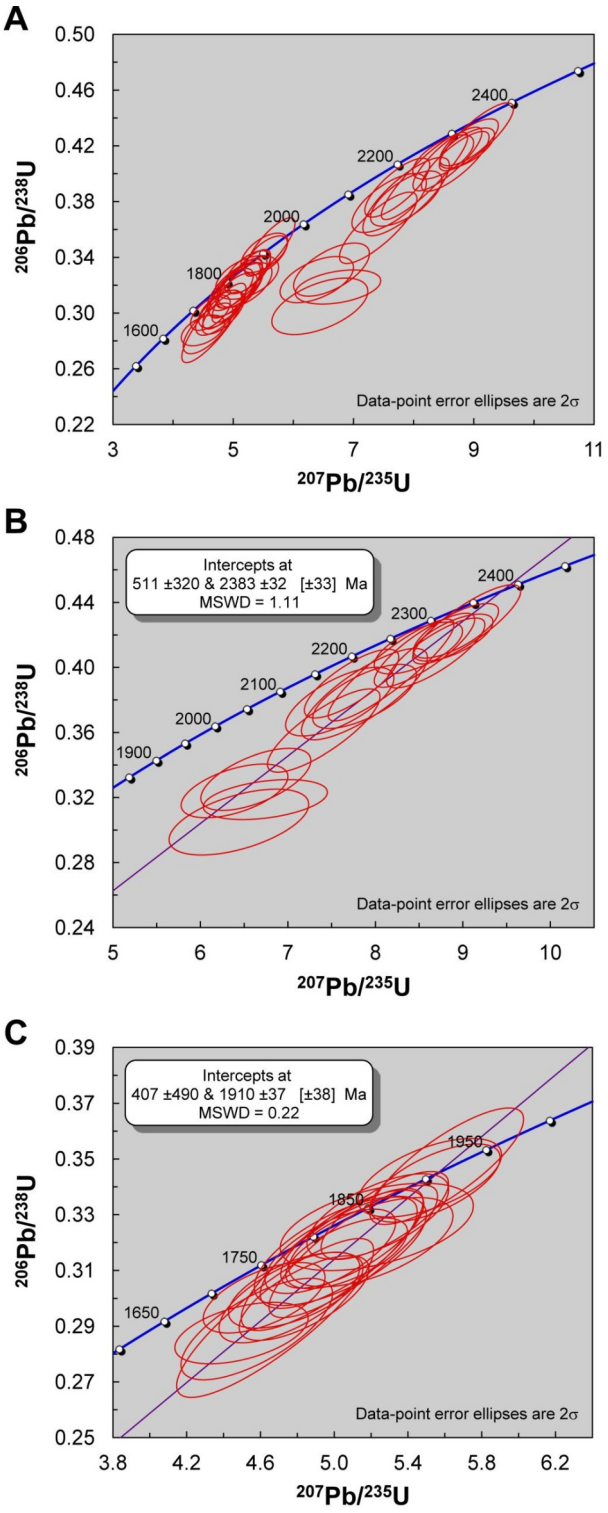

Figure AI-3 – Isotopic U-Pb LA-ICP-MS analytical results obtained on titanite from the Bear Lake REE occurrence: A) U-Pb isotopic results shown on a concordia diagram. At least two populations of discordant data can be distinguished: B) an older population of discordant data that has an upper intercept age of 2383 ± 32 Ma; and C) a younger population of discordant data that has an upper intercept age of 1910 ± 37 Ma.